



Institute for Molecular Science
annual review

2007

Published by

Institute for Molecular Science

National Institutes of Natural Sciences

Myodaiji, Okazaki 444-8585, Japan

Phone: +81-564-55-7418 (Secretary Room)

Fax: +81-564-54-2254 (Secretary Room)

URL: <http://www.ims.ac.jp/>

Editorial Committee 2007

Chairperson

KAWAGUCHI, Hiroyuki

Vice-Chairperson

KIMURA, Shin-ichi

ISHIDA, Tateki

YOSHIDA, Norio

HASEGAWA, Hirokazu

ITO, Takahiro

ISHIZUKI, Hideki

JIANG, Donglin

NAKAGAWA, Takeshi

SAKAMOTO, Youichi

TERO, Ryugo

WADA, Tohru

KURAHASHI, Takuya

KAMO, Kyoko

NAKAMURA, Rie



This is the fourth year of our new parent organization NINS (National Institutes of Natural Sciences). The severe financial circumstances are still continuing, unfortunately, because of the tight financial condition of the government. In spite of this we always have to strive to conduct excellent research at IMS as a Center of Excellence.

From April 2007 we have reorganized the structure of IMS into four Departments and seven Research Centers. The four departments include Department of Theoretical and Computational Molecular Science, Department of Photo-Molecular Science, Department of Materials Molecular Science, and Department of Life and Coordination-Complex Molecular Science. This reorganization is to meet recent developments of various branches of molecular science and to promote closer contacts and fruitful collaborations not only inside each department but also among the departments. The Research Centers play important roles, as usual, to offer their facilities to researchers inside and outside the institute. In order to enhance its function each Research Center is now associated with the corresponding department.

The four special programs of IMS are successfully to be continued: (i) Extreme photonics in collaboration with RIKEN, (ii) COE of molecular and materials simulations as a joint program of NINS, (iii) Nano-network project, including the joint research initiative using the cutting-edge 920MHz NMR, and (iv) Nano-science simulations for the “Grand Challenge Applications” of the national project of Petaflops super-computer. As for the international collaboration, in addition to the general program the Asian Core Program in Molecular Science started last fiscal year to promote collaborations and bring up young Asian scientists. In this fiscal year, the second annual meeting is to be held in Korea and the second winter school is planned in Okazaki in addition to many research collaborations.

The nationwide new network system has started as a test for efficient mutual use of experimental equipments covering 72 national universities. We really hope that this system will be strongly supported, since this is crucial to keep and promote basic research activities in Japan.

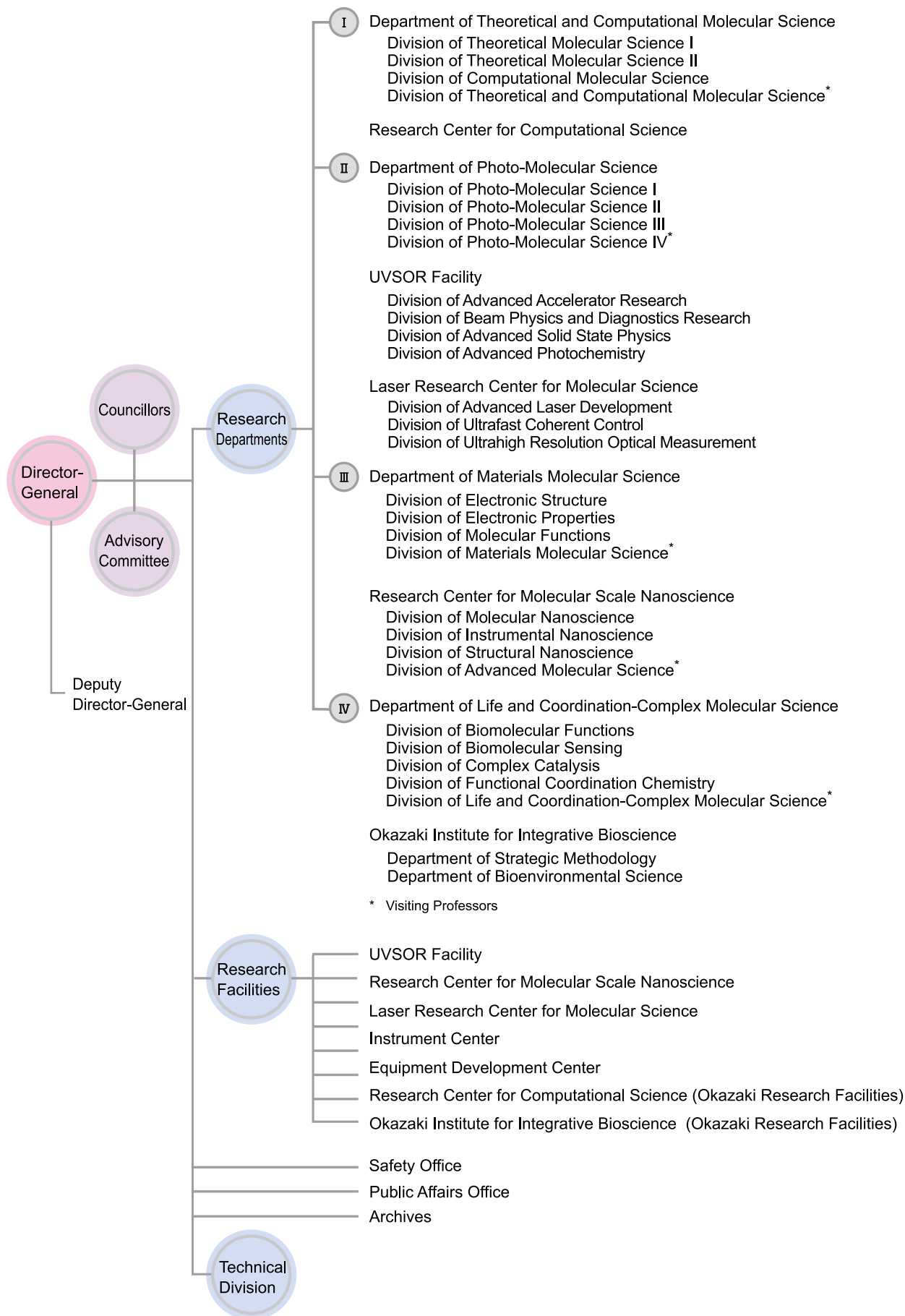
This volume of Annual Review is a comprehensive summary of research activities carried out at IMS in the period of September 2006-August 2007. During this period some people have left and some new people joined us, as listed in each research group. As usual, a lot of research activities are going on and we are proud of that. Any constructive comments and/or questions are welcome. It is also a great pleasure to announce that many colleagues received various prizes as explained in each research group and the end of this volume.

September, 2007

A handwritten signature in black ink that reads "H. Nakamura". The signature is written in a cursive style with a long, sweeping underline.

NAKAMURA, Hiroki
Director-General, Institute for Molecular Science

■ FROM THE DIRECTOR-GENERAL	i
■ CONTENTS	ii
■ ORGANIZATION	1
■ COUNCIL	2
■ ACTIVITIES IN EDUCATION AND COLLABORATION	4
■ RESEARCH ACTIVITIES	5
Theoretical and Computational Molecular Science	5
Photo-Molecular Science	23
Materials Molecular Science	47
Life and Coordination-Complex Molecular Science	77
■ RESEARCH FACILITIES	95
UVSOR Facility	96
Research Center for Molecular Scale Nanoscience	98
Laser Research Center for Molecular Science	99
Instrument Center	100
Equipment Development Center	101
Research Center for Computational Science	102
Okazaki Institute for Integrative Bioscience	103
Safety Office	104
■ SUPPORTING STAFF	105
■ PROGRAMS	106
Special Research Projects	106
Joint Study Programs	109
Collaboration Programs	112
■ AWARDS	114
■ LIST OF VISITING FOREIGN SCHOLARS	115
■ LIST OF PUBLICATIONS	118
■ LIST OF REVIEW ARTICLES AND TEXTBOOKS	130
■ INDEX	132
■ BUILDINGS AND CAMPUS	133



NAKAMURA, Hiroki

Director-General

Councillors

ESAKI, Nobuyoshi

Director, Institute for Chemical Research, Kyoto University

KATO, Shinichi

Chief Executive Officer, Toyota Central Research & Development Laboratories, Inc.

TSUCHIYA, Soji

Invited Professor, Josai University

NOGUCHI, Hiroshi

Culture News Editor, The Chunichi Shinbun Press

MILLER, H. William*

Professor, University of California, Berkeley

LAUBEREAU, Alfred*

Professor, Technische Universität München

The Council is the advisory board for the Director-General.

* Two of the councillors are selected among distinguished foreign scientists.

Distinguished Consultants

NAGAKURA, Saburo

The Japan Academy

INOKUCHI, Hiroo

Advisor, Japan Aerospace Exploration Agency

ITO, Mitsuo

Professor Emeritus, Institute for Molecular Science, The Graduate University for Advanced Studies, Tohoku University

KAYA, Koji

Director, RIKEN Discovery Research Institute

Research Consultants

HIROTA, Noboru

Professor Emeritus, Kyoto University

KONDOW, Tamotsu

Visiting Professor, Toyota Technological Institute

TAMAOKI, Kohei

Director, RIKEN Frontier Research System

Advisory Committee

AWAGA, Kunio

Professor, Nagoya University

ENOKI, Toshiaki

Professor, Tokyo Institute of Technology

FUJITA, Makoto

Professor, The University of Tokyo

KATO, Masako

Professor, Hokkaido University

MAEKAWA, Sadamichi

Professor, Tohoku University

NAKAJIMA, Atsushi

Professor, Keio University

SEKIYA, Hiroshi

Professor, Kyushu University

TANAKA, Kenichirou

Professor, Hiroshima University (Vice chair)

TERAZIMA, Masahide

Professor, Kyoto University

YAMASHITA, Kouichi

Professor, The University of Tokyo

HIRATA, Fumio

Professor, Institute for Molecular Science

KOSUGI, Nobuhiro

Professor, Institute for Molecular Science

NAGASE, Shigeru

Professor, Institute for Molecular Science

NISHI, Nobuyuki

Professor, Institute for Molecular Science

OGAWA, Takuji

Professor, Institute for Molecular Science

OKAMOTO, Hiromi

Professor, Institute for Molecular Science

OHMORI, Kenji

Professor, Institute for Molecular Science

TANAKA, Koji

Professor, Institute for Molecular Science

URISU, Tsuneo

Professor, Institute for Molecular Science

YAKUSHI, Kyuya

Professor, Institute for Molecular Science (Chair)

YOKOYAMA, Toshihiko

Professor, Institute for Molecular Science

Administration Bureau

KURATA, Yutaka	Director, Okazaki Administration Office Director, General Affairs Department
MURANO, Hiroaki	Director, Financial Affairs Department
HARADA, Eiichiro	Head, General Affairs Division
HIRAO, Koji	Head, International Relations and Research Cooperation Division
HAYASHI, Masanori	Head, Financial Affairs Division
KASSAI, Isamu	Head, Procurement Division
SHINOHARA, Kenji	Head, Facilities Division

Emeritus Professors

NAGAKURA, Saburo	The Japan Academy
HIROTA, Eizi	Professor Emeritus, The Graduate University for Advanced Studies
KIMURA, Katsumi	IMS, Professor Emeritus, Japan Advanced Institute of Science and Technology
MOROKUMA, Keiji	Research Leader, Fukui Institute for Fundamental Chemistry Kyoto University
INOKUCHI, Hiroo	Advisor, Japan Aerospace Exploration Agency
MARUYAMA, Yusei	Professor, Hosei University
YOSHIHARA, Keitaro	Professor, Japan Advanced Institute of Science and Technology
HANAZAKI, Ichiro	Professor Emeritus, The Graduate University for Advanced Studies
IWAMURA, Hiizu	Professor, University of the Air
SAITO, Shuji	Professor, Fukui University
IWATA, Suehiro	Professor, National Institution for Academic Degree
ITO, Mitsuo	Professor Emeritus, The Graduate University for Advanced Studies, Tohoku University
KAYA, Koji	Director, RIKEN Wako Institute, RIKEN Discovery Institute
KITAGAWA, Teizo	Fellow, Toyota Physical and Chemical Research Institute
KOABAYASHI, Hayao	Visiting Professor, Nihon University

Graduate Programs

IMS promotes pioneering and outstanding research by young scientists as a core academic organization in Japan. IMS trains graduate students in the Departments of Structural Molecular Science and Functional Molecular Science, Graduate School of Physical Sciences, the Graduate University for Advanced Studies (SOKENDAI). By virtue of open seminars in each research division, Colloquiums and the Molecular Science Forum to which speakers are invited from within Japan and all over the world, as well as other conferences held within IMS, graduate students have regular opportunities to be exposed to valuable information related to their own fields of research as well as other scientific fields. Graduate students can benefit from these liberal and academic circumstances, all of which are aimed at extending the frontiers of fundamental molecular science and to facilitate their potential to deliver outstanding scientific contributions.

For more details on the Departments of Structural Molecular Science and Functional Molecular Science, young scientists are encouraged to visit IMS through many opportunities such as the IMS Open Campus in May, Graduate-School Experience Program (Taiken Nyugaku) in August, Open Lectures in summer and winter, *etc.*



International Collaboration and International Exchange

IMS has accepted many foreign scientists and hosted numerous international conferences (*e.g.* Okazaki Conference) since its establishment and is now universally recognized as an institute that is open to foreign countries. In 2004, IMS initiated a new program to further promote international collaborations. As a part of this new program, IMS faculty members can (1) nominate senior foreign scientists for short-term visits, (2) invite young scientists for long-term stays, and (3) undertake visits overseas to conduct international collaborations. In 2006, IMS started a new program, JSPS Asian CORE Program on “Frontiers of material, photo- and theoretical molecular sciences” (2006–2011). This new program aims to develop a new frontier in the molecular sciences and to foster the next generation of leading researchers through the collaboration and exchange among IMS and core Asian institutions: ICCAS (China), KAIST (Korea), and IAMS (Taiwan). See the details in pages 112–113.



Joint Study Programs

As one of the important functions of an inter-university research institute, IMS facilitates joint study programs for which funds are available to cover the costs of research expenses as well as the travel and accommodation expenses of individuals. Proposals from domestic scientists are reviewed and selected by an interuniversity committee. See the details in pages 109–111.

The programs are conducted under one of the following categories:

- (1) Joint Studies on Special Projects (a special project of significant relevance to the advancement of molecular science can be carried out by a team of several groups of scientists).
- (2) Research Symposia (a symposium on timely topics organized as a collaborative effort between outside and IMS scientists).
- (3) Cooperative Research (a research program conducted by outside scientists with collaboration from an IMS scientist).
- (4) Use of Facilities (a research program conducted by outside scientists using the research facilities of IMS, except the UVSOR facility).
- (5) Joint Studies Programs using beam lines of UVSOR Facility.
- (6) Use of Facility Program of the Computer Center (research programs conducted by outside scientists at research facilities in the Research Center for Computational Science).





RESEARCH ACTIVITIES

Theoretical and Computational Molecular Science

It is our ultimate goal to develop theoretical and computational methodologies that include quantum mechanics, statistical mechanics, and molecular simulations in order to understand the structures and functions of molecules in gasses and condensed phases, as well as in bio and nano systems.

Theoretical Study and Design of Functional Molecules: New Bonding, Structures, and Reactions

Department of Theoretical and Computational Molecular Science
Division of Theoretical Molecular Science I



NAGASE, Shigeru
LU, Xin
CHOI, Cheol Ho
OHTSUKA, Yuki
ISHIMURA, Kazuya
TAKAGI, Nozomi
SLANINA, Zdenek
ZHOU, Zhen
KATOUDA, Michio
GAO, Xingfa
GUO, Jing-Doing
MIZOROGI, Naomi
SUTCLIFFE, Brian
KIM, Tae-Rae
YAMADA, Mariko
NAKAJIMA, Hikari

Professor
Visiting Professor*
Visiting Associate Professor
Assistant Professor
Technical Associate
Post-Doctoral Fellow[†]
Post-Doctoral Fellow[‡]
Post-Doctoral Fellow[§]
Post-Doctoral Fellow
Post-Doctoral Fellow
Post-Doctoral Fellow
Visiting Scientist
Graduate Student^{||}
Secretary
Secretary

In theoretical and computational chemistry, it is an important goal to develop functional molecules prior to or in cooperation with experiment. Thus, new bonds and structures provided by heavier atoms are investigated together with the reactivities. In addition, chemical modification and doping of cage-like molecules and clusters including fullerenes and carbon nanotubes are investigated to develop functional nano-molecular systems. Efficient computational methods are also developed to perform reliable quantum chemistry calculations even for large molecular systems.

1. New Parallel Algorithm of Energy Gradient Calculations for Second-Order Møller-Plesset Perturbation (MP2) Theory¹⁾

It is an important subject to determine molecular geometries and reaction paths. For this purpose, density functional theory (DFT) is widely used because of its low computational cost. However, the generally used DFT methods fail to describe non-covalent interactions that play an important role in supramolecules, host-guest interactions, self-assembly, molecular recognition, and the folding of proteins, and they tend to underestimate reaction barriers.

Second-order Møller-Plesset perturbation theory (MP2) is the simplest method that includes electron correlation important for non-covalent interactions and reaction barriers. MP2 is also helpful for checking DFT results. Despite these advantages, MP2 calculations are much more time-consuming than DFT calculations and require very large memory and hard disk. These make MP2 geometry optimization difficult for large molecules. Therefore, a new parallel algorithm of MP2 energy gradient calculations is developed using the MP2 energy algorithm that we have developed recently, which is

essential for the determination of molecular geometries and reaction paths. The algorithm decreases highly the FLOP (floating point operation) count as well as memory and disk sizes. Test parallel calculations are performed for taxol (C₄₇N₁₄H₅₁) and luciferin (C₁₁N₂O₃S₂H₈) with the 6-31G, 6-31G(d) and aug-cc-pVDZ basis sets. The results demonstrate the high parallel efficiency of the algorithm. In addition, the computational speed per CPU is considerably higher than that of other representative programs. Obviously, these make MP2 calculations feasible for considerably large molecules, and enriches the important applications, especially for molecular systems where DFT is inferior to MP2 in accuracy and reliability.

2. Accuracy of the Fragment Molecular orbital (FMO) Method Based MP2 Theory²⁾

The fragment molecular orbital (FMO) method permits high-speed *ab initio* calculations of large molecular systems by dividing them into small fragments. Since the MP2 code applicable to large molecules is developed, it is interesting to calibrate the accuracy of the MP2-based FMO method. Therefore, three-body interactions as well as two-body interactions are considered in the FMO method. These are named FMO2 (two-body) and FOM3 (three-body). Test calculations are carried out with the 6-31G(d) and 6-311G(d) basis sets for (H₂O)_n (*n* = 16, 32, 64), (alanine)_n (*n* = 10, 20, 40), and a small synthetic protein. FMO3-MP2 energies are closer to full MP2 energies than FMO2-MP2 energies. For example, the energy errors for the protein shown in Figure 1 are 4.61 (FMO2-MP2) and 0.81 (FMO3-MP2) mH for the 6-311G (d) basis set.

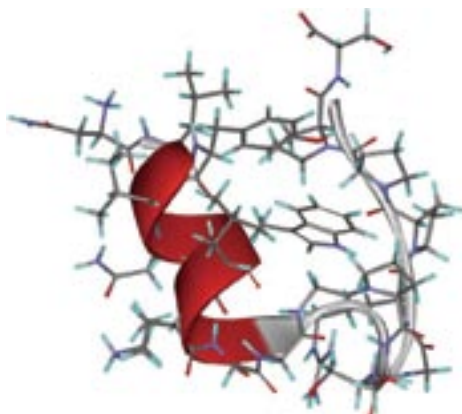


Figure 1. The synthetic protein IL2Y containing 304 atoms.

3. Multiple Bonds between Heavier Group 14 Elements: Structure and Reactivity^{3,4)}

Multiple bonds between heavier elements are of wide interest in main-group chemistry. Among these, heavier group 14 element analogues of alkynes, RMMR (M = Si, Ge, Sn, Pb), have attracted special interest as challenging synthetic targets. We have theoretically predicted that bulky substituent groups play an important role in making RMMR synthetically accessible and isolable as stable compounds. Accordingly, the Si, Ge, Sn, and Pb analogues of alkynes have been synthesized and isolated by introducing very bulky aryl and silyl groups. As shown by X-ray crystal structural analysis, the Si, Ge, and Sn analogues of alkynes have a multiply bonded structure, while the heaviest Pb analogue, Ar^{*}PbPbAr^{*} (Ar^{*} = C₆H₃-2,6-(C₆H₂-2,4,6-*i*Pr₃)₂), takes a singly bonded structure. Form theoretical calculations, however, we have revealed that even the heaviest analogue has a multiply bonded structure in solution, unlike the singly bonded structure found by X-ray crystal analysis. The different structures in solution and the crystal state are ascribed to packing forces. In addition, it is general that crystallization is significantly affected by the bulk of substituent groups. These have been also demonstrated for the recently synthesized tin analogues, Ar^{*}SnSnAr^{*} and Ar^{**}SnSnAr^{**} (Ar^{**} = C₆H₂-2,6-(C₆H₃-2,6-*i*Pr₂)₂-4-SiMe₃).

To provide insight to the unique reactivity of the silicon–silicon triple bond, the reactions of R^{Si}SiSiR^{Si} (R^{Si} = Si^{*i*}Pr [CH(SiMe₃)₂]₂) with 2-butenes (cis and trans) and alkynes are investigated. The cycloaddition of R^{Si}SiSiR^{Si} to 2-butenes proceeds in a stereospecific way, while its cycloaddition to phenylalkyne leads to an isolable aromatic 1,2-disilabenzene derivative. The reaction mechanisms are disclosed by theoretical calculations.

* Present Address; University of California, Berkeley, California 94720, U. S. A.

† Present Address; Fachbereich Chemie der Phillips-Universität, D-35032 Marburg, Germany

‡ Present Address; University of Tsukuba, Ibaraki 305-8577

§ Present Address; Nankai University, Tianjin 300071, P. R. China

|| carrying out graduate research on Cooperative Education Program of IMS with Seoul National University

4. Structures and Functionalization of Endohedral Metallofullerenes^{5,6)}

From MEM/Rietveld analysis of synchrotron X-ray powder diffraction data of Sc₂C₈₄, it was once believed that two Sc atoms are encaged inside the C₈₄ fullerene. From theoretical calculations and experiment, however, we have disclosed that two C atoms as well two Sc atoms are encapsulated inside the C₈₂ fullerene, forming Sc₂C₂@C₈₂.

We have predicted theoretically that the three-dimensional random motion of two La³⁺ cations in La₂@C₈₀ can be restricted to the circular motion in a plane by attaching an electron-donating molecule such as disilirane on the outer surface of the C₈₀ cage. This has been beautifully verified, as shown in Figure 2. Such circular motion in a plane is expected to induce unique electronic and magnetic fields in the direction perpendicular to the plane.

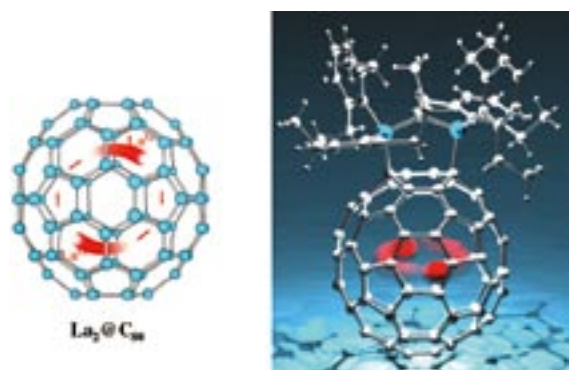


Figure 2. Random and two-dimensional circular motions of two La³⁺ cations in La₂@C₈₀ and its derivative.

References

- 1) K. Ishimura, P. Pulay and S. Nagase, *J. Comput. Chem.* **28**, 2034–2042 (2007).
- 2) D. G. Fedorov, K. Ishimura, T. Ishida, K. Kitaura, P. Pulay and S. Nagase, *J. Comput. Chem.* **28**, 1467–1484 (2007).
- 3) N. Takagi and S. Nagase, *Organometallics* **26**, 469–471 (2007); **26**, 3627–3629 (2007); *J. Organomet. Chem.* **692**, 217–224 (2007).
- 4) R. Kinjyo, M. Ichinohe, A. Sekiguchi, N. Takagi, M. Sumimoto and S. Nagase, *J. Am. Chem. Soc.* **129**, 7766–7767 (2007).
- 5) Y. Iiduka, T. Wakahara, K. Nakajima, T. Nakahodo, T. Tsuchiya, Y. Maeda, T. Akasaka, K. Yoza, M. T. H. Liu, N. Mizorogi and S. Nagase, *Angew. Chem., Int. Ed.* **46**, 5562–5564 (2007).
- 6) T. Wakahara, M. Yamada, S. Takahashi, T. Nakahodo, T. Tsuchiya, Y. Maeda, T. Akasak, M. Kako, Y. Yoza, E. Horn, N. Mizorogi and S. Nagase, *Chem. Commun.* 2680–2682 (2007).

Theoretical Studies of Electron Dynamics

Department of Theoretical and Computational Molecular Science
Division of Theoretical Molecular Science I



NOBUSADA, Katsuyuki	Associate Professor
YASUIKE, Tomokazu	Assistant Professor
KUBOTA, Yoji	Post-Doctoral Fellow
NODA, Masashi	Post-Doctoral Fellow
SHIRATORI, Kazuya	Graduate Student
IWASA, Takeshi	Graduate Student
YAMADA, Mariko	Secretary

Electron dynamics in nanometer-sized molecules and nanostructured materials is an intrinsic process related to a number of interesting phenomena such as linear and nonlinear optical response, electrical conduction, and also chemical reaction. Despite their importance, the electron dynamics has not been understood in detail. We have developed a computational method simulating the electron dynamics in real time and real space, and elucidated the dynamics.

1. Photoinduced Electric Currents in Ring-Shaped Molecules by Circularly Polarized Laser Pulses¹⁾

We have theoretically demonstrated that circularly polarized laser pulses induce electric currents and magnetic moments in ring-shaped molecules Na_{10} and benzene. The time-dependent adiabatic local density approximation is employed for this purpose, solving the time-dependent Kohn-Sham equation in real-space and real-time. It has been found that the electric currents are induced efficiently and persist continuously even after the laser pulses were switched off provided the frequency of the applied laser pulse is in tune with the excitation energy of the electronic excited state with the dipole strength for each molecular system. The electric currents are definitely revealed to be a second order nonlinear optical response to the magnitude of the electric field. The magnetic dipole moments inevitably accompany the ring currents, so that the molecules are magnetized. The production of the electric currents and the magnetic moments in the present procedure is found to be much more efficient than that utilizing static magnetic fields.

2. Theoretical Investigation of Optimized Structures of Thiolated Gold Cluster $[\text{Au}_{25}(\text{SCH}_3)_{18}]^+$

Geometric and electronic structures of a gold-methanethiolate $[\text{Au}_{25}(\text{SCH}_3)_{18}]^+$ are investigated by using density functional theory. Three types of optimized structures are

derived from two different Au_{25} core clusters protected by 18 methanethiolates. The most probable optimized structure (FCC2) consists of a Au_7 core cluster and Au-S complex-like ring clusters, $\text{Au}_{12}(\text{SCH}_3)_{12}$ and $\text{Au}_3(\text{SCH}_3)_3$. The Au_7 core cluster is enclosed by the $\text{Au}_{12}(\text{SCH}_3)_{12}$ ring cluster and then the Au_7 - $\text{Au}_{12}(\text{SCH}_3)_{12}$ core-ring subsystem is capped with the two $\text{Au}_3(\text{SCH}_3)_3$ ring clusters from both sides of the top and the bottom. This structural feature is in contrast to a general notion of gold-thiolate clusters that a core gold cluster is superficially protected by thiolate molecules. The optimized structure provides a large HOMO-LUMO gap, and its X-ray diffraction and absorption spectra successfully reproduce the experimental results.

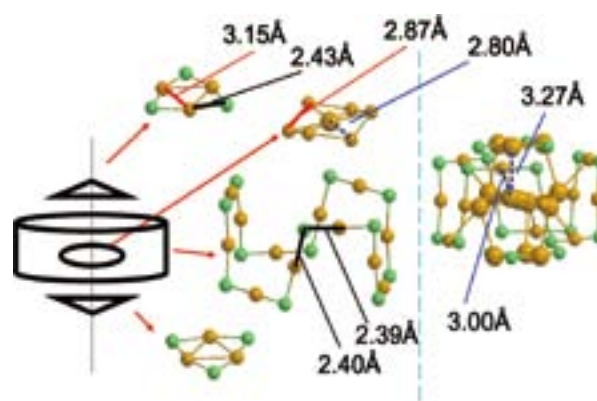


Figure 1. Fractionalized subsystems of FCC2 and their bond distances.²⁾

3. Efficient Numerical Method for Calculating Exciton States in Quantum Boxes³⁾

We have developed an efficient numerical method for exciton states confined in quantum boxes. The exciton wave function is expanded in terms of discrete variable representation basis functions. Our numerical approach has proved to be computationally much less demanding in comparison with the conventional configuration-interaction one.

4. Open-Boundary Cluster Model for Calculation of Adsorbate-Surface Electronic States

We have developed a simple embedded-cluster model approach to investigate adsorbate-surface systems. In our approach, the physically-relevant subsystem is described as an open-quantum system by considering a model cluster subject to an outgoing-wave boundary condition at the edge. This open-boundary cluster model (OCM) is free from artificial waves reflected at the cluster edge, and thus the adsorbate properties computed with the OCM are almost independent of the model cluster size. The exact continuous density of states (DOS) of a 1D periodic potential model is shown to be precisely reproduced with the OCM. The accurate DOS leads to an appropriate description of adsorbate-surface chemical bonding. Moreover, the open-boundary treatment of the OCM allows us to evaluate the electron-transfer rate from the adsorbate to the surface, whereas the conventional cluster model (CCM) does not give any information about such a dynamical process.

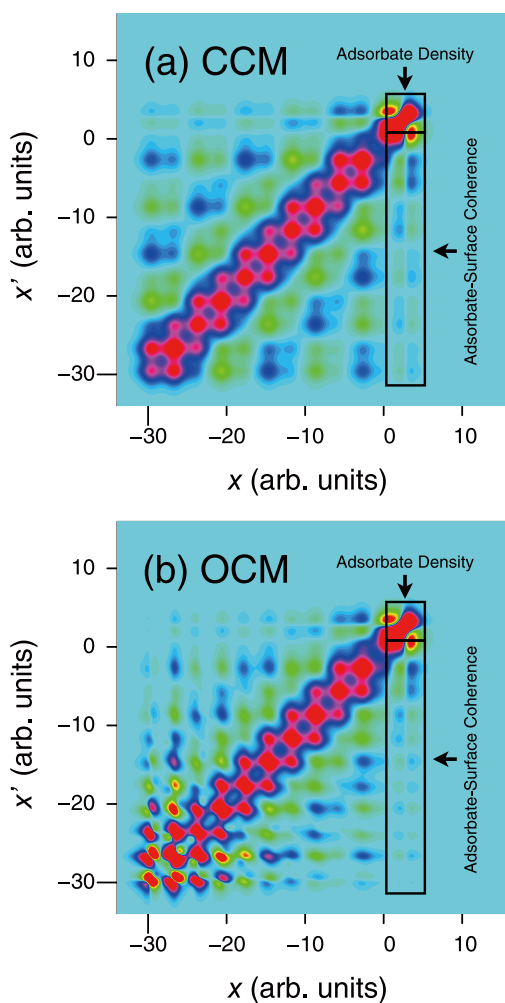


Figure 2. One-body reduced density matrix in the real space representation obtained with (a) CCM and (b) OCM. The adsorbate density and the adsorbate-surface coherence are illustrated in the square and rectangle regions, respectively. The adsorption distance and the chemical potential are set to be 2.5 and -1.3 , respectively.

5. Finite-Temperature Density Functional Calculation with Polarizable Continuum Model in Electrochemical Environment

We present a numerical methodology to calculate electronic structures of a molecule in electrochemical environment. The methodology is based on the finite temperature density functional theory (FTDFT) and allows us to study electronic properties of a molecule at a fixed chemical potential. The approach is applied to a reaction of $\text{NO}^+ + e^- \rightleftharpoons \text{NO}$ in chemical equilibrium. The solvent effect is taken into account by a conductor-like polarizable continuum model (C-PCM), and the size of the cavity in C-PCM is given in terms of the molecular charge so as to reproduce the experimental solvation energy of the cation. We demonstrate that the method combined with C-PCM (FTDFT/C-PCM) successfully describes the electronic structures of the molecule in electrochemical environment. Applicability of the present method to electrochemical properties is discussed in comparison with an alternative approach of statistically averaged DFT calculations.

References

- 1) K. Nobusada and K. Yabana, *Phys. Rev. A* **75**, 032518 (7 pages) (2007).
- 2) T. Iwasa and K. Nobusada, *J. Phys. Chem. C* **111**, 45–49 (2007).
- 3) Y. Kubota and K. Nobusada, *Phys. Lett. A* **369**, 128–131 (2007).

Advanced Electronic Structure Theory in Quantum Chemistry

Department of Theoretical and Computational Molecular Science
Division of Theoretical Molecular Science I



YANAI, Takeshi
YAMADA, Mariko

Associate Professor
Secretary

Aimed at predictive computational modelings of molecular electronic structures with *ab initio* quantum chemistry calculations, our scientific exploration is to establish a cutting-edge theoretical methodology that allows one to compute accurately and efficiently the complex electronic structures where the substantial multireference character in the wave functions has to be handled for the qualitative and quantitative descriptions. Our resultant works to be reported here are (1) to develop a new type of the multireference correlation model named Canonical Transformation (CT) theory, which can efficiently describe short-range dynamic correlation on top of the multi-configurational starting wave function, and (2) to construct the extensive complete active space self-consistent field (CASSCF) method combined with *ab initio* density matrix renormalization group (DMRG) method for making unprecedentedly larger active spaces available for the CASSCF calculations. These two pivotal developments are tailored to eventually be incorporated for solving large-scale multi-reference electronic structure problems.

1. Canonical Transformation (CT) Theory from Extended Normal Ordering¹⁾

We have presented a canonical transformation (CT) theory which is based on an exponential ansatz, is rigorously size extensive, and which may easily be combined with any multi-reference starting wave function such as CASSCF or DMRG wave functions. This study has derived a new formulation of the theory based on the extended normal ordering procedure of Mukherjee and Kutzelnigg.

Assuming that a reference wave function Ψ_0 is available that describes the nondynamic correlation in the problem, we incorporate the remaining dynamic correlation on top of the reference wave function Ψ_0 via an exponential operator that generates excitations between the active and external spaces, yielding

$$\Psi = e^A \Psi_0 \quad (\text{eq. 1})$$

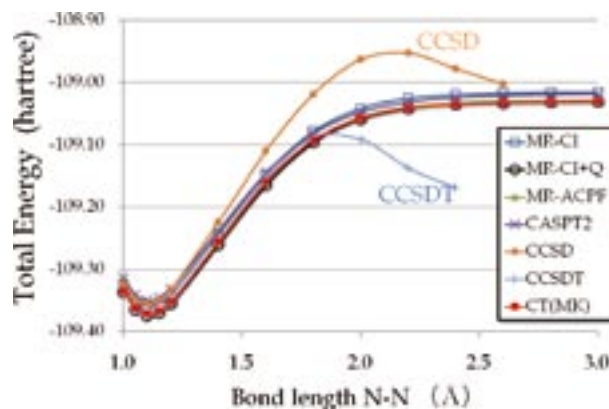


Figure 1. Bond-breaking curve of N_2 molecule with CAS(6e,6o) and cc-pVTZ Gaussian basis sets.

We will be concerned with a *unitary* formulation, where $A^\dagger = -A$. The excitations are understood to be both of external and semi-internal forms of up to two-particle operators. In a related picture, we can also view e^A as generating an effective *canonically transformed* Hamiltonian H^{CT} that acts only in the active space, but which has dynamic correlation folded in from the external space, where

$$H^{CT} = e^{-A} H e^A \quad (\text{eq. 2})$$

$$H^{CT} \Psi = E \Psi \quad (\text{eq. 3})$$

A central feature of the canonical transformation theory is the use of an *operator decomposition*, both to close the infinite expansions associated with an exponential ansatz and to reduce the complexity of the energy and amplitude equations that arise when working with a complicated reference function. Starting from the Baker-Campbell-Hausdorff expansion of the exact effective Hamiltonian, we replace each commutator by an approximate *decomposed* commutator to yield an approximate effective Hamiltonian,

$$H_{1,2}^{CT} = H_{1,2} + [H, A]_{1,2} + \frac{1}{2} [[H, A]_{1,2}, A]_{1,2} + \dots \quad (\text{eq. 4})$$

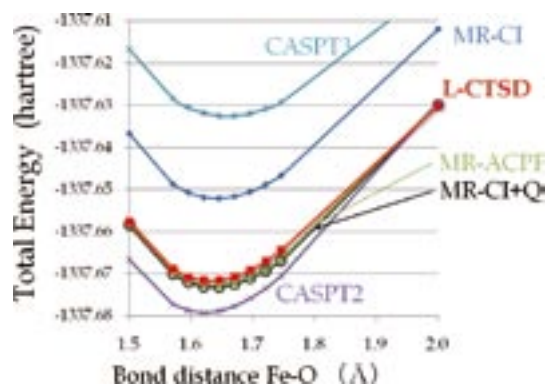


Figure 2. Bond-breaking curve of FeO molecule with CAS(12*e*,12*o*) and ANO-DZP Gaussian basis sets.

Table 1. Timings for different multireference methods for a single point calculation on the FeO curve. The time for the CASSCF calculation is not included. L-CTSD (present work) did not exploit the point-group symmetry of the molecule in the calculation.

	Time (sec)
CASPT2	5,900
CASPT3	17,000
MR-CT+Q	158,000
MR-ACPF	168,000
L-CTSD (present)	4,500

Each subscript denotes a decomposition, and the numbers “1,2” denote the particle ranks of the operators that remain after the decomposition. In this study, we have introduced a new-type operator decomposition, with some formal advantages, that is based on the concept of *extended normal ordering* as introduced by Mukherjee and Kutzelnigg. The study presented and exploited a form of the extended normal-ordered decomposition for three-particle operators. In the form implemented in the work, the computational cost is $O(a^2e^4)$, which is essentially the same as that of the single-reference coupled-cluster single and double (CCSD) model, where a is the number of active orbitals and e is the number of external orbitals.

A second focus of this work is to investigate in detail the behavior of the canonical transformation theory in a variety of chemical problems. For example, we study, with a range of basis sets, the bond-breaking potential energy curves of water, nitrogen, and iron oxide and compare our results against state-of-the-art multireference configuration interaction and perturbation theories. In addition, we examine numerically the size-extensivity and density-scaling properties of the canonical transformation energies. The results in the present study are much improved, in large part, because of improvements we have made to our numerical algorithms, and we describe in detail the numerical aspects of efficiently implementing and converging the CT equations.

Figure 1 shows the bond-breaking curve of the nitrogen molecule, which is a prototype multireference problem where the complication of breaking a triple bond occurs. For this application, the prevalent single-reference methods CCSD or

CCSDT are known to typically fail to describe the bond breaking. Figure 2 presents the potential curves of FeO computed by various multireference methods. The overall performance of our linearized CT method with single and double substitutes (L-CTSD) for these potential curves was competitive with the best multireference methods such as MR-ACPF. It is found that, for the FeO calculations, the multireference perturbation series CASPT2 and CASPT3 seemed to break down. Timings for the multireference calculations, which are listed in Table 1, reveal that CT method is two to three orders of magnitude faster than the most accurate MR-ACPF method, which though the CT is competitive with in accuracy.

2. Extensive Complete Active Space Self-Consistent Field (CASSCF) with *ab initio* Density Matrix Renormalization Group (DMRG)

To perform the large-scale multireference calculations with CT or other multireference methods, the extensive active-spaced reference wave functions where a large number of active electrons are highly (or fully) correlated within the active orbitals must be found. The CASSCF method provides the most desirable, optimal reference wave functions, in which the static correlations are effectively captured with the relaxed active orbitals that are optimized self-consistently at a high computational cost. We have developed a parallelized CAS optimization method that enables to handle unprecedentedly larger CAS with high-quality basis sets. Figure 3 shows timings for the orbital optimization steps of a single CASSCF iteration for all-trans $C_{12}H_{14}$ chain with a full π active space and cc-pVTZ Gaussian basis sets. The timings were measured on Pentium 4 2.2 GHz PC clusters connected within 100 MB bandwidth network. We have again performed the CASSCF calculation on the $C_{20}H_{22}$ chain with *ab initio* DMRG for an exact diagonalization of CAS(20*e*,20*o*). A single iteration of the extensive CASSCF calculation took just a couple of hours.

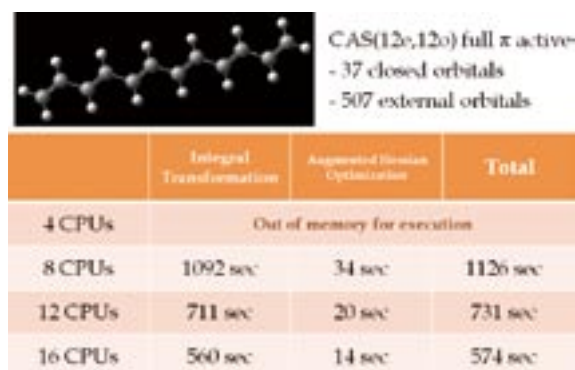


Figure 3. Timings for the parallelized CASSCF method with full π active space CAS(12*e*,12*o*) and cc-pVTZ basis.

References

- 1) T. Yanai and G. K.-L. Chan, *J. Chem. Phys.* **127**, 104107 (2007).

Developing the Statistical Mechanics Theory of Liquids in Chemistry and Biophysics

Department of Theoretical and Computational Molecular Science
Division of Theoretical Molecular Science II



HIRATA, Fumio	Professor
KIM, Bongsoo	Visiting Professor
CHONG, Song-ho	Assistant Professor
YOSHIDA, Norio	Assistant Professor
MARUYAMA, Yutaka	Post-Doctoral Fellow
MIYATA, Tatsuhiko	Post-Doctoral Fellow
IKUTA, Yasuhiro	Post-Doctoral Fellow
ISHIZUKA, Ryosuke	Post-Doctoral Fellow
PHONGPHANPHANEE, Saree	Graduate Student
YAMAZAKI, Yumi	Secretary
KATAYAMA, Naoko	Secretary
NAKAJIMA, Hikari	Secretary
YAMADA, Mariko	Secretary

We have been exploring the chemical and biological processes in solutions, based on the statistical mechanics of liquids, especially, on the integral equation theory of molecular liquids or the “RISM” and “3D-RISM” theories.¹⁻³⁾ Such exploration can be realized by combining the statistical mechanics theories with the other theoretical methods in the molecular science, which describes the different aspects of the physics such as the quantum processes and the liquid dynamics.

Our recent attention is focused on the “molecular recognition” and “fluctuation” of bio-molecules, which are the two key-processes in the living system. For examples, for an enzymatic reaction to take place, substrate molecules should be accommodated by the enzyme. The process is nothing but the molecular recognition which is regulated by the solvation free energy of the enzyme-substrate (ES) complex, and by the structural fluctuation of the protein.

1. Selective Ion-Binding by Protein Probed with the Statistical Mechanical Integral Equation Theory^{4,5)}

Molecular recognition is the most fundamental and important function of biomolecules. It is regarded as a process in which a host molecule makes a complex with a guest molecule through non-covalent chemical bonds including electrostatic, hydrophobic, and other interactions.

One of the most elementary processes of molecular recognition is the selective ion binding by protein. A variety of functions of protein is related to the ion binding: ion channels, ligand binding by a receptor, enzymatic reactions, and so on.

We have presented theoretical results for the ion binding by human lysozyme based on the 3D-RISM theory. The ion distribution around the wild type, Q86D, A92D and Q86D/A92D mutants in the several electrolyte solutions, KCl, NaCl and CaCl₂, has been evaluated. The doubly substituted mutant, Q86D/A92D, has two isomers distinguished with whether it has a Ca²⁺ ion or not: apo, without Ca²⁺; holo, with Ca²⁺. Since the difference between wild type and mutants lies only

in their active site, the discussion are focused on the active site, which consists of amino acid residues from Q83 to A92. The wild type and the Q86D mutant show no cation binding ability in accord with the experimental results. The 3D-RISM theory indicates that the A92D and Q86D/A92D mutants have cation binding ability. Na⁺ and Ca²⁺ ions are bound by the active site of the A92D and Q86D/A92D mutants, though K⁺ ions are not found in the active site. (see Figure 1)

The results are quite encouraging indicating the possibility of predicting protein functions by the theory. For example, it may become possible to find and/or design a protein, which has an ion binding ability. Such studies by means of the 3D-RISM theory are in progress.

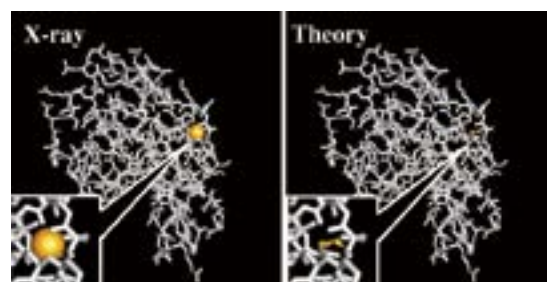


Figure 1. Comparison of Ca²⁺ position in holo-Q86D/A92D mutant between x-ray result and theoretical estimation. Threshold of 3D-DF is 25.0 for Ca²⁺ in the right hand side figure.

2. The Molecular Mechanism of the Pressure Denaturation of Protein Is Clarified by the 3D-RISM Theory⁶⁾

It has been well regarded that protein denatures by applying pressure, but nothing is known to date about the molecular mechanism. The key to solve the question is the “partial molar volume (PMV)” of protein, because the volume should “shrink” in the denatured state of the molecule due to the Le Chatelier law. Therefore, the question “why and how does pressure change the structure of protein” can be rephrased as “why and how is the PMV of the high pressure structure (HPS)

less than that of the low pressure structure (LPS).”

In order to answer the question, we have calculated the PMV of a protein called “ubiquitin,” associated with the transition from the low to high pressure structures, based on the 3D-RISM theory. The theory predicts that the PMV decreases upon the structural transition, which is consistent with the experimental observation. It is found from further analysis that the PMV reduction is ascribed substantially to the penetration of water molecules into a specific part of the protein. Based on the thermodynamic relation, this result implies that the water penetration causes the pressure-induced structural transition.

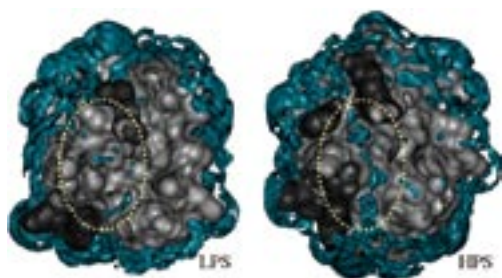


Figure 2. Isosurface representation of the three-dimensional distribution function of water oxygen around low-pressure (3 MPa) and high-pressure (300 MPa) structures (LPS and HPS, respectively) of ubiquitin. The blue surfaces show the area where the distribution function is larger than 2. The penetration of water molecules in the HPS is clearly seen in the area circled by the yellow dots.

3. Combination of Molecular Dynamics Method and 3D-RISM Theory for Conformational Sampling of Large Flexible Molecules in Solution⁷⁾

It has been a common understanding that the solvent plays an essential role in the thermodynamic stability of large molecules in solutions through, for instance, the hydrophobic and Coulomb interactions. In order to incorporate the solvent effects into the molecular simulations, we have developed a combination method of the molecular dynamics (MD) simulation with 3D-RISM theory. Using the proposed method, conformations of large flexible molecules in solution can be sampled along the free energy surface.

The solvent-induced force acting on solute atoms was evaluated as the gradient of the solvation free energy with respect to the solute-atom coordinates, which is obtained from 3D-RISM theory. In order to enhance the speed of computation, we have applied a multiple timestep algorithm based on the RESPA (Reversible System Propagator Algorithm) to the combined MD/3D-RISM method. To illustrate the present MD/3D-RISM simulation, we applied the method to a model of acetylacetone in aqueous solution, as a simple example of flexible solute.

To examine the validity of multiple timesteps, the dependence of energy conservation on timesteps was studied. Figure 3 shows the “time series” of the Hamiltonian H , where Δt_{RISM} denotes the timestep for performing the 3D-RISM calculation. The conformations of solute molecules were renewed with the

timestep of 1 fs. For $\Delta t_{\text{RISM}} = 1$ and 5[fs], H is conserved within a tolerable accuracy. For $\Delta t_{\text{RISM}} = 10$ and 20[fs], however, the values of H deviate from their initial values, with “time” elapsing. The result indicates that we can choose the timestep $\Delta t_{\text{RISM}} = 5$ [fs] without losing numerical accuracy: that is, the calculation of solvent-induced force once in 5 fs is sufficient for an accurate conformational sampling. This choice enhances the speed of computation by 3.4 times compared to a single timestep method, *i.e.* $\Delta t_{\text{RISM}} = 1$ [fs].

Acetylacetone possesses an intramolecular hydrogen bonding capability between the hydroxyl group and the carbonyl oxygen atom, and the molecule is significantly stabilized due to this hydrogen bond, especially in gas phase. The intramolecular hydrogen bond was kept intact during almost entire course of the MD simulation in gas phase, while in the aqueous solutions the bond is disrupted in a significant number of conformations. This result qualitatively agrees with the behavior on a free energy barrier lying upon the process for rotating a torsional degree of freedom of the hydroxyl group, where it is significantly reduced in aqueous solution by a cancellation between the electrostatic interaction and the solvation free energy.

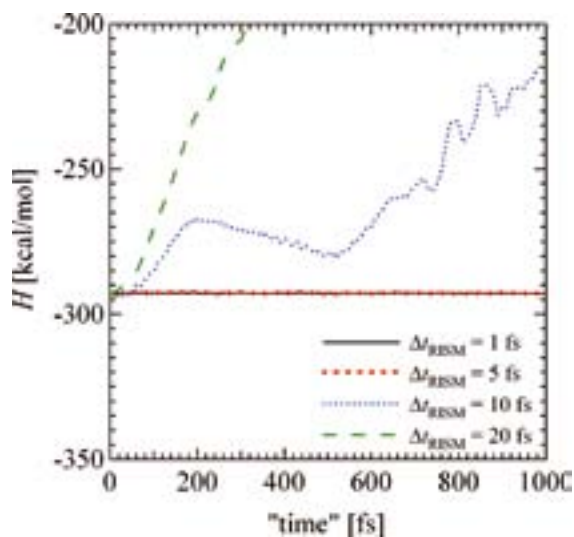


Figure 3. “Time series” of the Hamiltonian H . Δt_{RISM} denotes the timestep for performing the 3D-RISM calculation.

References

- 1) F. Hirata, *Molecular Theory of Solvation*, Kluwer; Dordrecht, Netherlands (2003).
- 2) A. Kovalenko and F. Hirata, *J. Chem. Phys.* **110**, 10095–10112 (1999).
- 3) T. Imai, R. Hiraoka, A. Kovalenko and F. Hirata, *J. Am. Chem. Soc. Communication* **127**, 15334–15335 (2005).
- 4) N. Yoshida, S. Phongphanphane, Y. Maruyama, T. Imai and F. Hirata, *J. Am. Chem. Soc.* **128**, 12042–12043 (2006).
- 5) N. Yoshida, S. Phonphanphane and F. Hirata, *J. Phys. Chem. B* **111**, 4588–4595 (2007).
- 6) T. Imai, S. Ohyama, A. Kovalenko and F. Hirata, *Protein Science* **16**, 1927–1933 (2007).
- 7) T. Miyata and F. Hirata, *J. Comput. Chem.* in press.

Theory of Photoinduced Phase Transitions

Department of Theoretical and Computational Molecular Science
Division of Theoretical Molecular Science II



YONEMITSU, Kenji
YAMASHITA, Yasufumi
MAESHIMA, Nobuya
MIYASHITA, Satoshi
TANAKA, Yasuhiro
KATAYAMA, Naoko

Associate Professor
Assistant Professor
Post-Doctoral Fellow
Post-Doctoral Fellow
Post-Doctoral Fellow
Secretary

Photoirradiation of materials usually creates electrons and holes, which are often accompanied by local structural deformation. With the help of cooperativity, the electronic and/or structural deformation can proliferate to change the physical property such as conductivity, permittivity, and magnetic susceptibility. The resultant nonequilibrium phase may not be reached by changing temperature or pressure because the energy of a photon is much higher than thermal energies. Our theoretical researches are focused on the mechanisms and dynamics of photoinduced phase transitions, how they are controlled, and how the photoinduced electron-lattice states are different from those which are realized in thermal equilibrium.

1. Relaxation Processes in Photoinduced Neutral-Ionic Pseudoferroelectric-Ferroelectric Phase Transitions¹⁾

To find characteristic properties of relaxation processes in the neutral-ionic, pseudoferroelectric-ferroelectric phase transition in the charge-transfer complex, tetrathiafulvalene-*p*-chloranil, we investigate stochastic processes in the classical spin-1 anisotropic Blume-Emery-Griffith model. Spins are assumed to obey the Markov process that is described by the master equation with the Arrhenius-type transfer probability. Time-evolution equations are derived from two standpoints. One is the mean-field approximation and the other is an extension of the Saito-Kubo treatment to the spin-1 and anisotropic case, which improves the mean-field approximation. Solving the equations numerically, we have found highly anisotropic relaxations during the neutral-to-ionic (thus, pseudoferroelectric-to-ferroelectric) transition: The interchain ordering develops much more slowly than the intrachain one. In contrast, the ionic-to-neutral (thus, ferroelectric-to-pseudoferroelectric) phase transition proceeds in a rather isotropic manner. This finding is relevant to the experimentally realized transition induced by intramolecular photoexcitations.

2. Charge-Transfer Excitations in One-Dimensional Dimerized Mott Insulators^{2,3)}

Dynamical properties of photoexcited states are theoretically studied in a one-dimensional Mott insulator dimerized by the spin-Peierls instability. Numerical calculations combined with a perturbative analysis from the decoupled-dimer limit have revealed that the lowest photoexcited state without nearest-neighbor interaction corresponds to an interdimer charge-transfer excitation that belongs to dispersive excitations. This excited state destabilizes the dimerized phase, leading to a photoinduced inverse spin-Peierls transition (Figure 1). We propose a purely electronic origin of midgap states that are observed in a latest photoexcitation experiment of an organic spin-Peierls compound, potassium-tetracyanoquinodimethane (K-TCNQ).

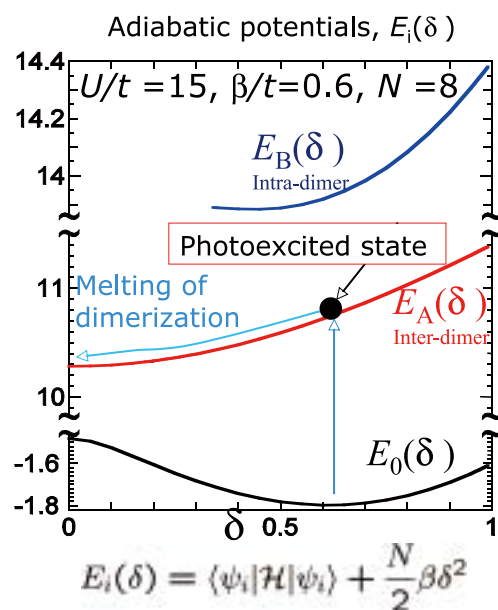


Figure 1. Adiabatic potentials of the ground state, the inter-dimer charge-transfer state, and the intra-dimer charge-transfer state.

The optical properties of one-dimensional dimerized Mott insulators are investigated further by using the one-dimensional dimerized extended Hubbard model, which contains nearest-neighbor interaction. Numerical calculations and a perturbative analysis from the decoupled-dimer limit clarify that there are three relevant classes of charge-transfer (CT) states generated by photoexcitation: interdimer CT unbound states, interdimer CT exciton states, and intradimer CT exciton states (Figure 2). This classification is applied to understanding the optical properties of an organic molecular material, 1,3,5-trithia-2,4,6-triazapentalenyl (TTTA), which is known for its photoinduced transition from the dimerized spin-singlet phase to the regular paramagnetic phase. We conclude that the lowest photoexcited state of TTTA is the interdimer CT exciton state and the second lowest state is the intradimer CT exciton state.

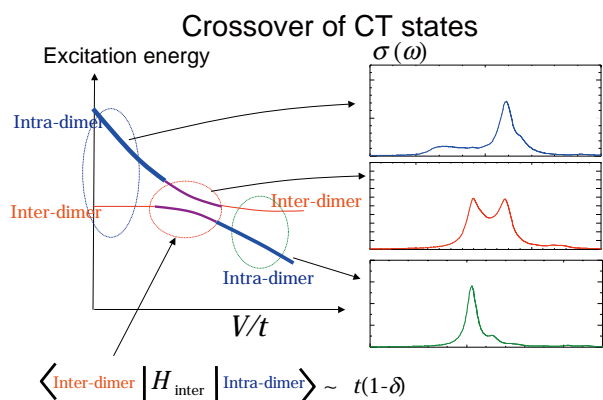


Figure 2. Energy diagram of relevant excited states. The solid (dotted) lines show the exciton (unbound) states, and the width of the lines indicate the strength of the spectral weight.

3. Effects of Electron Correlations and Lattice Distortions on Charge Order in Two-Dimensional Organic Salts^{4,5)}

Charge ordering accompanied by lattice distortion in quasi-two dimensional organic conductors θ -(BEDT-TTF)₂X [BEDT-TTF = bis(ethylenedithio)-tetrathiafulvalene] is studied by using a two-dimensional 3/4-filled extended Hubbard model with Peierls-type electron-lattice couplings first within the Hartree-Fock approximation. It is found that the horizontal-stripe charge-ordered state, which is experimentally observed in θ -(BEDT-TTF)₂RbZn(SCN)₄, is stabilized by the self-consistently determined lattice distortion. Furthermore, in the presence of the anisotropy in nearest-neighbor Coulomb interactions, the horizontal charge order becomes more stable than any other charge patterns such as diagonal, vertical, and three-fold-type states. At finite temperatures, we compare the free energies of various charge-ordered states and find a first-order transition from a metallic state with three-fold charge order to the insulating state with the horizontal charge order. The role of lattice degrees of freedom in the realization of the

horizontal charge order and the relevance to experiments on θ -(BEDT-TTF)₂X are clarified.

These combined effects of electron correlations and lattice distortions on the charge ordering in θ -(BEDT-TTF)₂RbZn(SCN)₄ are further investigated by means of the exact-diagonalization method. The findings are explained by the third-order perturbation theory from the strong-coupling limit. Electron-phonon interactions are found to be crucial to stabilize the horizontal-stripe charge order and to realize the low-symmetry crystal structure at low temperatures. Especially, modulations of transfer integrals not only by *c*- and *a*-axis molecular translations but also by molecular rotations are demonstrated to be important (Figure 3).

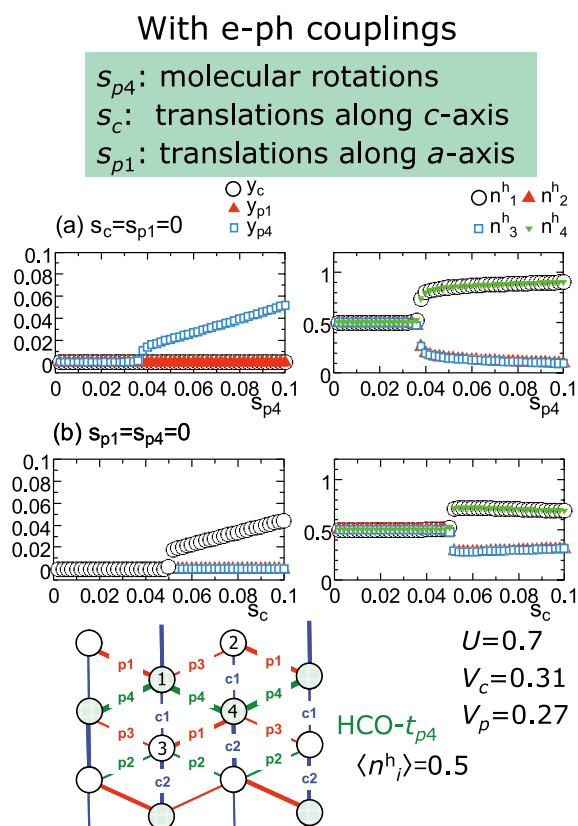


Figure 3. Electron-phonon coupling strength dependence of modulations of transfer integrals (left) and hole densities (right).

References

- 1) H. Inoue and K. Yonemitsu, *Phys. Rev. B* **75**, 235125 (13 pages) (2007).
- 2) N. Maeshima and K. Yonemitsu, *Phys. Rev. B* **74**, 155105 (11 pages) (2006).
- 3) N. Maeshima and K. Yonemitsu, *J. Phys. Soc. Jpn.* **76**, 074713 (5 pages) (2007).
- 4) Y. Tanaka and K. Yonemitsu, *J. Phys. Soc. Jpn.* **76**, 053708 (5 pages) (2007).
- 5) S. Miyashita and K. Yonemitsu, *Phys. Rev. B* **75**, 245112 (6 pages) (2007).

Molecular Dynamics Study of Classical Complex Systems and Quantum Systems in Condensed Phase

Department of Theoretical and Computational Molecular Science
Division of Computational Molecular Science



OKAZAKI, Susumu	Professor
MIURA, Shinichi	Assistant Professor*
YOSHII, Noriyuki	Assistant Professor†
YAMADA, Atsushi	Assistant Professor
MIKAMI, Taiji	Post-Doctoral Fellow
ANDOH, Yoshimichi	Post-Doctoral Fellow
KAJIMOTO, Shinji	Post-Doctoral Fellow‡
FUJIMOTO, Kazushi	Graduate Student

1. Free Energy of Water Permeation into Hydrophobic Core of Sodium Dodecyl Sulfate Micelle by Molecular Dynamics Calculation¹⁾

In our previous analysis of the structural stability of sodium dodecyl sulfate (SDS) micelle based on molecular dynamics calculation, vacancies were found in the center of the micelles (*Chem. Phys. Lett.* **425**, 58 (2006)). It is very interesting to clarify whether a water molecule is expected in the vacancy in thermodynamic equilibrium at room temperature. In order to investigate the stability of water in the core of micelle, free energy of transfer of water from bulk to the core has been calculated for the SDS micelle in water for two micelle sizes, $N = 61$ and 121 , at temperature $T = 300$ K and pressure $P = 1$ atm. The calculated free energy of transfer, $\Delta G_{c \leftarrow b}$, from the bulk to the core is about 28 ± 4 and 26 ± 4 kJ/mol for the micelle of size $N = 61$ and 121 , respectively, where the corresponding Boltzmann factor, $\exp(-\Delta G_{c \leftarrow b}/kT)$, is in the order of one over several ten thousand. Thus, water molecule hardly permeates into the core of the micelle.

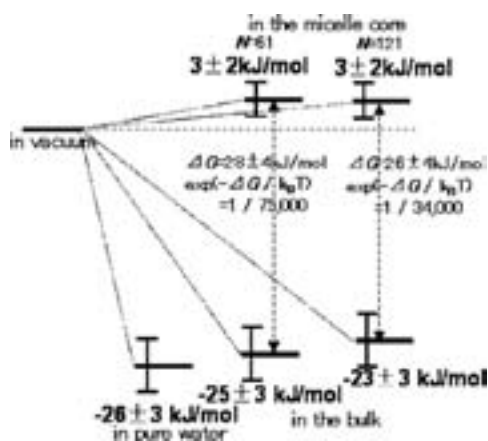


Figure 1. The calculated free energy of transfer of water molecule from vacuum to the core and to the bulk water for the micelle of the size $N = 61$ and 121 . The hydration free energy of water in pure water itself is also presented.

2. A Molecular Analysis of the Vibrational Energy Relaxation Mechanism of the CN^- Ion in Water Based upon Path Integral Influence Functional Theory Combined with a Dipole Expansion of the Solute–Solvent Interaction²⁾

The molecular mechanism of vibrational energy relaxation of the CN^- ion in water has been investigated using path integral influence functional theory combined with a dipole expansion of the solute–solvent interaction. First, in order to find out which solvent water molecules contribute most to the absorption of the solute excess vibrational energy, the normal modes of the solution, adopted for the harmonic oscillators

bath approximation in the influence functional theory, have been back-transferred to the molecular coordinates and a contribution to the relaxation has been assigned to each water molecule according to the transformation matrix. Then, the coupling intensity $C^{(i)2}$ between solute and solvent molecules playing a major role in the relaxation, has been analyzed by dipole expansion of the solute–solvent interaction, where bending, rotational and translational degrees of freedom were all represented by the standard variables μ_1 , μ_2 , R , θ_1 , θ_2 , and ϕ for the dipole expansion. From these analyses, it is clarified that (1) the contribution of the solvent water to the relaxation decreases rapidly in proportion to $1/R^6$, such that only water molecules in the first hydration shell take part in the relaxation, (2) water molecules located in the direction of C–N bond contribute much to the relaxation, and (3) the excess energy is transferred to the bending of the relevant water molecule and its rotational libration represented by the variable θ_2 .

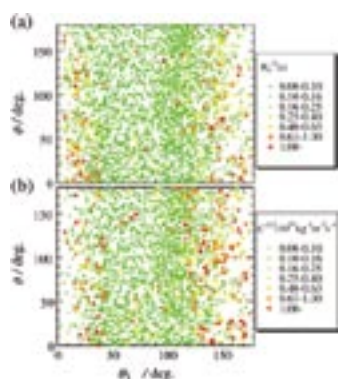


Figure 2. Actual (a) molecular relaxation $R^{(i)}$ and (b) molecular coupling intensity $C^{(i)2}$ for the water molecules in the first hydration shell.

3-1. Rotational Fluctuation of Molecules in Quantum Clusters. I. Path Integral Hybrid Monte Carlo Algorithm³⁾

We present a path integral hybrid Monte Carlo (PIHMC) method for rotating molecules in quantum fluids. This is an extension of our PIHMC for correlated Bose fluids [S. Miura and J. Tanaka, *J. Chem. Phys.* **120**, 2160 (2004)] to handle the molecular rotation quantum mechanically. A novel technique referred to be an effective potential of quantum rotation is introduced to incorporate the rotational degree of freedom in the path integral molecular dynamics or hybrid Monte Carlo algorithm. For a permutation move to satisfy Bose statistics, we devise a multilevel Metropolis method combined with a configurational-bias technique for efficiently sampling the permutation and the associated atomic coordinates. Then, we have applied the PIHMC to a helium-4 cluster doped with a carbonyl sulfide molecule. The effects of the quantum rotation on the salvation structure and energetics were examined. Translational and rotational fluctuations of the dopant in the superfluid cluster were also analyzed.

3-2. Rotational Fluctuation of Molecules in Quantum Clusters. II. Molecular Rotation and Superfluidity in OCS-Doped Helium-4 Clusters⁴⁾

Helium-4 clusters are studied as a function of cluster size N in a small-to-large size regime ($2 \leq N \leq 64$). The molecular rotation of the dopant shows nonmonotonic size dependence in the range of $10 \leq N \leq 20$, reflecting the density distribution of

the helium atoms around the molecule. The size dependence on the rotational constant shows a plateau for $N \geq 20$, which is larger than the experimental nanodroplet value. Superfluid response of the doped cluster is found to show remarkable anisotropy especially for $N \leq 20$. The superfluid fraction regarding the axis perpendicular to the molecular axis shows a steep increase at $N = 10$, giving the significant enhancement of the rotational fluctuation of the molecule. On the other hand, the superfluid fraction regarding the axis parallel to the molecular axis reaches 0.9 at $N = 5$, arising from the bosonic exchange cycles of the helium atoms around the molecular axis. The anisotropy in the superfluid response is found to be the direct consequence of the configurations of the bosonic exchange cycles.

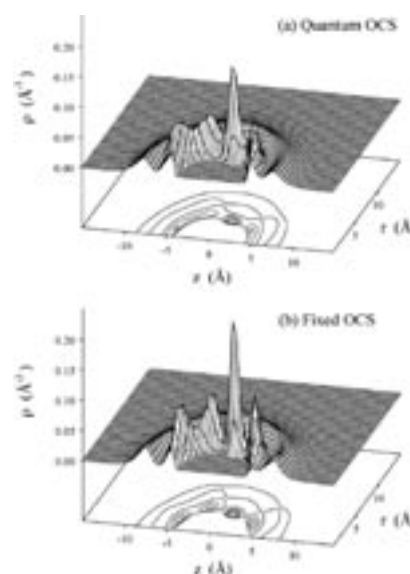


Figure 3. The total helium density distribution around the OCS molecule $\rho(z,r)$ in the $\text{OCS}({}^4\text{He})_{64}$ cluster [top: $\rho(z,r)$ for the quantum OCS case; bottom: $\rho(z,r)$ for the fixed OCS case]. z is the molecular axis and r the radial distance from the z axis. The OCS center of mass is located at the origin and the molecule is oriented as O–C–S from $+z$ to $-z$. All distances are in units of angstrom.

References

- 1) N. Yoshii and S. Okazaki, *J. Chem. Phys.* **126**, 096101(3 pages) (2007).
- 2) Y. Okamoto, T. Mikami, N. Yoshii and S. Okazaki, *J. Mol. Liq.* **134**, 34–39 (2007).
- 3) S. Miura, *J. Chem. Phys.* **126**, 114308 (10 pages) (2007).
- 4) S. Miura, *J. Chem. Phys.* **126**, 114309 (7 pages) (2007).

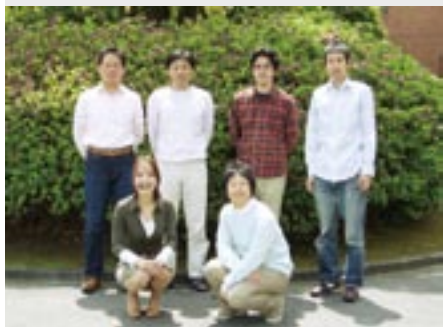
* Present Address; Kanazawa University, Kanazawa 920-1192

† Present Address; Himeji Dokkyo University, Himeji 670-8524

‡ Present Address; Tohoku University, Sendai 980-8577

Theoretical Studies on Condensed Phase Dynamics

Department of Theoretical and Computational Molecular Science
Division of Computational Molecular Science



SAITO, Shinji	Professor
KIM, Kang	Assistant Professor
KOBAYASHI, Chigusa	Post-Doctoral Fellow
YAGASAKI, Takuma	Post-Doctoral Fellow
ONO, Junichi	Graduate Student*
UENO, Harumi	Secretary

Liquids and biological systems show complicated dynamics because of their structural flexibility and dynamical hierarchy. Understanding these complicated dynamics is indispensable to elucidate the chemical reactions in solutions and the functions of proteins. We have been investigating liquid dynamics and chemical reactions in biological systems using molecular dynamics and electronic structure calculations. In addition, we have been analyzing complicated dynamics in terms of multi-dimensional spectroscopy.

1. Glass Transition in Porous Media: Test of Mode-Coupling Theory via Molecular Dynamics Simulation

When a liquid is supercooled below its freezing temperature, it becomes a metastable supercooled state. When the temperature is lowered further and crystallization could be avoided, the supercooled liquid undergoes the glass transition. In the glass transition region a drastic slowing-down occurs in dynamical properties, *e.g.* structural relaxation time, diffusion constant, and viscosity, whereas the static structure is almost the same as that of normal liquids.

The dynamics of glass forming liquids under confinement has attracted attention for its unusual thermodynamic properties; the glass transition temperature in a spatially confined system, *i.e.* a thin film or a porous media, is different from that in the bulk. A theoretical study for glass forming liquids confined in disordered immobile particles has been recently reported. In the study, the liquid-glass transition points for various densities of fluid and immobile particles were determined by using the mode-coupling theory (MCT).

We carried out molecular dynamics simulations of soft-sphere supercooled liquids in order to examine the above theoretical predictions, because the MCT is considered to be violated in the limit of low density for fluid particles. We confirmed that the structural relaxation becomes slow with the

increase in immobile particles. It is also found that the relaxation profile of the intermediate scattering function changes from the type B to the type A with the decrease in the density of fluid particles. In the type B, dynamics for high density of fluid particles, the well-known two-step relaxation is found and gradually stretched with increasing density of immobile particles. On the other hand, in the type A, dynamics for low density of fluid particles, the dynamics is significantly different from that of the type B, where the single-step relaxation decay with the long time tail has been observed. This long time tail is thought to be due to the diffusion localization, *i.e.* the fluid particles are trapped by the immobile obstacle particles for a long time. Moreover, we revealed that the system shows a reentry in the limit of low density for fluid particles at a certain high density for immobile particles as the prediction of the theoretical study. In the reentrant phenomenon, some delocalization is expected to occur due to fluid-fluid collisions. We are now examining this scenario and investigating the physical mechanism of the reentrant phenomenon using simulations.

2. Conformational Changes Associated with GTP Hydrolysis in Ras

Ras superfamily is a well-known signal transduction protein. Ras is activated by binding of GTP and binds to some effectors for regulation of cell proliferation, whereas it is inactivated by the hydrolysis of Ras-bound GTP. The hydrolysis rate is accelerated by five orders of magnitude by binding of GTPase-activating protein, GAP. Therefore, it is essential to investigate the binding effect of GAP on Ras for understanding the reaction.

We analyze the hydrolysis by dividing into the following four states; (i) active (reactant), (ii) GAP-bound, (iii) intermediate of hydrolysis, and (iv) inactive (product) states. We performed molecular dynamics (MD) calculation for the four states and analyzed the conformational changes and fluctuation.

tuations of Ras and GAP in these states. We also carried out QM/MM calculation to examine the details of structures.

In the step from the active to GAP-bound state, salt bridges between acidic residues in Ras and basic residues in GAP are formed. These bonds between Ras and GAP change the HB network structure around the active site and the structures in the switches I and II. In addition, the exchange of a water molecule near GTP is significantly suppressed by the binding of GAP to RAS. The present result implies that the bound water molecule near GTP makes the hydrolysis reaction facile.

GTP is converted to GDP and Pi by the hydrolysis. With MD and QM/MM methods we successfully constructed a stable intermediate state which was found in a recent experimental study. We found that the HB network structure around the active site and the conformation between Ras and GAP in the intermediate state are almost the same as those in the GAP-bound state. We clarified that the invasion of water required for the release of Pi and GAP does not take place in this state. We are also investigating how Pi and GAP are released from Ras in the last step.

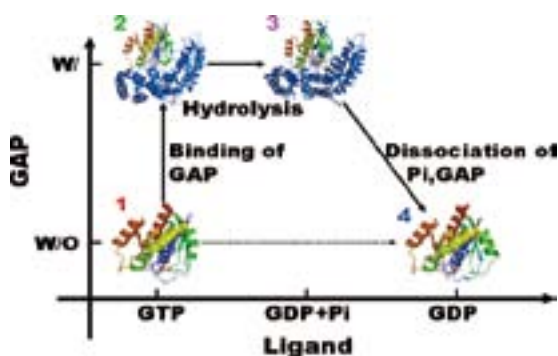


Figure 1. Conformational changes associated with GTP hydrolysis in Ras.

3. Two-Dimensional Infrared Spectroscopy of Intermolecular Modes in Liquid Water

Liquid water is an interesting system with a number of anomalous thermodynamic and dynamic properties. Its complicated dynamics has been analyzed with various kinds of spectroscopies. Great progresses have been achieved in developing multi-dimensional spectroscopies since late 90 s.

We have been investigating intermolecular water dynamics using two-dimensional (2D) infrared (IR) spectroscopy which is a powerful technique to provide detailed information on dynamics. In the 2D IR spectroscopy, the system interacts with electric fields at $t = 0$, t_1 , and $t_1 + T$, and the signal is detected at $t = t_1 + T + t_3$ and thus the response function is expressed in terms of a three-time correlation function. The so-called hybrid method in which equilibrium and non-equilibrium molecular

dynamics simulations are combined is employed in the calculation of 2D IR spectroscopy.

The peak width along the diagonal line in the 2D IR spectroscopy provides a measure of inhomogeneous broadening. The present result shows that the libration motion of water has inhomogeneous contribution. In addition, the present analysis shows that the initial inhomogeneity rapidly decays with ~ 100 fs, by analyzing the waiting time, T , dependence of the diagonal line shape. The loss of initial inhomogeneity slows down about three times, when the intermolecular translation motion which couples with the libration motion is removed. Consequently, we revealed the significant effect of the translation motion on the fast loss of initial inhomogeneity of the libration motion in liquid water.

We can obtain useful information about relaxation dynamics by analyzing off-diagonal peaks of the 2D IR spectroscopy. We found a strong off-diagonal peak located at $(\omega_1, \omega_3) = (\sim 700 \text{ cm}^{-1}, \sim 150 \text{ cm}^{-1})$. The cross peak arises from the coupling between the libration motion during t_1 and the intermolecular translation motion during t_3 . The intensity of the peak decreases for $T < 40$ fs and then it increases for $T > 40$ fs. The increase in the signal intensity can be attributed to the relaxation from the libration motion to intermolecular translation motion during t_2 . The present result shows that the time constant of the relaxation is about 150 fs.

Feynman diagrams for the 2D IR spectroscopy are usually classified into three kinds of Liouville pathways, S_I , S_{II} , and S_{III} : S_I represents rephasing pathways, on the other hand, S_{II} and S_{III} represent non-rephasing ones. We found that the third-order 2D IR response function of water contains several Feynman diagrams which cannot be classified into the above three pathways. The new pathways, S_{IV} , are related to the second overtone of the libration motion due to a three-quantum transition. The existence of the three-quantum transition shows the anharmonic dynamics in the libration motion. It is conceivable that S_{IV} can be observed by the intermolecular 2D IR experiment of water with two colors.

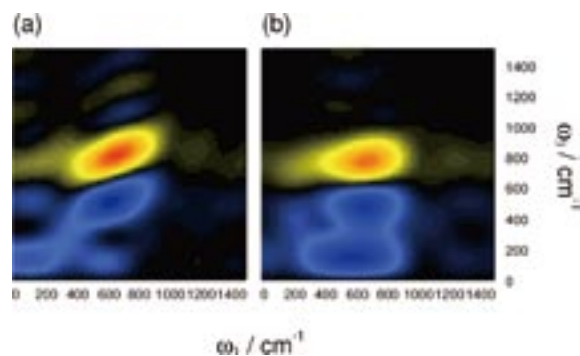
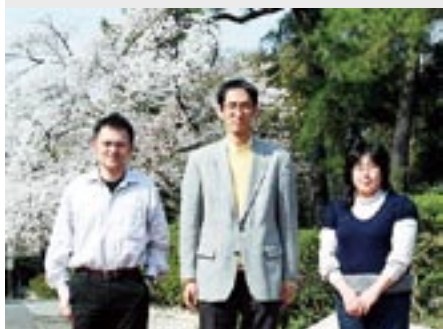


Figure 2. 2D IR spectra of water at (a) $T = 20$ and (b) 200 fs, respectively.

* carrying out graduate research on Cooperative Education Program of IMS with Kyoto University

Theory and Computation of Liquids and Liquid Interfaces

Department of Theoretical and Computational Molecular Science
Division of Computational Molecular Science



MORITA, Akihiro
ISHIDA, Tateki
SOKOLOV, Vladimir V.
ISHIYAMA, Tatsuya
KAWAGUTI, Ritsuko

Professor
Assistant Professor
IMS Fellow*
Post-Doctoral Fellow*
Secretary

The following projects 1–4 focus on the development of theory and computational analysis methods for interfacial sum frequency generation spectroscopy and its application to aqueous interfaces. The visible-infrared sum frequency generation spectroscopy is a powerful method to obtain interface-specific vibrational spectra. While this experimental technique is now widely used as an interface probe in a molecular level, reliable interpretation of the observed spectra is often lacking which significantly hinders the progress of this surface characterization method. We have proposed theoretical methods to compute the sum frequency spectra on the basis of *ab initio* molecular modeling and molecular dynamics simulation. These projects elucidated the sum frequency spectra of liquid interfaces, including aqueous salt and acid solutions, with the molecular modeling we have developed.

Projects 5 and 6 are mainly conducted by Dr. Ishida and his collaborators. Project 5 deals with the properties of room temperature ionic liquids in collaboration with Dr. Shiota at Chiba University. Project 6 is performed in collaboration with Dr. Yoshida and Prof. Hirata in the IMS about theoretical investigation of solvent effect on electron transfer reaction system.

1. Flexible and Polarizable Molecular Modeling for Describing Interfacial Properties of Gas-Liquid Aqueous Salt Solutions¹⁾

Gas-liquid interfacial structures of NaCl and NaI aqueous solutions are investigated via molecular dynamics simulations using a flexible and polarizable water model we have developed. The new five-site model of water aims at suitably describing interfacial properties, including vibrational sum frequency spectroscopy where both flexibility and polarization are crucial. The performance of the water model is system-

atically examined and demonstrated by a number of properties of bulk and interface, including density, vaporization energy, dipole moment, diffusion coefficient, radial distribution function, infrared and Raman spectra of the O–H stretching region, surface potential, and surface excess of ions. The orientational structure of surface water is investigated in detail in connection with the issue of surface solvation of anions. These investigations will be utilized to analyze the sum frequency generation spectra in relation to the orientational structure at the molecular level.

2. Computation of Sum Frequency Generation Spectra of Aqueous Salt Solution Interfaces²⁾

The vibrational sum frequency generation (SFG) spectra of gas-liquid interfaces of NaCl and NaI aqueous solutions are computed and analyzed by molecular dynamics (MD) simulations using a flexible and polarizable molecular model. The MD calculations have reproduced the experimental features of SFG spectra, including observed perturbation on the NaI spectra in contrast to little perturbation on NaCl. Analysis of the nonlinear susceptibility revealed that the intermolecular correlation has a significant contribution to the vibrationally resonant amplitude, which largely distorts the generally accepted relationship between the SFG intensity and orientation of individual molecules. In NaI solutions, modest enhancement of ssp intensity in the 3400 cm^{-1} region is thereby elucidated by this mechanism. Regarding the sps spectra, three spectral components are assigned and elucidated. Calculated remarkable enhancement in the $3400\text{--}3800\text{ cm}^{-1}$ region for NaI solutions is found to be sensitive to the electric double layer structure. It is also revealed that the sps intensity is augmented by the intermolecular water-water correlation effect.

3. Molecular Dynamics Analysis of Sum Frequency Generation Spectra of Aqueous Acid Solution Interfaces³⁾

Molecular dynamics simulation for gas/liquid interfaces of aqueous hydrochloric (HCl) and hydroiodic (HI) acid solutions is performed to calculate and analyze their sum frequency generation (SFG) spectra. The present MD simulation supports strong preference of hydronium ions at the topmost surface layer and a consequent formation of ionic double layers by the hydronium and halide ions near the interface. Accordingly, the orientational order of surface water in the double layers is reversed in the acid solutions from that in the salt (NaCl or NaI). The calculated SFG spectra of O–H stretching region well reproduce the experimental spectra of ssp and sps polarizations. In the ssp spectra, the strong enhancement in the hydrogen bonding region for the acid solutions is elucidated by two mechanisms, ordered orientation of water in the double layer and symmetric OH stretching of the surface hydronium ions. In the sps spectra, reversed orientation of surface water is evidenced in the spectral lineshapes, which are quite different from those of the salt solutions.

4. Modeling of C–H Vibrations for Alkyl Chain Molecules and Related Interfaces

The present work aims at applying our computational methods to the interfaces including alkyl chains. Alkyl chains have ubiquitous importance in organic films and polymer interfaces, and their C–H stretching vibration has been extensively studied by SFG and IR spectra. Their spectral structure in C–H stretching vibration is often complicated by those of CH₃ and CH₂ moieties and Fermi resonance with the CH bending overtone. As the first step to deal with such systems, we construct an appropriate model of methanol for describing interfacial vibrational spectra.

The present model of methanol is flexible and polarizable, and all the ingredient parameters are determined by density functional calculations. The present intramolecular force field appropriately includes the contribution of the Fermi resonance. For modeling of electrostatic interaction and polarization, we used the Charge Response Kernel (CRK) method. The present model takes account of geometry dependence of the partial charges and CRK, so that it is able to describe the dipole moment vector and polarizability tensor accurately as a function of molecular vibrational configuration. This molecular model of methanol will be extended to other molecules with alkyl chains for use of MD simulation.

5. Theoretical Investigation of Characteristics of Components of Room Temperature Ionic Liquids and Its Effect on Interplay between Cation and Anion Units

Room temperature ionic liquids (RTILs) show a wide variety of interesting physical and chemical properties, different from so-called molten salts. It is considered that many of them can be attributed to the character of both cation and anion which consist of RTILs. From these viewpoints, we can expect that the size of cation and anion, their geometric shapes, remarkable characteristics of elements in the cation and anion and so on, determine and explain some of essential properties and inside details. In particular, we focus on the characteristics of elements in the anion component in ionic liquids, 1-Butyl-3-Methylimidazolium cation (BMIM) with X⁻: PF₆⁻, AsF₆⁻ and SbF₆⁻. We compared important physical properties among them, referring to experimental data by molecular dynamics simulation procedures.

6. Theoretical Study of Temperature and Solvent Dependence of the Free Energy Surface of the Intramolecular Electron Transfer based on the RISM-SCF Theory; Application to 1,3-Dinitrobenzene Radical Anion in Acetonitrile and Methanol⁴⁾

The free energy surfaces along the intramolecular electron transfer reaction of 1,3-dinitrobenzene radical anion in acetonitrile and methanol are investigated with the reference interaction site model self-consistent field theory. Although acetonitrile and methanol have similar values of the dielectric constant, the free energy profiles are quite different. The electronic coupling strength exhibits an intriguing behavior in the temperature dependence: it increases with increasing temperature in acetonitrile, while that in methanol exhibits the opposite trend.

References

- 1) T. Ishiyama and A. Morita, *J. Phys. Chem. C* **111**, 721–737 (2007).
- 2) T. Ishiyama and A. Morita, *J. Phys. Chem. C* **111**, 738–748 (2007).
- 3) T. Ishiyama and A. Morita, *J. Phys. Chem. A* **111**, 9277–9285 (2007).
- 4) N. Yoshida, T. Ishida and F. Hirata, submitted to *J. Phys. Chem. B* (2007).

* Present Address; Department of Chemistry, Graduate School of Science, Tohoku University, Aoba-ku, Sendai 980-8578

Visiting Professors



Visiting Professor

ASAI, Yoshihiro (from *National Institute of Advanced Industrial Science and Technology*)

Theory of Electron Transport through Single Molecular Bridge Junctions

Theories of transport properties through single molecular bridges and atomic wires between the two electrodes have been investigated.¹⁻³⁾ Special attentions will be paid on heat dissipations accompanying the electron transport. Both fundamental theories and their implementations in terms of first principle electronic structure methods⁴⁾ have been studied, as well as their applications to real non-equilibrium open systems.

Both the physical reality and the chemical reality have been taken into account in the calculations.

References

- 1) Y. Asai and H. Fukuyama, *Phys. Rev. B* **72**, 085431 (2005).
- 2) Y. Asai, *Phys. Rev. Lett.* **93**, 246102 (2004); **94**, 099901(E) (2005).
- 3) Y. Asai and T. Shimazaki, "Vibronic Mechanism for Charge Transport and Migration Through DNA and Single Molecules" in *Charge Migration in DNA, Perspectives from Physics, Chemistry and Biology*, T. Chakraborty Ed., Springer-Verlag; Heidelberg (2007).
- 4) T. Shimazaki and Y. Asai, unpublished.



Visiting Associate Professor

AKIYAMA, Ryo (from *Kyushu University*)

Interaction between Like-Charged Colloidal Particles Immersed in Electrolyte Solution

Study of mesoscopic structure constructed by colloidal particles is important to discuss stability of cytoplasm, formation of rennet gel, and so on. The effective interaction between colloidal particles is necessary to calculate those systems using simulation method, because the molecular simulation with explicit solvent molecule and colloidal particle model is very hard. On the other hand, Kinoshita *et al.* are suggesting the importance of translational motion of solvent molecules to discuss the interaction. Then, we pay attention to the solvent granularity in this study.

We calculate the interaction between like-charged colloidal particles immersed in electrolyte solution using the OZ-HNC theory. Solvent molecules are modeled as neutral hard spheres, and ions and colloidal particles are modeled as charged hard spheres. The Coulomb potentials for ion-ion, ion-colloidal particle, and colloidal particle-colloidal particle pairs are divided by the dielectric constant of water. The van der Waals attraction between the colloidal particles, which is an essential constituent of the DLVO theory, is omitted in our model. Nevertheless, attractive regions appear in the interaction, when the electrolyte concentration is sufficiently high. Then the colloidal particles can adhere each other and can form aggregations or gels in spite of like-charged particles. In our model, the attraction arises from the granularity of solvent molecules. (R. Akiyama, N. Fujino, K. Kaneda, and M. Kinoshita, *Cond. Matt. Phys.* accepted.) We start in to study of Brownian dynamics simulation with the effective interaction and some related chemical reactions.



Visiting Associate Professor

HAYASHI, Michitoshi (from *National Taiwan University*)

Development of a Molecular Theory for Time-Resolved Sum-Frequency Generation and Its Applications to Vibrational Dynamics of Water

We developed a molecular theory for time-resolved sum-frequency generation (SFG). The molecular model for vibrational dynamics of water is constructed using the coupled-oscillator model in the adiabatic approximation. This model allows us to calculate vibrational energy transfer rate constants with two different ways; one is with the dipole-dipole interaction scheme and another is the anharmonicity scheme. An application of this theory is also provided for estimation of the time constants of the intermolecular vibrational energy transfer between water molecules using density functional theory method. This approach can provide a clue of a molecular mechanism as to how vibrational dynamics of water at the surface takes place.



RESEARCH ACTIVITIES

Photo-Molecular Science

Molecules respond to photon irradiation in a variety of ways, including photo-induced transitions and photochemical reactions. We have employed various light sources and experimental schemes to elucidate molecular structures and properties, and to control chemical reactions and molecular functions. We have also developed novel and advanced light sources for molecular science. Two of research facilities, the Laser Research Center for Molecular Science and the UVSOR Facility, conduct collaborative researches having intimate contacts with the Department of Photo-Molecular Science.

The main topics pursued in the Department include: Development of novel laser spectroscopic methods to reveal fundamental properties of molecules, development of high-resolution optical microscopic methods and application to nanomaterials, coherent control of molecules with ultrafast techniques, spectroscopy of inner-shell excited molecules and fundamental vacuum-UV photochemistry, investigation of the functionality of solid-state materials, developments of novel laser and synchrotron-orbit radiation sources, and so on.

Development of Advanced Near-Field Spectroscopy and Application to Nanometric Systems

Department of Photo-Molecular Science
Division of Photo-Molecular Science I



OKAMOTO, Hiromi	Professor
IMURA, Kohei	Assistant Professor
NARUSHIMA, Tetsuya	Assistant Professor
HORIMOTO, Noriko	IMS Fellow*
JIANG, Yuqiang	Post-Doctoral Fellow
WU, Huijun	Graduate Student
NOMURA, Emiko	Secretary

There is much demand for the study of local optical properties of molecular assemblies and materials, to understand mesoscopic phenomena and/or to construct optoelectronic devices in the nanometric scale. Scanning near-field optical microscopy (SNOM), which enables spatial resolution beyond the diffraction limit of light, has been remarkably progressed in technology in the past decade. Combination of this advanced optical technology with various nonlinear and ultrafast laser spectroscopic methods may offer a direct probe of molecular dynamical processes in mesoscopic materials systems. It may provide essential and basic knowledge for analyzing origins of characteristic features and functionalities of the mesoscopic systems. We have constructed apparatuses for near-field dynamic spectroscopy with the femtosecond time resolution and the nanometer spatial resolution. They are capable of measuring conventional near-field transmission, emission, and Raman-scattering, and unique near-field two-photon induced emission and ultrafast transient transmission as well. Based on these methods, we are observing the characteristic spatio-temporal behavior of various metal nanoparticles systems and molecular assemblies, for the purpose of understanding nano-optical characteristics, spatial coherence of excitations, dynamics, *etc.* We also investigate the basic characteristics of near-field microscopic measurements.

1. Near-Field Imaging of Locally Enhanced Optical Fields in Metal Nanoparticle Assemblies

It is of fundamental importance to reveal spatial distribution of localized optical field in metal nanostructures. In aggregated noble metal nanoparticles, for example, strong electric field is expected in the interstitial gaps between the nanoparticles, according to the electromagnetic theory. Such a localized strong optical field in the nanoparticle assembly is called as 'hot spot' and is considered as the major origin of the

huge Raman enhancement in single-molecule level surface-enhanced Raman scattering. However, since the conventional optical microscopy is unable to resolve nanometric structures, there has been no information on the detailed structure of hot spots given by spectroscopic measurements.

In this study, we applied the near-field two-photon induced emission measurement to obtain spatial distribution of the optical fields in the vicinity of metal nanoparticle assemblies. As a result, we succeeded in clear visualization of localized intense optical fields in the assemblies of gold nanoparticles.¹⁾ Figure 1 shows typical topographic and near-field two-photon

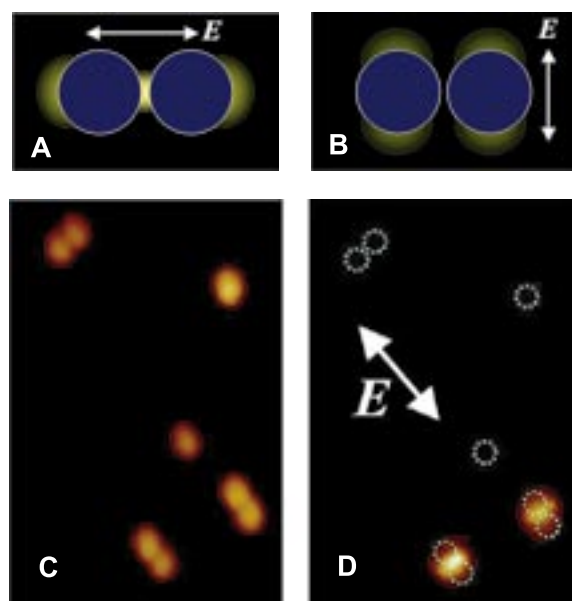


Figure 1. (A,B) Schematic view (theoretical prediction) of optical field strength in the vicinity of dimeric assemblies of metal nanoparticles. The field strength is shown by the brightness. (C) Observed topography and (D) near-field two-photon excitation images of gold nanoparticle (diameter 100 nm) assemblies. The dotted circles indicate positions of the nanoparticles, deduced from the topography.

excitation probability images for dimeric gold nanospheres (diameter 100 nm). The two-photon image shows that the optical fields are confined at interstitial sites in the aggregates, when the incident polarization is parallel to the interparticle axes. This result agrees well with the theoretical expectations. We also performed near-field Raman imaging experiments and found that the Raman excitation is also strongly enhanced at the interstitial gaps.¹⁾ The result gives a clear experimental proof to the hot-spot mechanism of surface-enhanced Raman scattering. In a similar way, we are examining fluorescence enhancements in the neighbor of gold nanoparticles of various shapes and their aggregates.

The methodology of visualizing the local optical field can be extensively applied to design metal nanostructures for the purpose of obtaining unique optical characteristics and/or optical fields strongly interacting with the nearby molecules. Studies in this line are under way.

2. Visualization of Plasmon Wavefunctions Induced in Various Metal Nanoparticles

We have reported that wavefunctions of localized plasmon resonances of metal nanoparticles can be visualized by using near-field transmission or two-photon excitation measurements.²⁾ The plasmons we visualized for chemically synthesized nanoparticles include the longitudinal modes in gold and silver nanorods and in-plane modes in gold triangular nanoplates. Figure 2 shows typical examples of near-field transmission images for longitudinal plasmon modes on a nanorod (the images correspond to the square moduli of the wavefunctions). We have reported that the images show excellent agreement with calculated images of local density of electromagnetic states which correspond to the square modulus of the resonant plasmon wavefunction.

We are extending the study to nanoparticles of other shapes and/or sizes, as well as the metal nanostructures manufactured by the electron-beam lithography technique, as a collaboration with the researchers outside of IMS. We have already obtained preliminary results for some metal nanostructures and have found peculiar plasmon waves in some cases. Such a study is also essential to design nanostructures of unique characteristics.

3. Ultrafast Transient Images of Gold Nanoparticles

We previously investigated ultrafast near-field transient transmission (space and time resolutions were *ca.* 50 nm and

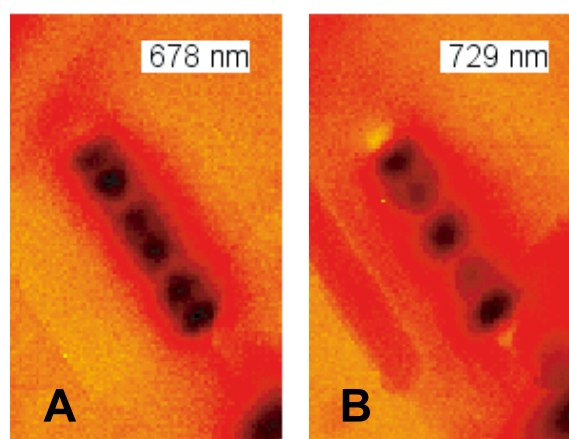


Figure 2. Near-field transmission images of a gold nanorod (diameter 20 nm, length 510 nm), observed at 678 nm (A) and 729 nm (B).

100 fs) of single gold nanorods to reveal dynamic behavior of the material.³⁾ We used a near-infrared pulse to excite longitudinal plasmon resonance of the rod and detect transient transmission change after that. The transient image of a nanorod at *ca.* 1 ps shows characteristic features: the sign of the transient transmission change (induced or bleached) depends on the position, and the transient image contrast is sometimes reversed depending on the size of the rod.

To understand the observed features, we simulated position-dependent transient transmission change based on electromagnetic density of states calculation. We have found that feature is qualitatively reproduced if we assume that the photoexcitation induces a homogeneous electronic temperature rise in the nanorod.

4. Near-Field Imaging of Organic Molecular Assemblies

We are studying mesoscopic structures and optical properties of organic molecular assemblies such as porphyrin wires, carbon nanotubes embedded in sugar molecule chains, Langmuir-Blodgett films of functional conjugated molecules, mainly as collaborations with other research groups.

References

- 1) K. Imura, H. Okamoto, M. K. Hossain and M. Kitajima, *Nano Lett.* **6**, 2173–2176 (2006).
- 2) H. Okamoto and K. Imura, *J. Mater. Chem.* **16**, 3920–3928 (2006).
- 3) K. Imura, T. Nagahara and H. Okamoto, *J. Phys. Chem. B* **108**, 16344–16347 (2004).

Awards

IMURA, Kohei; The Chemical Society of Japan Award for Young Chemists.

IMURA, Kohei; Spectroscopical Society of Japan Award for Encouragement of Young Scientists.

IMURA, Kohei; Research Foundation for Opto-Science and Technology Award for Young Researchers.

* Present Address; Tohoku University, Sendai 980-8578

Quantum-State Manipulation of Molecular Motions

Department of Photo-Molecular Science
Division of Photo-Molecular Science I



OHSIMA, Yasuhiro	Professor
HASEGAWA, Hirokazu	Assistant Professor
BAEK, Dae Yul	IMS Fellow
SUMA, Kosuke	JSPS Post-Doctoral Fellow
PAVLOV, Lubomir	Visiting Scientist*
KITANO, Kenta	Graduate Student
MIYAKE, Shinichiro	Graduate Student
INAGAKI, Itsuko	Secretary

Molecules in gas phase undergo translational, rotational and vibrational motions in a random manner, and the total molecular system is a statistical ensemble that contains a number of molecules in many different states of motions. This research group aims to establish methods to manipulate the quantum-state distribution pertinent to molecular motions, by utilizing the coherent interaction with laser lights. Here lasers with ultimate resolution in time and energy domains are employed complementally and cooperatively for manipulation of molecular motions. At the present stage, the following three subjects have been extensively explored. The first one is an exploit of impulsive interaction with ultrafast intense laser fields to achieve a nonadiabatic excitation of molecular rotation. The second subject is pertinent to creation and observation of vibrational wavepackets by fs pump–probe experiments. An experimental method newly developed in this laboratory has been applied to probing wavepackets associated with internal rotation of jet-cooled polyatomic systems. The third subject aims to realization of complete population transfer *via* an adiabatic interaction with high-resolution coherent light pulses. For this purpose, we are constructing ns laser systems, all of which are sufficiently coherent to drive the adiabatic interaction.

1. Quantum Control of Wavepacket and State Distribution *via* Nonadiabatic Rotational Excitation

When a gaseous molecular sample is irradiated by an intense nonresonant ultrafast laser pulse, the laser field exerts a torque that aligns the molecular axis along the laser polarization vector, due to the interaction with the molecular anisotropic polarizability. Because the interaction is nonadiabatic, *i.e.*, only remains in much shorter duration than the molecular rotational period, the torque is impulsive so that rotation of the molecules are excited. In a quantum mechanical point of view, this nonadiabatic rotational excitation (NAREX) creates a rotational wavepacket, a coherent superposition of rotational eigenstates.

We have recently developed a method for exploring the NAREX process in a quantum-state resolved manner by using resonance-enhanced multiphoton ionization, and reported state distribution of NO molecules, whose initial population was confined to the lowest state ($J = 0.5$), after the impulsive excitation with a fundamental output of a titanium-sapphire laser with ~ 120 fs duration.¹⁾ Population for each J after NAREX is proportional to the square of the probability amplitude of the corresponding eigenstate in the rotational wavepacket thus created. Therefore the state distribution is a useful experimental source for verifying the excitation process, and a model calculation has been performed to confirm it.

The present experimental method has been further applied to probe the state distribution after double-pulse excitation. As shown in Figure 1 (left), the population for each J changes oscillatory against the delay between the excitation pulses. Their beat patterns have been shown to provide definite information on excitation pathways in NAREX. Further theoretical consideration has proved that detailed examination in double-pulse experiments, in particular, on the population of the lowest rotational state will give rise to the full reconstruction of the rotational wavepacket even when arbitrary excitation pulses are employed. The experimental realization is now under way.

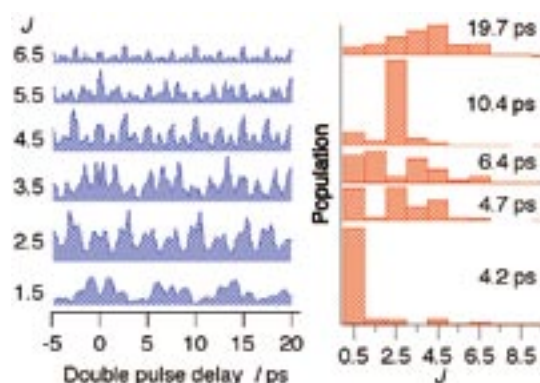


Figure 1. Population for each J state after the double-pulse NAREX against the pulse delay (left) and the corresponding state distributions at several delays (right).

Another important upshot from the double-pulse NAREX study is a partial attainment of control over rotational-state distribution with nonresonant ultrafast laser pulses. This is well demonstrated in Figure 1 (right): for instance, more than 80% of population comes back to the initial state when the delay is set to 4.2 ps, and almost 80% can be concentrated to a single eigenstate ($J = 2.5$, in this case) at delay of 10.4 ps. Implementation of elaborated shaping of excitation pulses is planned for further improvement in rotational-state control.

2. Wavepacket Dynamics of Methyl Internal Rotation Probed by fs Time-Resolved Fluorescence Depletion Spectroscopy

Real-time studies on low-frequency molecular vibrations with large amplitudes are of great significance, in particular, for potential application to control of isomerization reaction by coherent excitation of these motions. We have recently been exploring internal-rotation dynamics of methyl groups by utilizing ultrafast nonlinear spectroscopy, *i.e.*, fs time-resolved fluorescence depletion (fTRFD). While TRFD in ps regime has been applied previously for investigating slower intramolecular dynamics,²⁾ its implementation to fs regime for vibrational wavepacket studies is for the first time. We have performed fTRFD measurements in the S_1 - S_0 origin regions of several toluene derivatives in jet-cooled conditions. In particular, excitation-wavelength dependence has been examined in details for *m*-tolunitrile, as shown in Figure 2. Here the quantum interferences for the A_1 and E symmetry levels in both the S_0 and S_1 states are clearly observed. Beat components for each levels change their magnitudes for different excitation wavelengths. These dependences have been analyzed with model calculations numerically solving the time-dependent Liouville equations for methyl internal rotation.

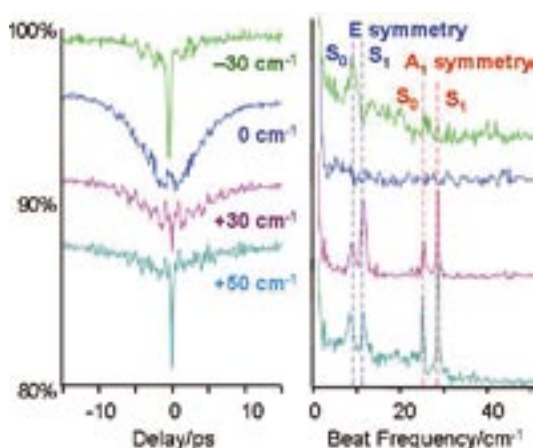


Figure 2. fTRFD spectra for different excitation wavelengths, indicated as offset wavenumbers from the origin band (left) and the corresponding power spectra (right).

Comparison of the observed fTRFD spectra with the calculated results shows that ca. 10% of population is transferred to the S_1 manifold in the present condition.

3. Construction of Coherent ns Pulsed Light Sources for Adiabatic Population Transfer

Highly efficient population transfer between quantum states can be accomplished with adiabatic interactions with ns coherent laser pulses, such as stimulated Raman adiabatic passage.³⁾ For realizing such an adiabatic quantum-state manipulation, we are constructing two independent laser systems, both of which will deliver pulsed outputs with almost Fourier-transform (FT) limited resolution. The first system, already in operation, is based on the pulsed amplification of the output from a cw ring titanium-sapphire laser. The third harmonics of the pulsed laser system has been applied for recording high-resolution excitation spectrum of the S_1 - S_0 6_0^1 band of jet-cooled benzene (Figure 3). Spectral Linewidth (0.013 cm^{-1}) of single ro-vibronic transitions is three times of FT limit. The second laser system is based on the optical parametric oscillation (OPO) injection-seeded by an extracavity cw diode laser. Quite recently, we have succeeded in single-mode operation of the OPO system, in which only a few mW of the cw light is necessary for stable injection seeding. The optical layout is now optimized for further increment of the output power up to the level sufficient for driving adiabatic population transfer.

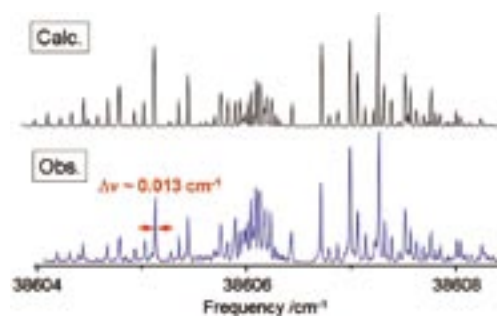


Figure 3. High-resolution excitation spectrum of benzene S_1 - S_0 6_0^1 band. Rotational temperature is set to 2 K for simulation.

References

- 1) H. Hasegawa and Y. Ohshima, *Phys. Rev. A* **74**, 061401 (4 pages) (2006).
- 2) M. J. Côté, J. F. Kauffman, P. G. Smith and J. D. McDonald, *J. Chem. Phys.* **90**, 2865–2873 (1989); G. V. Hartland, L. L. Connell and P. M. Felker, *J. Chem. Phys.* **94**, 7649–7666 (1991).
- 3) N. V. Vitanov, T. Halfmann, B. W. Shore and .K. Bergmann, *Annu. Rev. Phys. Chem.* **52**, 763–809 (2001).

Award

KITANO, Kenta; Best Poster Presentation Award in 23rd Symposium on Chemical Kinetics and Dynamics.

* from Bulgarian Academy of Science

Development of High-Precision Coherent Control and Its Applications

Department of Photo-Molecular Science
Division of Photo-Molecular Science II



OHMORI, Kenji	Professor
KATSUKI, Hiroyuki	Assistant Professor
HOSAKA, Kouichi	IMS Fellow
DELAGNES, Jean-Christophe	Post-Doctoral Fellow*
SHIMADA, Hiroyuki	Post-Doctoral Fellow
GOTO, Haruka	Graduate Student
INAGAKI, Itsuko	Secretary

Coherent control is based on manipulation of quantum phases of wave functions. It is a basic scheme of controlling a variety of quantum systems from simple atoms to nanostructures with possible applications to novel quantum technologies such as bond-selective chemistry and quantum computation. Coherent control is thus currently one of the principal subjects of various fields of science and technology such as atomic and molecular physics, solid-state physics, quantum electronics, and information science and technology. One promising strategy to carry out coherent control is to use coherent light to modulate a matter wave with its optical phase. We have so far developed a high-precision wave-packet interferometry by stabilizing the relative quantum phase of the two molecular wave packets generated by a pair of femto-second laser pulses on the attosecond time scale. We will apply our high-precision quantum interferometry to gas, liquid, solid, and surface systems to explore and control various quantum phenomena.

1. READ and WRITE Amplitude and Phase Information by Using High-Precision Molecular Wave-Packet Interferometry¹⁾

We demonstrate an experimental approach to read and write populations and relative phases of vibrational eigenstates within a wave packet created in the *B* state of the iodine molecule by using a pair of phase-locked femtosecond laser pulses. Our highly-stabilized optical interferometer keeps attosecond stability and resolution in the interpulse delay. These stability and resolution have realized an exquisite tuning of the interference of two vibrational wave packets to manipulate the relative populations and the relative quantum phases among the relevant vibrational eigenstates. These populations and phases have been retrieved by measuring fluorescence

from the upper *E* state induced by another nanosecond (ns) or femtosecond (fs) probe laser pulse. The bandwidth of the ns probe pulse is narrow enough to select only a small portion of the rotational progression of a particular vibrational band of the *E*-*B* transition. By scanning the probe wavelength, we measure the population distribution of the vibrational eigenstates within the wave packet. The fs probe pulse is used to measure quantum beats arising from the temporal evolution of the wave packet. Combining these two complementary measurements, we can read both population and phase information written and stored in the wave packet.

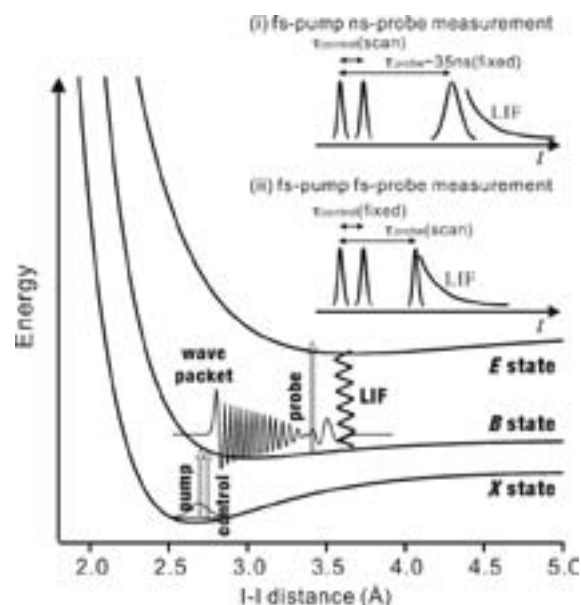


Figure 1. Pump-control-probe scheme for the real-time or state-resolved measurement of wave-packet interference with the femtosecond or nanosecond probe pulse. The potentials are only schematic.

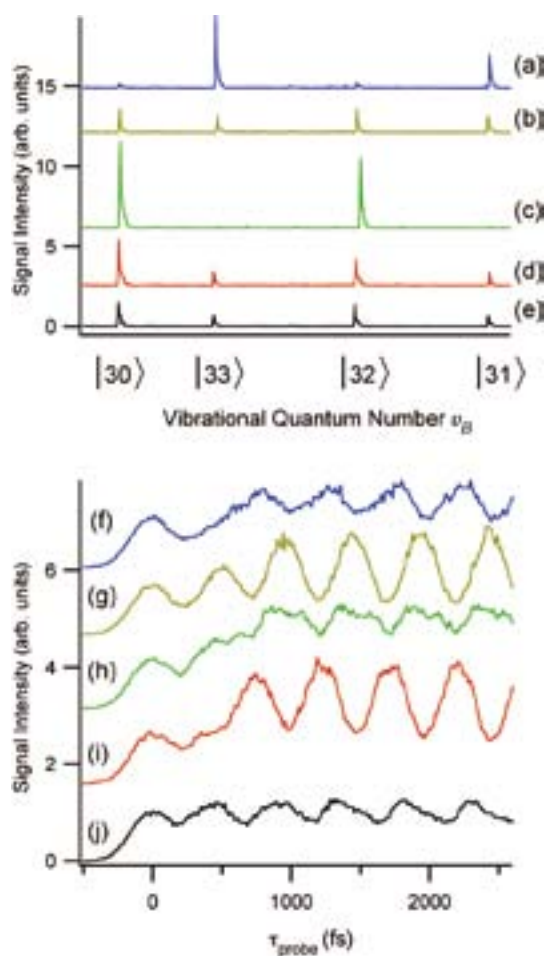


Figure 2. Wave packet interference measured with the pump and control delay τ_{control} tuned to $\sim(1+1/2) T_{\text{vib}}$ (~ 760 fs), where T_{vib} is a classical vibrational period of I_2 . (a)–(d) “POPULATION CODES” measured by scanning the wavelength of the ns probe pulse. The relative phase θ_{p-c} of the pump and control pulses is increased in steps of $\sim\pi/2$ in going from (a) to (d). (e) Population code written without the control pulse and displayed for reference. The five population codes are displaced vertically from one another for clarity. (f)–(i) “PHASE CODES” measured with almost the same θ_{p-c} 's as for (a)–(d), respectively. (j) Phase code written without the control pulse and displayed for reference. The five phase codes are displaced vertically from one another for clarity. A possible deviation of θ_{p-c} within each set of the population and phase codes is estimated to be $< 0.2\pi$ for the sets (a)–(f) and (c)–(h), and $< 0.03\pi$ for (b)–(g) and (d)–(i).

Reference

- 1) H. Katsuki, K. Hosaka, H. Chiba and K. Ohmori, *Phys. Rev. A* **76**, 013403 (13 pages) (2007).

Awards

OHMORI, Kenji; Japan Academy Medal.

OHMORI, Kenji; JSPS Prize.

Molecular Inner-Shell Spectroscopy: Electronic Structure and Intermolecular Interaction

Department of Photo-Molecular Science
Division of Photo-Molecular Science III



KOSUGI, Nobuhiro
HATSUI, Takaki
NAGASAKA, Masanari
KIMBERG, Victor
NAKANE, Junko

Professor
Assistant Professor
Assistant Professor
JSPS Post-Doctoral Fellow
Secretary

To reveal electronic structure and intermolecular interaction of free molecules and molecular solids and clusters, we are developing and improving soft X-ray spectrometers for resonant photoelectron spectroscopy and inelastic soft X-ray emission spectroscopy optimized to an undulator beamline BL3U at the UVSOR facility. We are also developing and improving an original *ab initio* quantum chemical program package GSCF, which is optimized to calculation of molecular inner-shell processes.

1. High-Resolution Soft X-Ray Emission Spectroscopy with a Transmission Grating

We have recently reported our new design of a transmission-grating spectrometer (TGS) for high resolution soft X-ray emission studies.¹⁾ The high resolution spectrometer generally requires high light gathering capability without sacrificing the energy resolution. This requirement can be fulfilled by use of the Wolter type-I mirror and the transmission grating (TG). Our spectrometer incorporates the basic concept for x-ray imaging and spectroscopy telescopes²⁾ into a compact and easy-to-use layout.

The present optical layout is a modification of the Rowland torus mount with facet gratings. In the ideal Rowland torus mount, the facet TGs should be mounted onto Rowland torus with keeping their normal to point the focus of the incoming x-rays. In our spectrometer, the facet TGs are positioned onto a single Si wafer. Such simplification might degrade optical properties. However, we demonstrated by ray-tracing simulations that the aberration in our geometry is small enough to realize the energy resolving power better than 5000.

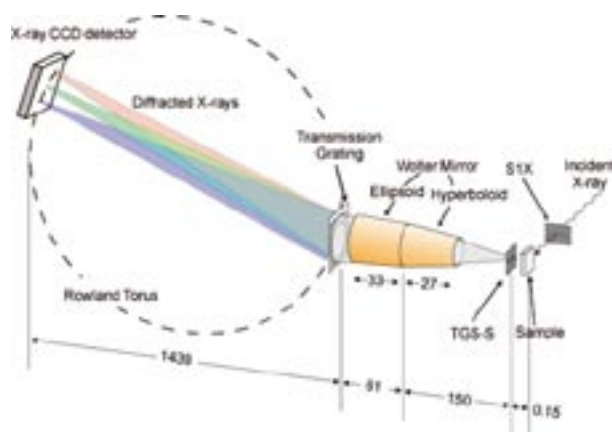


Figure 1. Layout of the present soft X-ray emission spectrometer.

Our TGS shown in Figure 1 is installed at the XES end-station of the undulator beamline BL3U. A soft x-ray emission spectrometer generally requires small beam size at the sample position, because a smaller opening of the spectrometer entrance slit is needed to achieve higher energy resolution. BL3U is designed to give small beam size of order of $10 \times 40 \mu\text{m}^2$. To check the stray light contamination, the profile of the 0th order diffraction was measured. The stray light intensity was less than 1% of the 1st diffraction order intensity. To check the energy resolution, diffuse scattering from aluminum samples illuminated by 60 eV soft x-rays was measured. Figure 2 shows the 1st order diffraction peak. The peak width was FWHM of 3 pixels, which corresponds to the energy resolving power of 4600. To our knowledge, the present resolving power is more than 4 times higher than the best record reported so far.

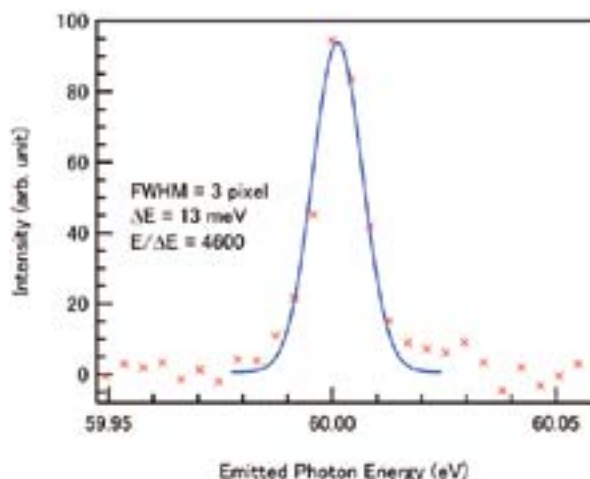


Figure 2. 1st order diffraction peak of the diffuse scattering from aluminum samples ($h\nu = 60$ eV), observed by using the present TGS.

2. X-Ray Natural Circular Dichroism of Amino Acids³⁾

X-ray absorption spectroscopy (XAS) is a powerful tool to study even large molecules. Due to the localized character of a core electron responsible for XAS, it is possible to correlate a specific XAS feature with a specific functional group or with an individual bond. In addition, even natural circular dichroism (NCD) is now observable in XAS of amino acids, though difference in XAS between the left and right circularly polarized X-rays proves to be tiny: $g = 2(I_L - I_R)/(I_L + I_R) \approx 10^{-3}$.

In the present work, we evaluate feasibility of different theoretical approaches for XNCD by using GSCF3 and other available *ab initio* codes. We describe the excited orbital set using the ground state Hartree-Fock (HF) orbital set employed in (i) RPA and (ii) static exchange approach (STEX) (unrelaxed), (iii) core-ionized state HF orbital set applied in STEX(relaxed) and (iv) HF excited state orbital set for each core-to-valence excited state. Furthermore in (i) the DFT-RPA method is compared with the RPA where the *ab initio* HF orbital set is used. In (iv), the oscillator and rotary strengths evaluated by different orbital sets for the initial and final states, namely, non-orthogonal ground-state and core-excited HF orbitals, are compared with those evaluated by using the core-excited HF orbital set to describe the initial (ground) state.

The basis set dependence of XNCD spectra of some amino acids in different approaches is systematically investigated using Woon and Dunning basis sets up to aug-cc-pCV5Z. The RPA calculation shows most satisfactory and self-consistent results for the low-lying core-to-valence excitations near the O K-edge. A clear convergence of the oscillator strength for the basis sets larger than triple-zeta is found for the RPA approach. Use of extended quadruple-zeta or larger basis sets are required to obtain satisfactory results for the rotary strength on the O K-edge. The relative simplicity of the RPA technique using the same ground-state HF orbital set for any core-to-valence excitation makes it applicable to chiral centers in rather large compounds such as proteins.

3. Inner-Shell Ionized and Excited States of Molecular Pyridine Clusters⁴⁾

Photoionization of clusters containing aromatic molecules shows characteristic redshifts of the appearance energies in the regime of the first ionization energy.⁵⁾ These redshifts are rationalized with the polarization (PL) effect by molecules surrounding a positively-charged core-ionized molecule. On the other hand, photoexcitation of clusters containing aromatic molecules does not show such a PL effect, because the core excited states are neutral. Recently, we have investigated the C 1s- π^* excitation in variable size benzene clusters,⁶⁾ whose excited states undergo substantial redshifts up to 60 meV relative to the isolated molecule. On the other hand, the N 1s- π^* excitations in pyridine clusters show ca. 60 meV-blueshifts. The mechanism of the energy shift in inner-shell excitation of molecular clusters could be different from that in inner-shell ionization.

The most stable pyridine dimer structure is theoretically found to be an anti-parallel displaced structure with the N atoms opposing each other, where the positively charged H atom of one ring lies on top of the negatively charged nitrogen atom of the other ring. In the parallel displaced geometry of pyridine trimer, the middle pyridine is displaced with respect to the top and bottom pyridine rings, such as two anti-parallel displaced pyridine geometries. In contrast to less stable parallel displaced stacking interaction in benzene dimer, the stacking interaction in pyridine dimer and trimer is stabilized electrostatically with the permanent dipole moment.

In the anti-parallel displaced dimer structure the blueshift is calculated to be 42 meV by using GSCF3. In the anti-parallel displaced trimer, the N 1s on the middle ring has the largest blueshift of 85 meV, whereas the top and bottom N 1s leads to the same blueshift of 42 meV as in the dimer. This means the second neighbor molecule is not contributive at all to the energy shift. We have also observed that the N 1s- π^* excitation energy shift is oscillating against a horizontal sliding in the anti-parallel displaced pyridine dimer. This indicates covalent intermolecular interaction is important; that is, a small π - π orbital interaction is visible as a small energy shift in the 1s- π^* excitation even in van der Waals clusters. In addition, this result indicates a possibility to know nearest neighbor molecular conformation by referring to the shift in core-to-valence excitation energy.

References

- 1) T. Hatsui, E. Shigemasa and N. Kosugi, *J. Electron Spectrosc. Relat. Phenom.* **144**, 1059 (2005).
- 2) K. P. Beuermann, H. Bräuninger and J. Trümper, *Appl. Opt.* **17**, 2304 (1978).
- 3) V. Kimberg and N. Kosugi, *J. Chem. Phys.* **126**, 245101 (2007).
- 4) I. Bradeanu and N. Kosugi, *AIP Conf. Proc.* **882**, 815 (2007).
- 5) E. Rühl, P. Bisling, B. Brutschy and H. Baumgärtel, *Chem. Phys. Lett.* **126**, 232 (1986).
- 6) I. L. Bradeanu, R. Flesch, N. Kosugi, A. Pavlychev and E. Rühl, *Phys. Chem. Chem. Phys.* **8**, 1906 (2006).

Extreme UV Photoionization Studies of Fullerenes by Using Synchrotron Radiation and High-Temperature Mass Spectrometer

Department of Photo-Molecular Science
Division of Photo-Molecular Science III



MITSUKE, Koichiro	Associate Professor
KATAYANAGI, Hideki	Assistant Professor
HUANG, Chaoqun	IMS Fellow
YAGI, Hajime	Post-Doctoral Fellow
KAFLE, Bhim Prasad	Graduate Student
PRODHAN, Md. Serajul Islam	Graduate Student

The interactions of C_{60} , C_{70} , C_{84} ... with high-energy photons have attracted considerable attention, since fullerenes provide unique molecular systems characterized by exceptionally stable electronic structures associated with dense and highly degenerated molecular orbitals and by extremely large vibrational degrees of freedom. In UVSOR we have investigated the yield curves of singly- and multiply-charged photoions from fullerenes by using a grazing incidence monochromator in the $h\nu$ range from 25 to 200 eV. We succeeded in absolutizing the partial and total photoionization cross section curves of $C_{60(70)}$. Moreover, we have measured the yield curves for $C_{60(70)-2n}^{z+}$ from $C_{60(70)}$ as a function of the internal energy of the parent $C_{60(70)}^{z+}$ ions to study the mechanisms and kinetics of sequential C_2 -release reactions.

1. Relative Partial Cross Sections for Single, Double and Triple Photoionization of C_{60} and C_{70} ¹⁾

Partial cross sections for the photoion formation from C_{60} and C_{70} were determined from the yields of singly, doubly and triply charged ions at $h\nu = 25$ –120 eV. The dependence of the detection efficiencies on the mass-to-charge ratio was evaluated by using the formula proposed by Twerenbold *et al.* Corrections of the detection efficiency were found to be critical to obtain accurate partial cross sections. Revisions were made of the partial cross-section curves for single and double photoionization of C_{60} and C_{70} . The curve for triple photoionization of C_{70} was newly proposed. The ratios between the cross sections for double and single photoionization increase with $h\nu$ and reach saturated values of 0.78 at 85 eV for C_{60} and ~ 1.3 at 100 eV for C_{70} . In contrast, the ratios at 120 eV between the cross sections for triple and single photoionization of C_{60} and C_{70} amount to be 0.14 and ~ 0.38 , respectively. Formation mechanism of multiply-charged fullerene ions was discussed in terms of valence-electron excitation to antibonding unoccupied orbitals and/or spherical

standing waves inside the cavity of a fullerene. This excitation could be followed by Spectator Auger processes and transmission of the excess electronic energy among numerous vibrational degrees of freedom.

2. Absolute Total Photoionization Cross Section of C_{60} in the Range of 25–120 eV²⁾

The absolute total photoionization cross section of C_{60} has been measured at $h\nu = 25$ –120 eV. Evaluation has been made on the detection efficiency of fullerene ions in different charge states. The present total photoionization cross section curve has been combined with the absorption cross section curves of C_{60} at $h\nu = 3.5$ –26 eV in the literature, after appropriate alterations of the vapor pressure being taken into account. The oscillator strengths are calculated from the combined cross section curve to be 230.5 and 178.5 at $h\nu = 3.5$ –119 and 3.5–40.8 eV, respectively. These oscillator strengths agree well with those expected from the TKR sum rule. Moreover, the total photoionization cross section curve of the present study is

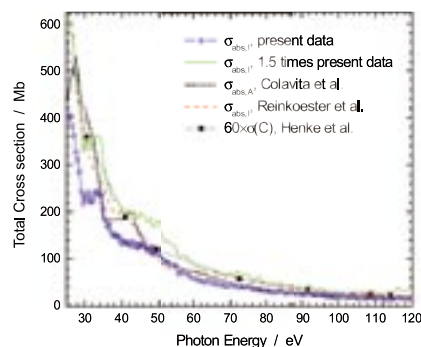


Figure 1. ○, total photoionization cross section $\sigma_{\text{abs,I}}$ of C_{60} of the present study; —, $\sigma_{\text{abs,I}}$ of the present study multiplied by 1.5; ---, experimental $\sigma_{\text{abs,I}}$ by Reinkoester *et al.*; ■, theoretical total photo-absorption cross section $\sigma_{\text{abs,A}}$ by Colavita *et al.*; ■, 60 times $\sigma_{\text{abs,A}}$ of a C atom by Henke *et al.*

consistent with those of recent experimental and theoretical studies (see Figure 1).

3. Relative Partial Cross Sections for Single, Double and Triple Photoionization of C₈₄

The partial cross sections for the photoion formation from C₈₄ were newly determined from the yields of singly, doubly and triply charged ions at $h\nu = 55\text{--}120$ eV. The ratios between the cross sections for double and single photoionization increase with $h\nu$ and reach saturated values of ~ 0.9 at 80 eV. In contrast, the ratios at 120 eV between the cross sections for triple and single photoionization amount to be ~ 0.18 , respectively.

4. Kinetic Energy Analysis of the Fragment Ions Produced from C₆₀ and C₇₀³⁾

We reported the yield curves of the fragments C_{60-2n}^{z+} and C_{70-2n}^{z+} ($n \geq 1, z \geq 1$) produced from C₆₀ and C₇₀, respectively, at $h\nu = 45\text{--}150$ eV. Then the mechanism of sequential loss of C₂ units has been proposed on a basis of comparison between the experimental ion yield curves and theoretical fractional abundance curves. The latter curves have been derived by employing the RRKM theory to individual unimolecular reactions, C_{60-2n+2}^{z+} \rightarrow C_{60-2n}^{z+} + C₂. More reliable calculations of the rate constants of these reactions are needed before closer comparison between the two curves. For such calculations we should know precise values of the activation energies for the reactions, together with the vibrational spectra of the transition states. This induced us to develop a new spectrometer for the fragment ions. It is likely that the magnitude of the potential barriers can be estimated from the average kinetic energy release measured by this spectrometer.

5. Scattering Distributions of the Photofragments from Fullerenes

We are developing an imaging spectrometer to measure the three-dimensional momentum distributions of the ionic photofragments produced from fullerenes at $h\nu > 50$ eV. High kinetic-energy resolution is expected to be achieved on the images by adopting the Eppink-Parker type velocity focusing lens system. We will be able to distinguish the two possible mechanisms of fragmentation of fullerene ions, *i.e.* stepwise C₂ ejection and direct fission into two species, since different momentum distributions result in different projected images on the position sensitive detector.

6. ZEKE Photoelectron Spectroscopy Using the Dark Gap of the Storage Ring

We have constructed a threshold photoelectron spectrometer for the purpose of measuring the signal of threshold electron-photoion coincidence (TEPICO), using the dark gap

of the UVSOR facility. Such measurements provide us with the detailed information about the excitation/de-excitation and decay processes of C₆₀ and C₇₀. We already succeeded in observing the electron signal from He and O₂ samples, but the spectra suffered from intense background counts. The background needs to be reduced to the utmost for performing the TEPICO measurement. It is also necessary to improve the efficiency of the spectrometer for threshold electrons. We are therefore developing an improved version of the spectrometer which has the capability to significantly reject the electrons with high kinetic energies and to guide slow electrons ($KE = 0$ to 10 meV) to the detector.

7. High Resolution Photoelectron Spectroscopy of Gaseous C₆₀

Photoelectron spectroscopy (PES) of solid C₆₀ has been performed by several groups to clarify its electronic structure. However, comprehensive PES studies of gaseous C₆₀ are few and the energy resolution was ~ 100 meV at the best. This resolution was not enough to distinguish closely spaced bands, though many degenerate bands are located in the 7–40 eV ionization energy range. We are developing an apparatus of high-resolution angle-resolved PES. Our goal is to carry out PES of various kinds of fullerenes with a total energy resolution of ~ 20 meV at the UVSOR facility. The partial photoionization cross section and anisotropy parameter of each band are expected to be determined at $h\nu = 25\text{--}150$ eV.

8. Photodissociation of Butyl Cyanides and Butyl Isocyanides⁴⁾

Photodissociation process to produce the electronically excited CN(B Σ^+) fragment has been studied for four structural isomers, *n*-C₄H₉CN, *t*-C₄H₉CN, *n*-C₄H₉NC and *t*-C₄H₉NC by using synchrotron radiation. Photoexcitation spectra for the CN(B² Σ^+ \rightarrow X² Σ^+) transition were measured in the excitation wavelength range of 85–165 nm (7.5–14.5 eV) and the CN(B² Σ^+ \rightarrow X² Σ^+) emission spectra were dispersed at several wavelengths in the range of 57–140 nm. Quantum yields for the production of the CN(B) state from photodissociative excitation of the isocyanides were larger than those from the cyanides. The quantum yields from the molecules consisting of a *tertiary*-butyl group were larger than those from the *normal*-butyl compounds.

References

- 1) K. Mitsuke, H. Katayanagi, C. Huang, B. P. Kafle, Md. S. I. Prodhon, H. Yagi and Y. Kubozono, *J. Phys. Chem. A* **111**, 8336–8343 (2007).
- 2) B. P. Kafle, H. Katayanagi, Md. S. I. Prodhon, H. Yagi, C. Huang and K. Mitsuke, *J. Phys. Soc. Jpn.* submitted.
- 3) B. P. Kafle, H. Katayanagi and K. Mitsuke, *AIP Conf. Proc.* **879**, 1809–1812 (2007).
- 4) K. Kanda, K. Mitsuke, K. Suzuki and T. Ibuki, *AIP Conf. Proc.* **879**, 1817–1820 (2007).

Molecules in Few-Cycle Intense Laser Fields

Department of Photo-Molecular Science
Division of Photo-Molecular Science III



HISHIKAWA, Akiyoshi
FUSHITANI, Mizuho
MATSUDA, Akitaka
NAKANE, Junko

Associate Professor
Assistant Professor
IMS Fellow
Secretary

When exposed to intense laser fields, molecules exhibit a variety of exotic features as the magnitude of the electric field component is comparable with that of the Coulomb field within a molecule. For a deeper understanding of the light-matter interaction, we investigate how atoms and molecules behave in strong and ultrashort laser fields, which carry only a few optical cycles within the pulse.

1. Electronic and Nuclear Responses of Fixed-in-Space H₂S to Ultrashort Intense Laser Fields¹⁾

The Coulomb explosion dynamics in non-resonant, ultrashort intense laser fields (12 fs, $\sim 10^{14}$ W/cm²) is studied for H₂S with its orientation fixed in space, to clarify how the electronic and nuclear responses change by the direction of laser polarization direction (ϵ) in the molecular frame (Figure 1). The momenta of the respective fragment ions, $p_1(\text{H}^+)$, $p_2(\text{H}^+)$ and $p_3(\text{S}^+)$ produced in the Coulomb explosion process, $\text{H}_2\text{S}^{3+} \rightarrow \text{H}^+ + \text{S}^+ + \text{H}^+$, were determined as three-dimensional vectors in the laboratory frame. The kinetic energy release (E_{kin}) and momentum angle (θ_{12}) distributions obtained for the respective directions revealed that the geometrical structure is almost frozen during the interaction with the laser fields for $x//\epsilon$, while it becomes elongated along the laser polarization vector when ϵ is parallel to the y - or z - axis, demonstrating that the Coulomb explosion dynamics of H₂S in intense laser fields can be manipulated by the polarization direction in the molecular frame.

The elongation in the molecular structure can be interpreted in terms of the induced dipole potential, $U_{\text{id}} = -\alpha\epsilon^2/2$. As the molecular structure stretches along ϵ , the corresponding component of polarizability tensor α becomes larger, which lowers the potential energy to induce the nuclear dynamics towards the elongated structures. Alternatively, the observed structural deformation can be explained by the population transfer to charge transfer (CT) states characterized with the ionic charge distribution and the large transition moments from

the ground state. Because of the ionic character, CT states can be stabilized in intense laser fields against the covalent ground state when the direction of the charge separation is parallel to the electric field ϵ . The large transition moments then facilitates the laser induced non-adiabatic population transfer from the ground state to the CT state, which leads to the enhanced ionization and dissociation in intense laser fields by the localized charge distribution.

In the case of H₂S, CT states with the H⁻-S-H⁺ (and H⁺-S-H⁻) type configuration and those with the H₂⁺-S⁻ or H₂⁻-S⁺ character are expected to contribute to the dynamical processes for the $y//\epsilon$ and $z//\epsilon$ directions, respectively. Possible candidates of such CT (ionic) states are the electronically excited 3^1B_2 and 5^1A_1 states located at 13.9 eV and 13.7 eV above the ground state at the equilibrium geometry. The transition moments from the ground state, $X^1\text{A}_1$, are $|\mu| = 1.57$ and 1.34 a.u., along the y - and z -axis, respectively.

On the other hand, no such CT states can be coupled with the ground state when ϵ is perpendicular to the molecular plane. The ionization process for $x//\epsilon$ should be dominated by the tunneling ionization from the HOMO $2b_1$ extending perpendicular to the plane. The ionized electron is then rescattered by the ion core to form highly charged parent ions within a few optical cycles, which minimizes the structural deformation prior to the Coulomb explosion.

In conclusion, we have demonstrated that the Coulomb explosion dynamics of H₂S in intense laser fields can be manipulated by the polarization direction ϵ in the molecular frame. The observed dependence of the electronic and nuclear responses to the non-resonant laser fields can be explained in terms of the character of the CT states, which serve as the “doorway states” to the structural deformation of small polyatomic molecules in intense laser fields as well as to the ionization and fragmentation processes discussed previously. The understanding of the electronic and nuclear response to the laser fields polarized in the molecular frame presented here will provide new prospects for efficient quantum control in the intense field regime.

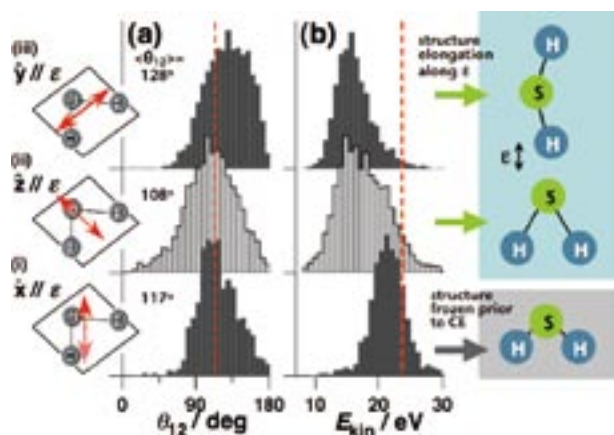


Figure 1. (a) Momentum angle θ_{12} distribution and (b) total kinetic energy E_{kin} distribution obtained for three different directions of ϵ , in the molecular frame, (i) $x//\epsilon$, (ii) $y//\epsilon$ and (iii) $z//\epsilon$.

2. Dalitz Plot Analysis of Coulomb Exploding O₃ in Ultrashort Intense Laser Fields²⁾

The three-body Coulomb explosion of ozone, $O_3^{3+} \rightarrow O^+ + O^+ + O^+$, in ultrashort intense laser fields (2×10^{15} W/cm²) is studied with two different pulse durations (9 and 40 fs) by the coincidence momentum imaging method. The nuclear dynamics in the laser fields is discussed using the Dalitz plot,³⁾ developed originally to describe the three-body reactions in elementary particle physics, which provides a compact two-dimensional representation of the relative momentum sharing among the three fragments produced through the dissociation of small polyatomic molecules.

In a Dalitz plot, normalized kinetic energy parameters of the three fragments are plotted in the Cartesian coordinate system (x, y),

$$x = (\epsilon_1 - \epsilon_2) / (\sqrt{3}E_{kin}), \quad (1)$$

$$y = \epsilon_3 / E_{kin} - 1/3, \quad (2)$$

where ϵ_i is the kinetic energy of the i -th fragment and $E_{kin} = \epsilon_1 + \epsilon_2 + \epsilon_3$. A set of three fragment momenta that fulfills the momentum conservation condition falls within a circle of $1/3$ in radius in this plot, and form a uniform distribution if there is no correlation among the three fragment momenta.

The Dalitz plot obtained for the 9-fs intense laser fields exhibits a sharp peak centered at the origin as shown in Figure

2, showing that all the three fragment ions tend to have the same momentum values, by the strong Coulombic interactions during the explosion process. When the pulse duration is increased from 9 to 40 fs, a broadening of the Dalitz plot distribution is identified, in addition to a decrease in the total kinetic energy release. The analysis based on a simple Coulomb explosion model shows that the geometrical structure of ozone remains almost unchanged during the interaction with the few-cycle intense laser fields, while a significant structural deformation along all the three vibrational coordinates, including the anti-symmetric stretching coordinate, is identified in the 40 fs laser fields. The observed nuclear dynamics are discussed in terms of the population transfer to the excited states of O₃.

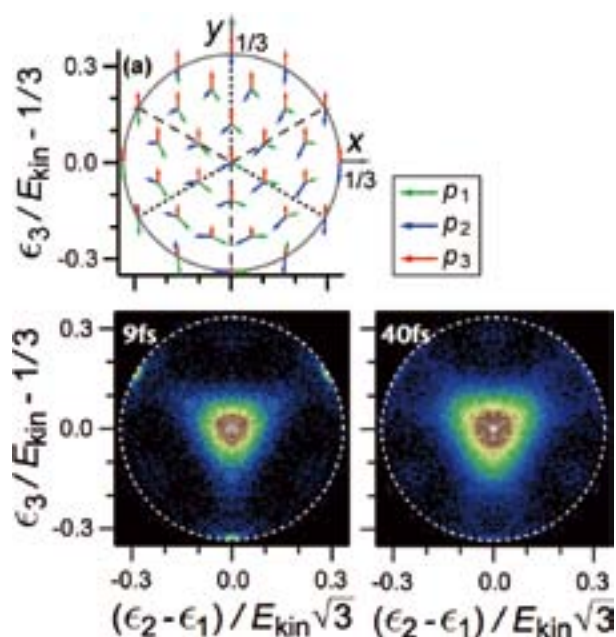


Figure 2. Dalitz plots obtained for the Coulomb explosion process of ozone, $O_3^{3+} \rightarrow O^+ + O^+ + O^+$, in 9 and 40 fs intense laser fields (2×10^{15} W/cm²).

References

- 1) A. Hishikawa, E. J. Takahashi and A. Matsuda, *Phys. Rev. Lett.* **96**, 243002 (2006).
- 2) A. Matsuda, E. J. Takahashi and A. Hishikawa, *J. Chem. Phys.* **127**, 114318 (2007).
- 3) R. H. Dalitz, *Philos. Mag.* **44**, 1068–1080 (1953).

Award

HISHIKAWA, Akiyoshi; Morino Foundation for Molecular Science.

Light Source Developments by Using Relativistic Electron Beams

UVSOR Facility
Division of Advanced Accelerator Research



KATOH, Masahiro	Professor
HOSAKA, Masahito	Assistant Professor*
MOCHIHASHI, Akira	Assistant Professor
SHIMADA, Miho	IMS Fellow
KOIKE, Masashi	Graduate Student [†]
SUZUKI, Yasuhiro	Graduate Student [†]
YOSHIDA, Mitsuhiro	Graduate Student [†]

This project involves researches and developments on synchrotron light source, accelerator technologies, beam physics, free electron laser and related technologies. All these works are performed at UVSOR-II electron storage ring and its injector.

1. Developments on UVSOR-II Accelerators

After the major upgrade in 2003,¹⁾ the UVSOR-II electron storage ring and its injector has been continuously improved. In this year an undulator was constructed and installed as the fourth undulator in the facility (Figure 1). The magnetic configuration is so-called APPLE-II type. The undulator can provide VUV light of various polarizations (horizontal /vertical plane and right-/left-handed circular) to a beam-line dedicated for photo-electron spectroscopy.²⁾ Its main parameters are summarized in Table 1. The commissioning was successful. The electron orbit movement caused by the magnetic field changes could be suppressed to smaller than 10 microns by a feed-forward system.



Figure 1. New variable polarization undulator for BL7U.

Table 1. Parameters of New Variable Polarization Undulator.

Configuration	APPLE-II
Number of Periods	40
Period Length	76 mm
Pole Length	3.04 m
Pole Gap	24–200 mm
Max. K Parameter	5.4 (horizontal) 3.6 (vertical) 3.0 (helical)

The beam lifetime of UVSOR-II is severely limited by Touschek effect due to its low emittance and low electron energy. The electron beam should be re-filled every 6 hours. To solve the lifetime problem eternally, we are preparing for top-up injection scheme. In this scheme, the electron beam is re-filled with a short interval, typically one minutes, to keep the beam current almost constant.



Figure 2. New magnet power supply for the booster synchrotron.

To realize the top up injection, the maximum operating energy of the injector and the beam transport line had to be increased from 600 MeV to 750 MeV. In this year, the magnet power supplies of the booster synchrotron and the beam transport line were replaced. The new power supplies are

capable of exciting the existing magnets sufficiently strong for the 750 MeV operation. The new power supplies were successfully commissioned. Soon, we have succeeded in accelerating electrons up to 750 MeV on the booster synchrotron and also in transporting those electrons to the storage ring. In July, we have started the full energy injection in the user runs. After some improvements on the beam transport efficiency and reinforcements on the beam monitor system and the safety interlock system, we will start testing the top-up injection soon.

2. New Method to Measure Touschek Lifetime

Touschek effect is a dominant beam loss mechanism in a low emittance and low energy storage ring such as UVSOR-II. It is difficult to measure the beam loss rate due to Touschek effect separately from those due to other effects such as scattering by residual gas molecules. We have developed a new method to measure the Touschek lifetime separately from other process.³⁾ The method is based on the single photon counting technique. By measuring the change of the relative intensities of two successive bunches, we can estimate the Touschek lifetime independently.

3. Storage Ring Free Electron Laser

The low emittance and the high peak current of UVSOR-II make the free electron laser oscillate in the deep UV region with high output power exceeding 1W.⁴⁾ At present the shortest wavelength is 215 nm. Lasing around 200 nm seems promising. Users' experiments using this high power and tunable laser beam are in progress.⁵⁾

The interaction between the electron beam and the laser pulse in the optical cavity produce strong electron bunch heating. This process limits the output power of the free electron laser. This heating process and its effects on the lasing were experimentally investigated.⁶⁾

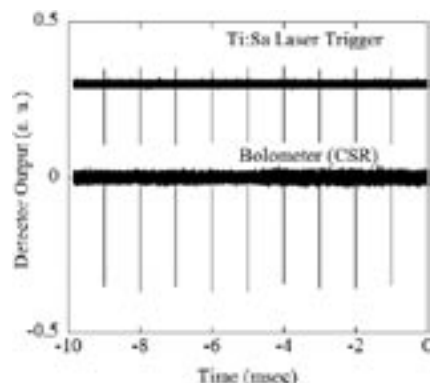


Figure 3. Coherent terahertz radiation induced by laser injection.

4. Terahertz Coherent Synchrotron Radiation by Laser-Electron Interaction

We have developed a system to create micro-density structure on electron bunches circulating in the storage ring.⁷⁾ The density structure, whose typical scale is ranging from a few hundred femtoseconds to a few picoseconds, is created through the interaction between the ultra-short laser pulses and electron bunches. Such electron bunches emit coherent synchrotron radiation in terahertz region, as shown in Figure 3. It was successfully demonstrated that, by controlling the shape of the micro-structure, the spectra of the coherent radiation could be controlled.

5. Coherent Harmonic Generation

Coherent harmonic generation is a method to produce coherent harmonics of laser light by using relativistic electron beam. The laser-electron interaction in an undulator produces density modulation of a period of laser wavelength. When the energy modulation is sufficiently larger than the natural energy spread, the density modulation contains higher harmonic component of the laser wavelength. Such an electron bunch emits coherent harmonics of the injected laser. We have successfully observed the coherent third harmonics of Ti:Sa laser.⁸⁾ Optical properties of the coherent harmonic radiation were experimentally investigated.

References

- 1) M. Katoh, M. Hosaka, A. Mochihashi, J. Yamazaki, K. Hayashi, Y. Hori, T. Honda, K. Haga, Y. Takashima, T. Koseki, S. Koda, H. Kitamura, T. Hara and T. Tanaka, *AIP Conf. Proc.* **705**, 49–52 (2004).
- 2) S. Kimura, T. Ito, E. Nakamura, M. Hosaka and M. Katoh, *AIP Conf. Proc.* **879**, 527–530 (2007).
- 3) A. Mochihashi, M. Katoh, M. Hosaka, Y. Takashima and Y. Hori, *Nucl. Instrum. Methods Phys. Res., Sect. A* **572**, 1033–1041 (2007).
- 4) M. Hosaka, M. Katoh, A. Mochihashi, M. Shimada, T. Hara and Y. Takashima, *Proc. 28th Internat. Free Electron Laser Conf.* (2006, Berlin), 368–370 (2006).
- 5) e.g. T. Nakagawa, T. Yokoyama, M. Hosaka and M. Katoh, *Rev. Sci. Instrum.* **78**, 023907 (2007).
- 6) M. Labat, M. E. Couprie, M. Hosaka, A. Mochihashi, M. Katoh and Y. Takashima, *Phys. Rev. STAB* **9**, 100701 (2006).
- 7) M. Katoh, M. Hosaka, A. Mochihashi, M. Shimada, S. Kimura, Y. Takashima and T. Takahashi, *AIP Conf. Proc.* **879**, 71–73 (2007).
- 8) M. Labat, M. Hosaka, A. Mochihashi, M. Shimada, M. Katoh, G. Lambert, T. Hara, Y. Takashima and M. E. Couprie, *Eur. Phys. J. D* **44**, 187–200, e2007-00177-6 (2007).

* Present address; Nagoya University, Nagoya, 464-8603

† carrying out graduate research on Cooperative Education Program of IMS with other graduate schools

Synchrotron Radiation Spectroscopy on Strongly Correlated Electron Systems

UVSOR Facility
Division of Advanced Solid State Physics



KIMURA, Shin-ichi
ITO, Takahiro
SAKURAI, Yoko
IM, Hojun
SUMII, Ryohei
MIZUNO, Takafumi
MIYAZAKI, Hidetoshi
OTA, Syunji
MIZUNUMA, Takuro
IIZUKA, Takuya

Associate Professor
Assistant Professor
IMS Fellow*
Post-Doctoral Fellow†
Post-Doctoral Fellow‡
Graduate Student
Graduate Student§
Graduate Student§,||
Graduate Student¶,**
Graduate Student††

Solids with strong electron–electron interaction, so-called strongly correlated electron systems (SCES), have various physical properties such as non-BCS superconducting, colossal magneto-resistance, heavy fermion and so on. The materials are one of candidates of the next generation functional materials. We are investigating the mechanism of the physical properties of SCES, especially rare-earth compounds, organic superconductors and transition-metal compounds, by infrared and angle-resolved photoemission spectroscopies using synchrotron radiation. Since experimental techniques using synchrotron radiation are evolved rapidly, the development is also one of our research subjects.

1. Optical Observation of Non-Fermi-Liquid Behavior in the Heavy Fermion State of YbRh_2Si_2 ¹⁾

The crossover between the localized and itinerant properties of rare-earth compounds is one of the main topics of recent solid state physics. We investigate the change of the electronic structure from the localized to itinerant states *via* the quantum critical point. The control from the localized to itinerant properties is usually done by applying pressure or changing the concentration of ligand atoms. YbRh_2Si_2 is a recently developed non-Fermi liquid material and is located near the quantum critical point. At the quantum critical point, the electrical resistivity is proportional to the temperature ($\rho \propto T$) below 10 K that is different from the Fermi liquid property ($\rho \propto T^2$). Then we measured far-infrared optical properties of YbRh_2Si_2 for photon energies down to 2 meV and temperatures 0.4–300 K. In the coherent heavy quasiparticle state, a linear dependence of the low-energy scattering rate on both temperature and photon energy was found (Figure 1). We relate this distinct dynamical behavior different from that of Fermi-liquid materials to the non-Fermi-liquid nature, *i.e.*, the electrodynamic property of YbRh_2Si_2 also indicates the non-Fermi liquid nature.

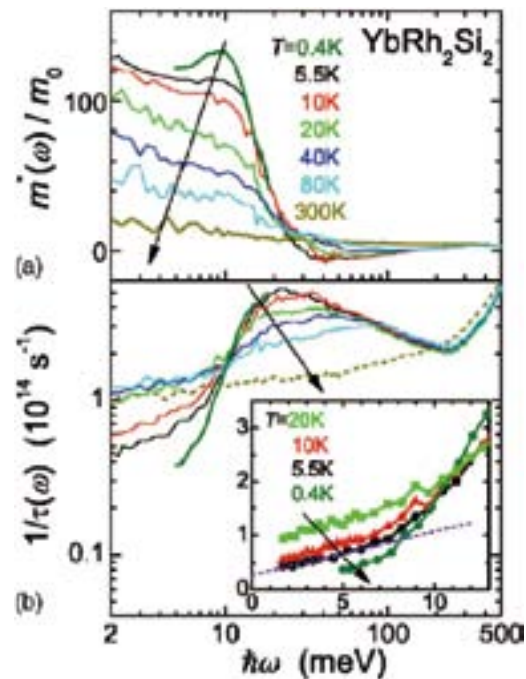


Figure 1. Temperature dependence of (a) the effective mass relative to the free-electron mass, $m^*(\omega)/m_0$, and (b) the scattering rate $1/\tau(\omega)$ as a function of photon energy. The inset of (b) is the low-energy part of $1/\tau(\omega)$. The dashed line emphasizes a $1/\tau(\omega) \propto \omega$ behavior.

2. Magnetic-Field-Induced Superconductor–Insulator–Metal Transition in an Organic Conductor: An Infrared Magneto-Optical Imaging Spectroscopic Study²⁾

The magnetic-field-induced superconductor–insulator–metal transition (SIMT) in partially deuterated κ -(BEDT-TTF)₂Cu[N(CN)₂]Br, which is just on the Mott boundary, has

been observed using the infrared magneto-optical imaging spectroscopy. The infrared reflectivity image on the sample surface revealed that the metallic (or superconducting) and insulating phases coexist and they have different magnetic-field dependences as shown in Figure 2. One of the magnetic-field dependence is SIMT that appeared on part of the sample surface. The SIMT was concluded to originate from the balance of the inhomogeneity in the sample itself and the disorder of the ethylene end groups resulting from fast cooling.

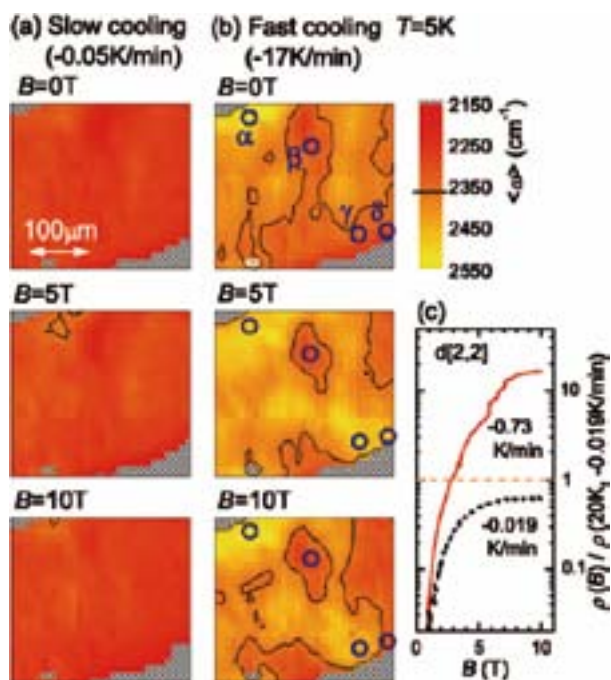


Figure 2. Magnetic-field and cooling-rate [slow cooling in (a) and fast cooling in (b)] dependencies of the spatial image of the center of the spectral weight $\langle\omega\rangle$ of 50% deuterated κ -(BEDT-TTF) $_2$ Cu [N(CN) $_2$]Br ($d[2,2]$) at $T = 5$ K. The wavenumber of $\langle\omega\rangle$ below (above) 2350 cm^{-1} is metallic (insulating) region. The black lines indicate the rough $M-I$ boundary (ω_M) of 2350 cm^{-1} and the lower and higher wave numbers indicate the insulating and metallic (superconducting) reflectivity spectra, respectively. The blue circles in (b) indicate the points of the different magnetic-field dependencies on the sample surface. The hatched area is the outside of the sample. (c) Magnetic-field and cooling-rate dependencies of the normalized resistivity of $d[2,2]$ at 5.5 K for the reference. Though the cooling rate of -0.73 K/min is different from that of (b), the physical character is the same.

3. Infrared Reflection-Absorption Spectroscopy of Al $_3$ Thin Film on Silver Surface Using Synchrotron Radiation³⁾

Infrared reflection-absorption spectra of Al $_3$ film on Ag surface have been measured as a function of thickness in the wave number region from 300 to 500 cm^{-1} using synchrotron radiation, UVSOR-II, to determine which of the geometrical isomers of Al $_3$ is dominant. The observed spectra of the Al-N stretching modes of Al $_3$ at around 420 cm^{-1} indicate that Al $_3$ film predominantly consists of the meridional isomer including the first monolayer adsorbed on the Ag surface as shown in Figure 3. In the spectrum of the monolayer Al $_3$, the Al-N stretching mode was observed to be located at wave number slightly lower than that of multilayer Al $_3$ probably due to the charge transfer between Al $_3$ and the Ag surface.

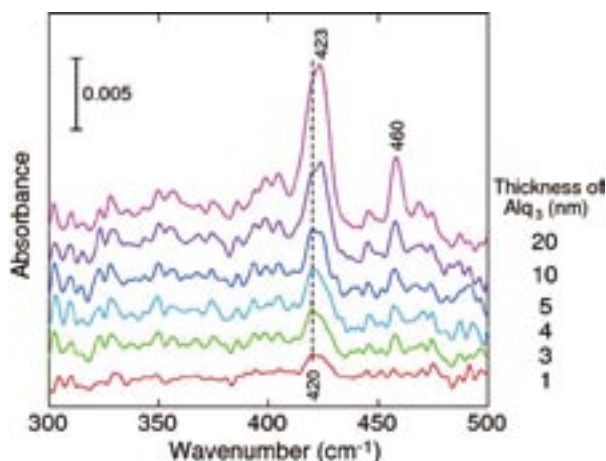


Figure 3. The thickness dependence of the IRAS spectra of an Al $_3$ film on Ag surface.

References

- 1) S. Kimura, J. Sichelschmidt, J. Ferstl, C. Krellner, C. Geibel and F. Steglich, *Phys. Rev. B* **74**, 132408 (4 pages) (2006).
- 2) T. Nishi, S. Kimura, T. Takahashi, H. J. Im, Y. S. Kwon, T. Ito, K. Miyagawa, H. Taniguchi, A. Kawamoto and K. Kanoda, *Phys. Rev. B* **75**, 014525 (5 pages) (2007).
- 3) Y. Sakurai, S. Kimura and K. Seki, *Appl. Phys. Lett.* **91**, 061922 (3 pages) (2007).

* Present Address; JAEA/SPring-8, Sayo, Hyogo 679-5148

† from Sungkyunkwan University, Korea

‡ from Nagoya University

§ carrying out graduate research on Cooperative Education Program of IMS with Nagoya University

|| Present Address; INAX Co. Ltd.

¶ carrying out graduate research on Cooperative Education Program of IMS with Meiji University

** Present Address; Department of Physics, Meiji University, Kawasaki 214-8571

†† carrying out graduate research on Cooperative Education Program of IMS with Kobe University

Electronic Structure and Decay Dynamics in Atoms and Molecules Following Core Hole Creation

UVSOR Facility
Division of Advanced Photochemistry



SHIGEMASA, Eiji
HIKOSAKA, Yasumasa
KANEYASU, Tatsuo
ITO, Masahiro

Associate Professor
Assistant Professor
IMS Fellow
Graduate Student*

The dynamics of the inner-shell photoexcitation, photoionization, and subsequent decay processes is much more complex, in comparison to outer-shell photo-processes. For instance, the inner-shell photoionization is concomitant with the excitation and ionization of valence electrons, which reveal themselves as shake-up and shake-off satellite structures in the corresponding photoelectron spectrum. The one-photon multi-electron processes, which are entirely due to the electron correlation in the system, are known to happen not only in the primary inner-shell hole creation processes, but also in their relaxation processes. Our research project is focused on elucidating the electronic structures and decay dynamics in core-excited atoms and molecules, by utilizing various spectroscopic techniques together with monochromatized synchrotron radiation in the soft x-ray region.

1. Dissociation Dynamics in Polyatomic Molecules Following Core Hole Creation

Auger electron-ion coincidence is a powerful method for studying the decay dynamics of core-excited/ionized molecules produced by soft x-ray irradiation. In order to exert the full potential of this method, the spectrometer should be equipped with a performance realizing analyses of vector correlations among the momenta of all the particles emitted. Coincidence imaging spectrometers, which enable us to measure three-dimensional momenta of both the electron and ions, have been widely used in the research field of atomic and molecular science. However it is difficult for such imaging technique to observe fast Auger electrons with a sufficient energy resolution. In this respect, a conventional electrostatic analyzer is suitable for observing the fast Auger electrons.

We have newly developed an Auger electron-ion coincidence spectrometer which consists of a double toroidal electron analyzer and a three-dimensional ion momentum

spectrometer.¹⁾ The performance has been evaluated by measuring Auger electrons and photoions emitted after inner-shell photoionization of OCS.

2. One-Photon Multi-Electron Emission Processes Studied by Multi-Electron Coincidence Spectroscopy

The double photoionization (DPI) of atoms and molecules has attracted special attention for a long time because this process is due entirely to electron correlation and, consequently, investigations of DPI reveal fundamental aspects of atomic and molecular physics. Until now, most DPI studies have concentrated on the removal of two valence electrons. Direct experimental observations of core-valence or core-core DPI are limited to a few cases. This is because investigations using conventional photoelectron spectroscopy offer neither direct spectroscopy of the doubly-ionized states nor the detailed DPI dynamics. By contrast, coincidence detection between the two photoelectrons emitted in DPI processes provides direct spectroscopic information on DPI processes; however, a sophisticated coincidence method is required, because the DPI cross section is unfavorable as compared with the main inner-shell ionization processes and, consequently, the events associated with these DPI processes are easily hidden behind ordinary inner-shell photoionization events. We have introduced a very efficient coincidence technique, the magnetic bottle time-of-flight electron coincidence method, into an investigation of DPI associated with the removal of a core electron. The powerful capabilities of this coincidence method on electron coincidence observations have recently been described.²⁻⁵⁾

A multi-electron coincidence dataset for Xe was accumulated at a photon energy of 301.6 eV.⁶⁾ Figure 1(a) shows the photoelectron spectrum in the kinetic energy range of 60–

250 eV, and Figure 1(b) displays a two-dimensional (2D) map showing coincidences between photoelectrons and slower electrons in the energy range 0–100 eV. Several diagonal stripes are observed on the 2D map. They are due to coincidences between two photoelectrons emitted through core-core or core-valence DPI. The intensity distributions along the diagonal stripes describe how the two photoelectrons produced from the DPI processes share the available energy. Resonance structures are discernable on the distributions: interactions and interference of the Xe^+ states with the DPI continua can be discussed from the resonance features.

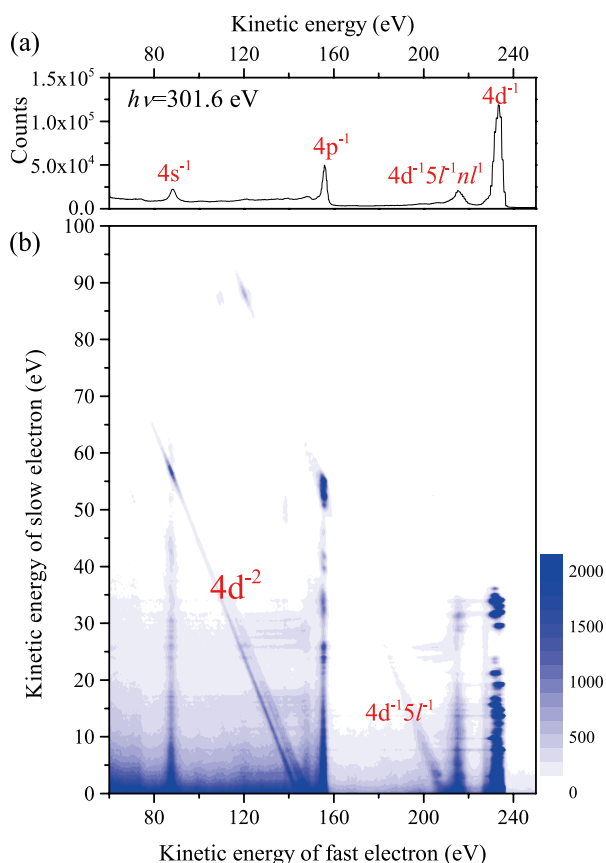


Figure 1. (a) Photoelectron spectrum of Xe obtained at a photon energy of 301.6 eV. (b) Two dimensional map of all coincidence pairs, represented as a function of the kinetic energies of fast and slow electrons.

3. Electronic Structures and Decay Dynamics in Multiply Excited States of Simple Molecules

Excitation of a core-electron in molecules can be accompanied by promotion of one or several valence electrons, due to the electron relaxation (valence polarization) and correlation effect. Such core-valence doubly or multiply excited states usually lie above the corresponding core ionization thresholds.

The doubly excited states of N_2 are exhibited on the photoabsorption spectrum in the photon energy range of 413–416 eV. We have performed an inner-shell photoelectron spectroscopic study of the autoionization of the core-valence doubly excited states.⁷⁾ The principal concern is the interplay between the autoionization from the doubly excited states and the femtosecond nuclear motion. The vibrational structure of the $\text{N}_2^+(1\sigma_{g/u}^{-1})$ states in photoelectron spectra manifests the relative rates for autoionization and nuclear motion.

In order to investigate all the autoionization features of the doubly excited states, we measured photoelectron spectra in the region of 412.5–417.3 eV with the photon energy intervals of 50 meV, at both 0° and 90° with respect to the electric vector. For an effective presentation of the obtained photoelectron spectra, 2D maps were used (Figures 2 (a) and (b)). The 2D maps show clearly that the vibrational features of the $\text{N}_2^+(1\sigma_{g/u}^{-1})$ states depends strongly on both photon energy and detection angle.

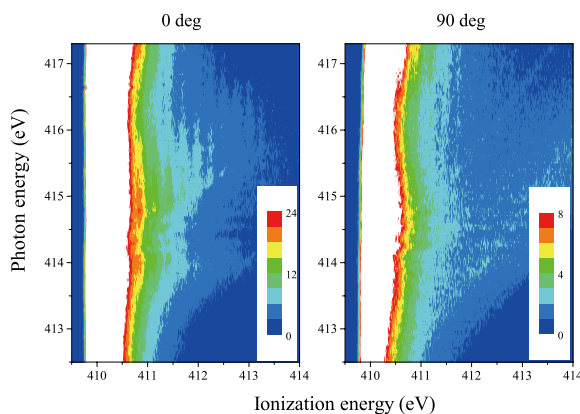


Figure 2. Two-dimensional maps of the inner-shell photoelectron yields from N_2 as a function of photon energy and ionization energy, measured in the photon energy region of 412.5–417.3 eV at (a) 0° and (b) 90° with respect to the electric vector.

References

- 1) T. Kaneyasu, Y. Hikosaka and E. Shigemasa, *J. Electron. Spectrosc. Relat. Phenom.* **156-158**, 279–283 (2007).
- 2) Y. Hikosaka, T. Aoto, P. Lablanquie, F. Penent, E. Shigemasa and K. Ito, *Phys. Rev. Lett.* **97**, 053003 (4 pages) (2006).
- 3) Y. Hikosaka, T. Aoto, P. Lablanquie, F. Penent, E. Shigemasa and K. Ito, *J. Phys. B* **39**, 3457–3464 (2006).
- 4) T. Kaneyasu, Y. Hikosaka, E. Shigemasa, F. Penent, P. Lablanquie, T. Aoto and K. Ito, *Phys. Rev. A* **76**, 012717 (7 pages) (2007).
- 5) Y. Hikosaka, T. Kaneyasu, E. Shigemasa, P. Lablanquie, F. Penent and K. Ito, *J. Chem. Phys.* **127**, 044305 (2007).
- 6) Y. Hikosaka, P. Lablanquie, F. Penent, T. Kaneyasu, E. Shigemasa, J. H. D. Eland, T. Aoto and K. Ito, *Phys. Rev. Lett.* **98**, 183002 (4 pages) (2007).
- 7) Y. Hikosaka, T. Kaneyasu, E. Shigemasa, Y. Tamenori and N. Kosugi, *Phys. Rev. A* **75**, 042708 (5 pages) (2007).

* carrying out graduate research on Cooperative Education Program of IMS with Niigata University

Micro Solid-State Photonics

Laser Research Center for Molecular Science
Division of Advanced Laser Development



TAIRA, Takunori
ISHIZUKI, Hideki
AKIYAMA, Jun
TSUNEKANE, Masaki
SATO, Yoichi
SAIKAWA, Jiro
OISHI, Yu
ONO, Yoko
INAGAKI, Yayoi

Associate Professor
Assistant Professor
IMS Fellow
Post-Doctoral Fellow*
Post-Doctoral Fellow
Post-Doctoral Fellow†
Post-Doctoral Fellow‡
Secretary
Secretary

The artistic optical devices should be compact, reliable, efficient and high power light sources. With the approaches of domain structures and boundaries engineering, it is possible to bring the new interaction in their coherent radiation. The high-brightness nature of Yb or Nd doped single crystal or ceramic microchip lasers can realize efficient nonlinear wavelength conversion. In addition, designed nonlinear polarization under coherent length level allows us new function, such as the quasi phase matching (QPM). The development of “*Micro Solid-State Photonics*,” which is based on the micro domain structure and boundary controlled materials, opens new horizon in the laser science.

1. High-Power Operation of Diode Edge-Pumped, Composite All-Ceramic Yb: Y₃Al₅O₁₂ Microchip Laser

A solid-state laser material of composite all-ceramic Yb: Y₃Al₅O₁₂ is applied as a source of a high-power, diode edge-pumped microchip laser. 520 W quasi-continuous-wave and 414 W continuous-wave (cw) output powers were obtained from the 3.7-mm-diameter, Yb doped ceramic core with a 200 μm thickness. The cw output power densities of 3.9 kW/cm² and 0.19 MW/cm³ in the core area and volume, respectively, are the highest for an active-mirror solid-state laser. The maximum thermal stress in the ceramic core is estimated to be 384 MPa at the non-cooled surface and is twice the tensile strength of single-crystal Y₃Al₅O₁₂. Figure 1 shows the input and output laser characteristics in quasi-cw (10 ms, 10 Hz) and cw operations of the composite all-ceramic Yb:YAG EPMCL.

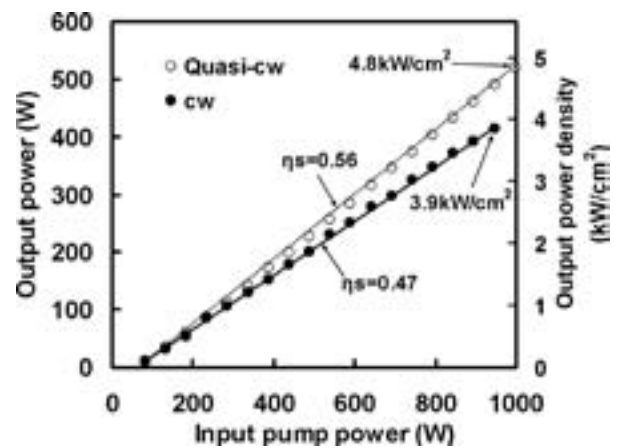


Figure 1. Incident pump power (peak) vs. laser output power (peak) of the edge-pumped all-ceramic EPMCL in quasi-cw and cw operations. The right axis shows output power density from the core area.

2. The Studies of Thermal Conductivity in GdVO₄, YVO₄, and Y₃Al₅O₁₂ Measured by Quasi-One-Dimensional Flash Method

We have measured thermal conductivity of Y₃Al₅O₁₂, GdVO₄, and YVO₄. In order to avoid the miss leading from three-dimensional (3D) thermal diffusion, we developed the quasi-one-dimensional (q1D) flash method. By taking in account the heat radiation effect in transparent materials for this measurement, YVO₄ was found to have larger thermal conductivity than GdVO₄. The measured thermal conductivities were 12.1, 10.5, 10.1, 8.9, and 8.5 W/mK for *c*-cut YVO₄, *c*-cut GdVO₄, YAG, *a*-cut YVO₄, and *a*-cut GdVO₄, respectively. The measured value in the range from room temperature to 200 °C is shown in Figure 2. The dependence of Nd-conductivity coefficient ($d\kappa/dC_{Nd}$) for convenient evaluation of the doping effect in thermal conductivity is also discussed.

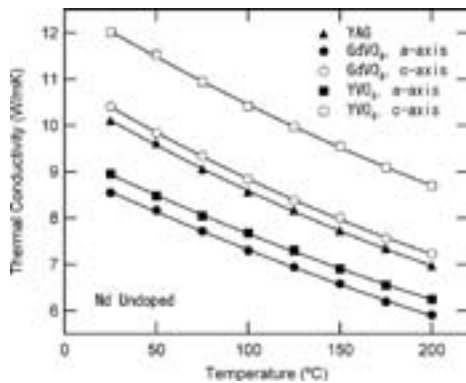


Figure 2. The measured value in the range from room temperature to 200 °C.

3. 52mJ Narrow-Bandwidth Degenerated Optical Parametric System with a Large-Aperture Periodically Poled MgO:LiNbO₃ Device

We have demonstrated efficient, high-energy, narrow-spectral-bandwidth 2.128 μ m pulse generation by use of periodically poled MgO:LiNbO₃ devices with a 36 mm length and 5 mm \times 5 mm large aperture. A free-running degenerated optical parametric oscillator (OPO) pumped with a Q-switched 1.064 μ m Nd:YAG laser exhibits a high slope efficiency of 75% and an optical-to-optical conversion efficiency of 70% with a broad spectral bandwidth (> 100 nm). In a configuration with a spectrally narrowed master oscillator followed by a power amplifier, we have achieved an output pulse energy of 52 mJ with a spectral bandwidth of less than 2 nm at the degeneracy point. The total optical-to-optical conversion efficiency of the system reached 50%.

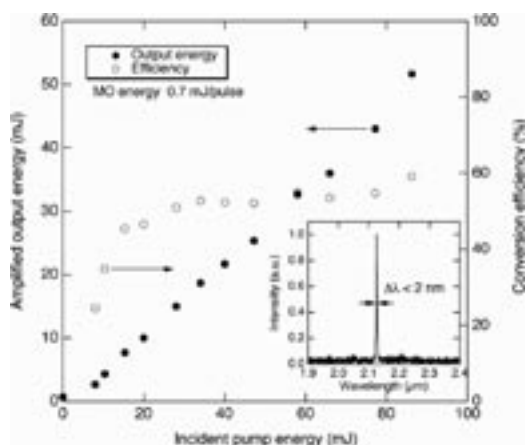


Figure 3. OPA output energy and conversion efficiency versus incident pump energy. The MO energy was 0.7 mJ/pulse. Closed circles, amplified pulse energy; open circles, conversion efficiency.

4. Tailored Spectral Designing of Layer-by-Layer Type Composite Nd:Y₃ScAl₄O₁₂/Nd:Y₃Al₅O₁₂ ceramics

We have fabricated the all-ceramic layered composite device with Nd:YAG and Nd:YSAG, which can perform efficient laser oscillation. From its spectroscopic properties, this layer-by-layer composite device will offer new function of laser oscillation by pump wavelength tuning. For example when pumped from YSAG side at 810.5 nm, it can oscillate at 1064 nm. On the other hand, it will oscillate at 1061 nm when pumped at 808.5 nm.

Due to the difference in the dependence on the wavelength of, the portion of the pumped power absorbed in Nd:YAG-layer and in Nd:YSAG-layer depends on the pumping wavelength. This resulted in the tuning of the component ratio of the Nd:YAG and Nd:YSAG in the fluorescence. The dependence of fluorescence profiles in this composite on the pump wavelength is shown in Figure. 4.

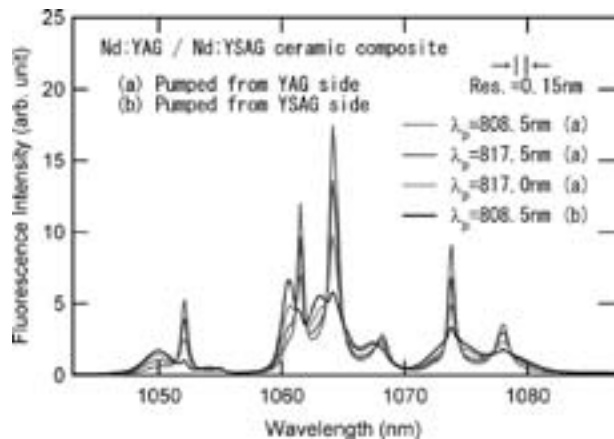


Figure 4. Measured fluorescent spectral profiles by changing pumping wavelength.

References

- 1) M. Tsunekane and T. Taira, *Appl. Phys. Lett.* **90**, 121101 (3 pages) (2007).
- 2) Y. Sato and T. Taira, *Opt. Express* **14**, 10528–10536 (2006).
- 3) J. Saikawa, M. Fujii, H. Ishizuki and T. Taira, *Opt. Lett.* **31**, 3149–3151 (2006).
- 4) Y. Sato, A. Ikesue and T. Taira, *IEEE J. Sel. Top. Quantum Electron.* **13**, 838–843 (2007).

* from JST Innovation Plaza Tokai

† from Tokyo Institute of Technology

‡ from RIKEN

Photo-Induced Dynamics and Reactions at Solid Surfaces

Laser Research Center for Molecular Science
Division of Ultrahigh Resolution Optical Measurement



MATSUMOTO, Yoshiyasu	Professor
WATANABE, Kazuya	Assistant Professor
MATSUMOTO, Taketoshi	Assistant Professor*
NAKAI, Ikuyo	Post-Doctoral Fellow†
FUYUKI, Masanori	Graduate Student‡

Solid surfaces provide an interesting environment where two completely different electronic systems meet to each other: localized electronic system, *i.e.*, atoms and molecules and delocalized one, *i.e.*, solid bulk surfaces. Charge transfer at surfaces is fundamental to adsorbate-metal interactions and reactions. Moreover, dynamic processes including chemical reactions on surfaces, particularly metal surfaces, are associated with continuous nonadiabatic transitions. This research program aims for understanding electron and nuclear dynamics at surfaces. Photo-induced processes including photochemistry at surfaces are the major focus in this program. Photons are used for not only exciting electronic states of adsorbate and substrate, but also for probing those states with various types of nonlinear optical spectroscopy.

1. Ultrafast Dynamics at Well-Defined Surfaces¹⁻³⁾

To understand the mechanism of surface photochemistry, it is vital to know how photoinduced electronic excitation induces adsorbate nuclear motions that ultimately lead to chemical reactions. We have demonstrated the real-time observations of surface phonons and adsorbate-substrate vibrational modes by fs time-resolved second harmonics generation (TRSHG). If an excitation light pulse has a duration sufficiently shorter than a period of a vibrational mode or a phonon mode, it can excite the mode with a high degree of temporal and spatial coherence. This coherent nuclear motion modulates the second-order susceptibility $\chi^{(2)}$. Thus, by monitoring the intensity modulation of the second harmonics (SH) generation of a probe pulse, we can observe the evolution of the coherent nuclear motion subsequent to the electronic excitation at the surfaces. We have focused on K on Pt(111), and Na and K on Cu(111) adsorption systems.

We have investigated coherently excited surface phonons at K-covered Pt(111) surfaces by using femtosecond time-resolved second harmonic generation spectroscopy. The frequency of the K–Pt stretching phonon mode depends on the superstructure of K: 5.0–5.3 and 4.5–4.8 THz for (2×2) and

($\sqrt{3}\times\sqrt{3}$)R30° superstructures, respectively. In addition to the stretching mode, a couple of Pt surface phonon modes are simultaneously observed when the ($\sqrt{3}\times\sqrt{3}$)R30° superstructure is formed. The dephasing time of the K–Pt stretching mode becomes shorter and its frequency redshifts as the absorbed fluence of a pump pulse increases. This is in stark contrast to the Pt surface phonon modes whose frequencies are independent of fluence. The fluence dependence of the K–Pt stretching mode is interpreted to be due to anharmonic coupling between the K–Pt stretching and lateral modes.

We have also observed time-resolved second harmonic signals from the Cu(111) surface with a full monolayer of Na in ultra-high vacuum and investigated the excitation-wavelength dependence of the wave packet dynamics of the coherently excited Na–Cu stretching mode. Changing the photon energy of the pump pulse (25 fs) from 2.0 to 2.5 eV, the oscillation amplitude derived from the Na–Cu stretching motion is enhanced. The careful measurements of photon-energy dependence indicates that the excitation efficiency mimics the absorbance of bulk Cu. Holes created in the d-bands by the optical transitions could be filled by electrons in the adsorbate-induced occupied state of the metallic quantum well by an Auger-type transition. Hence, holes can be created in the adsorbate-induced occupied state. Moreover, since this Auger decay can occur significantly faster than the oscillation period of the Na–Cu stretching mode, the substrate excitation may be a possible excitation mechanism for the coherent oscillation.

2. Spectroscopy and Chemistry of Metal Nanoclusters on Surfaces⁴⁾

The structure and reactivity of metal nanoclusters are important issues because of their relevance to heterogeneous catalysis. In particular, Au nanoclusters on titanium oxide surfaces has attracted a lot of interest since the discovery of its catalytic activity on CO oxidation. We apply various surface science techniques to clarify correlations between structures and reactivity of metal nanoclusters deposited on surfaces. We

use alkanethiolate-coated gold nanoclusters as a primary target in collaboration with Tsukuda (IMS) and Al-Shamery (U. Oldenburg) groups.

Deposition and fabrication of films of Au nanoclusters protected by alkanethiolate ligands are attempted on a TiO₂ (110) surface and the structures of films are observed by a scanning tunneling microscope (STM). Effects of oxygen- and hydrogen-plasma etching in addition to UV irradiation on the structure and chemical composition of the films are also investigated by using STM and X-ray photoelectron spectroscopy. Alkanethiolate Au nanoclusters are produced using a modified Brust synthesis method and their LB films are dip-coated on TiO₂(110). Alkanethiolate Au nanoclusters are weakly bound to the substrate and can be manipulated with an STM tip. Net-like structures of alkanethiolate Au nanoclusters are formed by a strong blast of air. Oxygen plasma etching removes alkanethiolate ligands and simultaneously oxidizes Au clusters. At room temperature, prolonged oxygen plasma etching causes agglomeration of Au nanoclusters. UV irradiation removes ligands partly, which makes Au nanoclusters less mobile. The net-like structure of alkanethiolate Au clusters produced by a blast of air is retained after oxygen- and hydrogen-plasma etching.

3. Observation of Spatial Patterning by a Sum Frequency Generation Microscope

For understanding of heterogeneous reactions on solid surfaces, it is crucial to obtain how reactions evolve in time and spatial domains. For this purpose, a new microscope for observation of spatial patterning of reactants and products at surfaces is needed. It is highly desirable that the microscope is capable to identify chemical species.

Sum frequency generation (SFG) is a nonlinear optical process. In particular, when visible and infrared beams are used, SFG is a powerful means for vibrational spectroscopy.

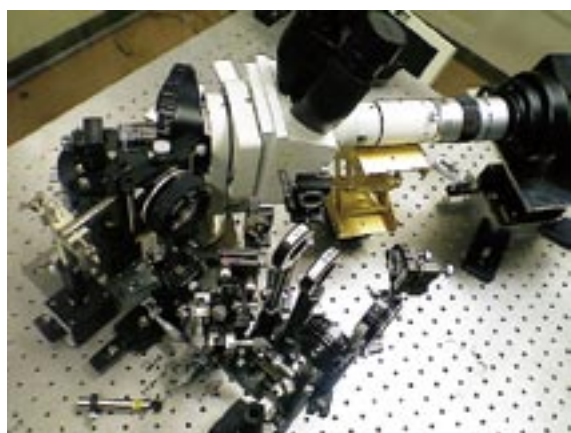


Figure 1. Setup of the sum frequency generation microscope.

Thus, we are developing a SFG microscope. So far, the first prototype of a microscope (Figure 1) has been built and micro-patterns of self-assembled monolayer have been observed. The spatial resolution of the current microscope is about 5 μm .

4. Chemistry of One-Dimensional Nano-Surface Compounds

The fluctuating configurations of low-dimensional structures can be thermodynamically favorable at finite temperatures, because the energy gain overcomes the energy cost that accompanies local structural fluctuation. In particular, one-dimensional (1D) systems have a propensity to be sensitive to these fluctuations as described by one of the maxims of condensed matter physics, *i.e.*, one chain does not make a crystal. Thus, the dynamical formation of active species and sites by these fluctuations is a key factor in establishing a microscopic model for chemical reactions at surfaces and nano-structured compounds. It is well known that the adsorption of O on Ag(110) results in the formation of quasi-1D structures, AgO chains, accompanied by the mass transfer of substrate atoms.

AgO chains arrange periodically to form $(n \times 1)$ ($n = 2 \sim 7$) depending on the fractional O coverage due to repulsive inter-chain interactions. On the added-row reconstructed Ag(110) $(n \times 1)$ -O surfaces, one-dimensional $-\text{Ag}-\text{O}-\text{Ag}-\text{O}-$ chains arrange periodically. Scanning tunneling microscopy was used for studying spatiotemporal evolution of the disproportionation reaction of H₂O with O adatoms on oxidized Ag(110) surfaces where quasi-one dimensional AgO chains form ordered structures. Initially the reaction takes place slowly on Ag(110)- (5×1) O at the end of AgO chain, whereas the reaction accelerates explosively upon the appearance of a chemical wave that propagates along the direction perpendicular to the chain. The surface morphology of the region swept over by the chemical wave completely changes from (5×1) -O to that with many rectangular islands, indicating the formation of H₂O (OH)₂. The induction time and explosive acceleration with the propagating chemical wave imply that the reaction is autocatalytic. Water clusters hydrating OH produced likely play a central role in serving as a reservoir of H₂O to feed to the reaction and enhancing the reactivity of H₂O with O adatoms in AgO chains.

References

- 1) M. Fuyuki, K. Watanabe and Y. Matsumoto, *Phys. Rev. B* **74**, 195412 (6 pages) (2006).
- 2) Y. Matsumoto, *Bull. Chem. Soc. Jpn.* **80**, 842–855 (2007).
- 3) Y. Matsumoto and K. Watanabe, *Chem. Rev.* **106**, 4234–4260 (2006).
- 4) T. Matsumoto, *et al.*, *Surf. Sci.* doi:10.1016/j.susc.2007.04.157

* Present Address; Osaka University, The Institute of Scientific and Industrial Research, Osaka 567-0047

† Present Address; Kyoto University, Graduate School of Sciences, Department of Chemistry, Kyoto 606-8502

‡ Present Address; Genesis Research Institute, Inc. Chiba 272-0001

Visiting Professors



Visiting Professor
KITAJIMA, Masahiro (*from National Institute for Materials Science*)

Electron-Phonon Interaction Dynamics and Optical Control of the Coherent Optical Phonons

We are studying on coherent phonons in metals and semiconductors, using fs pump-probe techniques. Our main interest is to know how excited carriers are coupled with the phonons coherently. We have recently started investigating optical control of coherent phonons in semimetals by using a pair of fs laser pulses whose relative timing is tuned on the attosecond time scale. This new challenge is being collaborated with the Prof. Ohmori's group of IMS, and would serve as a powerful tool for understanding the fundamental mechanism of the interaction between a photo-excited single particle and the constituents of the surrounding lattice.



Visiting Associate Professor
BABA, Masaaki (*from Kyoto University*)

Excited-State Structure and Dynamics of Isolated Molecules

Excited-state dynamics such as internal conversion (IC) to the ground state, intersystem crossing (ISC) to the triplet state, intramolecular vibrational redistribution (IVR), and predissociation are of great interest because these radiationless transitions are closely related to the energy level scheme and break down of Born-Oppenheimer or adiabatic approximation. Rotationally resolved ultrahigh-resolution laser spectroscopy is powerful to investigate not only the accurate level energies, but also the lifetime, magnetic moment, and coherence of the isolated molecules in a supersonic jet. These properties are very important to understand the origin of dynamical processes in the electronic excited state.



Visiting Professor
SODA, Kazuo (*from Nagoya University*)

Electronic Structure of Bulk Metallic Glasses and Heusler-Type Alloys

The electronic structures and their correlation with functional properties of bulk metallic glasses and Heusler-type Fe-based alloys have been investigated by means of photoelectron spectroscopy and photoabsorption spectroscopy with use of synchrotron radiation as a light source in order to clarify the origins of their fascinating functional properties. Bulk metallic glasses is bulky multi-component amorphous alloys, possessing useful engineering properties in spite of their thermodynamically metastable phase, while Heusler-type Fe-based alloys are promising thermoelectric materials, showing high mechanical strength and larger power factor than a conventional Bi-Te semiconductors.



Visiting Associate Professor
OKADA, Kazumasa (*from Hiroshima University*)

Study on the Fragmentation of Molecules and Clusters in the Inner-Valence and Inner-Shell Electron Excitation Regions

The knowledge of the mechanisms involved in the ionization helps us to understand various processes in which there exists interaction of molecules and photons or electrons. The fragmentation dynamics of highly-excited or multiply-ionized molecules and clusters is studied by means of time-of-flight mass spectrometry. Multiple modes of measurement are used to obtain branching ratios of fragment ions or breakdown diagrams. Kinetic energy distribution of fragments provides insight into the nature of the fragmentation process.



RESEARCH ACTIVITIES

Materials Molecular Science

Extensive development of new molecules, molecular systems and their higher-order assemblies is being conducted in the four divisions and in the research center for molecular scale nanoscience. Their electronic, optical and magnetic properties as well as reactivities and catalytic activities are being examined in an attempt to discover new phenomena and useful functions.

Structures and Functions of Metal–Carbon Nano-Systems Produced from Metal-Acetylides

Department of Materials Molecular Science
Division of Electronic Structure



NISHI, Nobuyuki
JUDAI, Ken
NISHIJO, Junichi
OISHI, Osamu
MATSUMOTO, Chie
FURUYA, Ari
NUMAO, Shigenori
UBAHARA, Wakana

Professor
Assistant Professor
Assistant Professor
Technical Associate
IMS Fellow
Post-Doctoral Fellow
Graduate Student
Secretary

Metal acetylides or metal ethynyl compounds are made of the M^+-C^- ionic bonds. However, the ionic states of the acetylides are essentially metastable resulting in the segregation into metal-carbon or metal-organic polymer nanophases. This segregation still maintains M^+-C^- ionic bonds around the interfaces of the metal wire, particles, and dendric sponges exhibiting various functions depending on the metal species.

1. Increased Electric Conductance through Physisorbed Oxygen on Copper Nanocables Sheathed in Carbon

Solid gas sensors, which are operated at high temperature, are normally based on chemisorption for modification of the electronic band conduction. Sensing of O_2 has been widely investigated. Recent advances in nanotechnology allow O_2 sensors, such as carbon nanotubes, to work at lower temperatures. We found that copper nanocables sheathed in carbon can detect physisorbed O_2 at room temperature by just measuring electric resistance. We have recently reported a low-cost, simple, and large-scale production method of nanowires involving the self-assembly of copper acetylide (Cu_2C_2) molecules in an aqueous solution. The conductance of a pressed tablet of nanocables fabricated by annealing Cu_2C_2 nanowires varies reversibly with adsorption and desorption of O_2 at room temperature.

Cu_2C_2 nanocables consist of metallic Cu nanowires sheathed in amorphous carbon layers. It is very simple to produce a sensor using Cu_2C_2 nanocables. Current-voltage (I - V) measurement of the Cu_2C_2 nanocables was carried out under O_2 - N_2 gas mixtures with a total pressure of 1 atm. The Cu_2C_2 nanocables exhibited an ohmic, proportional I - V character. The constant voltage used for the measurement was typically 1 V. Figure 1 shows the transient conductivity on the Cu_2C_2 nanocables obtained by alternately exposing the nanocables to pure O_2 (1 atm) and pure N_2 (1 atm) gas. The conductance more than doubled during the 10-min O_2 expo-

sure, and recovered reversibly during the subsequent N_2 exposures. It must be noted that the reversible fluctuations in conductance were observed at room temperature. The presence of the charged species changes the semiconductor's Fermi level and the conduction of carriers. However, reversible absorption and desorption cycles at room temperature are generally believed to involve physisorption of molecules. Physisorption of O_2 , which is not accompanied by charge transfer, is extremely unlikely to modify the electronic band structure for sensing by conductance.

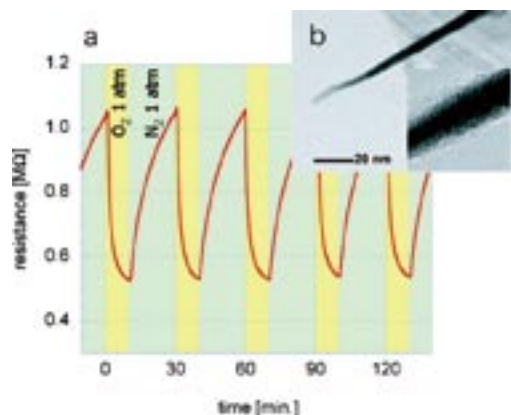


Figure 1. a: Reversible changes in Cu_2C_2 nanocable conductivity. The resistance of the Cu_2C_2 nanocables decreased under O_2 . b: TEM image of a Cu_2C_2 nanocable.

2. Template-Free Fabrication of One-Dimensional Ag Nanoparticle Arrays

Development of a new facile preparation method of one-dimensional (1D) metal nanoparticle (NP) arrays is significant for both application and fundamental studies. We demonstrate a new facile and mass productive fabrication method for diameter-controlled 1D NP arrays *via* decomposition of silver phenylacetylide [$Ag-C\equiv C-Ph$] nanowires. The ligand dissocia-

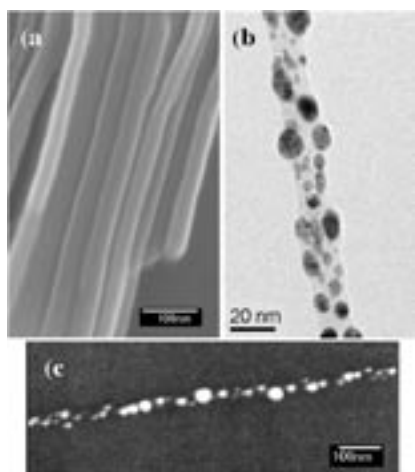


Figure 2. (a) SEM image of [Ag-C≡C-Ph] nanowires separated from EtOH. (b) TEM image of UV irradiated nanowire. (c) SEM image of nanowire after 1h of UV.

tion of [Me₃P-Ag-C≡C-Ph] in a polar solvent gives [Ag-C≡C-Ph] nanowires as shown in Figure 2a. The average diameter of nanowires depends on the solvent: for examples, using MeOH and 1-BuOH gives nanowires with the average diameter of 30 and 100 nm, respectively. The nanowire is easily decomposed into

an assembly of Ag NPs embedded in a polymerized phenylacetylene matrix by UV irradiation or heating thanks to the strong reducing power of ethynyl anions. The transmission electron microscope (TEM) image of UV irradiated nanowire is shown in Figure 2b. It is obvious that a nanowire is converted into an assembly of Ag NPs after irradiation, whereas the wire shape of an assembly is kept by polymerized phenylacetylene. The NP arrays can be easily fixed on the substrate by heating the nanowire above 150 °C under vacuum after 1 h of UV irradiation as shown in Figure 1c, where the surface of each Ag NP is covered with thin layer of polycyclic aromatic hydrocarbons.

3. Dendric Nano-Sponge of Silver Acetylide (Ag₂C₂) and Its Conversion to Silver Dendric-Skeletons Sheathed in Carbon Mantle

In contrast to the wire-type nano-structure formation of copper acetylide, silver acetylide (Ag₂C₂) produces nano-sponge composed of dendric nano-rods with diameters of 20–30 nm under a certain synthetic condition as seen in Figure 3. Annealing at a temperature lower than 85 °C exhibits the segregation into inner silver and outer carbon with maintaining the dendric shape. This heating procedure in vacuum sometimes causes explosive reaction when the temperature of the powder increases this upper limit. Nitric acid treatment removes metallic silver but remains carbon and a small amount of silver strongly bound to carbon. EDS and TGA spectra of this sample revealed the presence of the remaining metallic silver. BET area (number of molecules adsorbed \times area per an N₂ molecule) is estimated to be 157 m²/g from the BET adsorption isotherm equation for the acid treated sample.

Although the characterization of the residual silver remains, we expect high catalytic activities of the silver on the carbon sponge with mesopore structures.

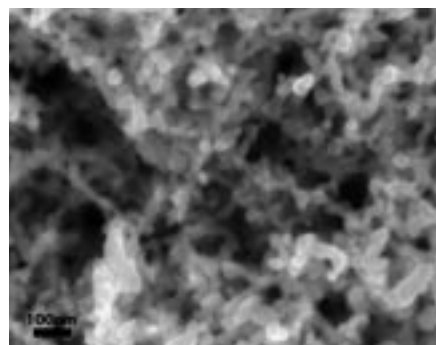


Figure 3. SEM image of the dendric nano-sponge structure of crystalline Ag₂C₂.

4. Hollow Graphitic Nano-Polyhedrons Produced from Silver Acetylide (Ag₂C₂)

A thoughtful graduate student can sometimes have a chance to change a bad accident to a very lucky discovery of a new material. The student performed the explosive reaction in a glass tube situated in a vacuum and collected the carbon product left inside the tube. Silver was evaporated and coated a mirror film inside the inner surface of the glass tube. Then he observed the TEM images of the carbon products. What he saw is the carbon onion type graphitic nano-structures with large empty holes, as shown in Figure 4. Strangely or reasonably, most of graphite layers are straight with bent corners with angles 90° ~ 120°. The SEM image in Figure 4-d shows the polyhedron balls of 20–100 nm. The presence of many defects (holes and layer mismatchings) in the graphitic shells suggests the potentials for gas storage.

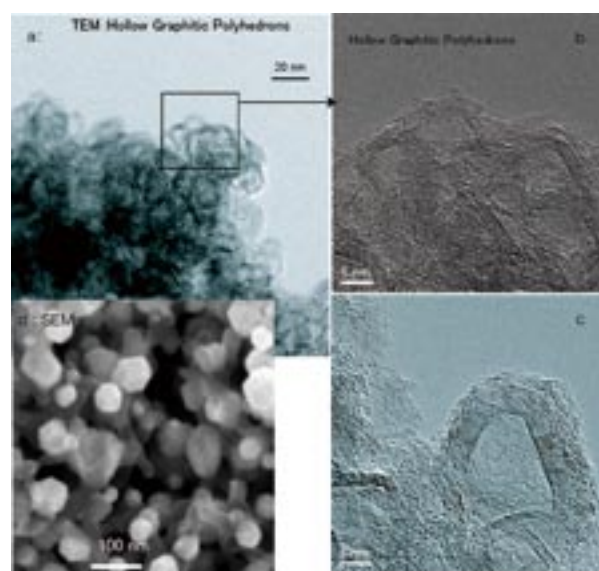


Figure 4. a: TEM image of Hollow Graphitic Polyhedrons. The part in the black frame is expanded in b. c: Another expanded TEM image exhibiting imperfect graphitic shells. d: SEM image of the samples.

Award

NISHIJO, Junichi; Excellent Presentation Award, 87th Spring Meeting of Chemical Society of Japan.

Characterization of Magnetic Ultrathin Films by Novel Spectroscopic Methods

Department of Materials Molecular Science
Division of Electronic Structure



YOKOYAMA, Toshihiko
NAKAGAWA, Takeshi
MA, Xiao-Dong
NOTO, Madomi

Professor
Assistant Professor
Graduate Student*
Secretary

Novel properties of magnetic metal ultrathin films have been attractive both from fundamental interest and from technological requirements. We are interested in drastic modification of metal thin films by surface chemical treatment such as adsorption-induced spin transitions and morphological changes. The magnetic properties are characterized by means of several kinds of spectroscopic methods like MOKE (Magneto-Optical Kerr Effect) using lasers and XMCD (X-ray Magnetic Circular Dichroism) using synchrotron radiation. Moreover, we are exploiting a new technique of ultraviolet (UV) magnetic circular dichroism (MCD) photoelectron emission microscopy (PEEM) in order to perform spatiotemporal magnetic imaging.

1. Enhanced Photoemission Magnetic Circular Dichroism Using Free Electron Laser at UVSOR-II

In 2006, we discovered surprising enhancement of the visible/ultraviolet photoemission MCD when the photon energy was tuned to the work function threshold.¹⁾ In the previous experiments, we employed Cs-coated films in order to reduce and control the work function of the magnetic thin film samples. It is essentially important to verify the enhancement of the photoemission MCD of the pure metal thin films without Cs deposition for the exclusion of some possible Cs-induced changes of the electronic structure. In this work, we have measured a magnetization curve of clean Ni films on Cu(001) by using a free electron laser (FEL) at UVSOR-II that is tunable and extremely intense.²⁾

Figure 1(a) shows the magnetization curve of 8 monolayer (ML) Ni on Cu(001) obtained by the total photoemission MCD measurement in the applied external magnetic field using the FEL,³⁾ whose photon energy was tuned around the work function of Ni. The MCD asymmetry, defined as $(I_{\text{left}} - I_{\text{right}})/(I_{\text{left}} + I_{\text{right}})$ where I_{left} and I_{right} are the photoemission intensities using left- and right-circularly polarized lights, respectively, is found to be $\pm 5\%$. The value is around two orders of magnitude more intense than the conventional

MOKE measurement, as in our previous observations.¹⁾ Moreover, we have measured a photoemission MCD magnetization curve of Gd-coated Ni on Cu(001) by using a HeCd laser. The work function is again close to the photon energy. The result is shown in Figure 1(b). A similar enhancement of the photoemission MCD was observed.

We have consequently confirmed that the enhancement of photoemission MCD around the work function threshold is a universal behavior, applicable to photoelectron emission microscopy. This work was carried out in collaboration with the UVSOR machine group of Prof. M. Kato and Dr. M. Hosaka (present affiliation: Nagoya University).

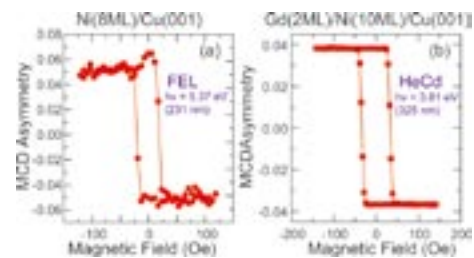


Figure 1. Photoemission MCD magnetization curves of Ni on Cu(001). (a) Clean 8 ML Ni using FEL at UVSOR-II and (b) 2 ML Gd coated 10 ML Ni using a HeCd laser. Both the films show the work functions close to the photon energies.

2. Novel Magnetic Microscope: Ultraviolet Magnetic Circular Dichroism Photoelectron Emission Microscopy

The enhancement of the photoemission magnetic circular dichroism in the UV region paves a new way to develop UV MCD PEEM for the investigation of nanostructured magnetism. At present, MCD PEEM is performed as XMCD PEEM using third-generation synchrotron radiation X-ray sources. UV MCD PEEM allows us to do in-laboratory experiments when tunable deep UV lasers are available. Moreover, when ultrashort pulsed lasers are employed, pump-and-probe UV MCD PEEM measurements provide us a time resolving

power of ~ 100 fs rather easily, which is two to three orders of magnitude faster than the present standard experiments using the third-generation synchrotron radiation sources. In the present experiment, we have constructed an UV laser PEEM apparatus and have successfully observed the first UV MCD PEEM images of the ultrathin film.²⁾

Figure 2 (left) is our UV MCD PEEM apparatus. In this experiment, as we had no deep UV lasers available, the Ni films was coated with Cs to match the work function to the photon energies of the employed UV lasers. A right panel of Figure 2 shows the magnetic image of the Cs-coated 12 ML Ni film on Cu(001) using a Ti:sapphire laser (second harmonics 400 nm). The image was given by the subtraction between the two images obtained by using the left- and right-circularly polarized lights. Beautiful magnetic domains can be seen; the light and dark areas are ascribed to the downward and upward magnetizations, respectively. This is the first observation of the UV MCD PEEM of the ultrathin film; although the UV MLD PEEM images (MLD: Magnetic Linear Dichroism) have been already reported, the results was given for a thick Fe film of 100 nm, and the contrast is only 0.19%.⁴⁾

We have succeeded in the observation of two-photon MCD PEEM of the same sample using a Ti:sapphire fundamental light (800 nm). Preliminary pump-and-probe data were also obtained with the time resolution of ~ 100 fs, which show the magnetization recovery with the time evolution. The experiments are in progress in collaboration with Prof. Y. Matsumoto (present affiliation: Kyoto University) and Dr. K. Watanabe.



Figure 2. (left) Photo of our UV MCD PEEM apparatus (Elmitec, PEEMspector) and (right) UV MCD PEEM image of Cs-coated 12 ML Ni on Cu(001), taken using the second-order harmonics of a Ti:sapphire laser (400 nm). In inset, the magnetization curve of a similar film is also shown.

3. Magnetism of Self-Assembled Co Nanorods Grown on Cu(110)-(2x3)N

Magnetic properties of low dimensional magnets has recently attracted much interest due to their importance for further dense magnetic recording media. From the view point of fundamental physics, these materials are interesting for their magnetic anisotropy, Curie/blocking temperature. In this work, we have investigated structural and magnetic properties of self-assembled Co nanorods⁵⁾ with ~ 1 nm thick grown on Cu(110)-(2x3)N. This work was performed in collaboration with Prof. F. M. Leibsle (University of Missouri, Kansas, U. S.

Award

NAKAGAWA, Takeshi; SSSJ Young-Researcher Lecture Award, The Surface Science Society of Japan (2006).

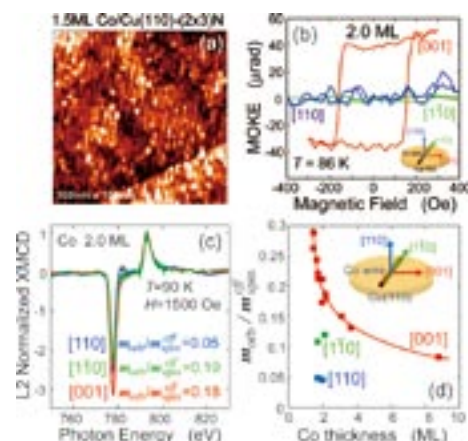


Figure 3. (a) STM image ($100 \text{ nm} \times 100 \text{ nm}$) of Co (1.5 ML equivalence) nanorods on Cu(110)-(2x3)N. (b) Angular dependent magnetization curves of 2.0 ML Co by longitudinal and polar MOKE. (c) Angular dependence of the Co L -edge XMCD spectra normalized to the L_{II} -edge peak at ~ 793 eV. (d) Thickness dependence of the relative orbital magnetic moment at 90 K.

A.) and Prof. M. Przybylski (Max-Planck Institut, Halle, Germany).

Figure 3(a) shows the STM images. The Co rods grows with the (1×6) periodicity. The superstructure is consistent with the LEED pattern. From the Auger electron spectra (no figure) it is found that the N atom is located always at the top of the surface in spite of Co deposition on the Cu(110)-(2x3)N surface. Magnetic properties have been characterized by MOKE and XMCD. Figure 3(b) shows the angular dependence of MOKE. A hysteresis loop was seen only along the [001] axis that is perpendicular to the rod axis within the surface plane. The magnetic easy axis is thus [001], which is interesting since macroscopic magnetic rods are likely to make their magnetization along the rod axis. In order to reveal the origin of the easy axis perpendicular to the rod axis, the Co L -edge XMCD spectra were recorded. Figure 3(c) shows the spectra. By comparing the relative intensity of the L_{III} -edge peak (~ 778 eV), one can find the sequence of the orbital magnetic moments m_{orb} as $[001] > [1\bar{1}0] > [110]$. This implies that the spin-orbit interaction determines the magnetic easy axis. It is also found that below the Co thickness of 2 ML, the orbital magnetic moment is enhanced drastically. This supports the [001] magnetic easy axis in the present nanorods.

References

- 1) T. Nakagawa and T. Yokoyama, *Phys. Rev. Lett.* **96**, 237402 (2006).
- 2) T. Nakagawa, T. Yokoyama, M. Hosaka and M. Katoh, *Rev. Sci. Instrum.* **78**, 023907 (2007).
- 3) M. Hosaka *et al.*, *Nucl. Instrum. Methods Phys. Res., Sect. A* **483**, 146 (2002).
- 4) G. K. L. Marx *et al.*, *Phys. Rev. Lett.* **84**, 5888 (2000).
- 5) S. M. York and F. M. Leibsle, *Phys. Rev. B* **64**, 033411 (2001).

* Present Address; Max-Planck-Institut für Mikrostrukturphysik, Weinberg 2, 06120 Halle, Germany

Structure and Properties of Metal Clusters Protected by Organic Molecules

Department of Materials Molecular Science
Division of Electronic Structure



TSUKUDA, Tatsuya	Associate Professor
NEGISHI, Yuichi	Assistant Professor
CHAKI, Nirmalya K.	IMS Fellow
TSUNOYAMA, Hironori	Post-Doctoral Fellow
YANAGIMOTO, Yasushi	Post-Doctoral Fellow
SHICHIBU, Yukatsu	Post-Doctoral Fellow
NAKAO, Satoru	Post-Doctoral Fellow
UBAHARA, Wakana	Secretary

1. Extremely High Stability of Glutathionate-Protected Au₂₅ Clusters against Core Etching¹⁾

It is well known that so-called magic-numbered clusters can be preferentially populated by dissociative excitation of larger precursors, because the energy required for removal of a single atom from a magic-numbered cluster is higher than from a neighbor. Thus, if the Au atoms can be removed sequentially from preformed thiolated-protected gold (Au:SR) clusters, one can anticipate a population growth of certain stable Au_n:SR clusters. Chemical etching by free thiols is one feasible method for core size reduction of the Au:SR clusters. The etching rate of Au_n:SR clusters must be determined as a function of core size, in order to provide a synthesis for well-defined Au_n(SR)_m clusters in large quantity, as well as to provide information regarding the stability of Au_n(SR)_m. In the present paper, we studied etching reactions of Au_n(SG)_m clusters with (n,m) = (10,10), (15,13), (18,14), (22,16), (25,18), (29,20), (33,22), (39,24) by free glutathione (GSH). It was found that Au₂₅:SG clusters show higher stability against etching than the others and as a result two different reaction modes are operative depending on the core size. The Au_n(SG)_m (n < 25) clusters are completely oxidized to Au(I):SG complexes while Au_n(SG)_m (n ≥ 25) clusters are etched into Au₂₅:SG by free GSH molecules. On the basis of this observation, a model is proposed to explain our recent finding that Au₂₅(SG)₁₈ clusters are selectively formed during the reaction of triphenylphosphine-stabilized Au₁₁ clusters and an excess amount of GSH.

2. Formation of Alkanethiolate-Protected Gold Clusters with Unprecedented Core Sizes in the Thiolation of Polymer-Stabilized Gold Clusters²⁾

We have investigated magic-number sequences of octadecanethiolate-protected gold (Au:SC₁₈) clusters obtained by thiolation of gold clusters stabilized by poly(*N*-vinyl-2-pyr-

rolidone) (PVP). The Au:SC₁₈ clusters were prepared by the reaction of C₁₈SH and PVP-stabilized Au clusters. Four samples were fractionated by recycling size exclusion chromatography (SEC) of the as-prepared Au:SC₁₈ clusters, and their core sizes were determined to be 8, 11, 21, 26 kDa by using laser desorption ionization mass spectrometry. Unexpectedly, the sequence of these core sizes is different from that (8, 14, 22, and 29 kDa) obtained by conventional reduction of Au(I)-SC₁₈ polymers, which is governed by kinetic factors. The present finding shows that the Au:SR (R = organic group) clusters with a high tolerance to thiol etching can be systematically synthesized by first populating precursory Au clusters in a PVP matrix with subsequent thiolation of the preformed Au clusters. Optical spectroscopy shows that the electronic structure changes drastically with a core size in the size range between *ca.* 40 and *ca.* 140 atoms.

3. Thiolate-Induced Structural Reconstruction of Gold Clusters Probed by ¹⁹⁷Au Mössbauer Spectroscopy³⁾

Several research groups have recently synthesized Au:SR clusters with well-defined chemical compositions, such as Au₂₅(SR)₁₈, Au₃₈(SR)₂₄, and Au₅₅(SR)₃₂, using size-separation techniques in combination with mass spectrometry. Nevertheless, geometric structures of Au:SR have not been determined experimentally mainly due to the unavailability of single crystals of these compounds. The lack of structural information for small Au:SR clusters hinders a full understanding of the origin of their stability and novel properties (*e.g.* photoluminescence, magnetism, and optical activity).

In the present study, we investigated the structures of a series of glutathionate-protected gold clusters, Au_n(SG)_m with n = 10–45, using ¹⁹⁷Au Mössbauer spectroscopy, which allows us to probe the local environment of the Au sites *via* isomer shift (IS) and quadrupole splitting (QS). The spectral analysis, with the help of recent theoretical results on methanethiolated gold clusters, revealed that Au-SG oligomeric rings are preferentially formed around the Au core. Specifically, a core-in-

cage structural motif theoretically predicted for $[\text{Au}_{25}(\text{SCH}_3)_{18}]^+$ explains the Mössbauer spectra of $\text{Au}_{25}(\text{SG})_{18}$ fairly well and thereby explains the high stability against the core etching reaction. The positive IS and QS values for the Au cores of $\text{Au}_n(\text{SG})_m$ suggest a nontrivial effect of thiolate ligation on the electronic structure of the underlying gold clusters.

4. Synthesis of Biicosahedral Gold Clusters, $[\text{Au}_{25}(\text{PPh}_3)_{10}(\text{SC}_n\text{H}_{2n+1})_5\text{Cl}_2]^{2+}$ ($n = 2-18$)⁴

Metal clusters have been gaining growing interest as elementary units of functional materials and building blocks of optoelectronic devices because of the novelty and controllability of their properties. Probably the most interesting aspect of “cluster-assembled materials” is that new collective properties can be imparted by controlling the distance between and arrangement of individual clusters. It is not trivial, however, to achieve this goal, since the interaction between clusters has to be enhanced without causing them to coalesce. One approach that has the potential to achieve such contradictory requirements is to use “magic clusters” as building units, since the interaction between these clusters is suppressed due to their inherent stability arising from their closed electronic and geometrical structures.

This paper reports the first chemical synthesis of Au_{25} cluster compounds in which two icosahedral Au_{13} units are directly connected by sharing a single vertex atom. The chemical reaction between $[\text{Au}_{11}(\text{PPh}_3)_8\text{Cl}_2]^+$ and n -alkanethiol $\text{C}_n\text{H}_{2n+1}\text{SH}$ ($n = 2, 8, 10, 12, 14, 16, 18$) serendipitously yielded stable Au_{25} cluster compounds with the formula, $[\text{Au}_{25}(\text{PPh}_3)_{10}(\text{SC}_n\text{H}_{2n+1})_5\text{Cl}_2]^{2+}$. Single-crystal X-ray structural analysis of $[\text{Au}_{25}(\text{PPh}_3)_{10}(\text{SC}_2\text{H}_5)_5\text{Cl}_2](\text{SbF}_6)_2$ revealed that the Au_{25} core is constructed by bridging two icosahedral Au_{13} clusters with thiolates sharing a vertex atom (Figure 1). Optical absorption spectroscopy showed that coupling between the Au_{13} building blocks gives rise to new electronic levels in addition to those of the Au_{13} constituents.

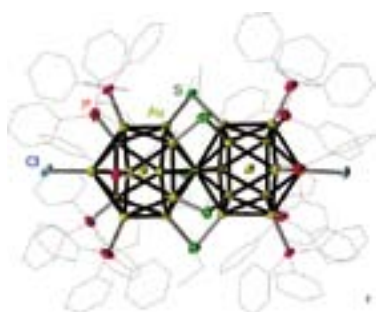


Figure 1. ORTEP drawing of the molecular structure of $[\text{Au}_{25}(\text{PPh}_3)_{10}(\text{SC}_2\text{H}_5)_5\text{Cl}_2]^{2+}$. Thermal ellipsoids are drawn at the 50% probability level.

Awards

NEGISHI, Yuichi; PCCP Award.

TSUKUDA, Tatsuya; GOLD 2006 Best Presentation Award.

5. Effect of Ag-Doping on the Catalytic Activity of Polymer-Stabilized Au Clusters in Aerobic Oxidation of Alcohol⁵

We have recently showed that Au clusters ($\phi = 1.3 \pm 0.3$ nm) stabilized by a representative hydrophilic polymer, poly(*N*-vinyl-2-pyrrolidone) [PVP; $(\text{C}_6\text{H}_9\text{ON})_n$], work as catalysts for various types of aerobic oxidation in water under mild conditions.^{6,7} The Au:PVP clusters not only work as practical catalysts for aerobic oxidations, but also provide an ideal opportunity to address fundamental questions regarding the reaction mechanism. Most importantly, a wet chemical approach has enabled us to prepare monodisperse Au:PVP clusters in the core-size range of 1.3–10 nm and to study the size dependent catalytic activity. The catalytic activity per unit cluster surface was found to increase with decreasing size, which is associated with non-metallic electronic structures. With the knowledge about size effect in hand, we have launched a further investigation into the nature of the active site of the small Au:PVP by tuning the charge state of Au *via* impurity doping.

A set of nearly monodisperse Au–Ag alloy clusters (size range 1.6 to 2.2 nm) with various Ag content (5–30%) was prepared by the co-reduction method in the presence of PVP. The catalytic activities of the Au–Ag:PVP clusters were investigated for aerobic oxidation of *p*-hydroxybenzyl alcohol as a model reaction to understand the effect of Ag on the catalytic activity of Au clusters. It was found that the rate constants per unit surface area for Au–Ag:PVP clusters with small Ag content (< 10%) were larger than those of monometallic Au:PVP clusters of comparable size. The enhancement of the catalytic activity by Ag doping is discussed in light of the electronic structure of the Au–Ag cores probed by X-ray photoelectron spectroscopy. The present results indicate that the partial anionic character of the Au core is important for the aerobic oxidation reactions of Au:PVP clusters.

References

- 1) Y. Shichibu, Y. Negishi, H. Tsunoyama, M. Kanehara, T. Teranishi and T. Tsukuda, *Small* **3**, 835–839 (2007).
- 2) H. Tsunoyama, P. Nickut, Y. Negishi, K. Al-shamery, Y. Matsumoto and T. Tsukuda, *J. Phys. Chem. C* **111**, 4153–4158 (2007).
- 3) K. Ikeda, Y. Kobayashi, Y. Negishi, M. Seto, T. Iwasa, K. Nobusada, T. Tsukuda and N. Kojima, *J. Am. Chem. Soc.* **129**, 7230–7231 (2007).
- 4) Y. Shichibu, Y. Negishi, T. Watanabe, N. K. Chaki, H. Kawaguchi and T. Tsukuda, *J. Phys. Chem. C* **111**, 7485–7487 (2007).
- 5) N. K. Chaki, H. Tsunoyama, Y. Negishi, H. Sakurai and T. Tsukuda, *J. Phys. Chem. C* **111**, 4885–4888 (2007).
- 6) H. Sakurai, H. Tsunoyama and T. Tsukuda, *J. Organomet. Chem.* **692**, 368–374 (2007).
- 7) H. Tsunoyama, T. Tsukuda and H. Sakurai, *Chem. Lett.* **36**, 212–213 (2007).

Optical Studies of Charge Ordering in Organic Conductors

Department of Materials Molecular Science
Division of Electronic Properties



YAKUSHI, Kyuya
YAMAMOTO, Kaoru
URUICHI, Mikio
KOWALSKA, Aneta
NAKANO, Chikako
TANAKA, Masayuki
YUE, Yue
TADA, Nao

Professor
Assistant Professor
Technical Associate
JSPS Post-Doctoral Fellow
Research Fellow
Graduate Student
Graduate Student
Secretary

In many organic charge-transfer salts, the electronic state of charge carriers is located at the boundary between localized and delocalized states. Recently the charge ordering (CO) originated from the localization of the charge carriers is widely found in organic conductors, and the electronic phase diagrams of typical organic conductors are re-considered taking CO into account. We are interested in the CO state, first because a CO phase is neighbored on a superconducting phase, wherein a new type of pairing mechanism for superconductivity is theoretically predicted, second because some compounds in a CO phase shows ferroelectricity, the origin of which is attributable to the electronic displacement, third because the narrow-band compounds have an inhomogeneous intermediate state between metallic and CO states. We employ infrared and Raman spectroscopy to study the CO state, since the infrared and Raman spectra change dramatically at the CO phase-transition temperature.

1. Two-Phase Coexistence in the Monovalent–Divalent Phase Transition of Dineopentylbiferrocene-Fluorotetracyanoquinodimethane, $(\text{npBifc}-(\text{F}_1\text{TCNQ})_3)^{1)}$

The Gibbs rule implies that two-phase coexistence is possible at a single temperature point in a single-component system. However, the phase coexistence has been reported in some temperature interval near the phase transition temperature, for example, in the neutral-ionic phase transition of TTF-CA (tetrathiafulvalene-chloranil), in the orientational ordering phase transition of C_{60} , in the spin-crossover temperature range of $[\text{Fe}(2\text{-pic})_3]\text{Cl}_2\cdot\text{MeOH}$ (2-pic: 2-picolylamine), and in the diffuse phase transition of relaxor ferroelectrics such as PMN ($\text{PbMg}_{1/3}\text{Nb}_{2/3}\text{O}_3$). Two mesoscopic phases are observed in a very narrow temperature interval of TTF-CA and C_{60} , in which the phase transformation occurs abruptly. On the other hand, microscopic domains are suggested in a wide temperature interval in $[\text{Fe}(2\text{-pic})_3]\text{Cl}_2\cdot\text{MeOH}$ and PMN, in which the phase transformation occurs gradually in a broad temperature interval.

Dineopentylbiferrocene-fluorotetracyanoquinodimethane, $(\text{npBifc})^{n+}(\text{F}_1\text{TCNQ})_3^{n-}$, undergoes a monovalent ($n = 1$)-divalent ($n = 2$) phase transition. The phase-transition behavior was studied using the magnetization, χT , which showed a continuous increase in the temperature interval of ~ 60 K from 160 to 100 K. Mochida *et al.* suggested the coexistence of LT and HT phases to explain the continuous transformation. If a domain structure causes the continuous phase transformation, the domain size seems to be microscopic like spin-crossover compounds and relaxor ferroelectrics. Contrary to this expectation, we found macroscopic domains in the temperature interval of gradual phase transformation. In this temperature interval, we found that the Bragg peaks split into two groups which correspond to the monovalent and divalent phases.

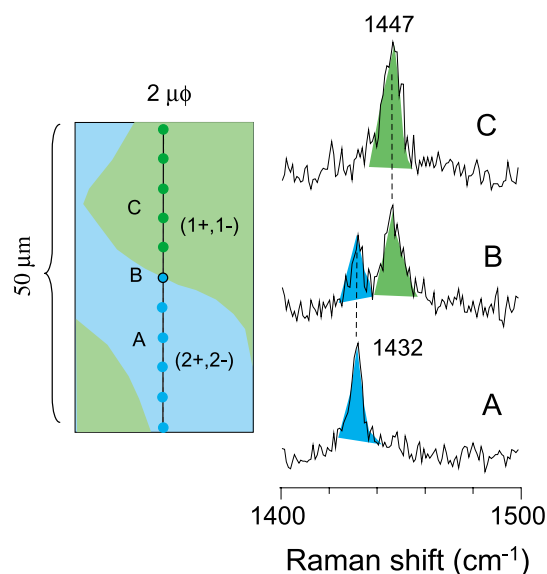


Figure 1. Position dependence of the Raman spectrum at 120 K. The Raman band at 1447 cm^{-1} appears in a monovalent ($n = 1$) state, whereas the 1432 cm^{-1} band appears in a divalent ($n = 2$) state. We have measured 11 points with the laser spot of $2\text{ }\mu\text{m}$ diameter. In the region A, only the 1432 cm^{-1} band is observed, whereas in other region C, 1447 cm^{-1} band is observed. At the boundary B, both are observed.

Below 100 K, the Bragg peaks of monovalent phase are completely replaced by the Bragg peaks of divalent phase. In addition, we found a strong position dependence of the Raman spectrum (See Figure 1). Both experiments show that the macroscopic domains of monovalent and divalent phases coexist in the transition temperature region. This finding is unique, because two *macroscopic domains* stably exist in a *wide* temperature interval near the gradual phase transformation. We consider that the large volume contraction ($\Delta V/V \sim 0.03$) at ~ 130 K is related to the stableness of the macroscopic coexistent domains. We examined a simple Landau-Ginzburg model including volumetric strain. According to this model, a stable coexistent state is obtained near the transition temperature region, and the coexistent temperature range increases as the elastic compliance and/or the volumetric strain is large. However, this model is very preliminary, and more realistic theory is necessary to fully understand the stable coexistent state.

2. Infrared and Raman Study of the Charge-Ordered State in the Vicinity of the Superconducting State in a Organic Conductor β -(*meso*-DMBEDT-TTF) $_2$ PF $_6$ ²⁾

The competition between charge ordering and superconductivity has been attracting attention, because in systems in which such competition occurs, charge fluctuation possibly contributes to the superconductivity pairing mechanism. Such competition can be depicted in an electronic phase diagram. From this viewpoint, the insulating charge-ordered (CO) phase in the vicinity of the superconducting phase has been studied in both organic and inorganic compounds.

β -(*meso*-DMBEDT-TTF) $_2$ PF $_6$ is possibly the typical compound, in which CO is competing with SC to be a ground state. We present spectroscopic evidence for the charge ordering in β -(*meso*-DMBEDT-TTF) $_2$ PF $_6$ below ~ 70 K. The infrared and Raman spectra abruptly changed at ~ 70 K, and the amplitude of charge order was estimated to be 0.5 from the splitting of the infrared-active C=C stretching mode. The

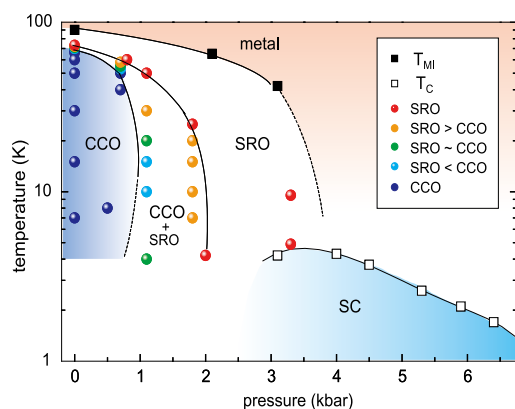


Figure 2. Pressure and temperature phase diagram. CCO and SRO respectively denote the checker-board type charge-order phase and short-range ordered fluctuating charge-order phase. CCO+SRO denotes the coexisting phase.

coexistence of the high-temperature and low-temperature signals was observed in a narrow temperature range (~ 4 K) at the phase transition temperature. The pressure and temperature phase diagram was obtained in the vicinity of the superconducting phase. The checkerboard-type charge-order (CCO) phase is not adjacent to the superconducting phase, but the short-range ordered charge-ordering (SRO) phase is next to the superconducting (SC) phase. The coexistent region significantly expands under the hydrostatic pressure. In the coexistent region, the crystal is inhomogeneous not only in macroscopic scale but also in mesoscopic scale.

3. Charge Ordered State and Frustration of the Site-Charges in (ET) $_3$ Te $_2$ I $_6$ and (BETS) $_2$ Te $_2$ I $_6$ ³⁾

The θ -type ET salt is most extensively studied for the charge-ordering (CO) phase transition. As the crystal lattice is uniform with herringbone structure, several electronic configurations are frustrating above the phase transition. The low-temperature horizontal CO is stabilized by the structural transformation, that is, electron-lattice interaction as well as Coulomb interaction takes part in the phase transition. To examine the role of Coulomb interaction, we have studied (ET) $_5$ Te $_2$ I $_6$ and (BETS) $_5$ Te $_2$ I $_6$ [ET = bis(ethylenedithio) tetrathiafulvalene and BETS = bis(ethylenedithio) tetraselenafulvalene], whose organic layer takes the non-uniform lattice with a herringbone structure. We have studied x-ray structural analysis, temperature dependence of vibrational spectra and temperature dependence of electrical resistivity under the uniaxial strain for (ET) $_5$ Te $_2$ I $_6$ and (BETS) $_5$ Te $_2$ I $_6$. In the low-temperature insulating phase for each salt, a charge sensitive mode, ν_2 , exhibits a peak splitting, and a vibronic ν_3 mode shows the factor group splitting. This observation confirms the charge ordered state. The distribution of the site charges is determined from the factor group analysis of the vibronic ν_3 mode, and the site charge takes an inner distribution. This result is in agreement with that suggested from the x-ray crystal structure analysis of the ET-salt. In the high temperature conducting phase, the vibronic ν_3 mode is smeared out whereas the frequencies of the two charge sensitive modes are almost unchanged in the whole temperature range. We have proposed the model that the highly conducting state is ascribed to the frustration between the inner distribution in the insulating state and the other charge distribution, which contributes to reducing the inter-site Coulomb interaction along the stacking and diagonal directions, respectively. Our conjecture is supported from the temperature dependence of the electrical resistivity under the uni-axial strain.

References

- 1) M. Uruichi, Y. Yue, K. Yakushi and T. Mochida, submitted.
- 2) M. Tanaka, K. Yamamoto, M. Uruichi, T. Yamamoto, K. Yakushi, S. Kimura and H. Mori, submitted.
- 3) T. Yamamoto, J. Eda, A. Nakao, R. Kato and K. Yakushi, *Phys. Rev. B* **75**, 205132 (18 pages) (2007).

Electrical Properties of Single-Component Molecular Crystals

Department of Materials Molecular Science
Division of Electronic Properties



KOBAYASHI, Hayao
TAKAHASHI, Kazuyuki
OKANO, Yoshinori
CUI, HengBo
OHTA, Akiyo

Professor*
Assistant Professor
Technical Associate
Post-Doctoral Fellow
Secretary

Since the discovery of the first single-component molecular metal, $[\text{Ni}(\text{tmdt})_2]$ (tmdt = trimethylenetetrathiafulvalenedithiolate), many analogous systems consisting of the transition metal complex molecules with similar extended-TTF type ligands were developed. However, the single-component molecular superconductor has not been developed yet. We have tried to prepare and characterize new analogous systems. The trial to examine the condition to metallize the insulating crystal of planar π donor molecule was made by using diamond anvil high-pressure cell.

1. Resistance Measurements of Microcrystals of Single-Component Molecular Metals Using Finely Patterned Interdigitated Electrodes

One of the largest problems in the studies on single-component molecular metals is the difficulties in the growth of sufficiently large single crystals. Therefore almost all the resistivity measurements ever made were performed on compacted crystalline powder pellets, which prevent to see the intrinsic resistivity behavior of the system. Recently, we have made the two-probe resistivity measurements on the as-grown polycrystalline samples of $[\text{Au}(\text{tmdt})_2]$ (tmdt = trimethylenetetrathiafulvalenedithiolate) using finely patterned interdigitated electrodes and confirmed the system to be anti-ferromagnetic molecular metal with unprecedentedly high magnetic transition temperature ($T_N = 110$ K). We used the commercially available gold or platinum electrodes with gap between interdigitated electrodes was $5 \mu\text{m}$ and the width of electrodes was $10 \mu\text{m}$. The microcrystals were grown on the interdigitated electrodes electrochemically from the acetonitrile solution containing $(\text{Me}_4\text{N})[\text{Au}(\text{tmdt})_2]$ and $(n\text{-Bu}_4\text{N})\text{PF}_6$. The resistivity measurements showed metallic behavior down to 3

K where the resistance ratio $\rho(3 \text{ K})/\rho(300 \text{ K})$ was 0.4. Despite of large decrease in the susceptibility at T_N suggesting the disappearance of a considerably large part of the Fermi surface, the resistivity showed no distinct anomaly around 110 K. This work was made under the collaboration with Dr. Hishashi Tanaka (AIST), Prof. Madoka Tokumoto (National Defense Academy) and Prof. Akiko Kobayashi (Nihon University).

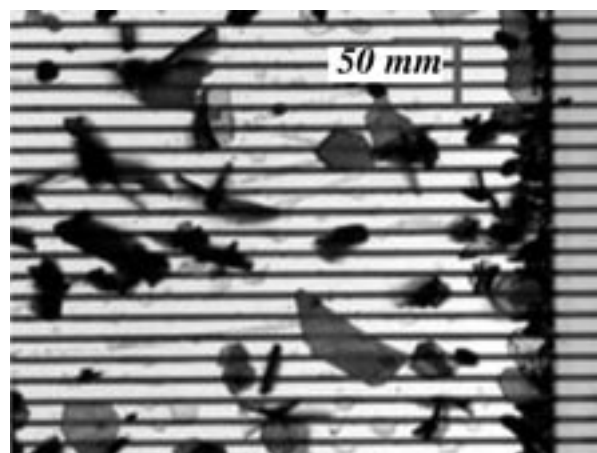


Figure 1. Microcrystals grown on interdigitated electrodes.

2. Structures and Physical Properties of Highly Conducting Single-Component Molecular Conductors Substituted with Selenium Atoms, $[\text{M}(\text{tmstfdt})_2]$ ($\text{M} = \text{Ni}$ and Au , tmstfdt = trimethylenediselenadithiafulvalenedithiolate)

With the aim of obtaining the single-component molecular metals with larger intermolecular interactions, that is, stronger

metallic properties, we have tried to prepare $[M(\text{tmstfdt})_2]$ ($M = \text{Ni}, \text{Au}$) with Se-containing extended-TTF ligands, tmstfdt. Microcrystals of $[M(\text{tmstfdt})_2]$ were grown by electrochemical oxidation of $(\text{Me}_4\text{N})_n[M(\text{tmstfdt})_2]$ ($n = 1$ (Au), 2 (Ni)) in the presence of tetra-*n*-butylammonium perchlorate in THF or acetonitrile. The crystal structures of $[M(\text{tmstfdt})_2]$ ($M = \text{Ni}, \text{Au}$) were determined by synchrotron radiation X-ray powder diffraction experiments. The crystals $[\text{Ni}(\text{tmstfdt})_2]$ and $[\text{Au}(\text{tmstfdt})_2]$ are isostructural to each other and have very simple triclinic unit cells with only one molecule on the lattice point. Although resistivity measurements were made on compressed polycrystalline pellet samples, the room temperature resistivities were very high ($\rho(\text{RT}) = 10^{-2} \Omega \text{ cm}$ (Ni), 10^{-1} (Au)). Furthermore, $[\text{Ni}(\text{tmstfdt})_2]$ showed metallic behavior down to about 50 K and kept high conductivities even at 4.2 K ($\rho(\text{RT}) \approx \rho(4 \text{ K})$). That is, $[\text{Ni}(\text{tmstfdt})_2]$ is a new Se-containing single-component molecular metal. On the other hand, the resistivity of $[\text{Au}(\text{tmstfdt})_2]$ increased slowly with lowering temperature. Magnetic measurements indicated Pauli paramagnetic behavior for $[\text{Ni}(\text{tmstfdt})_2]$ and antiferromagnetic transition below 10 K for $[\text{Au}(\text{tmstfdt})_2]$. This work was made under the collaboration with Dr. Emiko Fujiwara (the University of Tokyo) and Akiko Kobayashi (the University of Tokyo and Nihon University).

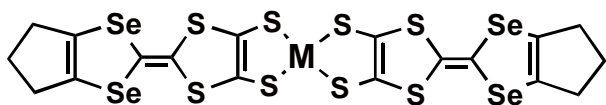


Figure 2. $M(\text{tmstfdt})_2$, $M = \text{Ni}, \text{Au}$.

3. Possibility of Metallization of π Molecular Crystal at High Pressure

It may be said that the science on the molecular conductors was started by the pioneer works by Eley, Vartanyan, Akamatu and Inokuchi around the middle of 20 century, who examined the conducting properties of the crystals of neutral π molecules such as phthalocyanine and condensed aromatic hydrocarbons. Since then an extremely large progress has been achieved in the field of molecular conductors. The first one-dimensional organic metal, $(\text{TTF})(\text{TCNQ})$ and the first organic superconductor, $(\text{TMTSF})_2\text{PF}_6$ were reported in 1973 and 1980, respectively and through the examination of these systems and analogous molecular conductors, the requirements for the

design of molecular metals became clear. That is, (1) the formation of conduction band by suitable molecular arrangement and (2) the carrier generation by charge transfer (CT) between the molecules forming conduction band and other chemical species were found to be two essential requirements. Due to the large success in the development of “*CT-type* molecular metals and superconductors,” almost all the chemists seemed to believe until recently that the crystal consisting of single kind of molecule could not be highly conducting at least at ambient pressure. However we have succeeded to develop the first single-component molecular metal in 2001 by designing the transition metal complex molecule with extremely small HOMO-LUMO gap and fairly large intermolecular interactions. It may be imagined that more straightforward way to metallize the single-component molecular crystal will be to apply extremely high pressure.

We have recently examined the possibility of metallization of the crystal of π donor molecule tetramethyltetrateluronaphthalene (TMTTeN) up to 30 GPa by performing high-pressure four-probe resistivity measurements using diamond anvil cell (DAC). The crystal of TMTTeN has monoclinic lattice with space group $P2_1/c$ and the lattice constants of $a = 10.130 \text{ \AA}$, $b = 6.069$, $c = 13.549$, $\beta = 110.572^\circ$, $V = 779.8 \text{ \AA}^3$, $Z = 2$. The room-temperature resistivity ($\rho(\text{RT})$) decreased smoothly with increasing pressure at $P < 10$ GPa, almost constant at $11 < P < 16$ GPa and decreased again at $17 < P < 25$ GPa. $\rho(\text{RT})$ became as small as $1.4 \times 10^{-3} \Omega \text{ cm}$ at 30 GPa. To our best knowledge, all the hitherto reported molecular conductors with $\rho(\text{RT})$ smaller than $10^{-2} \Omega \text{ cm}$ are metallic at around room temperature. However, TMTTeN was not metallic at least around room temperature. These results seem to support our conjecture that it is very difficult to metallize the crystal without destroying the molecular structure.

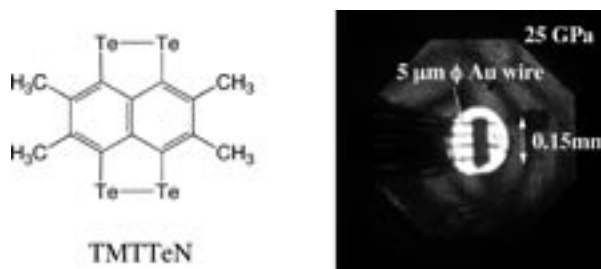


Figure 3. TMTTeN crystal put in the hole of metal gasket of DAC for 4-probe resistivity experiments.

* Present Address; Nihon University

Magnetic Resonance Studies for Molecular-Based Conductors

Department of Material Molecular Science
Division of Electronic Properties



NAKAMURA, Toshikazu Associate Professor
FURUKAWA, Ko Assistant Professor
HARA, Toshifumi IMS Fellow
MAEDA, Keisuke Graduate Student
TADA, Nao Secretary

Magnetic resonance measurements are advantageous for studying fundamental electronic properties and for understanding the detailed electronic structures of molecular based compounds. Developing an understanding of the electronic phases of these materials enables us to perform systematic investigations of low-dimensional, highly-correlated electron systems. Competition between the electronic phases in molecular-based conductors has attracted much attention. The investigations of such electronic phases by means of magnetic resonance measurements are important to understanding unsolved fundamental problems in the field of solid state physics.

In this study, we performed broad-line NMR and pulsed-ESR measurements on molecular-based conductors to understand electron spin dynamics in low-temperature electronic phases.

1. Redistribution of Charge in the Proximity of the Spin-Peierls Transition: ^{13}C NMR Investigation of $(\text{TMTTF})_2\text{PF}_6$

Organic conductors, $(\text{TMTTF})_2X$, have been extensively studied and are well-known quasi-one-dimensional conductors possessing various ground states, for example, spin-Peierls, antiferromagnetic, and superconductivity states realized by the application of pressure or variation of the counter-anion, X .¹⁾ However, recent progress in the investigation of charge-ordering (CO) phenomena has cast doubts on the validity of the simple Mott-Hubbard insulator model. TMTTF-based salts show a resistivity minimum at T_p in the paramagnetic phase because of 1D electronic Umklapp processes. Below T_p , they are well described with a localized picture. At low-temperatures, most of them undergo charge-ordering transitions in the intermediate paramagnetic states between T_p and the phase-transition temperature toward the ground state.²⁻⁴⁾ In our previous report,⁴⁾ the charge configuration patterns of the charge-ordering phases in the intermediate paramagnetic states, such as $-\text{O}-\text{O}-\text{O}-\text{O}-$ ($2k_F$) and $-\text{O}-\text{O}-\text{O}-\text{O}-$ ($4k_F$) along the stacking axes, were determined for several TMTTF salts

by ESR linewidth anisotropy analysis. We also clarified that the long-range Coulomb interaction along the stacking axis plays an essential role stabilizing the charge-ordering phases in the intermediate paramagnetic states.⁵⁻⁸⁾ However, the driving force and charge configuration of the ground state have not yet been clarified.

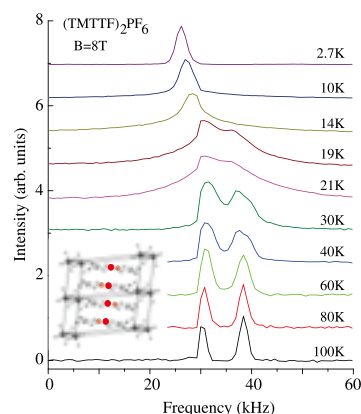


Figure 1. Temperature dependence of ^{13}C NMR spectra of $(\text{TMTTF})_2\text{PF}_6$. Measurements were performed at the so-called magic-angle configuration. The inset shows two inequivalent inner (solid large circles) and outer (small circles) ^{13}C sites in the zigzag TMTTF chains.

For example, the ground states of $(\text{TMTTF})_2\text{SbF}_6$ (antiferromagnet) and $(\text{TMTTF})_2\text{AsF}_6$ (spin-Peierls) are different from each other, although they possess the same charge configuration pattern in the intermediate paramagnetic phase. Moreover, the coexistence of two orders was established along with the existence of a tetracritical point in the temperature/pressure phase diagram.⁹⁾ Hence, it is also an open question whether charge separation in the spin-Peierls phase of $(\text{TMTTF})_2\text{MF}_6$ is likely or unlikely.

In this study, we performed pulsed ^{13}C NMR measurements on $(\text{TMTTF})_2\text{PF}_6$ to determine its low-temperature electric states. $(\text{TMTTF})_2\text{PF}_6$ shows a charge-ordering phase in the intermediate paramagnetic state below 65 K, and undergoes the spin-Peierls phase-transition at around 18 K. These

two successive phase-transition temperatures are the closest to each other among the family of TMTTF salts at ambient pressure. We present the electronic properties of this compound from a microscopic point of view.

2. Possible One-Dimensional Helical Conductor: Hexa-Peri-Hexabenzocoronene Nanotube

The discovery of electrically conductive carbon nanotube materials has expanded interest in exploring novel materials for functional electronic devices. Recently, new nanotubular objects have been developed by Aida and co-workers using novel hexa-*peri*-hexabenzocoronene (HBC) amphiphiles bearing hydrophilic oxyalkylene chains and lipophilic dodecyl chains. The amphiphilic HBC molecules have two lipophilic alkyl chains on one side, and two hydrophilic chains on the opposite side. Self-assembled graphitic nanotubes were obtained by cooling a hot tetrahydrofuran solution of the HBC derivative to room temperature. The HBC molecules stack to form well-defined nanotubes with a helical array of a large number of π -stacked HBC units.^{10–12} In ordinary carbon nanotubes, the conjugated two-dimensional π -molecular wave functions are spread on the surfaces of the nanotubes. However, in the case of the HBC nanotubes, the π -conjugated columns stack in the direction of the one-dimensional chain. The HBC nanotubes possess a uniform diameter of 20 nm with a wall thickness of 3 nm. Since the HBC molecules have a closed-shell, the resistivity of the pristine HBC nanotube is very high ($\sim M\Omega\text{cm}$). By chemical oxidation using iodine, however, the HBC nanotubes show high electrical conductivity.¹³

There have been remarkable recent developments in structural measurement techniques such as scanning electron microscopy (SEM) and X-ray crystallography. However, the HBC nanotubes are not crystalline and the iodine-doped phases are not stable in a vacuum: when placed in a vacuum, the iodine-doped HBC nanotubes return to reversibly to the form of pristine HBC nanotubes.¹³ Hence, it is difficult to use such structural measurement techniques for the iodine-doped HBC nanotubes. Magnetic resonances measurements, on the other hand, are non-contact, low-energy spectroscopy techniques that are powerful even for non-crystalline materials. Moreover, with magnetic resonance investigations we can obtain not only static information but also dynamic details. In order to understand the origin and dynamics of charged carriers, in the present study, ESR and ^1H NMR measurements were carried out on the iodine-doped HBC nanotubes.

3. Anomalous Temperature Dependence of g -Tensor in Organic Conductor, $(\text{TMTTF})_2\text{X}$ ($\text{X} = \text{Br}, \text{PF}_6$ and SbF_6)

The band-structures of organic conductors are deduced from frontier orbitals (for example, the highest occupied molecular orbital from a donor molecule) estimated by molecular orbital calculations applying the tight-binding approxima-

tion.¹⁾ The Fermi surfaces thus calculated are consistent with those estimated from quantum vibration and/or angular dependence magneto-resistance experiments.¹⁾ Most of the physical phenomena associated with organic conductors can be explained within a framework where the frontier orbital is treated as one rigid atomic orbital in an alkaline metal. It is commonly believed that the counter anions themselves do not affect the electronic properties of organic conductors.

An anomalous behavior of the g -tensor—a shift in principal value and rotation of the principal axes—was observed in $(\text{TMTTF})_2\text{X}$ salts with decreasing temperature.^{14–16} This behavior cannot be explained by a precursor effect (short-range magnetic fluctuation) just above the magnetic long-range order nor by molecular arrangement change.

In this study, we examined the magnetic properties for $(\text{TMTTF})_2\text{X}$ ($\text{X} = \text{Br}, \text{PF}_6$ and SbF_6) with ESR spectroscopy, X-ray diffraction, and quantum-chemical calculation of the g -tensor. We attempted to explain the anomalous behavior of the g -tensor using a scenario where the symmetry of the frontier orbital is deformed by the external counter-anion potential. The intra-molecular spin-distribution as a function of temperature is discussed from the microscopic point of view.

References

- 1) for example: T. Ishiguro, K. Yamaji and G. Saito, *Organic Superconductors*, 2nd ed., Springer-Verlag; Berlin/Heidelberg (1998).
- 2) D. S. Chow, F. Zamborszky, B. Alavi, D. J. Tantilto, A. Baur, C. A. Merlic and S. E. Brown, *Phys. Rev. Lett.* **85**, 1698 (2000).
- 3) P. Monceau, F. Ya. Nad and S. Brazovskii, *Phys. Rev. Lett.* **86**, 4080 (2001).
- 4) T. Nakamura, *J. Phys. Soc. Jpn.* **72**, 213 (2003).
- 5) F. Ya. Nad, P. Monceau, T. Nakamura and K. Furukawa, *J. Phys.: Condens. Matter* **17**, L399 (2005).
- 6) K. Furukawa, T. Hara and T. Nakamura, *J. Phys. Soc. Jpn.* **74**, 3288 (2005).
- 7) T. Nakamura, K. Furukawa and T. Hara, *J. Phys. Soc. Jpn.* **75**, 013707 (2006).
- 8) S. Fujiyama and T. Nakamura, *J. Phys. Soc. Jpn.* **75**, 014705 (2006).
- 9) F. Zamborszky, W. Yu, W. Raas, S. E. Brown, B. Alavi, C. A. Merlic and A. Baur, *Phys. Rev. B* **66**, 081103(R) (2002).
- 10) W. Jin, T. Fukushima, M. Niki, A. Kosaka, N. Ishii and T. Aida, *Proc. Natl. Acad. Sci. U.S.A.* **102**, 10801 (2005).
- 11) W. Jin, T. Fukushima, A. Kosaka, M. Niki, N. Ishii and T. Aida, *J. Am. Chem. Soc.* **127**, 8284 (2005).
- 12) J. P. Hill, W. Jin, A. Kosaka, T. Fukushima, H. Ichihara, T. Shimomura, K. Ito, T. Hashizume, N. Ishii and T. Aida, *Science* **304**, 1481 (2004).
- 13) Y. Yamamoto, T. Fukushima, W. Jin, A. Kosaka, T. Hara, T. Nakamura, A. Saeki, S. Seki, S. Tagawa and T. Aida, *Adv. Mater.* **18**, 1297 (2006).
- 14) M. Onoda, H. Nagasawa and K. Kobayashi, *J. Phys. Soc. Jpn.* **54**, 1240 (1985).
- 15) H. J. Pedersen, J. C. Scott and K. Bechgaard, *Solid State Commun.* **35**, 207 (1980).
- 16) H. J. Pedersen, J. C. Scott and K. Bechgaard, *Phys. Rev. B* **24**, 5014 (1981).

Macromolecular and Supramolecular Approaches to Spin-Functional Soft Materials

Department of Materials Science
Division of Molecular Functions



JIANG, Donglin
WANG, Wenping
ISHIZUKA, Tomoya
HE, Zheng
ISONO, Yukiko
MIZUKI, Hiroko
WAN, Shun
ISHIJIMA, Ryo
CHEN, Long
ODA, Masafumi
SUZUKI, Hiroko
OTA, Akiyo

Associate Professor
Visiting Associate Professor
Assistant Professor
IMS Fellow
Research Fellow
Research Fellow
Graduate Student
Graduate Student
Graduate Student
Graduate Student
Secretary
Secretary

The first-row transition metal ions of d^4-d^7 electronic configuration are of interest, due to their possibility for the coexistence of two spin states, *i.e.* low-spin and high-spin states. Under certain conditions, the two spin states are known to switch in response to external perturbations caused by changes in temperature and pressure or photoexcitation. This phenomenon, referred to as spin transition or spin crossover, leads to changes in the magnetic and optical properties of the materials and has great potential for memory, display, and sensor applications. Solid or crystalline inorganic materials have been studied most extensively so far as potential spin-crossover materials, and some show reversible spin transition in a narrow temperature range. On the other hand, recent attention has been focused on soft materials with spin-crossover properties, as these materials can be processed easily by casting and tuned by molecular design. However, because of a larger freedom of molecular ordering, one may anticipate a possible loss of long-range cooperativity among the spin-transition sites, with the result of non-abrupt spin crossover, as often observed in solution.

Recently, we have designed a series of dendritic triazole derivatives, which serve as bidentate ligands that covalently bridge the iron(II) centers to form rigid coordination polymers, whose spin-transition properties are controlled by the dimensions of the dendritic ligand.^{1,2)} Herein, we review our recent work on macromolecular and supramolecular approaches to the synthesis of newly designed spin-functional soft materials, with a focus on the possibility for the control of spin state and spin-spin interaction.

1. Synthesis and Functions of Multi Metallosalen Wheels

Salen units, due to their high binding affinity for various metal ions, are useful building blocks for the construction of

functional materials such as spin-crossover crystalline solids, components of molecular magnet, and catalysts for organic transformation and polymerization.

By appending dendritic metallosalen complexes with different generation numbers to di-, tri-, and hexakis-substituted benzene cores, a series of multi metallosalen wheels having different geometry and numbers of salen units on the exterior surface were synthesized (Figure 1) and unambiguously characterized by NMR and MALDI-TOF MS measurements. These molecular wheels are unique in that their metal sites are located on the identical single layer of the dendritic framework and thus allows for a clear correlation between function and structure. Studies on spin and catalytic functionalities are in progress.

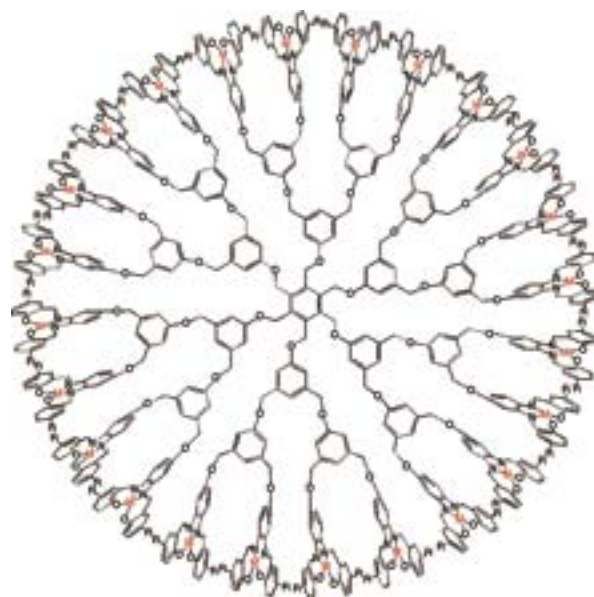


Figure 1. Schematic Representation of Multi Salen Wheels bearing 24 Metal Ions On the Exterior Surface.

2. Synthesis and Functions of TEG-Tethered Iron-Triazolate One Dimensional Chain

A series of newly designed Fe(II)-triazolate coordination polymers with TEG-tethered dendritic wedges ($G_n^m\text{trz}$)Fe (Figure 2; n = number of the generation of benzyl ether dendritic wedge; m = number of TEG chains) were synthesized and their spin-crossover properties were investigated both in solution and solid.

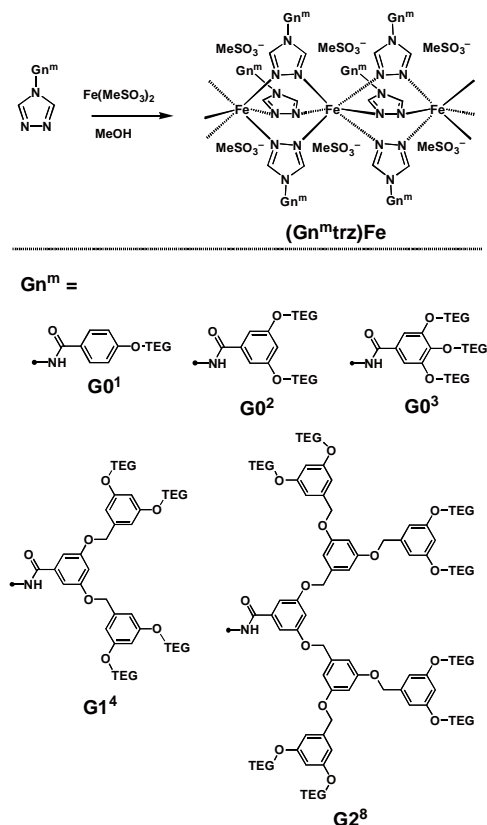


Figure 2. Schematic Representation of TEG-tethered Dendritic Iron-Triazolate Polymers.

TEG-tethered dendritic triazoles ($G_n^m\text{trz}$) with different numbers of TEG chains on the exterior surface were synthesized by convergent method and unambiguously characterized by NMR, MALDI-TOF-MS, IR measurements. Polymerization of $G_n^m\text{trz}$ with $\text{Fe}(\text{MeSO}_3)_2$ in MeOH at room temperature afford a series of coordination polymers ($G_n^m\text{trz}$)Fe with iron-triazolate backbone encapsulated in TEG-tethered dendritic wedges. These dendritic polymers are highly soluble in THF, MeOH, EtOH, *n*-propanol to give a stable solution over a long period. Since the 'naked' iron-triazolate polymer is not soluble, TEG-tethered dendritic wedges not only enhanced solubility but also prevented the polynuclear chain from decomposition in solution.

A MeOH solution of ($G_0^2\text{-trz}$)Fe at room temperature was colored violet, characteristic of low-spin state, and discolored

upon heating at 30 °C, whilst after cooling at 20 °C, the solution turned to violet again. This thermally induced coloration-discoloration process is reversible without any deterioration for many times. The above color change suggests that thermal spin crossover takes place even in MeOH. In fact, temperature variable electronic absorption spectroscopy display a heating profile with a decrease at 450-nm absorption band, originated from *d-d* absorption band of the low-spin state, together with the appearance of a new peak centered at 750 nm, characteristics of the high-spin state. The spin transition temperature was thus estimated to be 25 °C. This is also the case for $G_0^1\text{trzFe}$ with one TEG chain on the dendritic surface, to show a spin transition temperature at 25 °C. On the other hand, $G_0^3\text{trzFe}$ with three TEG chains on the surface of the dendritic wedges although displayed a reversible spin crossover in MeOH but with a much low transition temperature at 6 °C.

($G_1^4\text{trz}$)Fe and ($G_2^8\text{trz}$)Fe bearing large dendritic wedges were highly soluble in MeOH but displayed a colorless solution at room temperature, indicating a high-spin state of the focal metal chain. Upon cooling at 0 °C, the solution turned to violet, as a result of spin transition to low-spin state. The spin transition temperature in MeOH were estimated to be 8 and 5 °C, respectively. Therefore, when the size of dendritic wedge becomes large, the temperature for spin transition in MeOH decreased. In sharp contrast to the case of ($G_0^2\text{trz}$)Fe, solid samples of ($G_1^4\text{trz}$)Fe and ($G_2^8\text{trz}$)Fe retain high spin state even upon cooling at -78 °C. All these observations indicate that the TEG-tethered dendritic wedges play an important role in spin transition of the focal iron-triazolate chain.

XRD measurements of ($G_0^2\text{trz}$)Fe, ($G_1^4\text{trz}$)Fe, and ($G_2^8\text{trz}$)Fe exhibit that these dendrimers form hexagonal columnar structures. TEG-tethered dendritic wedges in the solution likely adopt stretched conformation, therefore, the decrease of spin transition temperature in solution is predominately affected by the size of the dendritic wedges. A large dendritic wedge causes steric hindrance between the neighboring metal sites and thus decreases the polymerization degree of the focal iron-triazolate chain. As a result, the spin transition temperature decreased. On the other hand, in solid state, the TEG chains become shrink to give a global conformation. Such a conformational change result in further increment of the steric hindrance between the two neighboring dendritic wedges, and eventually the focal iron-triazolate chain becomes distort, especially in the case of high-generation ($G_1^4\text{trz}$)Fe and ($G_2^8\text{trz}$)Fe. Therefore, the TEG-tethered dendritic wedges not only greatly improved the solubility of rigid coordination polymer chain, but much importantly *through* conformational change enables magneto-optical switching of the focal iron-triazolate chain.

References

- 1) T. Fuigaya, D. Jiang and T. Aida, *Chem. Asian J.* **2**, 106 (2007).
- 2) Z. He, T. Ishizuka and D. Jiang, *Polym. J.* in press (2007).

Award

JIANG, Donglin; SPSJ Wiley Award 2006.

and spatial modulation by MAS. Furthermore, the one also refocuses scalar coupling evolution during dipolar evolution time. One can therefore determine extremely averaged, weak dipolar coupling with lower limit of a hundred Hz for ^1H - ^{13}C spin pair, which corresponds to dynamic order parameter of 0.0043 with single rotor cycle at spinning speed less than 3 kHz. Total experimental time can also be appreciably reduced, as compared with acquiring full 2D-NMR spectra. Furthermore, by extending dipolar evolution time of multiple of unit cycle, lower detection limit can be extended as much as possible depending on effective T_2 under ^1H homonuclear dipolar decoupling multiple-pulse sequence of observed nuclei.

To prove efficacy and usefulness of this technique, we characterized lipids in fully hydrated multi-lamella vesicles (MLVs), 1-palmitoyl-2-oleyl-sn-glycero-3-phosphocholine (POPC). The time evolution of the recoupled, motionally averaged, weak ^1H - ^{13}C heteronuclear dipolar interactions was monitored by reduced high resolution NMR signal of natural abundant ^{13}C nuclei, prepared by either ^1H coherence transfer based on through-bond J -coupling mediated rotor synchronized INEPT or single pulse excitation of ^{13}C polarization. Dipolar couplings in each residue were determined by fitting the curves of reduced signals for ^1H - ^{13}C 2-spin, $^1\text{H}_2$ - ^{13}C 3-spin system $^1\text{H}_3$ - ^{13}C 4-spin system for CH and CH_2 and CH_3 , respectively. The segmental order parameters were shown in Figure 1 (c) with slice ^{13}C NMR spectra without and with maximally reduced signals. The obtained segmental order parameters for POPC in MLVs were slightly smaller, but similar as reported for saturated lipids. Further developments to characterize the local structures are in progress.

2. A Study of Local Mobility for Phospholipase C δ 1- Pleckstlin Homology Domain Bound to Fully Hydrated Multi-Lamella Vesicles by Solid State NMR²⁾

A peripheral membrane protein, phospholipase C (PLC)- δ 1, is one of membrane proteins related to signal transduction by conducting hydrolytic cleavage of phosphatidyl inositol-4,5-bisphosphate (PIP_2) on the surface of membrane bilayers and is known as one of essential proteins for mammals. Pleckstlin homology (PH) domain of PLC- δ 1 has been recognized as PIP_2 binding domain. In current study, characterization of local mobility of PLC- δ 1 PH domain bound to fully hydrated MLVs was explored. [3 - ^{13}C]Ala-labeled PLC- δ 1 PH domain was expressed as GST fusion protein in E Coli in [3 - ^{13}C]Ala contained in M9 culture and purified by affinity chromatography. The purified one was attached to the surface of MLVs prepared from POPC and PIP_2 with molar ratio 20:1. The molar ratio of protein to lipids was prepared to 1:20. PLC- δ 1 PH domain bound to MLVs were precipitated by ultracentrifuge of 6 hours at $541000\times g$ at 4°C . They were packed into sample tube as same way as mentioned above. Solid state NMR experiments were carried out under the same condition mentioned above. The magnified recoupling effects of motionally averaged weak ^1H - ^{13}C heteronuclear dipolar interactions were monitored as signal reduction of high resolution

^{13}C spectra of isotope enriched methyl carbon of Ala residues in PLC- δ 1 PH domain by SCREM-DIPSHIFT.¹⁾ Individual dipolar couplings were determined by fitting curves of the reduced signals for $^1\text{H}_3$ - ^{13}C 4-spin system with rotation effect around the C_3 rotation axis. Dynamic order parameters ($0 < \text{DOP} < 1.0$), were determined by the normalizing motionally averaged heteronuclear dipolar couplings with the one in rigid limit. Figure 2 (a) shows high resolution solid state NMR spectra with reduced signals due to recoupled heteronuclear dipolar couplings of methyl region. Dynamic order parameters for all Ala residues in PLC- δ 1 PH domain were determined similarly. Figure 2 (b) illustrates preliminary result of a pictorial representation of local mobility of PLC- δ 1 PH domain bound to fully hydrated POPC/ PIP_2 -MLVs, based on experimentally determined dynamic order parameters. The information of local mobility of PLC- δ 1 PH domain may give the understanding of a detailed mechanism as to a relationship between structure and function of PH domain, which is bound to PIP_2 . To the best of our knowledge, this is first example of successfully characterized local mobility for peripheral membrane protein bound to fully hydrated lipid bilayers by solid state NMR.

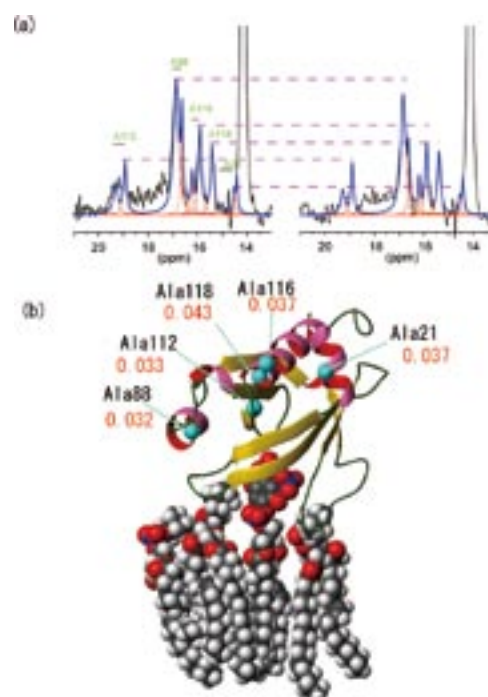


Figure 2. Pictorial representation of local mobility of PLC- δ 1 PH domain bound to fully hydrated POPC/ PIP_2 lipid bilayers surface of MLVs based on the experimentally determined order parameters (red colored) of Ala residues in PLC- δ 1 PH domain. Light blue spheres indicate the location of Ala residues in PLC- δ 1 PH domain. A model structure has been generated from the combination of X-ray derived structure bound to Inositol-1,4,5-triphosphate in the crystal and POPC lipid bilayers calculated from MD simulation.

References

- 1) K. Nishimura, *J. Chem. Phys.* submitted.
- 2) N. Uekama, M. Okada, H. Yagisawa, S. Tuzi and K. Nishimura, to be submitted.

Construction and Nano-scale Measurements of Molecular Nanostructures for Molecular Electronics

Research Center for Molecular Scale Nanoscience
Division of Molecular Nanoscience



OGAWA, Takuji	Professor
TANAKA, Hirofumi	Assistant Professor
HUANG, Wei	IMS Fellow*
HINO, Takami	Post-doctoral Fellow
SUGAWARA, Yoshitaka	Post-doctoral Fellow
TANEMURA, Hiroyo	Research Fellow†
IIDA, Yuko	Research Fellow‡
SATO, Hirokazu	Visiting Scientist§
SUBURAMANIAM, Chandramouli	Visiting Scientist
OZAWA, Hiroaki	Graduate Student¶
YAJIMA, Takashi	Graduate Student**
KAWAO, Masahiro	Graduate Student
YAMADA, Tetsuya	Graduate Student
SUZUKI, Hiroko	Secretary

Molecular electronics is a relatively new and fascinating area of research. However, as most single organic molecules are not conductive in a classical sense, long-range electronic transport through single molecules is unlikely to be useful for practical electronic circuits. Our group is interested in composites of conductive nano-materials with functional organic molecules as attractive bases for molecular electronics. Structures such as carbon nanotubes and metal nanoparticles incorporating functional organic molecules have been shown to be possible candidates. We have prepared two dimensional, one dimensional Au nano-particle assemblies using organic molecules, and carbon nanotube/organic molecule composites. Their electric properties were studied using nanogap electrodes and PCI-AFM.

The subjects of our group can be classified into three categories: (1) Preparation and self organization of functional organic molecules, metal nano-particles, and carbon nanotubes, (2) development of new scanning microscopic methods, and (3) development of new lithographic technique utilizing self assembling of molecules. By the combination of these three theme we are aiming to realize molecular scale electronics.

1. Metal-Semiconductor Transition Induced Visible Fluorescence in Single Walled Carbon-Nanotube/Noble Metal Nanoparticle Composites¹⁾

We show that single walled carbon nanotube (SWNT) bundles emit visible fluorescence in the presence of noble metal nanoparticles and nanorods in the solid state. Conductivity measurements with metallic nanotubes, isolated from pristine SWNTs show that they become semiconducting in the presence of the metal nanoparticles. Nanoparticle binding increases the defects in the nanotube structures which is evident in the Raman spectra. The metal-semiconductor transition removes the non-radiative decay channels of the excited states enabling visible fluorescence. Nanotube structures are imaged

using this emission with resolution below the classical limits.

2. A New Utilization of Organic Molecules for Nanofabrication Using the Molecular Ruler Method²⁾

Oligothiophenes and porphyrin oligomers were exploited as new molecules for the “molecular ruler” (MR) method in the form of simple molecular monolayers. When handled in air, oligothiophenes yielded extremely homogeneous nanogaps about 30 nm wide, while handling under N₂ produced nano-scale gaps of around 10 nm between parent and daughter structures. The difference between these two results indicated that it was possible to control the width of this gap by varying the extent of oxidation of the oligothiophenes. Porphyrin oligomers also yielded nanogaps about 10 nm wide. Therefore, these two types of molecules are promising candidates for use in MR methods.

3. Scanning Tunneling Microscopy Investigation of Vanadyl and Cobalt(II) Octaethylporphyrin Self-Assembled Monolayer Arrays on Graphite³⁾

Two-dimensional crystals of [2,3,7,8,12,13,17,18-octaethyl-21*H*,23*H*-porphine] vanadium(IV) oxide and cobalt(II) (VOOEP and CoOEP, respectively) at the interface of 1-tetradecene and highly oriented pyretic graphite (HOPG) were studied by scanning tunneling microscopy (STM). The lattice parameters were determined for VOOEP ($a = 1.6 \pm 0.1$ nm, $b = 1.46 \pm 0.05$ nm, $\Gamma = 61 \pm 3^\circ$) and CoOEP ($a = 1.48 \pm 0.08$ nm, $b = 1.42 \pm 0.07$ nm, $\Gamma = 62.0 \pm 4^\circ$). The lattice parameters were calibrated using the HOPG lattice as a reference. The center metal dependence observed by high-resolution STM analysis of octaethylporphyrin and the differences between VOOEP and CoOEP are proved.

4. Different *I-V* Characteristic of Single Electron Tunneling Induced by Using Double-Barrier Tunneling Junctions with Differing Symmetric Structures⁴⁾

I-V characteristics of single electron tunneling from a symmetric and an asymmetric double-barrier tunneling junction (DBTJ) were examined. A single Au nanoparticle was trapped in nanogap whose size was precisely controlled using a combination of electron beam lithography and molecular ruler technique. Though the symmetric junction showed a monotonic rise with a bias beyond the Coulomb gap voltage, the asymmetric junction showed Coulomb staircases. The capacitance of the junction estimated from the fitting curves using the Coulomb conventional theory was consistent with the capacitance calculated from the observed structure. The authors quantitatively found the correlation between the electrical and structural properties of DBTJ.

5. Halide Anion Mediated Dimer Formation of a *meso*-Unsubstituted N-Confused Porphyrin⁵⁾

The new N-confused porphyrin (NCP) derivatives, *meso*-unsubstituted *b*-alkyl, 3-oxo-N-confused porphyrin (3-oxo-NCP) and related macrocycles, were synthesized from appropriate pyrrolic precursors *via* a [3+1] type condensation reaction. 3-Oxo-NCP forms a self-assembled dimer in dichloromethane solution that is stabilized by complementary hydrogen bonding interactions arising from the peripheral amide-like moieties. The protonated form of 3-oxo-NCP was observed to bind halide anions (F⁻, Cl⁻) through the outer NH and the inner pyrrolic NH groups, affording a dimer in dichloromethane solution. The structure of the chloride-bridged dimer in the solid state was determined by X-ray diffraction analysis.

6. Photo Responsibility of Au Nanoparticle/Porphyrin Polymer Composite Device Using Nano-Gap Electrodes⁶⁾

Electrodes with a gap size of 15 ~ 80 nm could be bridged by porphyrin molecular wires with 50 ~ 300 nm length. The porphyrin units could be coordinated with Au nanoparticles having pyridinyl moiety. The device with both the porphyrin and Au nanoparticles showed photo-response characteristics while those without the Au nanoparticles showed no response.

7. Synthesis of Dendron Protected Porphyrin Wires and Preparation of a One-Dimensional Assembly of Gold Nanoparticles Chemically Linked to the π -Conjugated⁷⁾

A one-dimensional assembly of gold nanoparticles chemically bonded to π -conjugated porphyrin polymers was prepared on a chemically modified glass surface and on an undoped naturally oxidized silicon surface by the following methods: π -conjugated porphyrin polymers were prepared by oxidative coupling of 5,15-diethynyl-10,20-bis-(4-dendron)phenyl porphyrin, and its homologues (larger than 40-mer) were collected by analytical gel permeation chromatography. The porphyrin polymers were deposited using the Langmuir-Blodgett method on substrate surfaces, which were then soaked in a solution of gold nanoparticles (2.7±0.8 nm) protected with *t*-dodecanethiol and 4-pyridineethanethiol. The topographical images of the surface observed by tapping mode atomic force microscopy showed that the polymers could be dispersed on both substrates, with a height of 2.8±0.5 nm on the modified glass and 3.1±0.5 nm on silicon. The height clearly increased after soaking in the gold nanoparticle solution, to 5.3±0.5 nm on glass and 5.4±0.7 nm on silicon. The differences in height corresponded to the diameter of the gold nanoparticles bonded to the porphyrin polymers. The distance between gold nanoparticles observed in scanning electron microscopic images was *ca.* 5 nm, indicating that they were bonded at every four or five porphyrin units.

References

- 1) S. Chandramouli, T. S. Sreeprasad, T. Pradeep, G. V. P. Kumar, N. Chandrabhas, T. Yajima, Y. Sugawara, H. Tanaka, T. Ogawa and C. J., *Phys. Rev. Lett.* **99**, 167404 (4 pages) (2007).
- 2) T. Hino, H. Tanaka, H. Ozawa, Y. Iida and T. Ogawa, *Colloids Surf.*, A in press (2007).
- 3) Y. Miyake, H. Tanaka and T. Ogawa, *Colloids Surf.*, A in press (2007).
- 4) R. Negishi, T. Hasegawa, K. Terabe, M. Aono, H. Tanaka, H. Ozawa and T. Ogawa, *Appl. Phys. Lett.* **90**, 223112 (3 pages) (2007).
- 5) H. Furuta, H. Nanami, T. Morimoto, T. Ogawa, V. Král, J. L. Sessler and V. Lynch, *Chem. Asian J.* in press (2007).
- 6) T. Ogawa, H. Ozawa, M. Kawao and H. Tanaka, *J. Mater. Sci.: Mater. Electron.* **18**, 939–942 (2007).
- 7) H. Ozawa, M. Kawao, H. Tanaka and T. Ogawa, *Langmuir* **23**, 6365–6371 (2007).

Awards

MIYAKE, Yusuke; Outstanding Research Award, AsiaNano 2006.

MIYAKE, Yusuke; Best Poster Award, International Scanning Probe Microscopy Conference 2007.

* Present Address; Nanjin University, Nanjin, China

‡ Present Address; Tokai Regional Agricultural Administration Office, Nagoya

|| Present Address; Indian Institute of Technology, Chennai, India

** Present Address; Tokai Rubber Industries, Ltd., Komaki

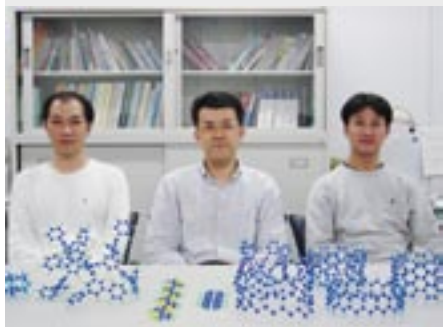
† Present Address; National Institute for Basic Biology, Okazaki

§ Present Address; Ebara Research Co., Ltd., Fujisawa

¶ Present Address; Nagoya University, Nagoya

Development of Organic Semiconductors for Molecular Thin-Film Devices

Research Center for Molecular Scale Nanoscience
Division of Molecular Nanoscience



SUZUKI, Toshiyasu
SAKAMOTO, Youichi
OKUBO, Kimitaka
WATANABE, Yoko

Associate Professor
Assistant Professor
Graduate Student
Secretary

Organic light-emitting diodes (OLEDs) and organic field-effect transistors (OFETs) based on π -conjugated oligomers have been extensively studied as molecular thin-film devices. Organic semiconductors with low injection barriers and high mobilities are required for highly efficient OLEDs and OFETs. Radical cations or anions of an organic semiconductor have to be generated easily at the interface with an electrode (or a dielectric), and holes or electrons must move fast in the semiconducting layer. Compared with organic p-type semiconductors, organic n-type semiconductors for practical use are few and rather difficult to develop. Recently, we found that perfluorinated aromatic compounds are efficient n-type semiconductors for OLEDs and OFETs.

1. Perfluoropentacene and Perfluorotetracene: Syntheses, Crystal Structures, and FET Characteristics¹⁾

We have synthesized perfluoropentacene and perfluorotetracene as potential n-type semiconductors for organic field-effect transistors (OFETs). Perfluoropentacene and perfluorotetracene are dark blue and reddish-orange crystalline solids, respectively. The HOMO-LUMO gaps of perfluorinated acenes are smaller than those of the corresponding acenes. The reduction potential of perfluoropentacene is almost the same as that of C₆₀, which is known as an excellent n-type semiconductor for FETs. Perfluoropentacene and perfluorotetracene are planar molecules that adopt herringbone structures with the angles of 91.2° and 91.1°, respectively. The short C–C contacts less than the sum of van der Waals radii were observed for both perfluorinated acenes. The interplanar distances are shorter than the layer separation of graphite, which may lead to high electron mobility along the stacking directions.

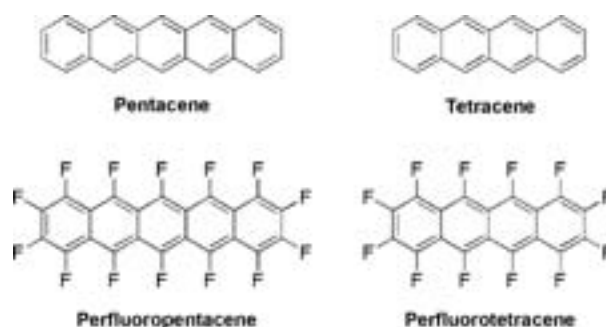
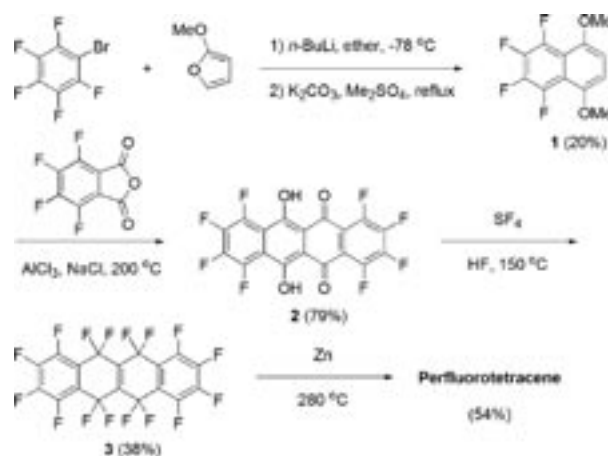


Figure 1. Structures of pentacene, tetracene, and their perfluorinated derivatives.



Scheme 1. Synthesis of perfluorotetracene.

2. Perfluorination of Tetracene: Effects on the Optical Gap and Electron-Acceptor Properties. An Electrochemical, Theoretical DFT, and Raman Spectroscopic Study

We report the synthesis and characterization of perfluorinated tetracene; a material with potential applications in organic electronics. The electrochemical behavior of the compound is analyzed by differential pulse voltammetry, and compared with that of tetracene. The structure of perfluorotetracene is planar as observed for pentacene. We also report a comparative Raman spectroscopic study of tetracene and perfluorotetracene in relation to their π -conjugational properties. Density functional theory calculations have been also performed, at the B3LYP/6-31G** level, to assess information regarding the topologies and energies of the frontier molecular orbitals around the gap, and about the vibrational normal modes associated with the Raman features selectively enhanced by the π -conjugation.

3. Optical Properties of Pentacene and Perfluoropentacene Thin Films

The optical properties of pentacene (PEN) and perfluoropentacene (PFP) thin films on various SiO₂ substrates were studied using variable angle spectroscopic ellipsometry. Structural characterization was performed using X-ray reflectivity and atomic force microscopy. A uniaxial model with the optic axis normal to the sample surface was used to analyze the ellipsometry data. Strong anisotropy was observed and enabled the direction of the transition dipole of the absorption bands to be determined. Furthermore, comparison of the optical constants of PEN and PFP thin films with the absorption spectra of the monomers in solution shows significant changes due to the crystalline environment. Relative to the monomer spectrum the HOMO-LUMO transition observed in PEN (PFP) thin film is reduced by 210 meV (280 meV). Surprisingly, a second absorption band in the PFP thin film shows a slight blueshift (40 meV) compared to the spectrum of the monomer with its transition dipole perpendicular to that of the first absorption band.

4. The Effect of Fluorination on Pentacene/Gold Interface Energetics and Charge Reorganization Energy²⁾

The energy level alignment at interfaces between conjugated organic semiconductors and metals is recognized as a

key factor determining the performance of organic-based (opto-) electronic devices. Experimentally, the hole injection barriers (HIBs) at organic/metal interfaces can be directly determined by ultraviolet photoelectron spectroscopy (UPS). In addition, angle-resolved UPS (AR-UPS) allows to assess important aspects of surface molecular orientation. In the present work, we used this method to investigate interfaces between two prototypical organic semiconductors pentacene (PEN) and perfluoropentacene (PFP) and Au. PEN can successfully be used as active material in organic field-effect transistors (OFETs) with high hole mobility of up to 5.5 cm²/Vs. The fabrication of integrated circuits requires also high electron mobility OFETs, which turns out to be difficult to achieve with pentacene, with reported electron mobilities up to 0.04 cm²/Vs. One approach to improve *n*-type performance of OFETs was to use perfluoropentacene, resulting in high electron mobilities of more than 0.2 cm²/Vs. Commonly, Au is used as source and drain contact metal in OFETs. Therefore, the interface energetics between organic semiconductors and Au are of interest, since charges have to be transported across these interfaces and minimized contact resistance is sought for.

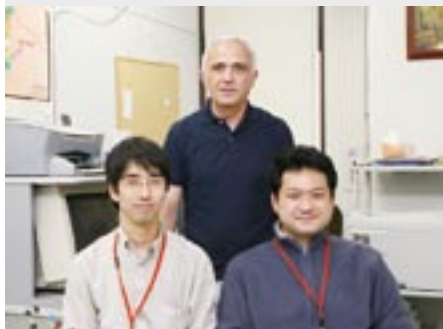
PEN and PFP monolayers on Au(111) exhibited very similar HIBs (0.60 eV vs. 0.65 eV), despite the significantly higher IE of the perfluorinated PEN analog. ϕ of Au(111) decreased upon PEN adsorption by 0.95 eV, while the decrease was only 0.5 eV for PFP. In the simple model of the “push-back” effect of surface metal electrons due to adsorption of molecules, our findings imply a larger bonding distance of PFP on Au compared to PEN. For PFP, four different layers away from Au were identified by significantly different HOMO binding energies, spreading by 0.8 eV. This spread was only 0.4 eV for PEN, and two layers could be resolved. PEN and PFP monolayers on Au(111) exhibited large charge reorganization energies, pointing towards strong charge localization at the interface.

References

- 1) Y. Sakamoto, T. Suzuki, M. Kobayashi, Y. Gao, Y. Inoue and S. Tokito, *Mol. Cryst. Liq. Cryst.* **444**, 225–232 (2006).
- 2) N. Koch, A. Vollmer, S. Duhm, Y. Sakamoto and T. Suzuki, *Adv. Mater.* **19**, 112–116 (2007).

Building Photosynthesis by Artificial Molecules

Research Center for Molecular Scale Nanoscience
Department of Nanomolecular Science



NAGATA, Toshi Associate Professor
ALLAKHVERDIEV, Suleyman I. Visiting Professor*
NAGASAWA, Takayuki Assistant Professor
WANATABE, Yoko Secretary

The purpose of this project is to build nanomolecular machinery for photosynthesis by use of artificial molecules. The world's most successful molecular machinery for photosynthesis is that of green plants—the two photosystems and related protein complexes. These are composed almost exclusively from organic molecules, plus a small amount of metal elements playing important roles. Inspired by these natural systems, we are trying to build up multimolecular systems that are capable of light-to-chemical energy conversion. At present, our interest is mainly focused on constructing necessary molecular parts.

1. An Approach towards Artificial Quinone Pools by Use of Photo- and Redox-Active Dendritic Molecules¹⁾

Mimicking individual processes of photosynthesis by use of artificial molecules is an interesting approach for chemists to build up new systems for light-to-chemical energy conversion. In this respect, particular success has been, and is being, achieved by studies on photoinduced electron transfer, models of antenna systems and oxygen evolving complexes. However, many other features of photosynthesis are still unexplored by model chemists. The quinone pool is one of such disregarded features.

We built a “single-molecular” quinone pool by use of synthetic molecules (Figure 1). The molecules are based on dendrimers with well-defined size and shape. A porphyrin (photoactive group) is attached at the center, and multiple quinones are attached at internal positions of the dendrimer.

When these molecules were irradiated with visible light ($\lambda > 500$ nm) in the presence of 4-*tert*-butylthiophenol, the quinones were gradually converted to the corresponding quinols. Figure 2 shows the time-dependent change of ¹H NMR under these conditions. This reaction is triggered by photoexcitation of the porphyrin. A particularly interesting observation in

Figure 2 is that the quinones of all layers in G3Q₁₄P were converted to quinols at similar apparent rates. We attribute this apparent layer independence of the conversion rate to the photoinduced exchange of quinone/quinol.

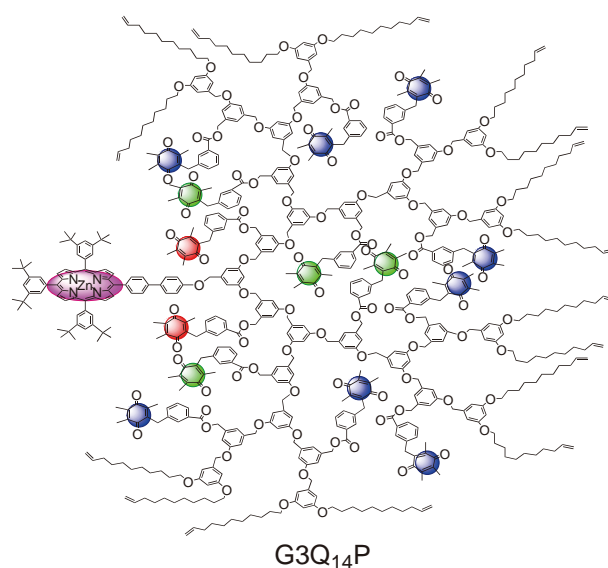


Figure 1. The artificial quinone pool compound.

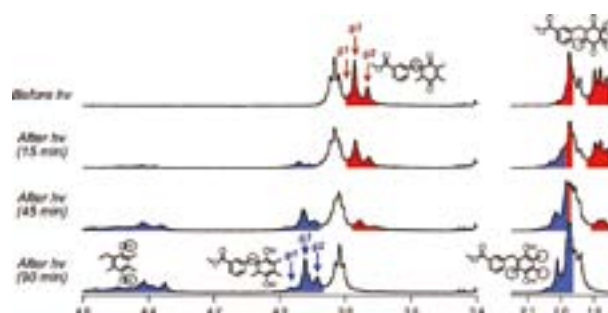


Figure 2. Time-dependent change of the ¹H NMR of G3Q₁₄P during photoreaction with 4-*tert*-butylthiophenol.

2. Rigid Tricarboxylate Ligands Derived from Triarylmesitylenes and Their Metal Complexes

Carboxylate ligands are widely found in active sites of metalloenzymes. From the synthetic point of view, however, there is one long-standing problem about metal-carboxylate clusters; carboxylate ligands can exist in various coordination modes (monodentate, η^1 -bridging, η^2 -bridging with *syn/anti* variations, *etc.*), hence it is very difficult to predict what structure(s) will result under particular reaction conditions. Even preformed clusters can easily rearrange to give products with very different structures.

To overcome these general difficulties in metal carboxylate chemistry, we developed a new tricarboxylate ligand **1**, which is designed suitably to bind to a particular trinuclear $M_3(\mu_3-O)$ core (Figure 3). The ligand **1** is a derivative of *syn*-2,4,6-tris(2'-X-aryl)-1,3,5-trimethylbenzene (triarylmesitylene), in which the three side chains (X) of the aryl groups are fixed in the same side of the central mesitylene ring because of the restricted rotation of the aryl-mesityl bonds. In addition, the carboxylate groups at the end of the side chains are located in suitable positions to bind to a $M_3(\mu_3-O)$ core.

We successfully prepared the triiron complex $[Fe_3(\mu_3-O)(\mathbf{1})_2(H_2O)_3]FeCl_4$ and characterized by X-ray crystallography (Figure 4). Interestingly, the similar compound lacking the 1,3,5-methyl groups did not give the similar complex. Such difference was rationalized by the molecular dynamic (MD) simulations (Figure 5). This ligand will serve as useful building blocks for constructing difficult metal clusters as observed in the photosynthetic oxygen-evolving center.

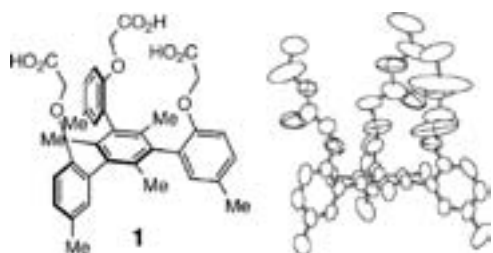


Figure 3. The ligand **1** and the X-ray structure of the triethyl ester.

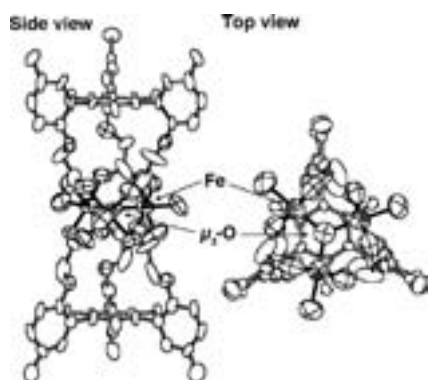


Figure 4. The X-ray structure of $[Fe_3(\mu_3-O)(\mathbf{1})_2(H_2O)_3]^+$.

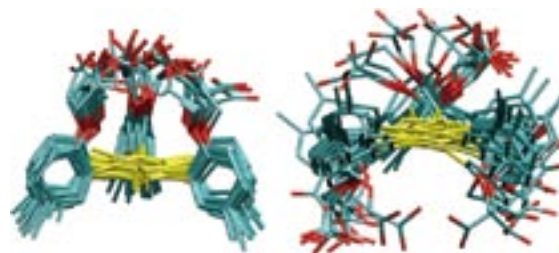


Figure 5. The MD trajectory of **1** (left) and that lacking the 1,3,5-methyl groups (right).

3. Reconstitution of the Water-Oxidizing Complex in Photosystem II Using Synthetic Mn Complexes: Production of Hydrogen Peroxide²⁾

Oxygen evolution is one of the most important, and most enigmatic, processes in plant photosynthesis. The function is performed at the oxygen-evolving complex (OEC), which contains, among others, four manganese ions as essential cofactors. The OEC resides at the oxidizing terminal of Photosystem II (PS2). Since the PS2 is a very efficient biomolecular device for photoinduced charge separation, replacing the OEC with other metal complexes is an interesting approach for developing new functions of photoinduced chemical conversion.

We attempted the reconstitution of the OEC with several dinuclear complexes of Mn(II) and Mn(IV). The reconstituted PS2 samples with these compounds regained the electron-transfer capability, but the oxygen evolution capability was less efficient. More interestingly, it was shown that hydrogen peroxide was produced by these reconstituted PS2 samples. This is the first example of reconstituted PS2 samples that exhibit non-natural photochemical functions.

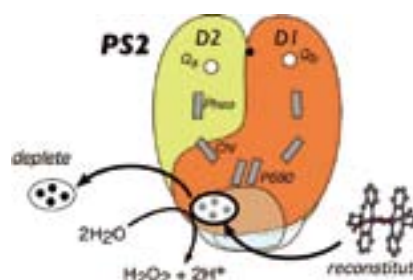


Figure 6. Schematic representation of PS2 reconstituted with an artificial Mn complex.

References

- 1) T. Nagata and Y. Kikuzawa, *Biochim. Biophys. Acta* **1767**, 648–652 (2007).
- 2) T. Nagata, T. Nagasawa, S. K. Zharmukhamedov, V. V. Klimov and S. I. Allakhverdiev, *Photosynth. Res.* **93**, 133–138 (2007).

* Present Address; Institute of Basic Biological Problems, Russian Academy of Sciences, Pushchino, Moscow Region 142290, Russia

Chemistry of Bowl-Shaped Aromatic Compounds and Metal Nanocluster Catalysts

Research Center for Molecular Scale Nanoscience
Division of Molecular Nanoscience



SAKURAI, Hidehiro Associate Professor
HIGASHIBAYASHI, Shuhei Assistant Professor
KAMIYA, Ikuyo IMS Fellow
NAKANO, Sachiko Research Fellow
REZA, A. F. G. Masud Graduate Student
KITAHARA, Hiroaki Graduate Student
ONOGI, Satoru Graduate Student
SASAKI, Tokiyo Secretary

Bowl-shaped π -conjugated compounds including partial structures of the fullerenes, which are called “buckybowls,” are of importance not only as model compounds of fullerenes but also as their own chemical and physical properties. Heteroatom-containing buckybowls (heterobuckybowls) have also been expected to exhibit unique physical characters. For example, in solution they show the characteristic dynamic behavior such as bowl-to-bowl inversion. On the other hand, they sometimes favor stacking structure in a concave-convex fashion in the solid state, giving excellent electron conductivity. Furthermore, some buckybowls are conceivable to possess the bowl-chirality if the racemization process, as equal as bowl-to-bowl inversion, is slow enough to be isolated. However, very few buckybowls/heterobuckybowls has been achieved for preparation mainly due to their strained structure, and no report on the preparation of chiralbowls has appeared. In the present project, we develop the rational route to the various kinds of buckybowls/heterobuckybowls with perfect chirality control using the organic synthesis approach.

We also investigate to develop novel catalytic properties of metal nanoclusters. We focus on the following projects: Preparation of size-selective gold nanoclusters supported by hydrophilic polymers and its application to aerobic oxidation catalysts: Synthetic application using metal nanocluster catalyst: Development of designer metal nanocluster catalyst using the highly- functionalized protective polymers: Catalytic activity of metal nanoclusters under the laser-irradiated conditions.

1. Synthesis of an Enantiopure *syn*-Benzocyclootrimer through Regio-Selective Cyclootrimerization of Halonorbornenes under Palladium Nanocluster Conditions¹⁾

An enantiopure *syn*-benzocyclootrimer (**1**) was selectively synthesized from an enantiopure halonorbornene (**2**) through

regio-selective cyclootrimerization catalyzed by palladium nanoclusters. The yield of **1** was dependent on the stability of the palladium clusters, which was ascertained from the appearance and TEM images of the reaction mixtures. The thus-prepared enantiopure benzocyclootrimer will serve as a key intermediate for the synthesis of C_{3v} symmetric chiral buckybowls.

Table 1.

Entry	Bu ₄ NX	Base	Solvent	Yield of 1
1	Bu ₄ NBr 100 mol %	NEt ₃ 250 mol %	DMF	trace
2	Bu ₄ NOAc 100 mol %	Na ₂ CO ₃ 1000 mol %	1,4-dioxane	34%
3	Bu ₄ NOAc 300 mol %	Na ₂ CO ₃ 1000 mol %	1,4-dioxane	42%
4	Bu ₄ NOAc 500 mol %	Na ₂ CO ₃ 1000 mol %	1,4-dioxane	47%
5	Bu ₄ NOAc 1000 mol %	Na ₂ CO ₃ 1000 mol %	1,4-dioxane	53%

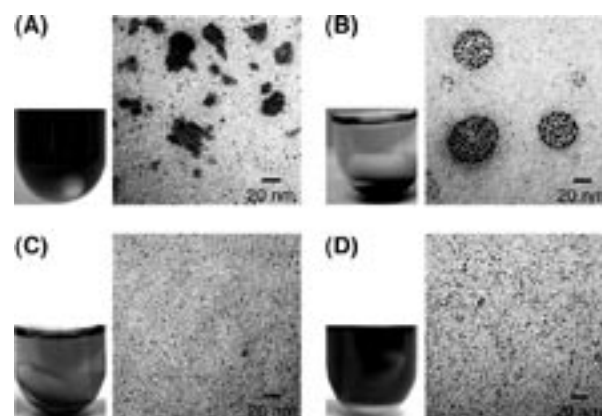
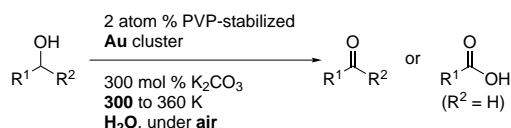


Figure 1.

Photographs and typical TEM images of the reaction mixtures under the conditions listed in entries 1, 2, 4, and 5 in Table 1 are shown in Figure 1. Judging from the appearance of the reaction mixtures, the Pd nanoclusters were well dispersed in the order of (B) < (C) < (D) which was consistent with the amount of Bu₄NOAc. The amount of precipitation of Pd black was observed in the opposite order, (B) > (C) > (D). The TEM images supported these observations. In Table 1, we show the result using the conditions which are considered typical reaction conditions for generation of Pd nanoclusters (Entry 1; Figure 1A). Indeed, the appearance of (A) was similar to that of (D), indicating the formation of nanoclusters. However, a considerable degree of aggregation of clusters was observed in the TEM images as well as in those of (B). Although both clusters in (C) and (D) were well dispersed judging from the TEM images, the concentration of clusters was much higher in (D), consistent with their appearance. These observations strongly suggest that the generation of Pd nanoclusters in appropriate conditions might be very important and that an excess amount of Bu₄NOAc could realize well-dispersed nanoclusters.

2. Synthetic Application of PVP-Stabilized Au Nanocluster Catalyst to Aerobic Oxidation of Alcohols in Aqueous Solution under Ambient Conditions²⁾

Gold nanoclusters ($\phi = 1.3$ nm) stabilized by poly(*N*-vinyl-2-pyrrolidone) (Au:PVP) were found to show a high catalytic activity toward the aerobic oxidation of alcohols. Various kinds of primary and secondary alcohols were converted to the corresponding carboxylic acids and ketones, respectively, in basic aqueous media at 300–360 K under air.



3. Lewis Acid Character of Zero-Valent Gold Nanoclusters under Aerobic Conditions: Intramolecular Hydroalkoxylation of Alkenes³⁾

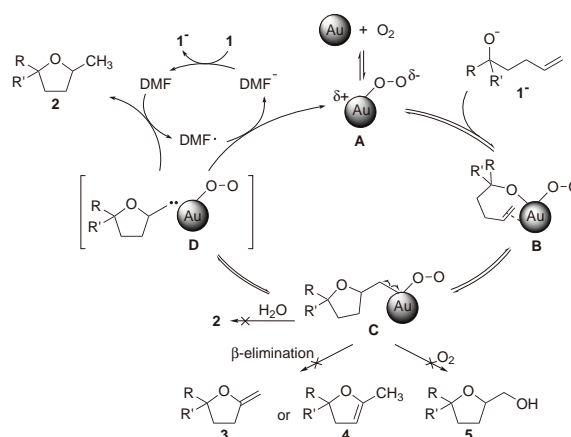
Gold nanoclusters stabilized by poly(*N*-vinyl-2-pyrrolidone) (Au:PVP NCs, $\phi = 1.3$ nm) behave as Lewis acid catalyst in aqueous media under aerobic conditions, to promote the intramolecular hydroalkoxylation of unactivated alkenes. Molecular oxygen generates a reaction center having

the Lewis acidic character on the surface of Au NCs in which constituent gold atoms are formally in zero-valence state.

Table 2. The role of molecular oxygen in the cyclization of **1a**.

entry	catalyst	conditions	yield, %
1	Au:PVP(1.3)	under air	87
2	Au:PVP(1.3)	under degassed conditions	0
3	Au:PVP(9.5)	under air	0

A possible mechanism is shown in Scheme 1. The reaction is initiated by formation of key intermediate **A**, which possesses an electron-deficient site generated by adsorption of O₂ onto the surface of the Au NCs. **A** acts as a Lewis acid, activating both the alkoxide and alkene by adsorption onto the surface (**B**), and giving **C** by the insertion of an alkene into the O–Au bond. From **C**, neither β -elimination, O₂ insertion, nor protonation proceeds; only homolytic dissociation takes place, generating the radical intermediate **D**, which afforded **2** via hydrogen abstraction from DMF accompanied by the regeneration of free Au NCs. Judging from the decrease in the reaction rate in DMF-*d*₇, all the steps between **A** and **D** may be in equilibrium.



Scheme 1. A possible mechanism for Au(0):PVP-catalyzed hydroalkoxylation.

References

- 1) S. Higashibayashi and H. Sakurai, *Chem. Lett.* **36**, 18–19 (2007).
- 2) H. Tsunoyama, T. Tsukuda and H. Sakurai, *Chem. Lett.* **36**, 212–213 (2007).
- 3) I. Kamiya, H. Tsunoyama, T. Tsukuda and H. Sakurai, *Chem. Lett.* **36**, 646–647 (2007).

Awards

KAMIYA, Ikuyo; Best Poster Presentation Award, The 3rd Organic Chemistry Young Researchers' Workshop, Nagoya University.
 HIGASHIBAYASHI, Shuhei; Best Presentation Award, The 87th Spring Meeting, Chemical Society of Japan.
 HIGASHIBAYASHI, Shuhei; Best Poster Presentation Award, Symposium on Molecular Chirality 2007.
 HIGASHIBAYASHI, Shuhei; Best Poster Presentation Award, The 17th International Symposium on Olefin Metathesis.

Structural Analyses of Biological Macromolecules by Ultra-High Field NMR Spectroscopy

Research Center for Molecular Scale Nanoscience
Division of Advanced Molecular Science



KATO, Koichi
SASAKAWA, Hiroaki
SUGIHARA, Takahiro
SUMIYOSHI, Akira
UTSUMI, Maho
AMEMIYA, Eiko
ENDA, Hiroki
OHNO, Erina
SASAKI, Tokiyo

Visiting Professor
Assistant Professor
Research Fellow
Graduate Student*
Graduate Student*
Graduate Student*
Graduate Student*
Graduate Student*
Secretary

Our research seeks the underlying molecular basis for the function of biological macromolecules. In particular, we are interested in the function of molecular machines that work in the cellular processes involving protein folding, transport and degradation, and of glycoproteins playing important roles in the humoral and cellular immune systems. By use of ultra-high field NMR spectroscopy, we aim to elucidate the three-dimensional structure, dynamics, and interactions of proteins and glycoconjugates at the atomic level. Here we report stable-isotope-assisted NMR studies of IgG-Fc glycoprotein, NEDD8 and protein disulfide isomerase.

fucosylated Fc crystals were both different from those in previously reported isomorphous Fc crystals.

1. Structural Comparison of Fucosylated and Nonfucosylated Fc Fragments of Human Immunoglobulin G1¹⁾

Removal of the fucose residue from the oligosaccharides attached to Asn297 of human immunoglobulin G1 (IgG1) results in a significant enhancement of antibody-dependent cellular cytotoxicity (ADCC) via improved IgG1-binding to Fcγ receptor IIIa (FcγRIIIa). To provide a structural insight into the mechanisms of affinity enhancement, we determined the crystal structure of non-fucosylated Fc fragment and compared it with that of fucosylated Fc. The overall conformations of the fucosylated and non-fucosylated Fc fragments were similar except for hydration mode around Tyr296. Stable-isotope-assisted NMR analyses confirmed the similarity of the overall structures between fucosylated and non-fucosylated Fc fragments in solution. These data suggest that the glycoform-dependent ADCC enhancement is attributed to a subtle conformational alteration in a limited region of IgG1-Fc. Furthermore, the electron density maps revealed that the traces between Asp280 and Asn297 of our fucosylated and non-

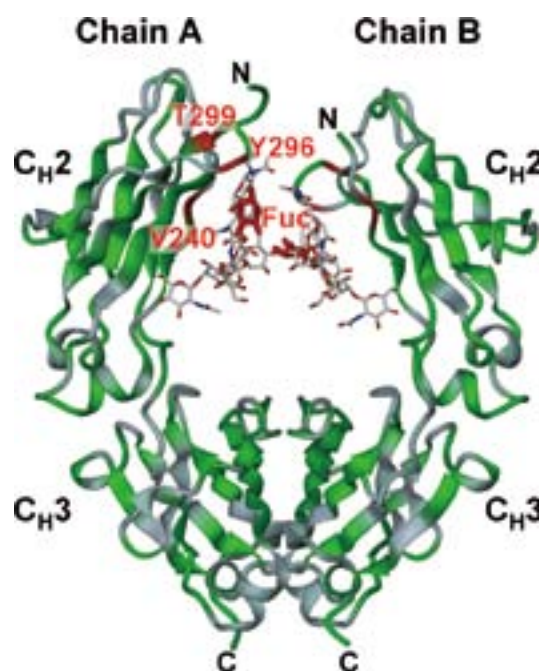


Figure 1. Mapping on the crystal structure of Fuc (+) of the amino acid residues showing the chemical shift difference between Fuc (+) and Fuc (-). The chemical shift differences are quantified for each residue according to the equation $(0.2\delta N^2 + \delta H^2)^{1/2}$, where δN and δH represent the differences in nitrogen and proton chemical shifts between Fuc (+) and Fuc (-). The amino acid residues showing and not showing observable chemical shift differences $[(0.2\delta N^2 + \delta H^2)^{1/2} > 0.1 \text{ ppm}]$ are colored red and green, respectively. The Fuc residues are colored magenta.

2. Direct Interactions between NEDD8 and Ubiquitin E2 Conjugating Enzymes Upregulate Cullin-Based E3 Ligase Activity²⁾

Although cullin-1 neddylation is crucial for the activation of SCF ubiquitin E3 ligases, the underlying mechanisms for NEDD8-mediated activation of SCF remain unclear. We demonstrated by NMR and mutational studies that NEDD8 binds the ubiquitin E2 (UBC4), but not NEDD8 E2 (UBC12). Our data imply that NEDD8 forms an active platform on the SCF complex for selective recruitment of ubiquitin-charged E2s in collaboration with RBX1, and thereby upregulates the E3 activity.

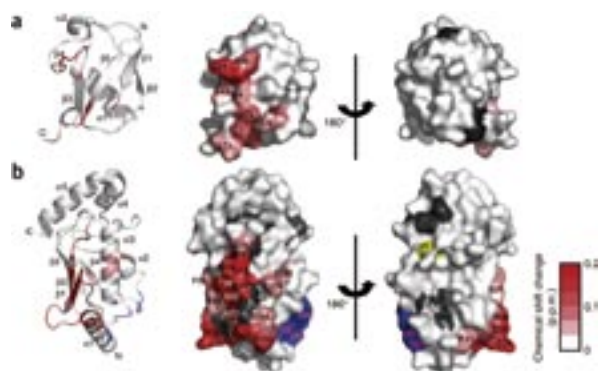


Figure 2. Identification of the binding sites on NEDD8 and UBC4. (a,b) Mapping of the perturbed residues of NEDD8 (a) and UBC4 (b) upon binding to each other. Residues are highlighted in red on the crystal structures of NEDD8 and UBC4. Red gradient indicates the strength of the perturbation. Blue, residues involved in the interaction with the RING-finger domain in the crystal structure of c-Cbl (PDB 1FBV); gray, prolines; yellow, catalytic cysteine (C85).

3. NMR Assignments of the *b'* and *a'* Domains of Thermophilic Fungal Protein Disulfide Isomerase³⁾

Protein disulfide isomerase (PDI) is a folding assistant in the endoplasmic reticulum that catalyzes the formation, break-

age and rearrangement of disulfide bonds of its substrate proteins. PDI comprises four structural domains, *a*, *b*, *b'*, *a'* plus C-terminal extension. To gain insight into the functions of PDI, we initiated NMR structure determinations of the *b'* and *a'* domains of thermophilic fungal PDI expressed in *E. coli*. Backbone NH signals of these domains were completely assigned except for His367 in the *a'* domain. In total, 87% (*b'* domain) and 86% (*a'* domain) of the observable proton signals were assigned. The secondary chemical shifts indicate that both domains assume thioredoxin folds.

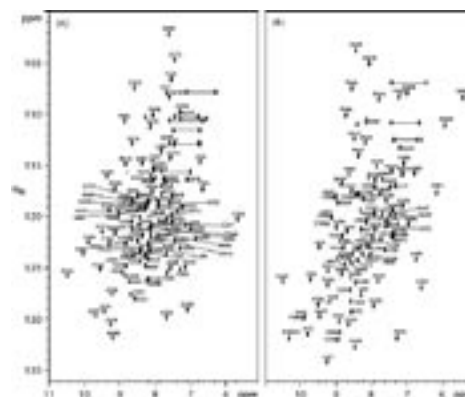


Figure 3. ¹H-¹⁵N HSQC spectra of 1 mM uniformly ¹³C/¹⁵N-labeled *b'* domain (a) and *a'* domain (b) of thermophilic fungal PDI in the presence of 10 mM [²H₁₀]dithiothreitol. Backbone amide cross peaks are indicated with assignments. The residue numbering of intact PDI was applied for each domain.

References

- 1) S. Matsumiya, Y. Yamaguchi, J. Saito, M. Nagano, H. Sasakawa, S. Otaki, M. Satoh, K. Shitara and K. Kato, *J. Mol. Biol.* **368**, 767–779 (2007).
- 2) E. Sakata, Y. Yamaguchi, Y. Miyauchi, K. Iwai, T. Chiba, Y. Saeki, N. Matsuda, K. Tanaka and K. Kato, *Nat. Struct. Mol. Biol.* **14**, 167–168 (2007).
- 3) M. Nakano, C. Murakami, Y. Yamaguchi, H. Sasakawa, T. Harada, E. Kurimoto, O. Asami, T. Kajino and K. Kato, *J. Biomol. NMR* **36**, 44 (2006).

Awards

UTSUMI, Maho; Physical Pharma Forum 2007 (The Pharmaceutical Society of Japan, Division of Physical Sciences) Award of Superior Excellence.

UTSUMI, Maho; 71st The Japanese Biochemical Society, Chubu Branch, Award for Young Scientists.

* carrying out graduate research on Cooperative Education Program of IMS with Nagoya City University

Development of Multifunction Integrated Macromolecules for Molecular-Scale Electronics

Research Center for Molecular Scale Nanoscience
Division of Molecular Nanoscience



TANAKA, Shoji

Assistant Professor

The concept of molecular-scale electronics is now realized for individual components such as wire, diode, switch, and memory cell, but the fabrication of complete molecular-scale circuits remains challenging because of the difficulty of connecting molecular modules to one another. Monomolecular Integration technology, which integrates the wiring, transistors, and the required passive elements on a single macromolecule, has been proposed as a promising solution to this problem. In this project we have been developing the architecture of this novel class of macromolecules and the protocols for their purposive organization on metal or semiconductor substrate surfaces.

1. Multipurpose Building Blocks for over 10 nm Long π -Conjugated System

“Stepwise synthesis” is the most flexible tool to construct tailor-made π -conjugated macromolecules with well defined functions for nanoscience and technology, however, the stepwise fabrication of over 10 nm long molecular skeleton is still a great challenge. As a solution to this problem, we have

developed a series of versatile building blocks (1-2) as shown in Figure 1, which are active for typical Pd or Ni-catalyzed Ar–Ar coupling reactions. It is facile to access to a wide variety of 1–75 nm long π -conjugated macromolecules from the combination of these blocks and 1–10 nm long molecular modules so far reported (3–9). The synthetic examples are presented in Figure 2.

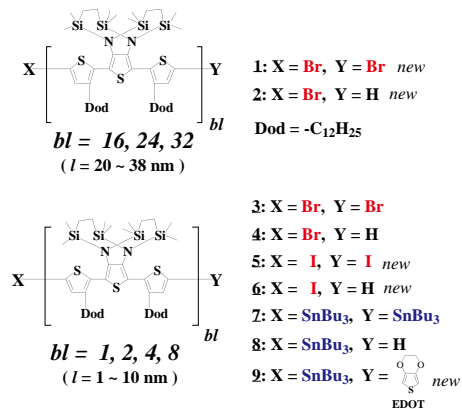
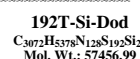
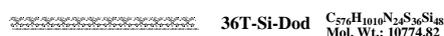
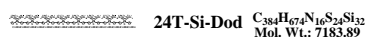
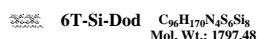


Figure 1. Molecular structures of building blocks (1-9).

Figure 2. Synthetic examples of precisely-defined α -oligothiophene derivatives.



Development of Novel Heterocyclic Compounds and Their Molecular Assemblies for Advanced Materials

Safety Office



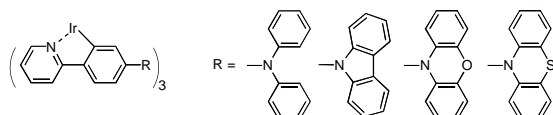
TOMURA, Masaaki

Assistant Professor

Heterocycles containing sulfur and/or nitrogen atoms are useful as components of functional materials since heteroatoms in their rings are helpful to stabilize ions or ion-radical species, and extended π -conjugation decreases Coulombic repulsion. In addition intermolecular interactions caused by heteroatom contacts can be expected to form novel molecular assemblies. In this project new electron acceptors, donors, and donor-acceptor compounds based on heterocycles such as 1,2,5-thiadiazole and 1,3-dithiole were synthesized and their physical properties including those of the charge-transfer complexes or ion-radical salts were investigated. Unique crystal structures were constructed by using weak intermolecular interactions such as hydrogen bonding or heteroatom contacts.

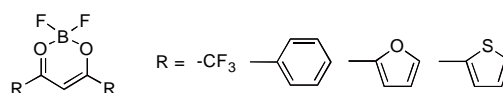
1. Synthesis and Electroluminescence Properties of *fac*-Tris(2-phenylpyridine)-iridium Derivatives Containing Hole-Accepting Moieties¹⁾

For effective organic electroluminescent (EL) devices, we synthesized *fac*-tris(2-phenylpyridine)iridium [Ir(ppy)₃] derivatives containing hole-trapping moieties, such as diphenylamine, carbazole, and phenoxazine. Their photoluminescent maxima were observed around the maximum of Ir(ppy)₃. These values were slightly shifted depending on the hole-trapping moieties. EL devices using an Ir complex with diphenylamine exhibited high EL performance because 1,1-bis[4-(di-*p*-tolylamino)phenyl]cyclohexane was employed as a hole-transporting layer. The maximum external quantum efficiency was recorded as 12.2% which is comparable to that observed in a device using Ir(ppy)₃.



2. Synthesis and Photoluminescence Properties of BF₂ Complexes with 1,3-Diketone Ligands²⁾

BF₂ complexes with 1,3-diketone ligands were synthesized, and their optical and electrochemical properties were studied. The colors of the complexes varied depending on the structures of the 1,3-diketone ligands. The absorption and emission maxima of the complexes with 1,3-diaryl-1,3-diketone ligands were considerably red shifted as compared to those of the complexes with 1-aryl-3-trifluoromethyl-1,3-diketone ligands, suggesting an extended p -conjugation of the 1,3-diaryl-1,3-diketone moieties. The molar absorption coefficients and quantum yields of the complexes with 1,3-diaryl-1,3-diketone ligands were larger than those of the complexes with 1-aryl-3-trifluoromethyl-1,3-diketone ligands. Cyclic voltammetry measurements revealed that the reduction potentials of the BF₂ complexes were higher than those of the free ligands. These complexes exhibited various emission colors in the solid states due to the intermolecular interactions.



References

- 1) K. Ono, M. Joho, K. Saito, M. Tomura, Y. Matsushita, S. Naka, H. Okada and H. Onnagawa, *Eur. J. Inorg. Chem.* 3676–3683 (2006).
- 2) K. Ono, K. Yoshikawa, Y. Tsuji, H. Yamaguchi, R. Uozumi, M. Tomura, K. Taga and K. Saito, *Tetrahedron* **63**, 9354–9358 (2007).

Visiting Professors



Visiting Professor
BABA, Yoshinobu (from Nagoya University)

Biomolecular Imaging by Quantum Dot

We developed new materials, which are synthesized by conjugation of quantum dots (QD) and biomolecules, including DNA, enzyme, and lectin. The QD-biomolecule conjugated materials are applied to single molecule imaging of real-time interaction between DNA and enzyme, real-time imaging of single DNA molecule trafficking into a single cell, and differentiation of a single cancer cell by selective labeling of QD-lectin conjugate and imaging. These techniques are extremely useful to understand the mechanism of an enzymatic reaction at the single molecule level, to enhance the gene transfection efficiency in the gene therapy, and to develop novel technology for cancer diagnosis in the very early stage of cancer.



Visiting Associate Professor
HIGUCHI, Masayoshi (from National Institute for Materials Science)

Creation of Novel Organic-Metallic Hybrid Polymers and their Electrochromic Functions

Organic-metallic hybrid polymers are expected to have unique electrochemical, photochemical, magnetic, or catalytic properties based on strong interaction between organic modules and metal ions. Novel hybrid polymers are formed by complexation of iron(II) acetate with bis(terpyridyl)benzenes as an organic module. The polymers have specific colors based on the metal-to-ligand charge transfer and the color disappears by electrochemical oxidation of the polymer. The electrochromic properties are caused by electrochemical redox of metal ions in the polymers. Interestingly, a single film of the hybrid polymer including both iron(II) and cobalt(II) ions shows multi-color electrochromic change: red, blue, and colorless at 0, 0.6, and 1.0 V vs. Ag/Ag⁺, respectively. The hybrid polymers with excellent electrochromic functions will be applied to “electronic papers,” one of next generation displays.



Visiting Associate Professor
MAEDA, Hiromitsu (from Ritsumeikan University)

Pyrrole-Based Molecular Assemblies and Supramolecular Structures

Acyclic π -conjugated oligopyrrole derivatives, though less extensively studied so far, often potentially have even more advantages as anion receptors and metal coordination ligands than cyclic ones. This is due to the formation of versatile complexes and supramolecular assemblies, although they require conformation changes by guest binding. Of the linear oligopyrroles, oligomeric derivatives of dipyrins bridged by π -conjugated spacers behave as building subunits and form coordination oligomers and discrete coordination nanorings. On the other hand, pyrrole oligomers with hydrogen bonding accepting site(s) have yielded unique morphologies as supramolecular assemblies and micro- and nanometer-scale structures by means of hydrogen bonding interactions. Furthermore, a new class of acyclic anion receptors, namely BF₂ complexes of dipyrrolyldiketones, have been shown to interact with anions by means of both pyrrole NH and bridging CH interactions. Ring inversion of pyrrole rings have been found to be essential to capture anions using these binding sites. Aryl-substitution of the receptors as π -extended derivatives has enabled the formation of assemblies such as supramolecular organogels that can be controlled by the addition of anions



RESEARCH ACTIVITIES

Life and Coordination-Complex Molecular Science

Department of Life and Coordination-Complex Molecular Science is composed of two divisions of Biomolecular science, two divisions of Coordination molecular science and one adjunct division. Biomolecular science divisions cover the studies on the elucidation of functions and mechanisms for various types of sensor proteins, protein folding, molecular chaperone, and metal proteins. Coordination complex divisions undergo to develop molecular catalysts for the transformation of organic molecules, activation small inorganic molecules, and reversible conversion between chemical and electrical energies. Based on the fundamental researches conducted by each division, interdisciplinary alliances in the Department aim at the creation of fundamental concepts for the molecular and energy conversion.

Bioinorganic Chemistry of Novel Hemeproteins

Department of Life and Coordination-Complex Molecular Science
Division of Biomolecular Functions



AONO, Shigetoshi
YOSHIOKA, Shiro
SAWAI, Hitomi

YASUHIRA, Kengo
YOSHIMURA, Hideaki
NISHIMURA, Muneto
TANIZAWA, Misako

Professor
Assistant Professor
IMS Fellow (–March '07)
JSPS Post-Doctoral Fellow (April '07–)
IMS Fellow
Graduate Student*
Graduate Student
Secretary

Heme-based sensor proteins show a novel function of the heme prosthetic group, in which the heme acts as the active site for sensing the external signal such as diatomic gas molecules and redox change. Aldoxime dehydratase is another novel hemeprotein, in which the heme prosthetic group tethers the substrate for its dehydration reaction. Our research interests are focused on the elucidation of the structure-function relationships of these novel hemeproteins.

1. Crystal Structure of CO-Sensing Transcription Activator CooA Bound to Exogenous Ligand Imidazole¹⁾

CooA is a CO-dependent transcriptional activator and transmits a CO sensing signal to a DNA promoter that controls the expression of the genes responsible for CO metabolism. CooA contains a b-type heme as the active site for sensing CO. CO binding to the heme induces a conformational change that switches CooA from an inactive to an active DNA-binding form. Here, we report the crystal structure of an imidazole-bound form of CooA from *Carboxydotherrmus hydrogeniformans* (Ch-CooA). In the resting form, Ch-CooA has a six-coordinate ferrous heme with two endogenous axial ligands, the α -amino group of the N-terminal amino acid and a histidine residue. The N-terminal amino group, which is coordinated to the heme in CooA, is replaced by CO. This substitution presumably triggers a structural change leading to the active form. The crystal structure of Ch-CooA reveals that imidazole binds to the heme, which replaces the N terminus, as does CO. The dissociated N terminus is positioned approximately 16 Å from the heme iron in the imidazole-bound form. In addition, the heme plane is rotated by 30° about the normal of the porphyrin ring compared to that found in the inactive form of *Rhodospirillum rubrum* CooA. Even though the ligand

exchange takes place, imidazole-bound Ch-CooA remains in the inactive form for DNA binding. These results indicate that the release of the N terminus resulting from imidazole binding is not sufficient to activate CooA. The structure provides new insights into the structural changes required to achieve activation.

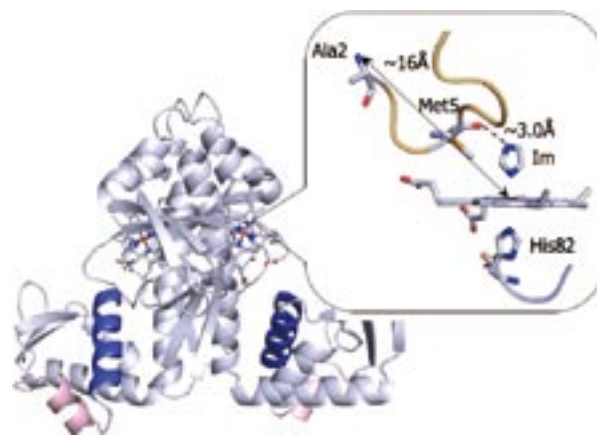


Figure 1. Structure of imidazole-bound Ch-CooA and the close-up view around the heme.

2. The Formation of Hydrogen Bond in the Proximal Heme Pocket of HemAT-Bs upon Ligand Binding²⁾

HemAT-Bs is the heme-based O₂ sensor responsible for aerotaxis control in *Bacillus subtilis*. In this study, we measured the time-resolved resonance Raman spectra of full-length HemAT-Bs wild-type (WT) and Y133F in the deoxy form and the photoproduct after photolysis of CO-bound form.

In WT, the $\nu_{\text{Fe-His}}$ band for the 10 ps photoproduct was observed at higher frequency by about 2 cm^{-1} compared with that of the deoxy form. This frequency difference is relaxed in hundreds of picoseconds. This time-dependent frequency shift would reflect the conformational change of the protein matrix. On the other hand, Y133F mutant does not show such a substantial $\nu_{\text{Fe-His}}$ frequency shift after photolysis. Since a hydrogen bond to the proximal His induces an up-shift of the $\nu_{\text{Fe-His}}$ frequency, these results indicate that Tyr133 forms a hydrogen bond to the proximal His residue upon the ligand binding. We discuss a functional role of this hydrogen bond formation for the signal transduction in HemAT-Bs.

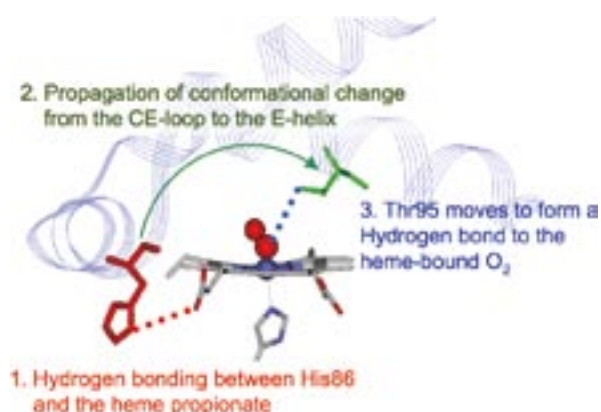


Figure 2. Signal transduction pathway of HemAT-Bs.

3. Two Ligand Binding Sites in the O_2 -Sensing Signal Transducer HemAT: Implication for Ligand Recognition/Discrimination and Signaling³⁾

We have identified a ligand (CO) accommodation cavity in the signal transducer sensor protein HemAT (heme-based aerotactic transducer) that allows us to gain single-molecule insights into the mechanism of gas sensor proteins. Specific mutations that are distal and proximal to the heme were designed to perturb the electrostatic field near the ligand that is bound to the heme and near the accommodated ligand in the cavity. We report the detection of a second site in heme proteins in which the exogenous ligand is accommodated in an internal cavity. The conformational gate that directs the ligand-migration pathway from the distal to the proximal site of the heme, where the ligand is trapped, has been identified. The

data provide evidence that the heme pocket is the specific ligand trap and suggest that the regulatory mechanism may be tackled starting from more than one position in the protein. Based on the results, we propose a dynamic coupling between the two distinct binding sites as the underlying allosteric mechanism for gas recognition discrimination that triggers a conformational switch for signaling by the oxygen sensor protein HemAT.

4. Systematic Regulation of the Enzymatic Activity of Phenylacetaldoxime Dehydratase by Exogenous Ligand⁴⁾

Phenylacetaldoxime dehydratase from *Bacillus* sp. OxB-1 (OxDB) contains a heme that acts as the active site for the dehydration reaction of aldoxime. Ferrous heme is the active form, in which the heme is 5-coordinated with His282 as the proximal ligand. In this work, we evaluated the functional role of the proximal ligand for the catalytic properties of the enzyme by “the cavity mutant technique.” H282G mutant of OxDB lost the enzymatic activity, though the heme, which was 5-coordinated with a water (or OH^-) as an axial ligand, existed in the protein matrix. The enzymatic activity was rescued by imidazole or pyridine derivatives that acted as the exogenous proximal ligand. By changing electron donation ability of these exogenous ligands with different substituents, the enzymatic activity could be regulated systematically. The stronger electron donation ability of the exogenous ligand, the higher restored enzymatic activity. Interestingly, H282G OxDB with 2-methyl imidazole showed a higher activity than wild type enzyme. Kinetic analyses revealed that the proximal His regulated not only the affinity of the substrate binding to the heme but the elimination of the OH group from the substrate.

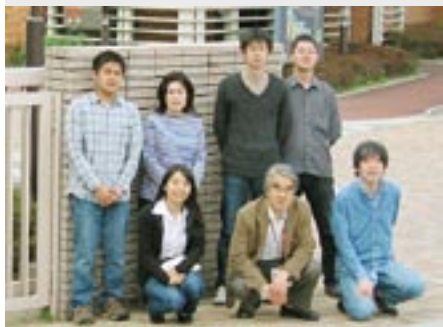
References

- 1) H. Komori, S. Inagaki, S. Yoshioka, S. Aono and Y. Higuchi, *J. Mol. Biol.* **367**, 864–871 (2007).
- 2) H. Yoshimura, S. Yoshioka, Y. Mizutani and S. Aono, *Biochem. Biophys. Res. Commun.* **357**, 1053–1057 (2007).
- 3) E. Pinakoulaki, H. Yoshimura, V. Daskalakis, S. Yoshioka, S. Aono and C. Varotsis, *Proc. Natl. Acad. Sci. U.S.A.* **103**, 14796–14801 (2006).
- 4) K. Kobayashi, M. Kubo, S. Yoshioka, T. Kitagawa, K. Kato, Y. Asano and S. Aono, *ChemBioChem* **7**, 2004–2009 (2006).

* Present Address; Kyoto University, Kyoto 606-8501

Elucidation of the Molecular Mechanisms of Protein Folding

Department of Life and Coordination-Complex Molecular Science
Division of Biomolecular Functions



KUWAJIMA, Kunihiro	Professor
CHAUDHURI, Tapan K.	Visiting Associate Professor
MAKI, Kosuke	Assistant Professor*
MUKAIYAMA, Atsushi	IMS Fellow
VOLETY, Srinivas	Visiting Scientist; JSPS Invited Fellow
NAKAMURA, Takashi	Post-Doctoral Fellow
MIZUKI, Hiroko	Research Fellow
TAKAHASHI, Kazunobu	Graduate Student†
ISOGAI, Miho	Secretary

Kuwajima group is studying mechanisms of *in vitro* protein folding and mechanisms of molecular chaperone function. Our goal is to elucidate the physical principles by which a protein organizes its specific native structure from the amino acid sequence. In this year, we studied the equilibrium and kinetics of canine milk lysozyme folding/unfolding by peptide and aromatic circular dichroism and tryptophan fluorescence spectroscopy, and the unfolding pathways of goat α -lactalbumin by high-temperature molecular dynamics simulations.

1. Equilibrium and Kinetics of the Folding and Unfolding of Canine Milk Lysozyme¹⁾

The equilibrium and kinetics of canine milk lysozyme folding/unfolding were studied by peptide and aromatic circular dichroism and tryptophan fluorescence spectroscopy. The Ca^{2+} -free apo form of the protein exhibited a three-state equilibrium unfolding, in which the molten globule state is well populated as an unfolding intermediate. A rigorous analysis of holo protein unfolding, including the data from the kinetic refolding experiments, revealed that the holo protein also underwent three-state unfolding with the same molten globule intermediate. Although the observed kinetic refolding curves of both forms were single-exponential, a burst-phase change in the peptide ellipticity was observed in both forms, and the burst-phase intermediates of both forms were identical to each other with respect to their stability, indicating that the intermediate does not bind Ca^{2+} . This intermediate was also shown to be identical to the molten globule state observed at equilibrium. The Φ -value analysis, based on the effect of Ca^{2+}

on the folding and unfolding rate constants, showed that the Ca^{2+} -binding site was not yet organized in the transition state of folding. A comparison of the result with that previously reported for α -lactalbumin indicated that the folding initiation site is different between canine milk lysozyme and α -lactalbumin, and hence, the folding pathways must be different between the two proteins. These results thus provide an example of the phenomenon wherein proteins that are very homologous to each other take different folding pathways. It is also shown that the native state of the apo form is composed of at least two species that interconvert.

2. Unfolding Pathways of Goat α -Lactalbumin as Revealed in Multiple Alignment of Molecular Dynamics Trajectories²⁾

Molecular dynamics simulations of protein unfolding were performed at an elevated temperature for the authentic and recombinant forms of goat α -lactalbumin. Despite very similar three-dimensional structures, the two forms have significantly different unfolding rates due to an extra N-terminal methionine in the recombinant protein. To identify subtle differences between the two forms in the highly stochastic kinetics of unfolding, we classified the unfolding trajectories using the multiple alignment method based on the analogy between the biological sequences and the molecular dynamics trajectories. A dendrogram derived from the multiple trajectory alignment revealed a clear difference in the unfolding pathways of the authentic and recombinant proteins, *i.e.* the former reached the

transition state in an all-or-none manner while the latter unfolded less cooperatively. It was also found in the classification that the two forms of the protein shared a common

transition state structure, which was in excellent agreement with the transition state structure observed experimentally in the Φ -value analysis.

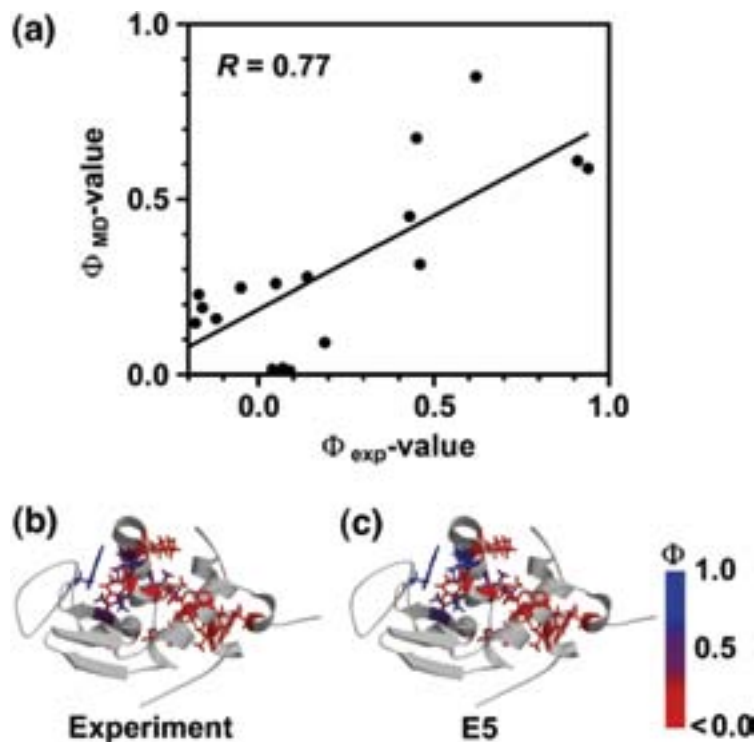


Figure 1. (a) Scatter plot showing the correlation between Φ_{exp} and Φ_{MD} of recombinant goat α -lactalbumin; Φ_{exp} contains small negative values, and Φ_{MD} was calculated for the structures around the center of cluster E5. (b) Φ_{exp} and (c) Φ_{MD} mapped onto the three-dimensional structure of goat α -lactalbumin.

References

- 1) H. Nakatani, K. Maki, K. Saeki, T. Aizawa, M. Demura, K. Kawano, S. Tomoda and K. Kuwajima, *Biochemistry* **46**, 5238–5251 (2007).
- 2) T. Oroguchi, M. Ikeguchi, M. Ota, K. Kuwajima and A. Kidera, *J. Mol. Biol.* **371**, 1354–1364 (2007).

* Present Address; Department of Physics, Nagoya University, Chikusa-ku, 464-8602 Nagoya

† carrying out graduate research on Cooperative Education Program of IMS with the University of Tokyo

Structure-Function Relationship of Metalloproteins

Department of Life and Coordination-Complex Molecular Science
Division of Biomolecular Functions



FUJII, Hiroshi
KURAHASHI, Takuya
KUJIME, Masato
TAKAHASHI, Akihiro
TANIZAWA, Misako

Associate Professor
Assistant Professor
Post-Doctoral Fellow*
Graduate Student
Secretary

Metalloproteins are a class of biologically important macromolecules, which have various functions such as oxygen transport, electron transfer, oxidation, and oxygenation. These diverse functions of metalloproteins have been thought to depend on the ligands from amino acid, coordination structures, and protein structures in immediate vicinity of metal ions. In this project, we are studying the relationship between the electronic structures of the metal active sites and reactivity of metalloproteins.

1. A Trigonal-Bipyramidal Geometry Induced by an External Water Ligand in a Sterically Hindered Iron Salen Complex, Related to the Active Site of Protocatechuate 3,4-Dioxygenase¹⁾

A unique distorted trigonal-bipyramidal geometry observed for the nonheme iron center in protocatechuate 3,4-dioxygenase (3,4-PCD) was carefully examined utilizing a sterically hindered iron salen complex, which well reproduces the endogenous His₂Tyr₂ donor set with water as an external ligand (Figure 1). X-ray crystal structures of a series of iron model complexes containing bis(3,5-dimesitylsalicylidene)-1,2-dimesitylethylenediamine indicate that a distorted trigonal-bipyramidal geometry is achieved upon binding of water as an external ligand. The extent of a structural change of the iron center from a preferred square-pyramidal to a distorted trigonal-bipyramidal geometry varies with the external ligand that is bound in the order Cl << EtO < H₂O, which is consistent with the spectrochemical series. The distortion in the model system is not due to steric repulsions, but electronic interactions between the external ligand and the iron center, as evidenced from the X-ray crystal structures of another series of iron model complexes with a less-hindered bis(3-xylylsalicylidene)-1,2-dimesitylethylenediamine ligand, as well as by DFT calculations. Further spectroscopic investigations indicate that a unique distorted trigonal-bipyramidal geometry

is indeed maintained even in solution. The present model study provides a new viewpoint that a unique distorted trigonal-bipyramidal iron site might not be preorganized by a 3,4-PCD protein, but could be electronically induced upon the binding of an external hydroxide ligand to the iron(III) center. The structural change induced by the external water ligand is also discussed in relation to the reaction mechanism of 3,4-PCD.

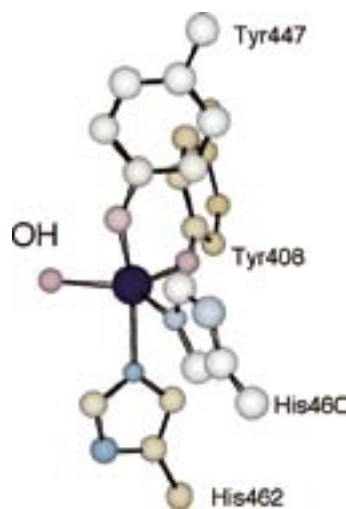


Figure 1. Active site structure of Protocatechuate 3,4-dioxygenase.

2. ⁶³Cu NMR Spectroscopy of Copper(I) Complexes with Various Tridentate Ligands: CO as a Useful ⁶³Cu NMR Probe for Sharpening ⁶³Cu NMR Signals and Analyzing the Electronic Donor Effect of a Ligand²⁾

⁶³Cu NMR spectroscopic studies of copper(I) complexes with various N-donor tridentate ligands, shown in Figure 1, are reported. As has been previously reported for most copper(I) complexes, ⁶³Cu NMR signals, when acetonitrile is coordi-

nated to copper(I) complexes of these tridentate ligands, are extremely broad or undetectable. However, when CO is bound to the above tridentate copper(I) complexes, the ^{63}Cu NMR signals become much sharper and show a large downfield shift, compared to those for the corresponding acetonitrile complexes. Temperature dependence of ^{63}Cu NMR signals for these copper(I) complexes show that a quadrupole relaxation process is much more significant to their ^{63}Cu NMR line widths than a ligand exchange process. Therefore, an electronic effect of the copper bound CO makes the ^{63}Cu NMR signal sharp and easily detected. The large downfield shift for the copper(I) carbonyl complex can be explained by a paramagnetic shielding effect induced by the copper bound CO, which amplifies small structural and electronic changes that occur around the copper ion to be easily detected in their ^{63}Cu NMR shifts. This is evidenced by the correlation between the ^{63}Cu NMR shifts for the copper(I) carbonyl complexes and their $\nu(\text{C}\equiv\text{O})$ values. Furthermore, the ^{63}Cu NMR shifts for copper(I) carbonyl complexes with imino type tridentate ligands show a different correlation line with those for amino type tridentate ligands. On the other hand, ^{13}C NMR shifts for the copper bound ^{13}CO for these copper(I) carbonyl complexes do not correlate with the $\nu(\text{C}\equiv\text{O})$ values. The X-ray crystal structures of these copper(I) carbonyl complexes do not show any evidence of a significant structural change around the Cu–CO moiety. The findings herein show that CO has great potential as a probe in ^{63}Cu NMR spectroscopic studies for characterizing the nature of the environment around copper ions in copper complexes.

3. Activation Parameters for Cyclohexene Oxygenation by Oxoiron(IV) Porphyrin π -Cation Radical Complex: Entropy Control of Allylic Hydroxylation Reaction³⁾

Cytochromes P450 (P450) are very versatile catalysts, which activate molecular oxygen and catalyze hydrocarbon hydroxylation or alkene epoxidation with high stereoselectivity. Reaction of P450 with cyclohexene yields a mixture of two major products: cyclohexene oxide (an epoxidation product) and 2-cyclohexen-1-ol (an allylic hydroxylation product). Interestingly, the ratio of epoxidation to allylic hydroxylation products, *i.e.*, the chemoselectivity, is changed by P450 isozymes and by mutation of a single amino acid near the proximal or distal side. In addition, P450 model studies using synthetic iron porphyrin complexes showed that the chemoselectivity depends on various other factors, such as the nature of the porphyrin and axial ligands, solvents, and reaction temperature. While these enzymatic and model studies suggest that chemoselectivity is dependent on the electronic structure of the reactive intermediate, oxoiron(IV) porphyrin π -cation

radical species (compound I), it is not clear how compound I controls chemoselectivity. Recently, the reaction mechanism and chemoselectivity of P450 have been studied by theoretical calculations based on density functional theory (DFT). In DFT studies, reaction mechanism and chemoselectivity are predicted from calculated activation energy, E_a , for epoxidation and allylic hydroxylation reactions of oxoiron(IV) porphyrin π -cation radical species. These studies are based on the assumption that the contribution of entropy of activation, ΔS^\ddagger , is much smaller than that of enthalpy of activation, ΔH^\ddagger . However, the validity of this assumption remains unproven because the activation parameters for epoxidation and allylic hydroxylation reactions of compound I species are yet to be determined. To better understand epoxidation and allylic hydroxylation reactions, the present study ascertained the activation parameters for epoxidation and allylic hydroxylation reactions of cyclohexene with compound I species, $\text{Fe}^{\text{IV}}\text{O}(\text{TMP})^+\text{Cl}$ (1), (Figure 2). This study demonstrated that epoxidation is an enthalpy-controlled reaction, while allylic hydroxylation is an entropy-controlled reaction. The large contribution of the entropy term, $-T\Delta S^\ddagger$, to the free energy of activation, ΔG^\ddagger , indicated that ΔG^\ddagger , rather than E_a , should be used to predict reaction mechanisms and chemoselectivity.

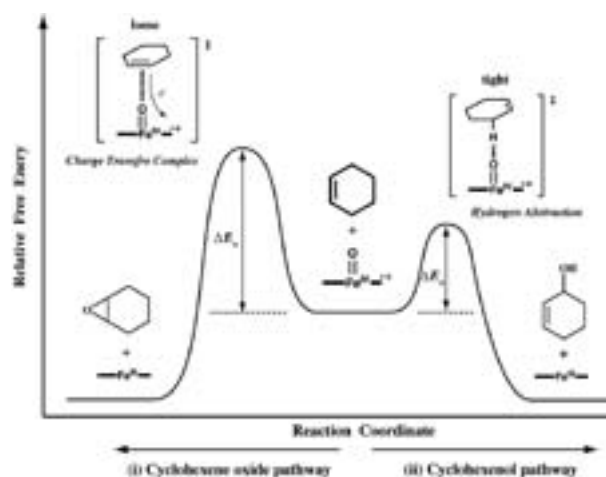


Figure 2. A cartoon of the reaction coordinates for allylic hydroxylation and epoxidation of cyclohexene by oxoiron(IV) porphyrin π -cation radical complex.

References

- 1) T. Kurahashi, K. Oda, M. Sugimoto, T. Ogura and H. Fujii, *Inorg. Chem.* **45**, 7709–7721 (2006).
- 2) M. Kujime, T. Kurahashi, M. Tomura and H. Fujii, *Inorg. Chem.* **46**, 541–551 (2007).
- 3) A. Takahashi, T. Kurahashi and H. Fujii, *Inorg. Chem.* **46**, 6227–6229 (2007).

Award

TAKAHASHI, Akihiro; Award for Oral Presentation by Graduate Student in Annual Meeting of Chemical Society of Japan.

* Present Address; Advanced Industrial Science and Technology, Tsukuba 305-8565

Fabrication of Silicon-Based Planar Ion-Channel Biosensors and Integration of Functional Cell Membrane Model Systems on Solid Substrates

Department of Life and Coordination-Complex Molecular Science
Division of Biomolecular Sensing



URISU, Tsuneo	Professor
TERO, Ryugo	Assistant Professor
MAO, Yangli	IMS Fellow
CHIANG, Tsung-Yi	Research Fellow
UNO, Hidetaka	Graduate Student
ZHANG, Zhen-Long	Graduate Student
SAYED, Abu	Graduate Student
NAKAI, Naohito	Graduate Student
ASANO, Toshifumi	Graduate Student
SHIMIZU, Atsuko	Secretary

To combining the human brain and the supercomputer is a dream of the scientist. To realize this dream we must develop several interface devices which can pick up several signals from neural cells such as electrical, optical and molecular signals. We run two main projects targeting the reactions on cell membranes. One is the fabrication of Si-based ion-channel biosensor, which is one of the above interface device to detect the neurotransmitter molecules. The other is the fundamental understanding of bilayer membrane properties using the artificial lipid bilayers on solid substrates, which is called supported bilayers, by means of atomic force microscope and fluorescence microscope-based techniques.

1. Supported Planar Lipid Bilayers on Step-and-Terrace TiO₂ Surfaces

We studied the influence of substrate surface properties on supported planar bilayer (SPB) using atomic force microscope

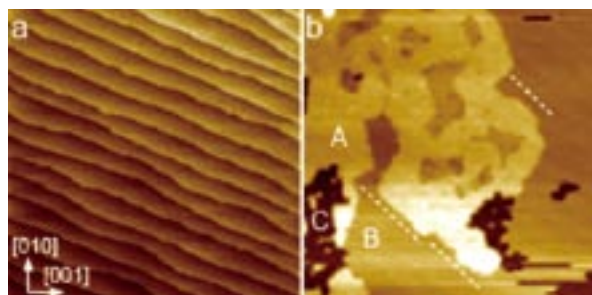


Figure 1. (a) AFM image ($2.0 \times 2.0 \mu\text{m}^2$) of the step-and-terrace TiO₂(100) surface. The image was obtained in air. (b) AFM image ($2.0 \times 2.0 \mu\text{m}^2$) of the DPoPC+DPPC binary bilayer on the TiO₂(100). The regions with the brightest (A), middle (B) and darkest (C) contrast are gel-phase domain, liquid crystal domain and defects (bare TiO₂), respectively. The dotted line represent the direction of the substrate atomic step. The image was obtained in a buffer solution.

and fluorescence microscope. Effects of surface hydrophilicity and atomic structures on the SPB formation process, morphology, and phase-separation were investigated on single-step-and-terrace rutile-TiO₂ low index surfaces. Step-and-terrace surfaces of rutile-TiO₂ (100), (110) and (001) were formed by etching in 10% HF *aq.* and annealing at O₂ flow (1.0 L min^{-1}) at 700–850 °C. Figure 1a shows the step-and-terrace TiO₂(100) surface. The height of each step was 0.25 nm, that corresponded to the height of the TiO₂(100) unit cell. Flat and continuous SPB was formed on both TiO₂ (100) and (001) surfaces by the vesicle fusion method. The dipalmitoleoylphosphatidylcholine (DPoPC)-SPB on the single- and double-step TiO₂(100) had a ratchet-like structure following the step-and-terrace structure of the substrate, but that on the half-step TiO₂(001) did not have the morphology reflecting the substrate structure. The atomic steps on the TiO₂(100) substrate affected the domain shapes in the binary bilayer of DPoPC and dipalmitoylphosphatidylcholine (DPPC). Some of the gel-phase domain (DPPC-rich) edges on the step-and-terrace TiO₂(100) surface run along the atomic step on the substrate (Figure 1b). This results shows the only 0.25 nm atomic structure on the substrate definitely affects to the lateral lipid assembly in several hundreds nanometer scale.

2. Analysis of Alzheimer's Disease Pathogenesis by *in situ* AFM

Alzheimer's disease (AD) is one of the most common age-associated pathologies, which inevitably leads to dementia and death. Amyloid plaques and neurofibrillary tangles containing beta-amyloid (A β) are two of the pathological hallmarks of AD. A key event in AD pathogenesis is the conversion of A β peptide from soluble to toxic aggregation in the brain. In particular, how to aggregate and interact with lipid membranes is one of the most important researches because the membrane

surface might be responsible for both neurotoxicity and senile plaque formation.

Supported planar bilayers (SPBs) are useful *in vitro* mimicking system for natural biological membranes. Recently, several reports showed that these inert substrates affected to the SPB fluidity, phase-transition, formation rate, and domain structures. Detailed substrate effects of such systems are of paramount importance for SPBs to mimic cell membranes successfully and for the design of new applications in biosensors and surface bio-functionalization.

In this study, we investigated the interaction of A β 40-GM1 on the ternary-SPB of Ganglioside (GM1), sphingomyelin (SM) and cholesterol (Chol), which is used as the natural membrane raft, by AFM, fluorescence microscopy, and CTX-B and Thioflavin T assay. The novel phase-separations with triangle domains are observed on mica surface by AFM (Figure 2a), whereas the second bilayers were formed on SiO₂ substrate at the same conditions (Figure 2b).

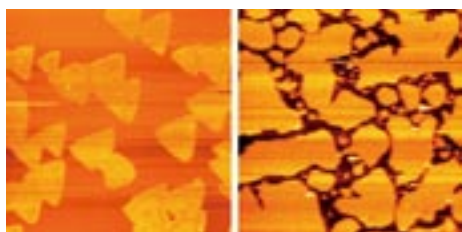


Figure 2. (a, b) AFM images of GM1/SM/Chol (20:40:40 molar ratio)-SPBs on mica (a: 10 \times 10 μ m²) and SiO₂ (b: 5.0 \times 5.0 μ m²) substrates.

3. Fabrication of Si-Based Planar Type Patch Clamp Biosensor Using Silicon on Insulator Substrate¹⁾

The aim of this study is to fabricate the planar type patch clamp ion-channel biosensor, which can detect the neurotransmitter molecules, using silicon-on-insulator (SOI) substrate. The micropore with 1.2 μ m diameter was formed through the top Si layer and the SiO₂ box layer of the SOI substrate by focused ion beam (FIB). Then the substrate is

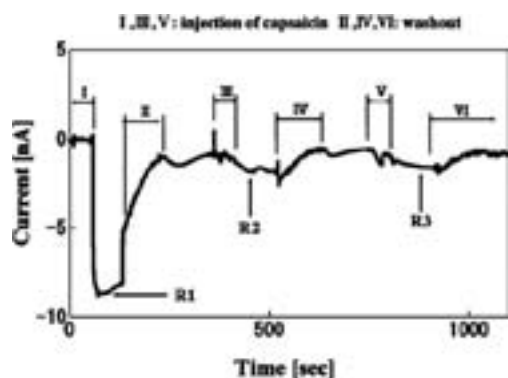


Figure 3. Whole-cell current of TRPV1-transfected HEK-293 cell activated by repeated capsaicin (7.1 μ M) applications, which shows desensitization in the extracellular solution containing Ca²⁺. The holding voltage was -30 mV.

assembled into the microfluidic circuit. The human embryonic kidney 293 (HEK-293) cell transfected with transient receptor potential vanilloid type 1 (TRPV1) was positioned on the micropore and the whole-cell configuration was formed by the suction. We succeeded to measure the capsaicin-induced Ca²⁺ channel current of the TRPV1 (Figure 3), when we added capsaicin to the extracellular solution as a ligand molecule. The channel current showed the desensitization unique to the TRPV1.

4. Synchrotron Radiation Stimulated XeF₂ Etching Beam-Line with Focusing to Differential Pumping Pinhole

In the synchrotron radiation (SR) etching using XeF₂ gas, a high etching rate in addition to the unique characteristics of anisotropic etching and material selectivity is expected. We constructed a system for the SR-induced dry etching of Si using XeF₂ as etching gas in UVSOR. However, in the previous XeF₂ SR etching experiments, LiF₂ windows have been used at the beam entrance to the etching chamber to protect the upper stream part of the beam line from the corrosive XeF₂ gas. Due to the significant absorption of irradiation beam by this LiF₂ window and its rapid radiation damage, it was difficult to obtain a practical etching rate. Based on these our experiences, we have constructed a new XeF₂ etching beam line with expected high etching rate at UVSOR beam line 4A (Figure 4). The second focusing deflecting mirror ($f = 2$ mm) was set at 406cm down stream position from the first bent cylindrical pre-mirror. The pinhole (1 mm in diameter, 10 mm in length) is set at this second mirror focusing point. The sample surface position is 5 mm down-stream from this pinhole. The second mirror chamber is pumped by turbo-molecular pump (0.48 m³ s⁻¹). And the sample chamber is pumped (4 $\times 10^{-4}$ m³ s⁻¹) through XeF₂ gas line by rotary pump. According to this pinhole, sufficiently high vacuum ($\sim 10^{-4}$ Torr) in the second mirror chamber to protect the mirror from the contamination damage is kept with realizing a quite high XeF₂ gas pressure and high photon flux in the reaction chamber.

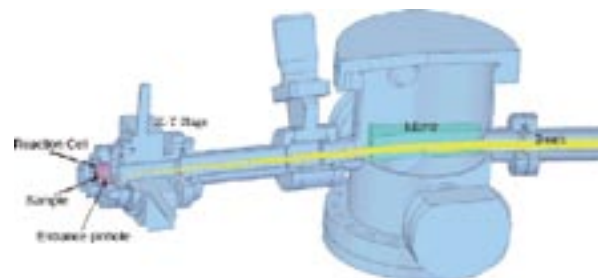


Figure 4. Schematic view of the etching chamber, pinhole and second focusing mirror.

Reference

- 1) Z. L. Zhang, T. Asano, H. Uno, R. Tero, M. Suzui, S. Nakao, T. Kaito, K. Shibasaki, M. Tominaga, Y. Utsumi, Y. L. Gao and T. Urisu, *Thin Solid Films* in press.

Development of Fluorescent and Bioluminescent Proteins for Imaging Biomolecules

Department of Life and Coordination-Complex Molecular Science
Division of Biomolecular Sensing



OZAWA, Takeaki	Associate Professor
TAKEUCHI, Masaki	Assistant Professor
HIDA, Naoki	IMS Fellow
MUHAMMAD, Awais	Post-Doctoral Fellow

Current focus on biological research is to quantify and image biomolecules in living cells and animals. To probe biomolecular functions and dynamics, we are exploring a new way for developing fluorescent and bioluminescent reporter proteins based on protein splicing and complementation techniques. The reporter proteins can be applied to development of analytical methods for detecting protein-protein interactions, intracellular localization of proteins and their dynamics, enzyme activities, gene expression and production of small biomolecules.

1. Imaging Dynamics of Endogenous Mitochondrial RNA in Single Living Cells

Location of cytoplasmic mRNA directs proteins to particular intracellular compartments, thereby controlling local cellular functions. Distinct localization of mitochondrial RNA (mtRNA) and the molecular mechanism are, however, poorly understood. We developed genetically-encoded RNA probes for characterizing localization and dynamics of mtRNA in single living cells. The probes consist of two RNA-binding domains of PUMILIO1, each connected with split fragments of a fluorescent protein capable of reconstituting upon binding to a target RNA. We designed the probes to specifically recognize a 16-base sequence of mtRNA encoding NADH dehydrogenase subunit 6 (ND6) and to be targeted into mitochondrial matrix, which allowed real-time imaging of ND6 mtRNA localization in living cells. We showed that ND6 mtRNA is localized within mitochondria and concentrated particularly on mtDNA. Movement of the ND6 mtRNA is restricted but oxidative stress with H₂O₂ induces the mtRNA

to diffuse in mitochondria, and the mtRNA gradually decomposed thereafter. The present observation of mtRNA demonstrates that the RNA probes provide a means to understand mtRNA dynamics controlled both temporally and spatially in intracellular compartments in living cells.

2. A Genetically Encoded Optical Probe for Detecting Release of Proteins from Mitochondria toward Cytosol in Living Cells and Animals

We developed a genetically encoded bioluminescence indicator for monitoring the release of proteins from mitochondria in living cells. The principle of this method is based on reconstitution of split *Renilla reniformis* luciferase (Rluc) fragments by protein splicing with an Ssp DnaE intein. A target mitochondrial protein connected with an N-terminal fragment of Rluc and an N-terminal fragment of DnaE is expressed in mammalian cells. If the target protein is released from the mitochondria toward the cytosol upon stimulation with a specific chemical, the N-terminal Rluc meets the C-terminal Rluc connected with C-terminal DnaE in the cytosol, and thereby, the full-length Rluc is reconstituted by protein splicing. The extent of release of the target fusion protein is evaluated by measuring activities of the reconstituted Rluc. To test the feasibility of this method, we monitored the release of a Smac/DIABLO protein from mitochondria during apoptosis in living cells and mice. The present method allowed high-throughput screening of an apoptosis-inducing reagent, staurosporine, and imaging of the Smac/DIABLO release in cells and in living mice. This rapid analysis can be used for

screening and assaying chemicals that would increase or inhibit the release of mitochondrial proteins in living cells and animals.

3. Nongenomic Activity of Ligands in the Association of Androgen Receptor with Src

Androgen receptor (AR) induces cell proliferation by increasing the kinase activity of Src. We developed an approach for discriminating agonist and antagonist in a nongenomic steroid-signaling pathway using an association of AR with Src. We constructed a pair of genetically encoded indicators, where N- and C-terminal fragments of split firefly luciferase (FLuc) were fused to AR and Src, respectively. The fusion proteins with AR and Src are localized in the cytoplasm and on the plasma membrane, respectively. Upon being activated with androgen, AR undergoes an intramolecular conformational change and binds with Src. The association causes the complementation of the split FLuc and recovery of FLuc activity. The resulting luminescence intensities were taken as a measure of the rapid hormonal activity of steroids in the nongenomic AR signaling. Ten minutes were required for the AR-Src association by 5 α -dihydroxytestosterone (DHT), which was completely inhibited by an antagonist, cyproterone acetate. The activities of ligands in the nongenomic pathway of AR were compared with those in the genomic pathway obtained on the basis of the nuclear trafficking of AR in mammalian cells. The comparison revealed that DHT and testosterone activate both genomic and nongenomic pathways of AR. 17 β -Estradiol and progesterone were found to be specific activators only for the genomic signaling pathway of AR. On the other hand, procymidone exhibited a specific activity only for the nongenomic signaling pathway of AR. The present approach is the first example addressing the agonistic and antagonistic activities of ligands in a nongenomic pathway of AR.

4. Cyclic Luciferase for Real-Time Sensing of Caspase-3 Activities in Living Mammals

Programmed cell death (apoptosis) is a crucial process involved in pathogenesis and progression of diseases, which is executed by Cysteine Aspartyl Proteases (caspases). The caspase activities in living subjects and their regulation with small chemical compounds are of great interest for screening drug candidates or pathological agents. We developed a genetically encoded bioluminescent indicator for high-throughput sensing and noninvasive real-time imaging of caspase activities in living cells and animals. Firefly luciferase connected with a substrate sequence of caspase-3 (Asp-Glu-Val-Asp) is cyclized by an intein DnaE (a catalytic subunit of DNA polymerase III). When the cyclic luciferase is expressed in living cells, the luciferase activity greatly decreases due to a steric effect. If caspase-3 is activated in the cells, it cleaves the substrate sequence embedded in the cyclic luciferase and the luciferase activity is restored. We demonstrated quantitative sensing of caspase-3 activities in living cells upon extracellular stimuli. Furthermore, the indicator enabled noninvasive imaging of the time-dependent caspase-3 activities in living mice. This cyclic luciferase indicator provides a general means for understanding the mechanism of physiological proteolytic processes and for screening novel pharmacological chemicals among candidates in living subjects.

References

- 1) T. Ozawa, Y. Natori, M. Sato and Y. Umezawa, *Nat. Methods* **4**, 413–419 (2007).
- 2) A. Kanno, T. Ozawa and Y. Umezawa, *Anal. Chem.* **78**, 8076–8081 (2006).
- 3) S. B. Kim, A. Kanno, T. Ozawa, H. Tao and Y. Umezawa, *ACS Chem. Biol.* **2**, 484–492 (2007).
- 4) A. Kanno, Y. Yamanaka, H. Hirano, Y. Umezawa and T. Ozawa, *Angew. Chem., Int. Ed.* **46**, 7595–7599 (2007).

Heterogeneous Catalytic Systems for Organic Chemical Transformations in Water

Department of Life and Coordination-Complex Molecular Science
Division of Complex Catalysis



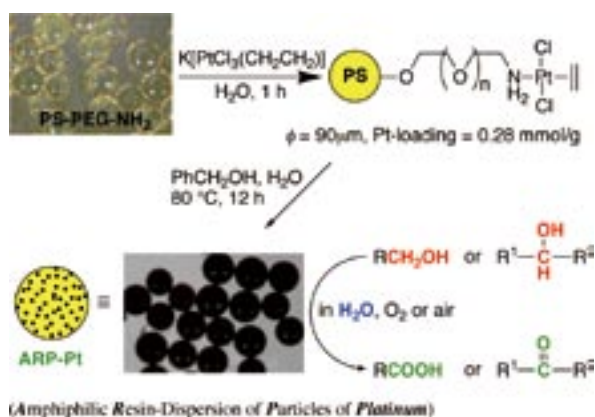
UOZUMI, Yasuhiro
YAMADA, Yoichi M. A.
OE, Yohei
SUZUKA, Toshimasa
KIMURA, Tsutomu
MINAKAWA, Maki
MATSUURA, Yutaka
TAKENAKA, Hiroe
TORII, Kaoru
ARAKAWA, Takayasu
BEPPU, Tomohiko
SASAKI, Tokiyo
HIGASHIBAYASHI, Azumi
TANIWAKE, Mayuko

Professor
Assistant Professor
IMS Fellow
Post-Doctoral Fellow
Post-Doctoral Fellow
Post-Doctoral Fellow
Post-Doctoral Fellow
Research Fellow
Research Fellow
Graduate Student
Graduate Student
Secretary
Secretary
Secretary

Various organic molecular transformations catalyzed by transition metals were achieved under heterogeneous aqueous conditions by use of amphiphilic resin-supported metal complexes or metal nanoparticles which were designed and prepared by this research group. In particular, highly stereoselective asymmetric allylic substitutions and aerobic alcohol oxidation, both of which were performed in water under heterogeneous conditions with high recyclability of the polymeric catalysts, are highlights among the achievements of the 2006–2007 period to approach what may be considered ideal chemical processes of next generation. Representative results are summarized hereunder.

1. Nanometal Particle Catalysts Dispersed in Amphiphilic Resin Supports^{1,2)}

An amphiphilic polystyrene-polyethylene glycol (PS-PEG) resin-dispersion of nanoparticles of platinum (ARP-Pt) was developed which had a mean diameter of 5.9 nm with a narrow size distribution throughout the resin (Scheme 1). ARP-Pt was found to be a useful and readily recyclable catalyst for aerobic oxidation of a wide variety of alcohols, including non-activated aliphatic and alicyclic alcohols, in water with an oxygen or air

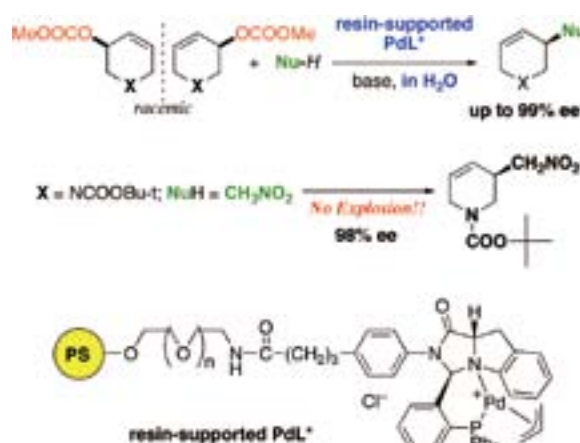


Scheme 1. Catalytic Aerobic Oxidation of Alcohols in Water with Amphiphilic Resin-Dispersion of Nanoparticles of Platinum.

atmosphere under heterogeneous conditions to meet green chemical requirements. A PS-PEG resin-dispersion of nanopalladium catalyst was also prepared which catalyzed aerobic oxidation of alcohols and hydrodechlorination of aryl halides under heterogeneous aqueous conditions.

2. Chiral Palladium Complexes Immobilized with Amphiphilic Resin Supports^{3,4)}

Stereoselective polymeric palladium catalysts supported on an amphiphilic polystyrene-poly(ethylene glycol) (PS-PEG) resin were developed to realize asymmetric allylic substitutions in water under heterogeneous conditions. A polymeric (*R*)-2-(*d* iphenylphosphino)binaphthyl (MOP) ligand anchored onto the PS-PEG resin by an (*S*)-alanine tether unit was identified through the library-based screening to be an effective chiral ligand for the asymmetric palladium-catalyzed π -allylic substitution of 1,3-diphenylpropenyl acetate with malonate nucleophiles under heterogeneous aqueous conditions. Nitromethane was safely applied as a C1 nucleophile for palladium-catalyzed

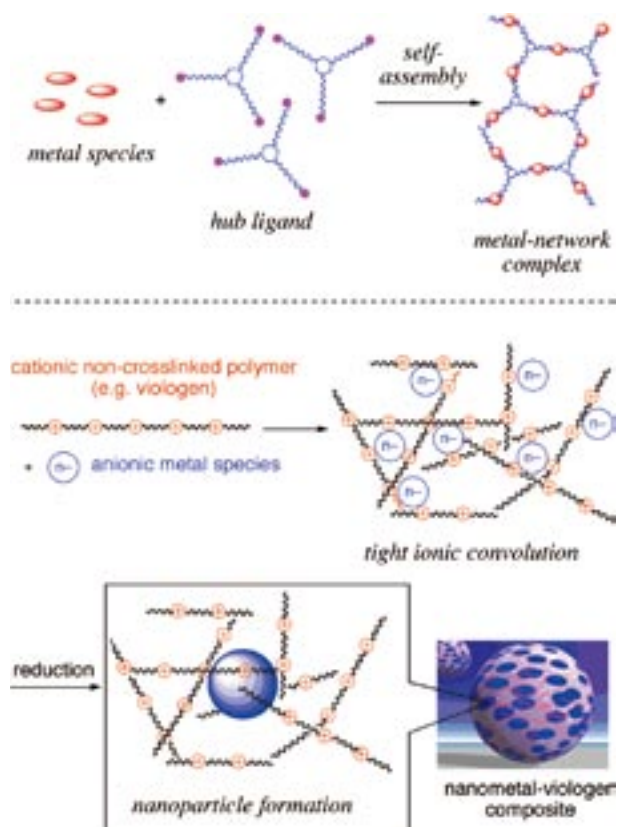


Scheme 2. Catalytic Asymmetric Allylic Substitution of Cycloalkenyl Esters in Water with an Amphiphilic Polymeric Chiral Palladium Complex.

π -allylic substitution of cyclic allylic substrates in water with amphiphilic PS-PEG resin-supported chiral imidazoindolephosphine-palladium complexes (Scheme 2). Catalytic asymmetric nitromethylation of cycloalkenyl esters was achieved in water as a single reaction medium under heterogeneous conditions using 5 mol% palladium of a PS-PEG resin-supported palladium-imidazoindolephosphine complex to give optically active (cycloalkenyl)nitromethanes with up to 98% ee.

3. Self-Organized Polymeric Metal Complexes^{5,6,7}

A novel solid-phase 3D metal-organic coordination network catalyst was prepared *via* self-assembly from PdCl₂(CH₃CN)₂ and a trisphosphine hub with three flexible alkyl-chain linkers. This insoluble network complex efficiently catalyzed the Suzuki-Miyaura reaction under atmospheric conditions in water. This catalyst was reused without loss of catalytic activity. A novel solid-phase self-organized catalyst of palladium nanoparticles was also prepared from PdCl₂ with main-chain viologen polymers *via* ionic convolution and



Scheme 3. Concepts of Self-Organized Network Complexation and Ionic Convolution.

Awards

UOZUMI, Yasuhiro; Chemical Society of Japan Award for Creative Research.

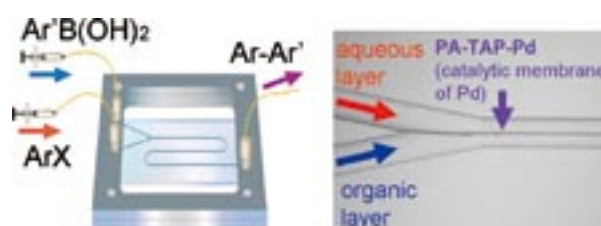
UOZUMI, Yasuhiro; Green-Sustainable Chemistry Award and MEXT Minister Award for Green-Sustainable Chemistry.

YAMADA, Yoichi M. A.; Thieme Journal Award.

reduction. This insoluble nanocatalyst nano-Pd-Viologen efficiently promoted α -alkylation of ketones with primary alcohols in the presence of Ba(OH)₂·H₂O under atmospheric conditions without organic solvents. The nano-Pd-Viologen catalyst was reused without loss of catalytic activity. The both concepts of network complexation and ionic convolution are depicted in Scheme 3.

4. Microchannel Reactor with a Catalytic Membrane⁸⁾

Instantaneous catalytic carbon-carbon bond forming reactions were achieved in a microchannel reactor having a polymeric palladium complex membrane (Scheme 4). The catalytic membrane was constructed inside the microchannel *via* self-assembling complexation at the interface between the organic and aqueous phases flowing laminarly, where non-crosslinked polymer-bound phosphine and ammonium tetrachloropalladate dissolved, respectively. Palladium-catalyzed coupling reaction of aryl halides and arylboronic acids was performed using the microchannel reactor to give quantitative yields of biaryls within 4 seconds of retention time in the defined channel region.



Scheme 4.

References

- 1) Y. M. A. Yamada, T. Arakawa, H. Hocke and Y. Uozumi, *Angew. Chem., Int. Ed.* **46**, 704–706 (2007).
- 2) Y. Uozumi, R. Nakao and H. Rhee, *J. Organomet. Chem.* **692**, 420–427 (2007).
- 3) Y. Kobayashi, D. Tanaka, H. Danjo and Y. Uozumi, *Adv. Synth. Catal.* **348**, 1561–1566 (2006).
- 4) Y. Uozumi and T. Suzuka, *J. Org. Chem.* **71**, 8644–8646 (2006).
- 5) Y. M. A. Yamada, Y. Maeda and Y. Uozumi, *Org. Lett.* **8**, 4259–4262 (2006).
- 6) Y. M. A. Yamada and Y. Uozumi, *Org. Lett.* **8**, 1375–1378 (2006).
- 7) Y. M. A. Yamada, H. Guo and Y. Uozumi, *Org. Lett.* **9**, 1501–1504 (2007).
- 8) Y. Uozumi, Y. M. A. Yamada, T. Beppu, N. Fukuyama, M. Ueno and T. Kitamori, *J. Am. Chem. Soc.* **128**, 15994–15995 (2006).

Metal Complexes Aiming Conversion between Chemical and Electrical Energies

Department of Life and Coordination-Complex Molecular Science
Division of Functional Coordination Chemistry



TANAKA, Koji	Professor
WADA, Tohru	Assistant Professor
OZAWA, Hironobu	IMS Fellow
KIMURA, Masahiro	Post-Doctoral Fellow
KOSHIYAMA, Tamami	Post-Doctoral Fellow
FUKUSHIMA, Takashi	Graduate Student
INOUE, Ayako	Graduate Student
YAMAGUCHI, Yumiko	Secretary
NAKAGAKI, Shizuka	Secretary

Metal ions involved in various metal proteins play key roles to generate metabolic energies through oxidation of organic molecules. Metal complexes having an ability to oxidize organic molecules at potentials more negative than that of reduction of dioxygen, therefore, are feasible catalysts to convert chemical energy to electrical one when combined with dioxygen reduction. Aqua-Ru complexes can be converted to high valent Ru=O ones by sequential proton and electron loss, and some of the latter can oxidize organic molecules. However, the redox potentials to generate high valent Ru=O complexes are too positive to use as energy converters. We have succeeded in smooth conversion from aqua to oxo ligands on Ru-dioxolene framework through proton coupled intramolecular electron transfer from the deprotonated form of Ru-OH species to dioxolene ligand. The aqua-oxo conversion using the unique redox behavior of Ru-dioxolene frameworks enabled us to isolate unprecedented metal-oxo and -amino radical complexes. We are elucidating the reactivity of those complexes as electrocatalysts toward the oxidation of hydrocarbons.

1. Experimental and Theoretical Evaluation of the Charge Distribution over Ruthenium and Dioxolene Framework of [Ru(OAc)-(dioxolene)(terpy)] (terpy = 2,2':6',2''-terpyridine) Depending on Substituents¹⁾

Ru complexes [Ru(OAc)(dioxolene)(terpy)] having various substituents on the dioxolene ligand (dioxolene = 3,5-*t*-Bu₂C₆H₂O₂ (**1**), 4-*t*-BuC₆H₃O₂ (**2**), 4-ClC₆H₃O₂ (**3**), 3,5-Cl₂C₆H₂O₂ (**4**), Cl₄C₆O₂ (**5**); terpy = 2,2':6',2''-terpyridine) were prepared. EPR spectra of these complexes in glassy frozen solutions (CH₂Cl₂:MeOH = 95:5, vol./vol.) at 20 K showed anisotropic signals with *g* tensor components 2.242 > *g*₁ > 2.104, 2.097 > *g*₂ > 2.042, and 1.951 > *g*₃ > 1.846. An anisotropic value, Δ*g* = *g*₁ - *g*₃, and an isotropic *g* value, <*g*> =

$[(g_1^2 + g_2^2 + g_3^2)/3]^{1/2}$, increase in the order **1** < **2** < **3** < **4** < **5**. The resonance between the Ru^{II}(sq) (sq = semiquinone) and Ru^{III}(cat) (cat = catecholato) frameworks shifts to the latter with an increase of the number of electron-withdrawing substituents on the dioxolene ligand. DFT calculations of **1**, **2**, **3**, and **5** also support the increase of the Ru spin density (Ru^{III} character) with an increase of the number of Cl atoms on the dioxolene ligand. The singly occupied MOs (SOMOs) of **1** and **5** are very similar to each other and stretch out the Ru-dioxolene frameworks, whereas the LUMO of **5** is localized on Ru and two O atoms of dioxolene in comparison with that of **1**. Electron-withdrawing groups decrease the energy levels of both the SOMO and LUMO. An increase in the number of Cl atoms in the dioxolene ligand results in an increase of the positive charge on Ru. Successive shifts in the electronic structure between the Ru^{II}(sq) and Ru^{III}(cat) frameworks caused by the variation of the substituents are compatible with the experimental data (Figure 1).

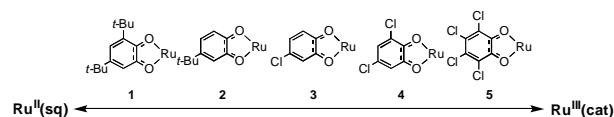


Figure 1. Charge distribution on the Ru-dioxolene framework depending on substituents.

2. Generation of Ru^{II}-Semiquinone-Anilino Radical through Deprotonation of Ru^{III}-Semiquinone-Anilido Complex²⁾

Aminyl radicals are thermodynamically unstable and have an ability to oxidize organic substrates through H-atom abstraction. Metal complexes bearing an aminyl radical may, therefore, have potential uses as new oxidation catalysts in organic synthesis. Actual electronic states of aminyl radical metal

complexes would lie somewhere between two limiting resonance structures such as the amido state $\{M^{(n+1)+}-NR_2\}$ and the aminyl radical $\{M^{n+}-\cdot NR_2\}$ and would usually be shifted toward the former. Recently, metal complexes having aminyl radicals were isolated by means of chemical and electrochemical oxidation of the corresponding metal amido complexes. On the other hand, a Ru^{II} -semiquinone-oxyl radical complex, $[Ru^{II}(terpy)(Bu_2sq)(O^{\cdot-})]$ ($terpy = 2,2':6',2''$ -terpyridine, $Bu_2sq^- = 3,5$ -di-*tert*-butylsemi-quinonate), was isolated through deprotonation of $[Ru^{III}(terpy)(Bu_2sq)(OH)]^+$ under basic conditions without using any oxidants. Furthermore, the deprotonated species of $[Ru^{III}(terpy)(Bu_2sq)(NH_3)]^{2+}$ and $[Ru^{III}(NH_2-bpa)(Bu_2sq)]^{2+}$ ($NH_2-bpa =$ bis(2-pyridylmethyl)-2-aminoethylamine) were proved to oxidize alcohols to aldehydes or ketones with the generation of $[Ru^{II}(terpy)(Bu_2sq)(NH_3)]^+$ and $[Ru^{II}(NH_2-bpa)(Bu_2sq)]^+$, respectively. The most plausible active species for the oxidation of alcohols is a Ru^{II} -semiquinone-aminyl radical that is a limiting resonance structure of an Ru^{III} -semiquinone-amido complex. Although the Ru^{II} -semiquinone-aminyl radical intermediate was too labile to identify its existence in oxidation reactions, an analogous Ru^{III} -semiquinone-anilino radical complex that also would be formed from the corresponding Ru^{III} -semiquinone-anilino complexes may be stabilized due to the π -conjugated system of anilino group. We successfully isolated the Ru^{II} -semiquinone-anilino radical, $[Ru^{II}(*NPh-bpa)(Bu_2sq)]-2H_2O$ (**2**), and its one-electron reduced species, *i.e.*, the Ru^{II} -catechol-anilino radical, $[Ru^{II}(*NPh-bpa)(Bu_2cat)]^-$ (**3**), complexes bearing the 2-[Bis(2-pyridylmethyl)aminomethyl]-anilido ligand ($NPh-bpa^{2-}$). The anilino radical characters of **2** and **3** are proved by EPR spectroscopy, resonance Raman spectroscopy, and DFT calculations (Figure 2).

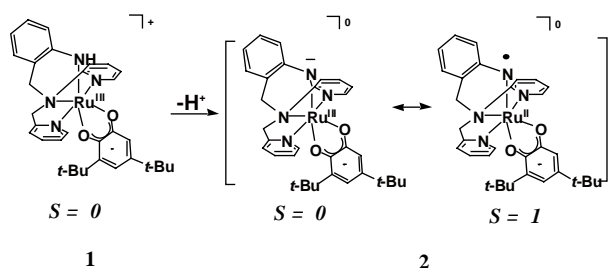
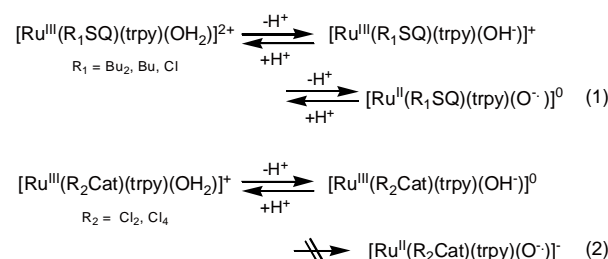


Figure 2. The formation of anilino radical complex.

3. Proton Coupled Electron Transfer Driven by the Acid-Base Equilibrium of Aqua-Ruthenium-Dioxolene Complexes

Ruthenium-dioxolene complexes with an aqua ligand, $[Ru^{III}(trpy)(R_1\text{-dioxolene})(OH_2)](ClO_4)_2$ ($R_1 = Bu_2$ [**6**]

(ClO_4)₂, Bu [**7**](ClO_4)₂, Cl [**8**](ClO_4)₂), and $[Ru^{III}(trpy)(R_2\text{-dioxolene})(OH_2)](BF_4)$ ($R_2 = Cl_2$ (**9**) and Cl_4 (**10**)) were prepared by the hydrolysis of the correspondent acetato complexes, $Ru^{III}(trpy)(R_3\text{-dioxolene})(OAc)$ ($R_3 = Bu_2$ (**1**), Bu (**2**), Cl (**3**), Cl_2 (**4**) and Cl_4 (**5**)). The EPR spectra of ruthenium-acetato complexes, suggest that the $Ru^{III}(SQ)$ framework is the principal contribution to the electronic structure of the complexes, **1–3**, whereas the $Ru^{III}(Cat)$ one became the main contribution to the complexes **4** and **5**. The electronic structures of the analogous aqua complexes are also largely influenced by the substituents of the dioxolene ligand. The dicationic complexes [**6**](ClO_4)₂, [**7**](ClO_4)₂, and [**8**](ClO_4)₂ have the $Ru^{III}(SQ)$ frameworks. The acid-base reaction of the aqua ligand of [**7**]²⁺, whose redox potentials lied between those of [**6**]²⁺ and [**8**]²⁺, proceeds *via* two subsequent proton dissociations. The CVs of those complexes also indicate the formation of oxyl radical complexes $[Ru^{II}(trpy)(SQ)(O^{\cdot-})]^0$, because addition of two equivs of BuOK to $[Ru^{III}(trpy)(SQ)(OH_2)]^{2+}$ resulted in shift of the rest potential of the solution to negative directions across the $Ru^{III}(SQ)/Ru^{II}(SQ)$ redox potential. On the other hand, the aqua complexes [**9**]⁺ and [**10**]⁺ that have mainly the $Ru^{III}(Cat)$ character due to more electron-withdrawing dioxolene ligands dissociate only one proton in the experimental conditions. The CV did not show the formation of the $Ru^{II}(Cat)$ core by an addition of large excess of BuOK to $[Ru^{III}(SQ)(trpy)(OH_2)]^{2+}$. It is, therefore, concluded that the conversion from $[Ru^{III}(SQ)(trpy)(OH^-)]^+$ to $[Ru^{II}(SQ)(trpy)(O^{\cdot-})]^0$ through $[Ru^{III}(SQ)(trpy)(O^{2-})]^0$ is achieved by the neutralization energy generated by treatment of the Ru-OH bond with BuOK, whereas it is not enough to convert from $[Ru^{III}(SQ)(trpy)(OH^-)]^+$ to $[Ru^{II}(Cat)(O^{\cdot-})]^0$ *via* $[Ru^{III}(SQ)(trpy)(O^{2-})]$ $[Ru^{III}(SQ)(trpy)(O^{2-})]^0$.

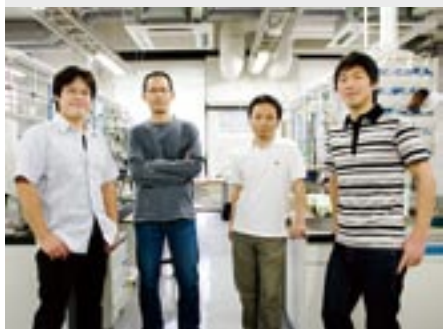


References

- 1) T. Wada, M. Yamanaka, T. Fujihara, Y. Miyazato and K. Tanaka, *Inorg. Chem.* **45**, 8887–8894 (2006).
- 2) Y. Miyazato, T. Wada, K. Tanaka, E. Fuhita and J. T. Muckerman, *Angew. Chem., Int. Ed.* **46**, 5728–5730 (2007).

Synthesis and Reactions of Transition Metal Complexes Having Aryloxy-Based Ligands, Especially with Regard to Activation of Small Molecules

Department of Life and Coordination-Complex Molecular Science
Division of Functional Coordination Chemistry



KAWAGUCHI, Hiroyuki
MATSUO, Tsukasa
WATANABE, Takahito
AKAGI, Fumio
ARII, Hidekazu
FUKAWA, Tomohide
ISHIDA, Yutaka

Associate Professor
Assistant Professor*
IMS Fellow
Post-Doctoral Fellow
Post-Doctoral Fellow
Post-Doctoral Fellow
Post-Doctoral Fellow

This project is focused on the design and synthesis of new ligands that are capable of supporting novel structural features and reactivity. Currently, we are investigating multidentate ligands based on aryloxy and thiolate. In addition, we set out to study metal complexes with sterically hindered aryloxy and arylthiolate ligands. Our recent efforts have been directed toward activation of small molecules.

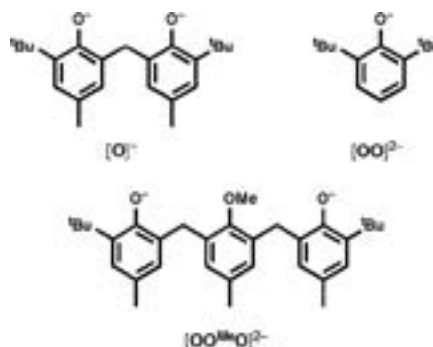
Development of ligands that play important roles in coordination chemistry has been the subject of intense interest. The chemistry of metal aryloxy complexes has shown that aryloxy ligands can promote various important transformations at metal centers. Therefore, aryloxy ligands complement the well-studied cyclopentadienyl-based systems, with the major difference being the greater reactivity of the aryloxy complexes due to their relatively higher unsaturation and lower coordination numbers for a $(ArO)_nM$ fragment. However, coordinatively unsaturated metal complexes undergo facile ligand redistribution reactions, which are occasionally a severe obstacle to synthetic efforts.

One of strategies for overcoming this problem is the use of covalently linked ancillary ligands, thereby limiting ligand mobility and leaving little possibility to reorganize the molecule. This feature has led to the isolation and structural characterization of a number of metal complexes that are difficult to obtain with aryloxy monodentate ligands. In this context, we set out to investigate aryloxy-based multidentate ligands as new ancillary ligands.

1. Reduction of Carbon Dioxide with Hydrosilanes Catalyzed by Zirconium-Borane Complexes¹⁾

Carbon dioxide is the stable carbon end product of metabolism and other combustions, and it is an abundant yet low-value carbon source. This molecule would be very valuable as

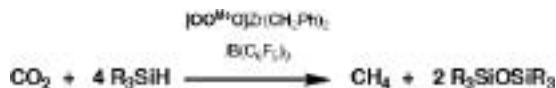
a renewable source if it were to be effectively transformed into reduced organic compounds under mild conditions. However, thermodynamic stability of CO_2 has prevented its utilization in industrial chemical processes, and thus this represents a continuing scientific challenge. In this study, we found that CO_2 is catalytically converted into CH_4 and siloxanes via bis(silyl)acetals with a mixture of a zirconium benzyl phenoxide complex and tris(pentafluorophenyl)borane ($B(C_6F_5)_3$).



Scheme 1.

In a first set of experiments, we studied the catalytic activity of cationic zirconium benzyl complexes bearing phenoxide ligands (Scheme 1) in the course of reducing CO_2 with $PhMe_2SiH$ as the test substrate. The catalysts used in this study were synthesized by treatment of the dibenzyl complexes with $B(C_6F_5)_3$ in toluene. The reaction of CO_2 with $PhMe_2SiH$ proceeded exothermically to form $(PhMe_2Si)_2O$ (Scheme 2). Performing the analogous reaction in benzene- d_6 in a NMR tube revealed the release of CH_4 as the byproduct. The resonance due to CH_4 was observed as singlet at 0.15 ppm in the 1H NMR spectrum. Mono- and bis-phenoxide ligands $[O]^-$ and $[OO]^{2-}$ gave zirconium complexes that preformed with low activity relative to the tridentate ligand $[OO^MeO]^{2-}$. The combination of a zirconium complex with $B(C_6F_5)_3$ is responsible

for this result, because the analogous reaction using $[(\text{O}^{\text{Me}}\text{O})\text{Zr}(\text{CH}_2\text{Ph})][\text{B}(\text{C}_6\text{F}_5)_4]$ did not give CH_4 but led to formation of $\text{Ph}_2\text{Me}_2\text{Si}$ and Me_2SiH_2 . Thus, neither zirconium cationic species nor $\text{B}(\text{C}_6\text{F}_5)_3$ alone provided an active catalyst.



Scheme 2.

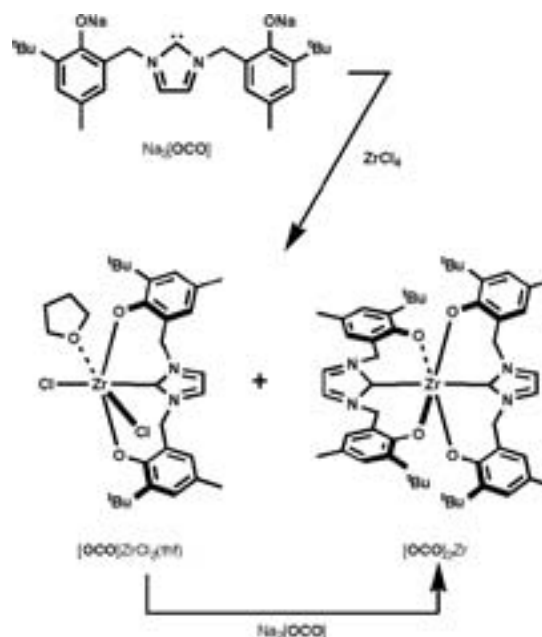
In order to obtain insight into the intervening processes in the reaction, isotopically enriched $^{13}\text{CO}_2$ (99 atom% ^{13}C) was admitted into a resealable NMR tube containing a solution of $(\text{O}^{\text{Me}}\text{O})\text{Zr}(\text{CH}_2\text{Ph})_2$, $\text{B}(\text{C}_6\text{F}_5)_3$, and Et_3SiH in benzene- d_6 at room temperature. The reaction requires approximately one week for completion and is monitored by NMR spectroscopy. The reaction proceeded cleanly, during which time $^{13}\text{CO}_2$ and Et_3SiH were fully consumed. Monitoring the reaction by $^{13}\text{C}\{^1\text{H}\}$ NMR spectroscopy indicates the presence of bis(silyl)acetal $^{13}\text{CH}_2(\text{OSiEt}_3)_2$ as a detectable intermediate. The resonance at 84.5 ppm due to $^{13}\text{CH}_2(\text{OSiEt}_3)_2$ grew to a maximum relative intensity over a period of about 7 h and then decreased as that at -4.4 ppm due to $^{13}\text{CH}_4$ continued to grow until, after about 1 week, it was the only resonance attributable to a ^{13}C -labeled product. Additionally, in the absence of proton decoupling, the resonances due to $^{13}\text{CH}_2(\text{OSiEt}_3)_2$ and $^{13}\text{CH}_4$ split into a triplet and a quintet with a coupling constant of 161.5 and 125.6 Hz, respectively. This observation unambiguously confirms that the carbon atom of CH_4 originates from CO_2 , and the source of its hydrogen atoms is added Et_3SiH .

The method for catalytic reduction of CO_2 presented here offers some significant advantages, since it proceeds under mild conditions and permits complete reduction of CO_2 to CH_4 . Another curious aspect of this system is the formation of polysiloxane from CO_2 and hydrosilane in chemical CO_2 fixation. The present results are promising, but we note that catalytic activity will need to be improved and the long-term stability and performance of the catalyst demonstrated.

2. Zirconium Complexes of a Tridentate Bis(aryloxide)-NHC Ligand²⁾

The chemistry and application of *N*-heterocyclic carbenes (NHCs) have been extensively explored. They can bind as two-electron donors to a wide range of transition metal, main group, and *f*-block derivatives. Especially, NHCs have been found extensive use as ancillary ligands in late transition metal complexes, in which they have shown enhanced catalytic activity compared to their phosphine analogues. In contrast, NHC complexes of early transition metals are considerably less developed despite the great potential of this class of molecules. This is mainly due to the ease of dissociation of the NHC ligand from the electron deficient metal center, which

makes it difficult to study the chemistry of NHCs in early transition metals and *f*-elements. A potential means of directing metal–NHC interactions is the covalent tethering of the anionic functional groups to the NHC ligand system, where the NHC moiety is held in proximity of the metal center by a covalent tether and should affect reactivity in a specific way. In this study, we show the synthesis of zirconium complexes having a bis(aryloxide)-NHC ligand ($[\text{OCO}]^{2-}$, Scheme 3)



Scheme 3.

The disodium salt of a ligand $\text{Na}_2[\text{OCO}]$, was prepared by reaction of $\text{H}_3[\text{OCO}]\text{Br}$ with 3 equiv of $\text{NaN}(\text{SiMe}_3)_2$. Reaction of $\text{ZrCl}_4(\text{thf})_2$ with 1 equiv of $\text{Na}_2[\text{OCO}]$ gave a mixture of $[\text{OCO}]\text{ZrCl}_2(\text{thf})$ and $[\text{OCO}]_2\text{Zr}$. When the amount of $\text{Na}_2[\text{OCO}]$ was increased to 2 equiv, $[\text{OCO}]_2\text{Zr}$ was obtained in good yield. The complex $[\text{OCO}]\text{ZrCl}_2(\text{thf})$ is a precursor to organometallic derivatives, and treatment with PhCH_2MgCl or $\text{Me}_3\text{SiCH}_2\text{Li}$ yielded $[\text{OCO}]\text{ZrR}_2$ ($\text{R} = \text{CH}_2\text{Ph}$, CH_2SiMe_3). The disodium salt $\text{Na}_2[\text{OCO}]$ is unstable and undergoes 1,2-benzyl migration, while zirconium complexes of the $[\text{OCO}]^{2-}$ ligand are found to be thermally stable in solid and solution.

Compounds $[\text{OCO}]\text{ZrCl}_2(\text{thf})$ and $[\text{OCO}]\text{ZrR}_2$ should provide excellent starting materials for investigation of the reactivity of this class of group 4 metal complexes. We expect it to demonstrate a rich and varied chemistry.

References

- 1) T. Matsuo and H. Kawaguchi, *J. Am. Chem. Soc.* **128**, 12362–12363 (2006).
- 2) D. Zhang, H. Aihara, T. Watanabe, T. Matsuo and H. Kawaguchi, *J. Organomet. Chem.* **692**, 234–242 (2007).

* Present Address; RIKEN Wako Institute, Frontier Research System

Visiting Professors



Visiting Professor
KITAGAWA, Hiroshi (from *Kyushu University*)

Creation of Novel Functional Nano Materials Based on Proton-Coupled Electronic Properties

Dynamics of molecules and ions in “coordination nano-space” are acted by characteristic nano-fields such as intermolecular interaction, coulomb interaction, catalytic action, *etc.* This project is to reveal a basic principle of an unusual nano-field acting on coordination space, and to create the nano space where the energy conversions can be easily operated. In particular, we aim at the construction of coordination nano space system which is able to control a series of energy operations such as generation, separation, storage, material conversion of an energy molecule H₂, or electron/ion transport. In this year, we have explored a novel hydrogen-energy functional coordination nano-space by using proton-coupled redox and electron-proton interaction. In the present project, we will create new 1) hydrogen-storage nano-materials, 2) highly proton-conductive coordination polymers, 3) highly electron-proton conductive materials, *etc.*



Visiting Associate Professor
KANAMORI-KATAYAMA, Mutsumi (from *RIKEN*)

Development of the Assay System for Protein-RNA Interactions

Recently, it has been cleared that a large amount of non-coding RNA (ncRNA) existed in mammalian cells. Though some ncRNAs are analyzed and cleared to have important functions, what most ncRNAs do is largely unknown. These ncRNAs are thought to function with Protein, RNA or DNA rather than by themselves. Therefore, it is thought that the information of interactions will play an important role to annotate the function of ncRNAs.

So, we focused on the protein-RNA interaction (PRI), and have been developing the assay system to obtain PRI information efficiently.



Visiting Associate Professor
KONDO, Mitsuru (from *Shizuoka University*)

Synthesis of Coordination Polymers with Metallocene Units

Network materials obtained by connections of metallocene units with organic components have attracted intense attentions toward the developments of new functional materials because of the high redox properties and versatile flexibilities based on the metallocene units. Nevertheless, assembled materials with metallocene units excepting ferrocene moieties are still limited. We have prepared the coordination polymers with cobaltocene and rhodocene units. Recently, we have selected ruthenocene-1,1'-dicarboxylic acid (H₂rudc) toward creations of new network materials with ruthenocene units, and have succeeded in syntheses and characterizations of two new network materials, (dpe)(H₂rudc) (dpe = bipyridylethylene) (**1**) and (Hdpp)(Hrudc) (dpp = dipyriddypropane) (**2**). The effects of the free rotations of the Cp rings on the network structures have been shown by their structural characterizations. That is, although both compounds **1** and **2** give linear networks constructed by intermolecular hydrogen bonds, compound **2** demonstrates a quite unique folding structure compared to the simple linear structure of **1**.



RESEARCH FACILITIES

The Institute includes five research facilities. This section describes their latest equipment and activities. For further information please refer to older IMS Annual Review issues (1978–2006).

UVSOR Facility

KOSUGI, Nobuhiro	Director
KATO, Masahiro	Professor
SHIGEMASA, Eiji	Associate Professor
KIMURA, Shin-ichi	Associate Professor
HOSAKA, Masahito	Assistant Professor*
MOCHIHASHI, Akira	Assistant Professor
ITO, Takahiro	Assistant Professor
HIKOSAKA, Yasumasa	Assistant Professor
HORIGOME, Toshio	Technical Associate
NAKAMURA, Eiken	Technical Associate
YAMAZAKI, Jun-ichiro	Technical Associate
HASUMOTO, Masami	Technical Associate
SAKAI, Masahiro	Technical Associate
HAYASHI, Kenji	Technical Associate
KONDO, Naonori	Technical Associate
HAGIWARA, Hisayo	Secretary



Outline of UVSOR

The UVSOR accelerator complex consists of a 15 MeV injector linac, a 600 MeV booster synchrotron, and a 750 MeV storage ring. The magnet lattice of the storage ring is the so-called double-bend achromat. The double RF system is routinely operated for the user beam time, and the lifetime of the electron beam has been improved to around 6 hours at 200 mA. The storage ring is normally operated under multi-bunch mode with partial filling. The single bunch operation is also conducted about two weeks per year, which provides pulsed synchrotron radiation (SR) for time-resolved experiments. Initial beam currents stored under multi-bunch and single-bunch modes are 350 mA and 70 mA, respectively.

Eight bending magnets and three insertion devices are available for utilizing SR. The bending magnet with its radius of 2.2 m provides SR, whose critical energy is 425 eV. After completing the upgrade project, there are 14 beamlines available in total (13 operational, and 1 under construction) at UVSOR, which can be classified into two categories. 9 of them are the so-called “Open beamlines,” which are open to scientists of universities and research institutes belonging to the government, public organizations, private enterprises and those of foreign countries. The rest of the 5 beamlines are the

so-called “In-house beamlines,” which are dedicated to the use of the research groups within IMS. We have 1 soft X-rays (SX) station equipped with a double-crystal monochromator, 8 EUV and SX stations (one of them is under construction) with a grazing incidence monochromator, 3 VUV stations with a normal incidence monochromator, 1 (far) infrared station equipped with FT interferometers, 1 station with a multi-layer monochromator.

Collaborations at UVSOR

Variety of investigations related to molecular/material science is carried out at UVSOR by IMS researchers. In addition, many researchers outside IMS visit UVSOR to conduct their own research work. The number of visiting researchers per year tops about 800, whose affiliations extend to 60 different institutes. International collaboration is also pursued actively and the number of visiting foreign researchers reaches over 80, across 10 countries. UVSOR invites new/continuing proposals for research conducted at the open beamlines twice a year. The proposals from academic and public research organizations (charge-free) as well as enterprises (charged) are acceptable. The fruit of the research activities using SR at UVSOR is published as a UVSOR ACTIVITY REPORT annually. The refereed publications per year count more than 60 since 1996. In recent five years, the number of beamlines has been reduced from 22 to 14. The upgrade project of the UVSOR storage ring, in which the creation of four new straight sections and the achievement of much smaller emittance (27 nm-rad) were planned in 2002–2003, has been accomplished on schedule. The upgraded storage ring is named UVSOR-II. As seen in Figure 2, the numbers of users and related publications have shown an apparent upward tendency, since 2004.

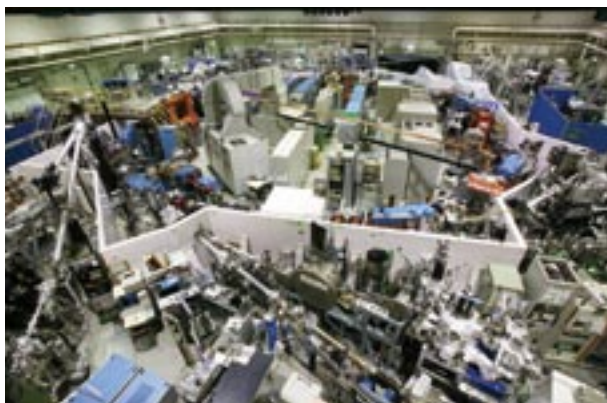


Figure 1. Overview of the UVSOR storage ring room.

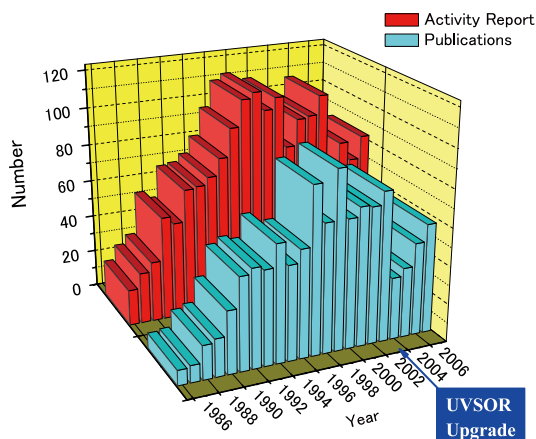


Figure 2. Number of publications resulting from UVSOR work and of users' reports in UVSOR ACTIVITY REPORT.

Highlights of Users' Researches 2006

1) VUV Reflectance Spectroscopy of Strongly Correlated Electron System

J. Fujioka, S. Miyasaka, Y. Tokura (*Univ. Tokyo, Osaka Univ.*)

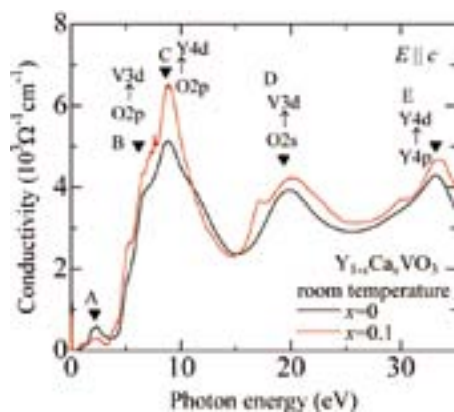


Figure 3. The optical conductivity spectra of $Y_{1-x}Ca_xVO_3$ $x=0$ (black line) and $x=0.1$ (red line), respectively.

The spin, orbital and charge degrees of freedom in the correlated electron system have been attracting much attention. The interplay among them leads to the versatile magnetic and/or electronic structure, even though the crystal structure is nearly cubic. The investigation of the electronic structure over wide energy range by the measurements of the reflectivity spectra is indispensable to reveal the spin-orbital-charge coupled phenomena associated with the insulator to metal transition.

We have measured the reflectivity spectra of the several transition metal oxides, including the V, Mn, Fe, Ni, and Cu ions, for an energy range between 4 eV and 35 eV. As an

example, we focus on the optical conductivity spectra of the single domain crystals of the perovskite-type vanadium oxide $Y_{1-x}Ca_xVO_3$ as the prototypical Mott-Hubbard insulator, with two valence electrons in the $3d$ orbital of the nominally trivalent V ion with the spin configuration of $S=1$.

In Figure 3, we show the optical conductivity spectra of $Y_{1-x}Ca_xVO_3$ $x=0$ and $x=0.10$ for $E \parallel c$, which was measured at room temperature. We assigned the peak A around 2 eV to the Mott-gap excitation. A more intense peak (B) is observed around 7 eV, which is assigned to the charge transfer excitation from O_{2p} to V_{3d} level. Above 7 eV, three peaks (C, D, and E) are observed and we have assigned them to the excitations from O_{2p} to Y_{4d} , from O_{2s} to V_{3d} , and from Y_{4p} to Y_{4d} , respectively.

2) Phase Change of EUV Reflection Multilayer Measured by Total Electron Yields

T. Ejima, T. Harada, A. Yamazaki (*Tohoku Univ.*)

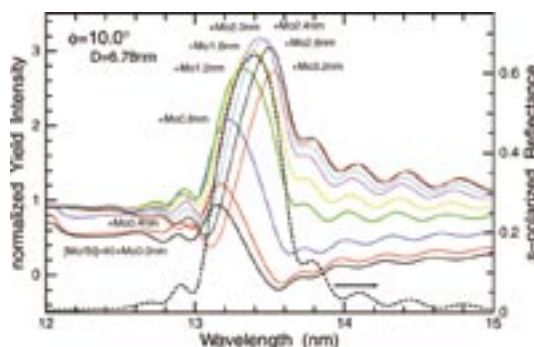


Figure 4. Total electron yield (solid curves) and reflection (broken curve) spectra of Mo/Si multilayers with varying top Mo layer thicknesses.

In the extreme ultraviolet (EUV) wavelength region, normal incidence mirrors are required to have extremely low aberrations. The surface milling method has been proposed for accurate correction of figure errors. It is essential to obtain information regarding the reflection phase in multilayer mirrors. In this study, reflection phase values for multilayer optics were obtained according to the formula derived from the total electron yield intensity and reflection in the multilayer.

Simultaneous reflection and TEY measurements for aperiodic Mo/Si multilayers are shown in Figure 4. In the TEY spectra, the main peak is observed clearly around 13.4 nm and the peak position shifts from 13.2 nm to 13.6 nm as the thickness of the top Mo layer increases. The phase term differences obtained from the reflection and TEY spectra are in accordance with the change in thickness of the top Mo layer. To evaluate the phase information, the present TEY intensity analysis has proved much easier than the Kramers-Kronig analysis of the reflection spectrum.

* Present Address; Nagoya University

Research Center for Molecular Scale Nanoscience

YOKOYAMA, Toshihiko	Director, Professor
OGAWA, Takuji	Professor
NISHI, Nobuyuki	Professor
OKAMOTO, Hiromi	Professor
NAGAYAMA, Kuniaki	Professor (OIIB)
UOZUMI, Yasuhiro	Professor
NAGASE, Shigeru	Professor
KATO, Koichi	Visiting Professor
SUZUKI, Toshiyasu	Associate Professor
NAGATA, Toshi	Associate Professor
SAKURAI, Hidehiro	Associate Professor
NISHIMURA, Katsuyuki	Associate Professor
TSUKUDA, Tatsuya	Associate Professor
TANAKA, Shoji	Assistant Professor
TANAKA, Hirofumi	Assistant Professor
SAKAMOTO, Yoichi	Assistant Professor
NAGASAWA, Takayuki	Assistant Professor
HIGASHIBAYASHI, Shuhei	Assistant Professor
SASAKAWA, Hiroaki	Assistant Professor
NOTO, Madomi	Secretary
SUZUKI, Hiroko	Secretary
WATANABE, Yoko	Secretary
ITO, Yumi	Secretary (Nanonet project)
FUNAKI, Yumiko	Secretary (Nanonet project)



Research Center for Molecular Scale Nanoscience was established in 2002 with the mission of undertaking comprehensive studies of “Molecular Scale Nanoscience.” The Center consists of one division staffed by full-time researchers (Division of Molecular Nanoscience), two divisions staffed by adjunctive researchers (Divisions of Instrumental Nanoscience and Structural Nanoscience), one division staffed by visiting researchers (Division of Advanced Molecular Science). Their mandates are

- 1) Fabrication of new nanostructures based on molecules
- 2) Systematic studies of unique chemical reactions
- 3) Systematic studies of physical properties of these nanostructures.

The Center administers offers public usage of the advanced ultrahigh magnetic field NMR (Nuclear Magnetic Resonance, 920 MHz) spectrometer not only for solution specimens but for solid samples. Since 2004 a number of collaborating researches with the 920 MHz NMR measurements have been examined. Figure shows the apparatus, together with a typical example of the NMR spectra, where one can easily find much better resolving power than that of a standard 500 MHz NMR spectrometer. The research activity in the period of Sep. 2006 through Aug. 2007 was outlined as: (1) Study of folding a De Novo designed peptide, (2) Structure determination of bio-active natural products, (3) Characterization of metal ion complexes by solid state NMR, and (4) Dynamic structures of biological macromolecules. This research division will continuously call for the collaborating research applications using the 920MHz NMR spectrometer with a view to use the NMR of a wide scientific tolerance (*e.g.* structural biology, organic chemistry, catalyst chemistry, *etc.*).

Since 2005, Nanoforum has been organized, which supports small international/domestic meetings and seminars

related to nanoscience. The Center also conducts the Nanotechnology Network Project of the Ministry of Education, Culture, Sports, Science and Technology (MEXT) as a core organization, and provides various kinds of nanotechnology public support programs to Japanese and foreign researchers. This project will be described in the other section in this book.



Figure 1. 920 MHz NMR spectrometer and an example measured using 920 and 500 MHz spectrometers. Much higher resolution in 920 MHz can be clearly seen.

Laser Research Center for Molecular Science

OHMORI, Kenji	Director, Professor
KATOH, Masahiro	Professor
OKAMOTO, Hiromi	Professor
OHSHIMA, Yasuhiro	Professor
MATSUMOTO, Yoshiyasu	Professor
TAIRA, Takunori	Associate Professor
HISHIKAWA, Akiyoshi	Associate Professor
ISHIZUKI, Hideki	Assistant Professor
WATANABE, Kazuya	Assistant Professor
UEDA, Tadashi	Technical Associate
CHIBA, Hisashi	Technical Associate
NAKAGAWA, Nobuyo	Secretary



The center aims to develop new experimental apparatus and methods to open groundbreaking research fields in molecular science, in collaboration with the Department of Photo-Molecular Science. Those new apparatus and methods will be served as key resources in advanced collaborations with the researchers from the community of molecular science. The

main targets are (1) advanced photon sources covering wide energy ranges from terahertz to soft X-ray regions; (2) novel quantum-control schemes based on intense and ultrafast lasers; and (3) high-resolution optical imaging and nanometric microscopy. The center also serves as the core of the joint research project "Extreme Photonics" between IMS and RIKEN.

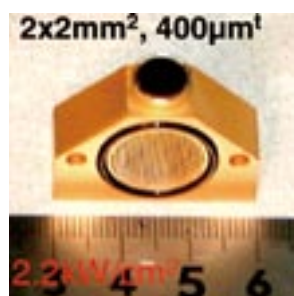


Figure 1. Microchip laser developed at the center.

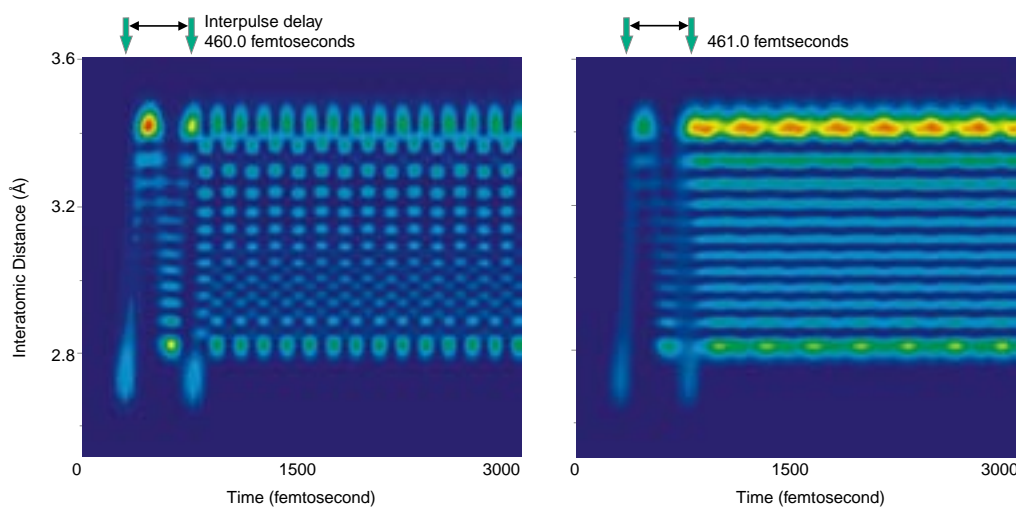


Figure 2. Theoretical simulation of quantum interferometric images generated in a single molecule with a pair of two laser pulses whose timing is controlled on the attosecond (10^{-18} sec) timescale.

Instrument Center

YAKUSHI, Kyuya	Director
YAMANAKA, Takaya	Technical Associate
TAKAYAMA, Takashi	Technical Associate
FUJIWARA, Motoyasu	Technical Associate
OKANO, Yoshinori	Technical Associate
MIZUKAWA, Tetsunori	Technical Associate
MAKITA, Seiji	Technical Associate
NAKANO, Michiko	Technical Associate
SAKAI, Yasuko	Secretary
OTA, Akiyo	Secretary



Instrument Center was organized in April of 2007 by integrating the general-purpose facilities of research center for molecular-scale nanoscience and laser research center for molecular science. The mission of Instrument Center is to support the in-house and external researchers in the field of molecular science, who are conducting their researches using general-purpose instruments such as ESR, x-ray diffractometer, fluorescence spectrometer, *etc.* The staffs of Instrument Center maintain the best condition of the machines, and provide consultation for how to use them. The main instruments are NMR, mass spectrometer, powder x-ray diffractometer in Yamate campus and ESR, SQUID magnetometer, powder and single-crystal diffractometer, dilution refrigerator with superconducting magnet, fluorescence spectrophotometer, UV-VIS-

NIR spectrophotometer, circular dichroic spectrometer in Myodaiji campus. Instrument Center provides liquid nitrogen and liquid helium using helium liquefiers. The staffs of Instrument Center provide consultation for how to treat liquid helium, and provide various parts necessary for low-temperature experiments. Instrument Center supports also the network sharing system of the chemistry-oriented instruments, which starts in the April of 2007. From April to July of 2007, Instrument Center accepted 17 applications from 17 institutions outside of IMS. The users applied SQUID (9), ESR (8), x-ray diffractometer (4), mass spectrometer (3), NMR (2), and UV-VIS spectrometer (1), where the numbers in parenthesis shows the application number.

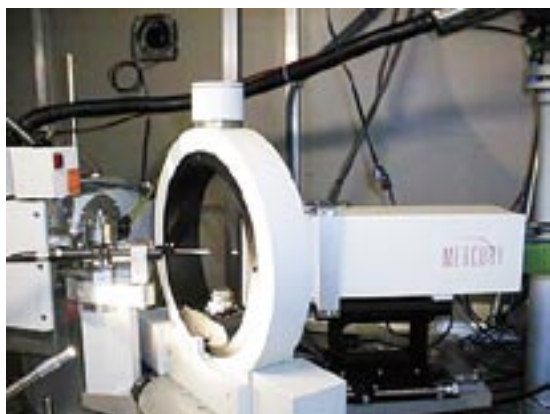


Figure 1. CCD X-ray diffractometer.

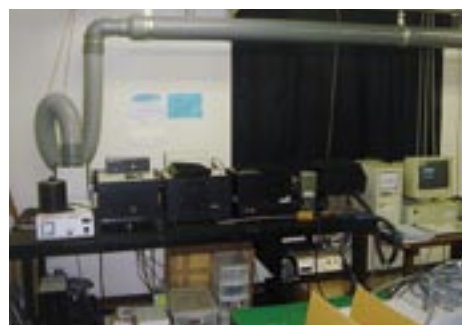


Figure 2. Fluorescence spectrophotometer.

Equipment Development Center

URISU, Tsuneo
SUZUI, Mitsukazu
MIZUTANI, Nobuo
AOYAMA, Masaki
YANO, Takayuki
KONDOU, Takuhiko
YOSHIDA, Hisashi
UTCHIYAMA, Kouichi
TOYODA, Tomonori
NAGATA, Masaaki
MIYASHITA, Harumi
TAKAMATSU, Yoshiteru
URANO, Hiroko

Director
Technical Associate
Reserch Fellow
Reserch Fellow
Secretary



Design and fabrication including the research and developments of the new instruments necessary for the molecular science are the mission of this center, which consists of the mechanical, electronics and glass work sections.

We expanded our service to the outside researchers of universities and research institutes since 2005. The main aims of this new attempt are to contribute to the molecular science community and to improve the technology level of the center staffs.

The technical staff of the Equipment Development Center is engaged in planning, researching, designing and constructing high technology experimental instruments in collaboration with the scientific staff. And these experimental instruments are manufactured by incorporating with new technologies and new mechanical ideas. A part of our activity in the current fiscal year is described below.

Fabrication of a Micro Channel for a Micro Mixer

The micro mixer is a powerful apparatus that enables us to mix liquids efficiently in the micro channels as small as tens of micrometer. However, the products obtained by the mixer are sometimes contaminated by unwanted chemical reactions between the liquid and the base metal since the most of the micro mixers commercially available are made of metal. In order to prevent this, fabrication of a mixer made of a glass is required which is a technical challenge.

At the start of the project, we decided to fabricate the micro mixer by metal in order to optimize the dimensions and geometries of the micro mixer. We made micro channel of brass as shown in Figure 1 by using NC milling machine with minute end mill. The thickness of a channel wall and the distance between the channels are 100 micrometer. The channel depth is estimated to be 100 micrometer by considering the effective cutting length of an end mill used. The micro mixer we designed and fabricated consists of three parts, as shown in Figure 2.

Test experiment showed that efficiency of the mixing was not satisfactory; the results of the mixing were nearly the same with those obtained by conventional mixing. Although the reason is not clear at this moment, we believe that this is due

to the fact that the wall thickness is too large. Then, we are now making an effort to reduce the wall thickness by using an end mill with a spherical shape.



Figure 1. Micro mixer outline view.

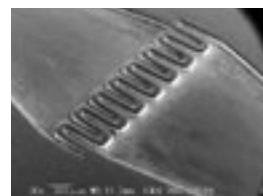


Figure 2. Micro channel.

Manufacture of the Stainless Steel Electrode Parts Using the Elliptical Vibration Cutting Method

To suppress the field emission dark current of various electron guns by high electric field sufficiently, it is required that the surface of the electrode is mirror-finish and Rz value is less than 0.1 micrometer. Titanium, molybdenum, and stainless steel are used as composition components. Currently the mirror-finish is attained by polishing. Therefore the discharge is induced by the abrasive grain remained on the surface. We applied the elliptical vibration cutting method to get a mirror-finish only by cutting those parts.

The elliptical vibration cutting method is the technique which Professor Shamoto of Nagoya University developed. The validity of this technique clarified by the ultra-precision machining using the diamond turning tool of the material, which was impossible due to the problem of a tool life until now.

Figure 3 shows photograph of the SUS304 material surface-of-a-sphere made by the elliptical vibration cutting. The best Rz value of the mirror-finished surface is 0.025 micrometer.



Figure 3. The 28mm diameter, surface-of-a-sphere with R60mm made by sending speed 10 micrometer/rev, spindle rotation speed 20 rpm, the vibration radius 2 micrometers and vibration frequency 39 kHz.

Research Center for Computational Science

OKAZAKI, Susumu	Director, Professor
SAITO, Shinji	Professor
MORITA, Akihiro	Professor
OONO, Hitoshi	Assistant Professor
MIZUTANI, Fumiyasu	Technical Associate
TESHIMA, Fumitsuna	Technical Associate
NAITO, Shigeki	Technical Associate
SAWA, Masataka	Technical Associate
IWAHASHI, Kensuke	Technical Associate
MATSUO, Jun-ichi	Technical Associate
YAZAKI, Toshiko	Secretary
KANO, Seiko	Secretary
TOKUSHI, Hitomi	Secretary



Research Center for Computational Sciences, Okazaki Research Facilities, National Institutes of National Science, provides up-to-date computational resources to academic researchers in molecular science and related fields. In 2006, this facility was used by 555 scientists in 141 project groups.

The computer systems, currently consisting of Fujitsu PRIMEQUEST, SGI Altix4700, NEC SX-7, and NEC TX-7, cover a wide range of computational requests in quantum chemistry, molecular simulation, chemical reaction dynamics and solid state physics. These systems are linked to international networks through Science Information Network (SINET3). Detailed information on the hardware and software of the Center is available on the web site (<http://ccinfo.ims.ac.jp/>).

The Center provides a number of program suites, including Gaussian 03, GAMESS, Molpro2002, Hondo2003, AMBER, etc, which are installed to the computer systems and kept updated for immediate use of the users. The Center also maintains and offers the Quantum Chemistry Literature Database (QCLDB, <http://qcldb2.ims.ac.jp/>), which has been developed by the Quantum Chemistry Database Group in collaboration with staff members of the Center. The latest release,

QCLDB II Release 2006, contains 89,624 data of quantum chemical studies.

In addition to offering computer resources to wide range of molecular scientists, another vital aspect of the Center is to perform leading computational researches with massive computations. In 2003 the Center joined the National Research Grid Initiative (NAREGI) project, a three-year national project by National Institute of Informatics (NII) and IMS. This joint project aimed at developing grid computing system (NII) and thereby realizing extremely large-scale computational studies in the frontier of nanoscience (IMS). For these purposes, two supercomputer systems, Hitachi SR11000 and HA8000, were introduced to the Center in 2004, with combined performance exceeding 10TFlops. In 2006, the NAREGI project was reformed to join a new national project Development & Application of Advanced High-Performance Supercomputer Project by RIKEN, where IMS plays an important role in the application of the PFlops-scale supercomputer to nanoscience. Further information on next-generation supercomputer project and computer systems at the Center is found on the web site (<http://ims.ac.jp/nanogrid/>).



Figure 1. Super-High-Performance Molecular Simulator.

Okazaki Institute for Integrative Bioscience

AONO, Shigetoshi	Professor
KUWAJIMA, Kunihiro	Professor
FUJII, Hiroshi	Associate Professor
KURAHASHI, Takuya	Assistant Professor
MAKI, Kosuke	Assistant Professor*
YOSHIOKA, Shiro	Assistant Professor
ISOGAI, Miho	Secretary
TANIZAWA, Misako	Secretary



The main purpose of Okazaki Institute for Integrative Bioscience (OIIB) is to conduct interdisciplinary, molecular research on various biological phenomena such as signal transduction, differentiation and environmental response. OIIB, founded in April 2000, introduces cutting edge methodology from the physical and chemical disciplines to foster new trends in bioscience research. OIIB is a center shared by and benefited from all three institutes in Okazaki, thus encouraging innovative researches adequately in advance of academic and social demands. The research groups of three full professors and one associate professor who have the position in IMS join OIIB. The research activities of these groups are as follows.

Aono group is studying the bioinorganic chemistry of hemeproteins that show a novel function. They solved the crystal structure of CO sensor protein from a thermophilic CO oxidizing bacterium and discussed the molecular mechanism of CO sensing. They also reported the structure and function relationships of aldoxime dehydratase, which is a novel heme-containing dehydrase enzyme. Kuwajima group is studying mechanisms of *in vitro* protein folding and mechanisms of molecular chaperone function. Their goals are to elucidate the physical principles by which a protein organizes its specific native structure from the amino acid sequence. In this year,

they studied the equilibrium and kinetics of canine milk lysozyme folding/unfolding by peptide and aromatic circular dichroism and tryptophan fluorescence spectroscopy. Fujii group is studying molecular mechanisms of metalloenzymes, which are a class of biologically important macromolecules having various functions such as oxygen transport, electron transfer, oxygenation, and signal transduction, with synthetic model complexes for the active site of the metalloenzymes. In this year, they studied molecular mechanisms of metalloenzymes relating to monooxygenation reactions and denitification processes.

OIIB is conducting the cooperation research program, "Frontiers of Membrane Protein Research," with Institute for Protein Research, Osaka University from 2005. In this program, the following projects have been carried out to elucidate the role of membrane proteins in life: (i) the development of expression systems, purification methods, and chemical synthesis of membrane proteins, (ii) the development of new methods for analyzing the structure and function of membrane proteins. As a part of this cooperation program, International Symposium on Electro-chemical Signaling by Membrane Proteins—Biodiversity and Principle, was held in Okazaki Conference Center from March 14 to March 16, 2007, where

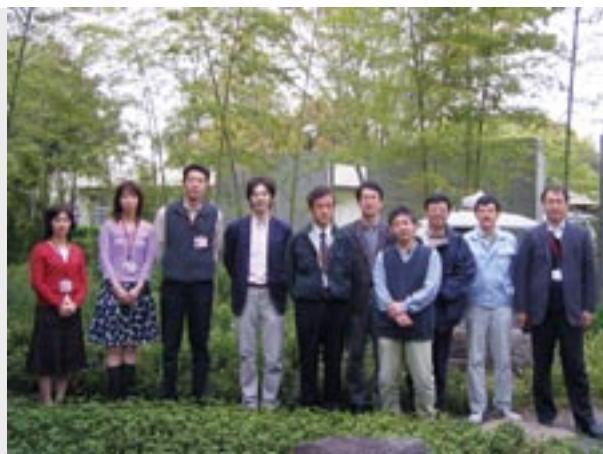
19 invited lectures and 40 poster presentations were provided, and we had more than 200 participants. This symposium was co-organized as a SOKENDAI International Symposium.



* Present Address: Nagoya University, Nagoya 464-8601

Safety Office

OKAMOTO, Hiromi	Director
TOMURA, Masaaki	Assistant Professor
TANAKA, Shoji	Assistant Professor
KATO, Kiyonori	Technical Associate
HORIGOME, Toshio	Technical Associate
NAGATA, Masaaki	Technical Associate
YAMANAKA, Takaya	Technical Associate
TAKAYAMA, Takashi	Technical Associate
HAYASHI, Kenji	Technical Associate
MAKITA, Seiji	Technical Associate
ONITAKE, Naoko	Secretary
TSURUTA, Yumiko	Secretary



The Safety Office was established in April 2004. The mission of the Office is to play a principal role in the institute to secure the safety and health of the staffs by achieving a comfortable workplace environment, and improvement of the working conditions. In concrete terms, it carries out planning, work instructions, fact-findings, and other services for safety and health in the institute. The Office is comprised of the following staffs: The Director of the Office, Safety-and-Health

Administrators, Safety Office Personnel, Operational Chiefs, and other staff members appointed by the Director General. The Safety-and-Health Administrators patrol the laboratories in the institute once every week, and check whether the laboratory condition is kept sufficiently safe and comfortable to conduct researches. The Office also edits the safety manuals and gives safety training courses, for Japanese and foreign researchers.

Public Affairs Office

HIRATA, Fumio	Head
OHSHIMA, Yasuhiro	Vice-Head
HARADA, Miyuki	Technical Associate
NAKAMURA, Rie	Secretary

Archives

YAKUSHI, Kyuya	Head
MINAMINO, Satoshi	Technical Associate
KIMURA, Katsumi	Professor Emeritus
SUZUKI, Satomi	Secretary

Technical Division

KATO, Kiyonori	Head
----------------	------

Reception

OHHARA, Kyoko	Secretary
SUGIYAMA, Kayoko	Secretary
TSURUTA, Yumiko	Secretary
KAMO, Kyoko	Secretary

NOGAWA, Kyoko	Secretary
---------------	-----------

The commission of the Technical Division is mainly to provide support for maintaining and managing Research Centers and Facilities of IMS. Most of the members belong to these stations.

In addition, we also support Safety Office, Research groups, Public Affairs Office, Archives and Reception of the IMS.

The Research Centers and Facilities are;

- (1) UVSOR Research Center: Operation and maintenance of the Synchrotron Radiation Facility and support of visiting researchers.
- (2) Laser Research Center for Molecular Science: Maintenance of the laser devices and support of visiting researchers.
- (3) Instrument Center: Maintenance and support of general-use research devices such as NMR, ESR, SQUID, MS, X-

ray diffractometers, dilution refrigerator and several kinds of spectrometers. The network system for efficient use of research equipments is also taken care for. Liquid nitrogen and liquid helium are also provided.

- (4) Equipment Develop Center: R&D center consisting of mechanical engineering, electrical engineering and manufacturing of chemical glass tools.
- (5) Research Center for Computational Science: Operation and maintenance of the computer resources including super computers and support of users outside IMS. In addition, Orion and IMS networks are maintained.

The annual meeting is regularly organized since 1975 for technical staff of research Institutes and Universities. Various technical problems related to research are discussed. The proceedings are published and stored in the computer server.



Special Research Projects

IMS has special research projects supported by national funds. Four projects in progress are:

- (a) Next Generation Integrated Nanoscience Simulation Software
Development & Application of Advanced High-Performance Supercomputer Project
- (b) Formation of Interdisciplinary and International Bases for Natural Sciences, NINS
“Development of New Computational Methods for Large-Scale Systems and Establishment of Advanced Simulation Center for Molecules and Materials”
- (c) Extreme Photonics
- (d) MEXT Nanotechnology Network
Nanotechnology Support Project in Central Japan: Synthesis, Nanoprocessing and Advanced Instrumental Analysis

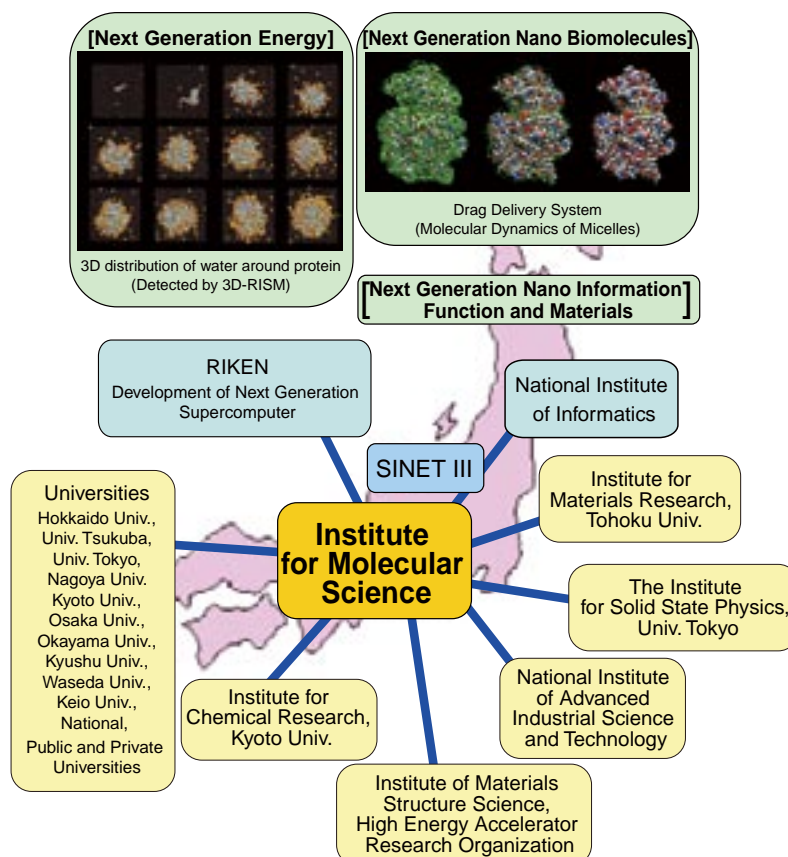
These four projects are being carried out with close collaboration between research divisions and facilities. Collaborations from outside also make important contributions. Research fellows join these projects.

(a) Next Generation Integrated Nanoscience Simulation Software Development & Application of Advanced High-Performance Supercomputer Project

A national project entitled, “Next Generation Integrated Nanoscience Simulation Software” was initiated on April 1, 2006 at Institute for Molecular Science (IMS). The project is a part of the “Development & Application of Advanced High-Performance Supercomputer Project” of MEXT, which aims to develop a next generation supercomputer and application software to meet the need in the computational science nation-wide.

The primary mission of our project is to resolve following three fundamental problems in the field of nanoscience, all of which are crucial to support society’s future scientific and

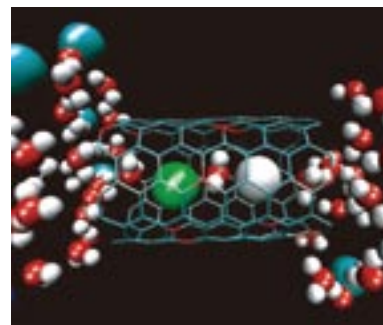
technological demands: (1) “Next Generation Energy” (*e.g.*, effective utilization of the solar energy), (2) “Next Generation Nano Biomolecules” (*e.g.*, scientific contributions toward overcoming obstinate diseases), and (3), “Next Generation Nano Information Function and Materials” (*e.g.*, molecular devices). In these fields, new computational methodologies and programs are to be developed to clarify the properties of nanoscale substances such as catalysts (enzymes), biomaterials, molecular devices, and so forth, by making the best use of the next generation supercomputer.



(b) Formation of Interdisciplinary and International Bases for Natural Sciences, NINS “Development of New Computational Methods for Large-Scale Systems and Establishment of Advanced Simulation Center for Molecules and Materials”

This project aims to establish a core computational science center for molecular and material systems and to develop advanced methodologies for large-scale calculations. The project has been organized by five institutes of the National Institutes of Natural Sciences, *i.e.* Institute for Molecular Science, National Astronomical Observatory of Japan, National Institute for Fusion Science, National Institute for Basic Biology, and National Institute for Physiological Sciences, and other universities and research institutes. We are trying to create a new interdisciplinary field by integrating the different views and methodologies traditionally associated with each field that belongs to a different hierarchy of natural sciences. Structures and dynamics of large-scale complex systems, such as nanomaterials and biological systems, are investigated by using a variety of sophisticated computational methods based

on theories of electronic structure, molecular dynamics method, statistical mechanics, and so on. The development of new computational methods utilizing parallel computation has also been furthered organizing the members having different scientific backgrounds. Seminars and workshops for the advanced calculations and for the development of human resources are also conducted by this project.



Ion permeation in a mode channel.

OKAZAKI, Susumu	Large-Scale Molecular Dynamics Calculations for Aqueous Solution of Amphiphilic Molecules
HIRATA, Fumio	Theoretical Study of Molecular Recognition Based on the 3D-RISM Theory
NAGASE, Shigeru	Quantum Chemistry Calculations of Nanomolecules
SAITO, Shinji	Theoretical Analyses of Condensed Phase Dynamics by Using Molecular Dynamics Simulation
NOBUSADA, Katsuyuki	Theoretical Calculations for Electron Dynamics Strongly Coupled to the Electromagnetic Field
YONEMITSU, Kenji	Theory for Nonequilibrium Control of Collective Dynamics in Quantum-Classical Hybrid Many-Particle Systems
YANAI, Takeshi	Theory Development for Multireference Electronic Structures with <i>ab initio</i> Quantum Chemical Methods

(c) Extreme Photonics

Institute for Molecular Science has a long-standing tradition of promoting spectroscopy and dynamics of molecules and molecular assemblies. Accordingly, photo-molecular science is one of major disciplines in molecular science. This field is not confined in the traditional spectroscopy, but makes solid basis for other disciplines including nanoscience and bioscience, *etc.* Therefore, continuing developments in spectroscopy and microscopy are vital to enhance our abilities to elucidate more complex systems in time and spatial domains.

In order to achieve full developments of photo-molecular science, we need to pursue three branches in developing: (1) new light source, (2) new spatio-temporally resolved spectroscopy, and (3) new methods to control chemical reactions. Since 2005, we have started the program of “Extreme Photonics” in collaborating with the RIKEN institute. Currently 7 groups in IMS are involved in this program, and the specific research titles are as follows:

- (1) Development of new light sources

TAIRA, Takunori	Micro Solid-State Photonics
-----------------	-----------------------------
- (2) Development of new spatio-temporally resolved spectroscopy

OKAMOTO, Hiromi	Development of Extreme Time-Resolved Near-Field Spectroscopy
MATSUMOTO, Yoshiyasu	Development of Spatio-Temporally Resolved Spectroscopy for Surfaces and Interfaces
OZAWA, Takeaki	Developments of Luminescent Probes based on Protein Structures and Analysis System of Biological Functions
- (3) Development of new methods to control chemical reactions

OHMORI, Kenji	Development of Attosecond Coherent Control and Its Applications
HISHIKAWA, Akiyoshi	Reaction Imaging and Control with Extremely Short Laser Pulses
OHSHIMA, Yasuhiro	Quantum-State Manipulation of Molecular Motions by Intense Coherent Laser Pulses

(d) MEXT Nanotechnology Network Nanotechnology Support Project in Central Japan: Synthesis, Nanoprocessing and Advanced Instrumental Analysis

The Ministry of Education, Culture, Sports, Science and Technology (MEXT), Japan started the Nanotechnology Network Project in April 2007 in order to support Japanese nanotechnology researches not only for university and government institutes but also for private companies. IMS participates in this project as a core organization (project leader: YOKOYAMA, Toshihiko, Prof. & Director of Research Center for Molecular Scale Nanoscience) with Nagoya University (representative: BABA, Yoshinobu, Prof.), Nagoya Institute of Technology (representative: SUMIYAMA, Kenji, Prof.) and Toyota Technological Institute (representative: SAKAKI, Hiroyuki, Prof. & Vice President of TTI), and establishes a nanotechnology support center in central Japan area for these five years. We will support

- 1) Public usage of various advanced nanotechnology instruments such as ultrahigh magnetic field NMR (920 MHz), advanced transmission electron microscopes, and so forth
- 2) Design, synthesis and characterization of organic, inorganic and biological molecules and materials,
- 3) Semiconductor nanoprocessing using advanced facilities and technologies.

We will promote applications not only to each supporting element, but to combined usage of several supporting elements such as a nanobiotechnology field that is highly efficient in this joint project. In 2007 Apr.–2007 Spt., the number of accepted projects applied to IMS amounted 39.



300kV Transmission Electron Microscopy and Some Typical Examples.

List of Supports in IMS

Person in Charge	Support Element
OKAMOTO, Hiromi	Space- and Time-Resolved Near-Field Microspectroscopy
YOKOYAMA, Toshihiko	Magneto-Optical Characterization of Surface Nanomagnetism
YOKOYAMA, Toshihiko	Electron Spectroscopy for Chemical Analysis
NISHI, Nobuyuki	Tunable Picosecond Raman Spectroscopy
NISHI, Nobuyuki	300kV Transmission Analytical Electron Microscopy
TSUKUDA, Tastsuya	Focus Ion Beam Processing & Field Emission Scanning Electron Microscopy
NAGAYAMA, Kuniaki	Phase Contrast Transmission Electron Microscopy for Nanobiological materials
UOZUMI, Yasuhiro	920 MHz NMR Spectrometer
OGAWA, Takuji	Preparation of Molecular Electronic Devices and Electric Conductivity Measurements
NAGASE, Shigeru	Quantum Chemical Calculation for Molecular Design
TSUKUDA, Tastsuya; SUZUKI, Toshiyasu; NAGATA, Toshi; SAKURAI, Hidehiro	Synthesis & Design of Functional Organic Nanomaterials

Joint Study Programs

As one of the important functions of an inter-university research institute, IMS facilitates joint study programs for which funds are available to cover the costs of research expenses as well as the travel and accommodation expenses of individuals. Proposals from domestic scientists are reviewed and selected by an interuniversity committee.

(1) Special Projects

A. New Developments in Spin Science Using Pulsed and High-Frequency ESR

KATO, Tatsuhisa (*Josai Univ.*)
 MIZOGUCHI, Kenji (*Tokyo Metropolitan Univ.*)
 SAKAMOTO, Hirokazu (*Tokyo Metropolitan Univ.*)
 NAKAMURA, Toshikazu (*IMS*)
 FURUKAWA, Ko (*IMS*)

In order to develop advanced ESR (electron spin resonance) spectroscopy for materials science, we performed functional materials studies, both on isolated molecules and on molecular assemblies. The following two topics were investigated: 1) We determined the molecular structure of novel systems such as $\text{Gd}@C_{82}$ and their spin interaction using ESR spectroscopy, and explored the functionality of the complicated molecule system. 2) We carried out an analysis of spin dynamics for functional molecular assemblies, including molecular conductors and magnetic materials. We searched for cooperative phenomena involved in intra-molecule freedom, and new functional physical-properties originating in molecular assemblies.

A-1 ESR Spectra of Bingel Monoadducts of $\text{Gd}@C_{82}$

Two kinds of Bingel monoadducts of $\text{Gd}@C_{82}$ exhibited a sharp contrast in the ESR spectra. The reaction of $\text{La}@C_{82}$ with diethyl bromomalonate in the presence of a base (the Bingel reaction) generated five mono-adducts. Akasaka and coworkers recently synthesized two monoadducts of $\text{Gd}@C_{82}$, mono-A and mono-E, at high purity. ESR spectra of the adducts were obtained using a high-field (W-band) ESR spectrometer at low temperature in solution, which showed remarkable contrast between mono-A and mono-E. The ESR spectrum of mono-A was unambiguously assigned to the spin state of $S = 7/2$, and that of mono-E to $S = 3$.

A-2 Peculiar Ground State of β'' -(BEDT-TTF)-TCNQ Revealed by ESR

One of the two segregated stack isomers of (BEDT-TTF)-TCNQ (abbreviated as ET-TCNQ), β'' -ET-TCNQ, has been studied. Since the unit cell of β'' -ET-TCNQ has one ET and one TCNQ molecule with a charge transfer of 0.5 electrons, a quarter-filled band with strong on-site Coulomb correlation

determines the electronic states.

It is known that (1) the β'' -form has metallic characteristics at low temperatures with definite Fermi surfaces, (2) the charge separation within the ET layer melts away below 170 K, and (3) the 1D TCNQ stack has weak dimerization at all temperatures. However, several open questions still remain for this system, including anomalies in the electrical resistivity at 80 K and 20 K, and heat capacity anomalies at 10 K and 20 K.

Here, on the basis of ESR and ^1H NMR spectra, and spin susceptibility for each of the ET and TCNQ stacks deduced from the ESR g -shift, we propose a model with partial CDW nesting in ET sheets below 80 K, spin-Peierls transition at 20 K within the TCNQ 1D stacks, and the RKKY broadening of the ESR spectra of the TCNQ soliton-like spins via conduction electrons of the ET layer with a Kondo temperature of 10 K.

A-3 Spin-Dynamics Investigation by Pulsed ESR for Spin-Peierls Phases in Conventional Systems and Charge-Ordered TMTTF Salts

TMTTF-based salts undergo charge-ordering (CO) transitions in the intermediate paramagnetic states between the resistivity minimum temperature and the phase-transition temperature towards the ground state. In our previous report, the charge configuration patterns of the charge-ordering phases in the intermediate paramagnetic states were determined to be $-\text{O}-\text{o}-\text{O}-\text{o}-$ ($4k_{\text{F}}$) along the stacking axes for $(\text{TMTTF})_2\text{MF}_6$ salts ($M = \text{P, As, Sb}$) by ESR linewidth anisotropy analysis. However, the charge configuration of the ground state (for example, $(\text{TMTTF})_2\text{PF}_6$ (spin-Peierls)) has not yet been clarified. Moreover, the co-existence of the CO ($4k_{\text{F}}$) and spin-Peierls ($2k_{\text{F}}$) phases seems unlikely.

To determine spin dynamics in the proximity of the spin-Peierls phase, pulsed ESR investigations were carried out for one-dimensional organic conductors, $(\text{TMTTF})_2\text{X}$, compared to a conventional spin-Peierls system, $\text{MEM}(\text{TCNQ})_2$. While the ESR spin-lattice relaxation rate, $\text{ESR}-T_1^{-1}$, of $\text{MEM}(\text{TCNQ})_2$ shows ordinal spin-gap behavior at around the spin-Peierls phase transition temperature, T_{SP} , the $\text{ESR}-T_1^{-1}$ of $(\text{TMTTF})_2\text{PF}_6$ cannot be explained within the framework of simple spin-gap formation in the proximity of T_{SP} . Possible reorientation of charge configuration is likely. We discuss the electronic properties from a microscopic point of view.

B. Construction of the Research Methodology for Biomolecular Sensing System

URISU, Tsuneo (*IMS*)
 TOMINAGA, Makoto (*OIIB*)
 MORIGAKI, Kennichi (*AIST*)
 ISOBE, Hiroko (*Univ. Tsukuba*)
 ISHII, Kiyoshi (*Chubu Univ.*)

The target of this project is the development of a kind of neural cell chips as shown in Figure 1, in which a couple of cells is combined by synapse and the detection of action potential, fluorescence or FRET signal and neurotransmitter molecules.

Figure 2 is shown the first device which we have developed last year.¹⁾ Transient receptor potential V1 (TRPV1) transfected HEK293 cell is positioned on the micropore of the Si chip. The chip is integrated into the microfluidic circuit. Channel current triggered by capsaicin was successfully observed. The desensitization unique to the TRPV1 channel was observed.

Reference

1) Z. L. Zhang *et al.*, *Thin Solid Film* (2007) in press.

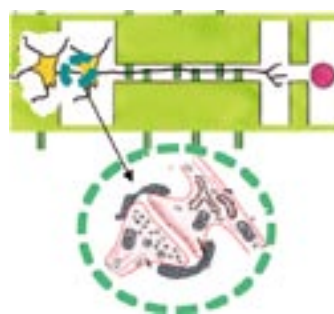


Figure 1. Schematic image of the target neural cell chip in this project.

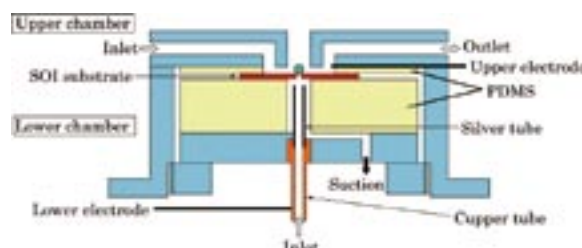


Figure 2. Planer patch clamp device fabricated in this project using Si-SOI substrate.

(2) Research Symposia

(From 2006 Oct. to 2007 Sep.)

Dates	Theme	Chair
Nov. 7– 8, 2006	Approach from Interstellar and Molecular Sciences to the Origin of Homochirality	KAWAGUCHI, Kentaro OHSHIMA, Yasuhiro
Nov. 17–18, 2006	Workshop on Research for VUV Luminescence	ITOH, Minoru SHIGEMASA, Eiji
Nov. 29–30, 2006	Large-Amplitude Vibration by High-Resolution Molecular Spectroscopy	BABA, Masaaki OHSHIMA, Yasuhiro
Dec. 5– 6, 2006	Recent Advances in Molecular Science via Sum Frequency Generation Spectroscopy	OUCHI, Yukio MORITA, Akihiro
Dec. 21–22, 2006	Hierarchy of Molecular Interactions in Complicated Systems: A Basis for Understanding of Biological Functions	TAHARA, Tahei NISHI, Nobuyuki
Mar. 11–12, 2007	New Development of Materials Molecular Science	KATO, Reizo YAKUSHI, Kyuya
Mar. 14–15, 2007	Functions and Properties of Nano-Structure Controlled Hybrid Inorganic-Organic Composites	OHBA, Masaaki TANAKA, Koji
Mar. 19–20, 2007	Progress in Science of Nanoclusters and Nanoparticles —Reactivity, Structure, and Dynamics	MAFUNE, Fumitaka TSUKUDA, Tatsuya
Mar. 19–20, 2007	Molecular Science of Enzymes Relating to Heme Degradation	FUJII, Hiroshi

May 22–23, 2007	Molecular Science for Living Cells	OHTA, Nobuhiro OZAWA, Takeaki
Jun. 1– 3, 2007	Metals and Molecular Assemblies —The Way to Frontier of Supramolecular Science—	UENO, Takashi KAWAGUCHI, Hiroyuki
Jun. 23, 2007	Physical Chemistry Symposium for Young Scientists in Molecular Science	HAMAGUCHI, Hiroo HISHIKAWA, Akiyoshi
Aug. 29–31, 2007	Coupled Simulation in Molecular Science: Theories and Applications	AOYAGI, Mutsumi SAITO, Shinji
Sep. 10–11, 2007	Synchrotron Radiation and Surface Electron Emission Microscopy: Recent Progress in Microscopic Techniques for Nanomaterials Science	ASAKURA, Kiyotaka YOKOYAMA, Toshihiko
Sep. 28–29, 2007	Scientific Basis of New Field “Molecular Communication”	URISU, Tsuneo

(3) Numbers of Joint Study Programs

Categories		2006 Oct.–2007 Mar.	2007 Apr.–2007 Sep.	Total
Special Projects		0	2	2
Research Symposia		9	6	15
Cooperative Research		39	44	83
Use of Facility	Laser Research Center for Molecular Science	1	–	1
	Research Center for Molecular Scale Nanoscience	21	–	21
	Instrument Center	–	23	23
	Equipment Development Center	5	2	7
Use of UVSOR Facility		62	70	132
Use of Facility Program of the Computer Center				141

Collaboration Programs

(a) IMS International Program

IMS has accepted many foreign scientists and hosted numerous international conferences since its establishment and is now universally recognized as an institute that is open to foreign countries. In 2004, IMS initiated a new program to further promote international collaborations. As a part of this

new program, IMS faculty members can (1) nominate senior foreign scientists for short-term visits, (2) invite young scientists for long-term stays, and (3) undertake visits overseas to conduct international collaborations.

Leader	Title	Partner
OHMORI, Kenji	Quantum Control of Atoms and Molecules with Amplitude- and Phase-Shaped Optical Pulses	France: Prof. GIRARD, Bertrand and his group members U.S.A.: Prof. LEVIS, Robert J. and his group members
SHIGEMASA, Eiji	Dynamics in Resonant Auger Decay Studied by Electron-Ion Coincidence Spectroscopy	France: Dr. SIMON, Marc Dr. GUILLEMIN, Renaud Dr. JOURNEL, Loic U.K.: Dr. ELAND, John H. D.
KIMURA, Shin-ichi	Optical and Photoelectrical Studies on the Local to Itinerant Electronic Structure of Strongly Correlated Electron Systems	Korea: Prof. KWON, Yong-Seung Dr. IM, Hojun Dr. KIM, Hyeong-do and group members
TAIRA, Takunori	Passively Q-Switched Nd-Lasers with YCOB Doubler	France: Prof. AKA, Gerard Philippe Dr. LOISEAU, Pascal Dr. XU, Ke
KATOH, Masahiro	Beam Dynamics in Free Electron Laser	France: Dr. COUPRIE, Marie Emmanuelle and group member Dr. BIELAWSKI, Serge and group member
KOSUGI, Nobuhiro	Resonant Soft X-Ray Spectroscopic Study at UVSOR BL3U	Germany: Prof. RUEHL, Eckart and group members Sweden: Prof. AGREN, Hans Prof. PETERSSON, Lars G. M. Prof. NORDGREN, Joseph and group members U.S.A.: Dr. GUO, Jinghua
TANAKA, Koji	Photochemical Water Oxidation and Multi-Electron Reduction of Carbon Dioxide	U.S.A.: Dr. FUJITA, Etsuko Dr. MUCKERMAN, James T.
JIANG, Donglin	Studies on Molecular Design and Self-Assembly of Light-Harvesting Antennae	China: Prof. WANG, Changchun and group members

SAKURAI, Hidehiro

Studies on Columnar Structure of Buckybowl
Supramolecules

India:

Dr. SASTRY, Narahari G.
and group members

NAGASE, Shigeru

Theoretical Study on Chemical Modification
and Functionalization of Single-Walled Carbon
Nanotubes

China:

Prof. LU, Jing
and group members

(b) Asian Core Program “Frontiers of Material, Photo- and Theoretical Molecular Sciences”

Asian Core Program is a multilateral international collaboration program carried out by JSPS (Japan Society for the Promotion of Science). It is designed to create world-class research hubs in selected fields within the Asian region, while fostering the next generation of leading researchers. The program is based on a principle of equal partnership among core institutions in Japan and other Asian countries, so that each institution is expected to secure its own matching fund. Institute for Molecular Science has launched a new collaboration project “material, photo- and theoretical molecular

sciences” (2006–2011) within the framework of this Asian Core Program with three key institutes in east Asian countries: Institute of Chemistry, Chinese Academy of Science (China); The College of Natural Science, Korea Advanced Institute of Science and Technology (Korea); and Institute of Atomic and Molecular Sciences, Academia Sinica (Taiwan). At present, nine joint researches are in progress, three joint seminars have so far been carried out, and another seven seminars are planned.



Professor Emeritus Inokuchi's Scientific Achievement

Professor Hiroo Inokuchi, the former Director-General of IMS (1987–1993), was awarded the Kyoto Prize of 2007 for his pioneering and fundamental contributions to organic molecular electronics. The Kyoto Prize is an international award to honor those who have contributed significantly to the scientific, cultural, and spiritual betterment of mankind. The Prize is presented annually in each of the following three categories: Advanced Technology, Basic Sciences, and Arts and Philosophy. Professor Inokuchi was honored in the field of Materials Science and Engineering in the category of Advanced Technology. Professor Inokuchi initiated pioneering research on electrical conduction between molecules in aromatic hydrocarbons which had been believed to be a typical insulator, and established the scientific foundation for studying the electrical conductivity of organic materials. Further, he

systematically elucidated an electronic structure of a wide variety of organic materials by photoelectron spectroscopy. Through a series of such studies, he established the academic base essential for studying the electronic properties of organic

solids, making fundamental contributions to the subsequent development of organic molecular electronics.



Mr. Suzui's Technical Achievements

Mr. Mistukazu Suzui, the leader of the machine group of Equipment Development Center, has received The CSJ Award for Technical Achievement from The Chemical Society of Japan, by his work "Design and fabrication of advanced



experimental systems using the precision machine technologies." Mr. Suzui has developed many equipments necessary for molecular science experiments through the cooperation with scientists who need the instruments, and attained a great contribution to the molecular science. His main achievements awarded are "High mass TOF mass spectrum analyzer," "High density oriented molecular beam generator," "Microchip laser system," and "Biosensor and biochip," etc. All these instruments and devices require fine machinery design and fabrication technologies to make. Not only these recent works, he also contributed to the construction of many kinds of monochromators in the synchrotron radiation facility of IMS, UVSOR. We expect him continuing important contribution to molecular science research field.

Professor Suzuki's Scientific Achievement

Professor Toshinori Suzuki, Chief Scientist of Chemical Dynamics Laboratory, RIKEN (Institute of Physical and Chemical Research), a former associate professor of Department of Electronic Structure, IMS, received the 20th IBM Japan Science Prize in 2006 for his contribution to "development and accomplishment of the ultrafast photoelectron imaging spectroscopy to directly observe the change of quantum states of reacting molecules, or activated complexes." This prize was founded by Japan IBM Co. at 1987 in order to commemorate the 50th anniversary of the founding of the company. Candidates of the award are researchers who conduct outstanding studies in the extensive field of physics, chemistry, computer science and electronics at universities and public institutes. He received the prize in the chemistry division.

Professor Suzuki had studied chemical reaction dynamics by means of molecular beam technique, laser spectroscopy as well as photoion and photoelectron imaging at IMS since 1992. He moved to RIKEN in 2002 and presides over the Chemical Dynamics Laboratory.

The observation of the change of quantum states was hitherto believed to be impossible, so that the state-to-state chemistry, in which electronic states of

reactant (entrance) and product (exit) were determined, were regarded as the most precise science of chemical reactions. The ultrafast photoelectron imaging spectroscopy exploded this belief. This spectroscopy allows us to measure changes of energy and angular distributions of photoelectrons from reacting molecules. Changes of shapes of electron orbitals and wave packet motions of molecular vibration and rotation can be obtained from the analysis of the photoelectron images. This spectroscopy enables us to experimentally investigate how chemical reactions proceed with accuracy which has not been fulfilled by existing techniques.



Visitors from abroad are always welcome at IMS and they have always played an important role in the research activities of the Institute. The foreign scientists who visited IMS during the past year (September 2006–August 2007) are listed below.

(1) MONKASHO (Ministry of Education, Culture, Sports, Science and Technology, Japan) or JSPS (Japan Society for the Promotion of Science) Invited Fellow

Prof. R. Rodgers Kenton	North Dakota State Univ.	U.S.A.	Nov. '06
Prof. Michael K. Chan	Ohio State Univ.	U.S.A.	Nov. '06
Dr. Bielawski Serge	Univ. of Sci. and Tech. of Lille	France	Nov. '06–Dec. '06
Prof. Pavlov Lubomir	Inst. for Nuclear Res. and Nuclear Energy	Bulgaria	Jun. '07–Mar. '08
Dr. Volety Srinivas	Center for Cellular and Mol. Bio.	India	Jul. '07–Apr. '08

(2) IMS Visiting Professor or Associate Professor from Abroad (period of stay from 3 to 12 months)

Dr. Dascalu Traian	Natl. Inst. for Laser Plasma and Radiation Phys.	Romania	Sep. '06–Mar. '07
Prof. Bongsoo Kim	Changwon Natl. Univ.	Korea	Mar. '07–Feb. '08
Prof. Choi Cheol Ho	Kyungpook Natl. Univ.	Korea	Mar. '07–Jan. '08
Prof. Chaudhuri Tapan Kumar	Indian Inst. of Tech.	India	Jul. '07–Jul. '08

(3) JSPS Post-Doctoral or Ronpaku Fellow

Dr. Kowalska Aneta	Tech. Univ. of Lodz	Poland	Oct. '06–Oct. '08
Prof. Dai Hai-Lung	Temple Univ.	U.S.A.	Mar. '07
Prof. Chen Ying-Cheng	Inst. of Atomic and Mol. Sci., Academia Sinica	Taiwan	Mar. '07
Dr. Cheng Wang-Yau	Inst. of Atomic and Mol. Sci., Academia Sinica	Taiwan	Mar. '07
Dr. Wei Ching-Min	Inst. of Atomic and Mol. Sci., Academia Sinica	Taiwan	Mar. '07
Dr. Tzeng Wen-Bih	Inst. of Atomic and Mol. Sci., Academia Sinica	Taiwan	Mar. '07
Prof. Lee Yoon Sup	KAIST	Korea	Mar. '07
Prof. Kim Sang Yul	KAIST	Korea	Mar. '07
Prof. Choi In Sung	KAIST	Korea	Mar. '07
Prof. Churchill David	KAIST	Korea	Mar. '07
Prof. Ihee Hyocherl	KAIST	Korea	Mar. '07
Prof. Kim Sang Kyu	KAIST	Korea	Mar. '07
Prof. Liu Ming-Hua	Inst. of Chem., Chinese Acad. of Sci.	China	Mar. '07
Prof. Zhang De-Qing	Inst. of Chem., Chinese Acad. of Sci.	China	Mar. '07
Prof. Yang Guo-Qiang	Inst. of Chem., Chinese Acad. of Sci.	China	Mar. '07
Prof. Xia An-Dong	Inst. of Chem., Chinese Acad. of Sci.	China	Mar. '07
Prof. Mao Lan-Qun	Inst. of Chem., Chinese Acad. of Sci.	China	Mar. '07
Prof. Yang Zhen-Zhong	Inst. of Chem., Chinese Acad. of Sci.	China	Mar. '07
Prof. Bian Wen-Sheng	Inst. of Chem., Chinese Acad. of Sci.	China	Mar. '07

(4) IMS Visiting Scientist

Mr. Utschig Thomas	Indian Inst. of Tech. Madras	India	Sep. '06–Oct. '06
Prof. Ruehl Eckart	Free Univ. of Berlin	Germany	Nov. '06
Dr. Mortier Michel	CNRS Ecole Natl. Superieure de Chem. Paris	France	Nov. '06
Mr. Pornputtpong Natapol	Chulalongkorn Univ.	Thailand	Nov. '06
Dr. Innis Vallerie Ann A.	Philippine Nuclear Res. Inst.	Philippines	Nov. '06
Ms. Chu Yiwen	Fudan Univ.	China	Nov. '06
Dr. Yang Wuli	Fudan Univ.	China	Nov. '06
Mr. Mao Weiyong	Fudan Univ.	China	Nov. '06
Mr. Chen Wei	Fudan Univ.	China	Nov. '06
Mr. Ji Minglei	Fudan Univ.	China	Nov. '06
Mr. Gao Jia	Fudan Univ.	China	Nov. '06
Ms. Shao Dandan	Fudan Univ.	China	Nov. '06
Mr. Bhuiyan Mohammad Tauhidul Islam	Kyungpook Natl. Univ.	Korea	Nov. '06
Ms. Lin Li-Chuan	Pohang Univ. of Sci. and Tech.	Korea	Nov. '06
Mr. Rashid Mohammad Harun Or	Kyungpook Natl. Univ.	Korea	Nov. '06
Mr. Choi Heechol	Kyungpook Natl. Univ.	Korea	Nov. '06
Mr. Khandelwal Manish	Pohang Univ. of Sci. and Tech.	Korea	Nov. '06

LIST OF VISITING FOREIGN SCHOLARS

Ms. Kumar Anupriya	Pohang Univ. of Sci. and Tech.	Korea	Nov. '06
Mr. Reigh Shang Yik	Seoul Natl. Univ.	Korea	Nov. '06
Mr. Kim Dong Young	Pohang Univ. of Sci. and Tech.	Korea	Nov. '06
Mr. Keum Changsoo	Pohang Univ. of Sci. and Tech.	Korea	Nov. '06
Mr. Min Seung Kyu	Pohang Univ. of Sci. and Tech.	Korea	Nov. '06
Mr. Kim Woo Youn	Pohang Univ. of Sci. and Tech.	Korea	Nov. '06
Ms. Park Mina	Pohang Univ. of Sci. and Tech.	Korea	Nov. '06
Ms. Choi Sunyoung	Korea Adv. Inst. of Sci. and Tech.	Korea	Nov. '06
Mr. Park Seong Byeong	Korea Adv. Inst. of Sci. and Tech.	Korea	Nov. '06
Mr. Cho Eunseo	Seoul Natl. Univ.	Korea	Nov. '06
Mr. Son Won-joon	Seoul Natl. Univ.	Korea	Nov. '06
Mr. Subramaniam Chandramouli	Indian Inst. of Tech. Madras	India	Nov. '06–Dec. '06
Mr. Evain Clement	Univ. of Sci. and Tech. of Lille	France	Nov. '06–Dec. '06
Dr. Szwaj Christophe	Univ. of Sci. and Tech. of Lille	France	Nov. '06–Dec. '06
Mr. Petre Cristian	Natl. Inst. for Laser, Plasma and Radiation Phys.	Romania	Dec. '06
Prof. Zhou Zhen	Inst. of New Energy Mater. Chem.	China	Jan. '07–Mar. '07
Prof. Segonds Patricia	Univ. Joseph Fourier	France	Feb. '07–Mar. '07
Prof. Boulanger Benoit	Univ. Joseph Fourier	France	Mar. '07
Dr. Thomas Richard	Stockholm Univ.	Sweden	Apr. '07–May '07
Mr. Zhaumechyk Vitali	Stockholm Univ.	Sweden	Apr. '07–May '07
Ms. Zhou Jing	Peking Univ.	China	Apr. '07–Jul. '07
Prof. Lu Jing	Peking Univ.	China	Apr. '07–May '07
Dr. Jiang Yuqiang	Inst. of Mol.Sci.	China	May '07
Ms. Vijay Dolly	Indian Inst. of Chem. Tech.	India	May '07–Jul. '07
Dr. Shailesh R Shah	MS Univ. of Baroda	India	May '07–Jun. '07
Dr. Kelly Kevin	Rice Univ.	U.S.A.	May '07
Prof. Aka Gerard	Univ. Pierre & Marie Curie	France	Jun. '07
Ms. Xu Ke	Univ. Pierre & Marie Curie	France	Jun. '07
Prof. Loiseau Pascal	Univ. Pierre & Marie Curie	France	Jun. '07
Prof. Toy Patrick H.	Univ. of Hong Kong	China	Jun. '07
Dr. Guo Jinghua	Lawrence Berkeley Natl. Lab.	U.S.A.	Jun. '07
Prof. Huang Wei	Nanjing Univ.	China	Jun. '07–Sep. '07
Dr. Guo JIng Dong	Jiangxi Sci. and Tech. Normal Univ.	China	Jun. '07
Prof. Boo Bong Hyun	Chungnam Natl. Univ.	Korea	Jul. '07
Dr. Chen Zhongfang	Univ. of Georgia	U.S.A.	Jul. '07
Prof. Lu Jing	Peking Univ.	China	Jul. '07
Prof. Zhao Xiang	Xi'an Jiaotong Univ.	China	Jul. '07–Aug. '07
Prof. Xian-He Bu	Nankai Univ.	China	Jul. '07–Aug. '07
Mr. Kim Tae-Rae	Seoul Natl. Univ.	Korea	Jul. '07–Jan. '08
Prof. Sutcliffe Brian Terence	Univ. Libre Bruxelles	Belgium	Aug. '07–Nov. '07
Prof. Kotora Martin	Charles Univ.	Czech	Aug. '07
Prof. Wang Changchung	Fudan Univ.	China	Aug. '07

(5) Visitor to IMS

Prof. Park Jaiwook	Pohang Univ. of Sci. and Tech.	Korea	Oct. '06
Prof. Wüthrich Kurt	Swiss Federal Inst. of Tech.	Swiss	Oct. '06
Prof. Giratd Bertrand	Univ. Paul Sabatier	France	Nov. '06
Prof. Hsu Yen-Chu	Inst. of Atomic and Mol. Sci.	Taiwan	Nov. '06–Dec. '06
Prof. Merer Anthony	Univ. of British Columbia	Canada	Nov. '06–Dec. '06
Prof. Hougen Jon T.	Univ. of Wisconsin	U.S.A.	Nov. '06–Dec. '06
Prof. Cramer Roger E.	Univ. of Hawaii	U.S.A.	Dec. '06
Dr. Saxena Avadh Behari	Los Alamos Natl. Lab.	U.S.A.	Dec. '06
Prof. Kincaid James R	Marquette Univ.	U.S.A.	Mar. '07
Prof. Zhang Bin	Inst. of Chem.	China	Mar. '07
Prof. Brooks James S.	Florida State Univ.	U.S.A.	Mar. '07
Prof. Ouahab Lahcene	UMR CNRS	France	Mar. '07
Dr. Xantheas Sotiris, S	Pacific Northwest Natl. Lab.	U.S.A.	Mar. '07

Prof. Kovalenko Andriy	Univ. of Alberta	Canada	Mar. '07
Prof. Prezhdo Oleg, V.	Univ. of Washington	Ukraine	Apr. '07–Apr. '07
Prof. Hayward Steven	Univ. of East Anglia	U.S.A.	Apr. '07–Apr. '07
Prof. Chandrajit Bajaj	Univ. of Texas at Austin	India	May '07
Prof. Day Peter	Royal Inst. of Great Britain	U.K.	Jul. '07
Prof. Castner Edward	State Univ. of New Jersey	U.S.A.	Aug. '07
Prof. Wright Peter	Scripps Res. Inst.	U.S.A.	Aug. '07–Aug. '08

Scientists who would like to visit IMS under programs (1) and (2) are invited to make contact with IMS staff in their relevant field.

Theoretical and Computational Molecular Science

- T. TSUCHIYA, H. KURIHARA, K. SATO, T. WAKAHARA, T. AKASAKA, T. SHIMIZU, N. KAMIGATA, N. MIZOROGI and S. NAGASE, "Supramolecular Complexes of La@C₈₂ with Unsaturated Thiocrown Ethers," *Chem. Commun.* 3585–3587 (2006).
- T. ADACHI, S. MATSUKAWA, M. NAKAMOTO, K. KAJIYAMA, S. KOJIMA, Y. YAMAMOTO, K. -Y. AKIBA, S. RE and S. NAGASE, "Experimental Determination of the $n_N \rightarrow \sigma^*_{P-O}$ Interaction Energy of O-Equatorial C-Apical Phosphanes Bearing a Primary Amino Group," *Inorg. Chem.* **45**, 7269–7277 (2006).
- Y. MAEDA, Y. SATO, M. KAKO, T. WAKAHARA, T. AKASAKA, J. LU, S. NAGASE, Y. KOBORI, T. HASEGAWA, K. MOTOMIYA, K. TOHJI, A. KASUYA, D. WANG, D. YU, Z. GAO, R. HAN and H. YE, "Preparation of Single-Walled Carbon Nanotubes—Organosilicon Hybrids and Their Enhanced Field Emission Properties," *Chem. Mater.* **18**, 4205–4208 (2006).
- Y. MAEDA, M. KANDA, M. HASHIMOTO, T. HASEGAWA, S. KIMURA, Y. LIAN, T. WAKAHARA, T. AKASAKA, S. KAZAOUL, N. MINAMI, T. OKAZAKI, Y. HAYAMIZU, K. HATA, J. LU and S. NAGASE, "Dispersion and Separation of Small-Diameter Single-Walled Carbon Nanotubes," *J. Am. Chem. Soc.* **128**, 12239–12242 (2006).
- T. SASAMORI, E. MIEDA, N. NAGAHORA, K. SATO, D. SHIOMI, T. TAKUI, Y. HOSOI, Y. FURUKAWA, N. TAKAGI, S. NAGASE and N. TOKITOH, "One-Electron Reduction of Kinetically Stabilized Dipnictenes: Synthesis of Dipnictene Anion Radicals," *J. Am. Chem. Soc.* **128**, 12582–12588 (2006).
- N. MIZOROGI and S. NAGASE, "Do Eu@C₈₂ and Gd@C₈₂ Have an Anomalous Endohedral Structure?" *Chem. Phys. Lett.* **431**, 110–112 (2006).
- T. WAKAHARA, H. NIKAWA, T. KIKUCHI, T. NAKAHODO, G. M. A. RAHMAN, T. TSUCHIYA, Y. MAEDA T. AKASAKA, K. YOZA, E. HORN, K. YAMAMOTO, N. MIZOROGI, Z. SLANINA and S. NAGASE, "La@C₇₂ Having a Non-IPR Carbon Cage," *J. Am. Chem. Soc.* **128**, 14228–14229 (2006).
- T. TSUCHIYA, K. SATO, H. KURIHARA, T. WAKAHARA, Y. MAEDA, T. AKASAKA, K. OHKUBO, S. FUKUZUMI, T. KATO and S. NAGASE, "Spin-Site Exchange System Constructed from Endohedral Metallofullerenes and Organic Donors," *J. Am. Chem. Soc.* **128**, 14418–14419 (2006).
- T. TSUCHIYA, T. WAKAHARA, Y. LIAN, Y. MAEDA, T. AKASAKA, T. KATO, N. MIZOROGI and S. NAGASE, "Selective Extraction and Purification of Endohedral Metallofullerene from Carbon Soot," *J. Phys. Chem. B* **110**, 22517–22520 (2006).
- Z. SLANINA, F. UHLIK and S. NAGASE, "Computed Structures of Two Known Yb@C₇₄ Isomers," *J. Phys. Chem. A* **110**, 12860–12863 (2006).
- Z. SLANINA and S. NAGASE, "A Computational Characterization of N₂@C₆₀," *Mol. Phys.* **104**, 3167–3171 (2006).
- W. SONG, J. LU, Z. GAO, M. NI, L. GUAN, Z. SHI, Z. GU, S. NAGASE, D. YU, H. YE and X. ZHANG, "Structural and Electronic Properties of One Dimensional K_xC₆₀ Crystal Encapsulated in Carbon Nanotube," *Int. J. Mod. Phys. B* **21**, 1705–1714 (2007).
- Z. SLANINA, S. -L. LEE, F. UHLIK, L. ADAMOWICZ and S. NAGASE, "Computing Relative Stabilities of Metallofullerenes by Gibbs Energy Treatments," *Theor. Chem. Acc.* **117**, 315–322 (2007).
- N. TAKAGI and S. NAGASE, "Effects of Bulky Substituent Groups on the Si–Si Triple Bonding in RSi≡SiR and the Short Ga–Ga Distance in Na₂[RGaGaR]. A Theoretical Study," *J. Organomet. Chem.* (a special issue) **692**, 217–224 (2007).
- Y. -K. CHOE, S. NAGASE and K. NISHIMOTO, "Theoretical Study of the Electronic Spectra of Oxidized and Reduced States of Lumiflavin and Its Derivative," *J. Comput. Chem.* **28**, 727–739 (2007).
- N. TAKAGI and S. NAGASE, "Tin Analogues of Alkynes. Multiply Bonded Structures vs Singly Bonded Structures," *Organometallics* **26**, 469–471 (2007).
- B. WANG, S. NAGASE, J. ZHAO and G. WANG, "Structural Growth Sequences and Electronic Properties of Zinc Oxide Clusters (ZnO)_n (n = 2–18)," *J. Phys. Chem. C* **111**, 4956–4963 (2007).
- D. G. FEDOROV, K. ISHIMURA, T. ISHIDA, K. KITaura, P. PULAY and S. NAGASE, "Accuracy of the Three-Body Fragment Molecular Orbital Method Applied to Møller-Plesset Perturbation Theory," *J. Comput. Chem.* **28**, 1467–1484 (2007).
- Z. SLANINA, F. UHLIK and S. NAGASE, "Computational Evaluation of the Relative Production Yields in the X@C₇₄ Series (X = Ca, Sr, and Ba)," *Chem. Phys. Lett.* **440**, 259–262 (2007).
- F. UHLIK, Z. SLANINA and S. NAGASE, "Mg@C₇₄ Isomers: Calculated Relative Concentrations and Comparison with Ca@C₇₄," *Phys. Status Solidi A* **204**, 1905–1910 (2007).
- Z. SLANINA, F. UHLIK, S. LEE, L. ADAMOWICZ and S. NAGASE, "Calculations on Endohedral C-74 Complexes," *J. Nanosci. Nanotechnol.* **7**, 1339–1345 (2007).
- Z. SLANINA, F. UHLIK, X. ZHAO, L. ADAMOWICZ and S. NAGASE, "Relative Stabilities of C-74 Isomers," *Fullerenes, Nanotubes, Carbon Nanostruct.* **15**, 195–205 (2007).
- R. KINJO, M. ICHINOHE, A. SEKIGUCHI, N. TAKAGI, M. SUMIMOTO and S. NAGASE, "Reactivity of a Disilyne RSi≡SiR (R = SiⁱPr[CH(SiMe₃)₂]₂) toward π -Bonds: Stereospecific Addition and a New Route to an Isolable 1,2-Disilabenzene," *J. Am. Chem. Soc.* **129**, 7766–7767 (2007).

- K. ISHIMURA, P. PULAY and S. NAGASE**, "New Parallel Algorithm of MP2 Energy Gradient Calculations," *J. Comput. Chem.* **28**, 2034–2042 (2007).
- T. WAKAHARA, M. YAMADA, S. TAKAHASHI, T. NAKAHODO, T. TSUCHIYA, Y. MAEDA, T. AKASAKA, M. KAKO, K. YOZA, E. HORN, N. MIZOROGI and S. NAGASE**, "Two-Dimensional Hopping Motion of Encapsulated La Atoms in Silylated $\text{La}_2@C_{80}$," *Chem. Commun.* 2680–2682 (2007).
- Y. IIDUKA, T. WAKAHARA, K. NAKAJIMA, T. NAKAHODO, T. TSUCHIYA, Y. MAEDA, T. AKASAKA, K. YOZA, M. T. H. LIU, N. MIZOROGI and S. NAGASE**, "Experimental and Theoretical Studies of the Scandium Carbide Endohedral Metallofullerene $\text{Sc}_2\text{C}_2@C_{82}$ and Its Carbene Derivative," *Angew. Chem., Int. Ed.* **46**, 5562–5564 (2007).
- N. TAKAGI and S. NAGASE**, "Do Lead Analogues of Alkynes Take a Multiply Bonded Structure?" *Organometallics* **26**, 3627–3629 (2007).
- Z. SLANINA, F. UHLIK, S. -L. LEE, L. ADAMOWICZ and S. NAGASE**, "Computed Structure and Relative Stabilities of $\text{Be}@C_{74}$," *Int. J. Quantum Chem.* **107**, 2494–2498 (2007).
- T. IWASA and K. NOBUSADA**, "Theoretical Investigation of Optimized Structures of Thiolated Gold Cluster $[\text{Au}_{25}(\text{SCH}_3)_{18}]^+$," *J. Phys. Chem. C* **111**, 45–49 (2007).
- K. NOBUSADA and K. YABANA**, "Photoinduced Electric Currents in Ring-Shaped Molecules by Circularly Polarized Laser Pulses," *Phys. Rev. A* **75**, 032518 (7 pages) (2007).
- Y. KUBOTA and K. NOBUSADA**, "Efficient Numerical Method for Calculating Exciton States in Quantum Boxes," *Phys. Lett. A* **369**, 128–131 (2007).
- T. IWASA and K. NOBUSADA**, "Gold-Thiolate Core-in-Cage Cluster $\text{Au}_{25}(\text{SCH}_3)_{18}$ Shows Localized Spins in Charged States," *Chem. Phys. Lett.* **441**, 268–272 (2007).
- K. IKEDA, Y. KOBAYASHI, Y. NEGISHI, M. SETO, T. IWASA, K. NOBUSADA, T. TSUKUDA and N. KOJIMA**, "Thiolate-Induced Structural Reconstruction of Gold Clusters Probed by ^{197}Au Mössbauer Spectroscopy," *J. Am. Chem. Soc.* **129**, 7230–7231 (2007).
- Y. KUBOTA and K. NOBUSADA**, "An Efficient Numerical Method for Exciton States in Quantum Boxes," *Comput. Phys. Commun.* **177**, 43 (2007).
- K. SHIRATORI and K. NOBUSADA**, "Electronic Structure Calculations at Constant Chemical Potential toward the Application to Electrochemistry," *Comput. Phys. Commun.* **177**, 47 (2007).
- K. NOBUSADA and K. YABANA**, "Electric Currents in Ring-Shaped Molecules Induced by Circularly Polarized Laser Pulses," *Comput. Phys. Commun.* **177**, 54 (2007).
- N. YOSHIDA, S. PHONGPHANPHANEE, Y. MARUYAMA, T. IMAI and F. HIRATA**, "Selective Ion-Binding by Protein Probed with the 3D-RISM Theory," *J. Am. Chem. Soc.* **128**, 12042–12043 (2006).
- A. E. KOBRYN and F. HIRATA**, "Statistical-Mechanical Theory of Ultrasonic Absorption in Molecular Liquids," *J. Chem. Phys.* **126**, 044504 (2007).
- T. IMAI, R. HIRAOKA, A. KOVALENKO and F. HIRATA**, "Locating Missing Water Molecules in Protein Cavities by the Three-Dimensional Reference Interaction Site Model Theory of Molecular Solvation," *Proteins: Struct., Funct., Bioinf.* **66**, 804–813 (2007).
- Y. IKUTA, Y. MARUYAMA, M. MATSUGAMI and F. HIRATA**, "Probing Cations Recognized by a Crown Ether with the 3D-RISM Theory," *Chem. Phys. Lett.* **433**, 403–408 (2007).
- A. TANIMURA, A. KOVALENKO and F. HIRATA**, "Structure of Electrolyte Solutions Sorbed in Carbon Nanospaces, Studied by the Replica RISM Theory," *Langmuir* **23**, 1507–1517 (2007).
- T. YAMAZAKI, T. IMAI, F. HIRATA and A. KOVALENKO**, "Theoretical Study of the Cosolvent Effect on the Partial Molar Volume Change of Staphylococcal Nuclease Associated with Pressure Denaturation," *J. Phys. Chem. B* **111**, 1206–1212 (2007).
- N. YOSHIDA, S. PHONPHANPHANEE and F. HIRATA**, "Selective Ion-Binding by Protein Probed with the Statistical Mechanical Integral Equation Theory," *J. Phys. Chem. B* **111**, 4588–4595 (2007).
- Y. IKUTA, Y. MARUYAMA, F. HIRATA and S. TOMODA**, "Theoretical Study of Solvent Effect on Diastereo Selectivity in Protonation of Methyl 3-Fluorobutanoate Anion by Ethanol: Application of the 3D-RISM Theory," *THEOCHEM* **811**, 183–190 (2007).
- T. IMAI, S. OHYAMA, A. KOVALENKO and F. HIRATA**, "Theoretical Study of the Partial Molar Volume Change Associated with Pressure-Induced Structural Transition of Ubiquitin," *Protein Sci.* **16**, 1927–1933 (2007).
- T. IMAI, H. HARANO, M. KINOSHITA and A. KOVALENKO**, "A Theoretical Analysis on Changes in Thermodynamic Quantities upon Protein Folding: Essential Role of Hydration," *J. Chem. Phys.* **126**, 225102–225102 (2007).
- K. YONEMITSU**, "Interchain-Coupling Effects on Photoinduced Neutral-Ionic Transition Dynamics in Mixed-Stack Charge-Transfer Complexes," *J. Low Temp. Phys.* **142**, 503–506 (2006).
- N. MAESHIMA and K. YONEMITSU**, "Dynamics of Photoexcited States in One-Dimensional Dimerized Mott Insulators," *Phys. Rev. B* **74**, 155105 (11 pages) (2006).

LIST OF PUBLICATIONS

- Y. TANAKA and K. YONEMITSU**, “Effects of Electron-Lattice Coupling on Charge Order in θ -(ET)₂X,” *J. Phys. Soc. Jpn.* **76**, 053708 (5 pages) (2007).
- H. INOUE and K. YONEMITSU**, “Relaxation Process in the Photoinduced Neutral-Ionic Paraelectric-Ferroelectric Phase Transition in Tetrathiafulvalene-*p*-chloranil,” *Phys. Rev. B* **75**, 235125 (13 pages) (2007).
- S. MIYASHITA and K. YONEMITSU**, “Charge Ordering in θ -(BEDT-TTF)₂RbZn(SCN)₄: Cooperative Effects of Electron Correlations and Lattice Distortions,” *Phys. Rev. B* **75**, 245112 (6 pages) (2007).
- N. MAESHIMA and K. YONEMITSU**, “Charge-Transfer Excitations in One-Dimensional Dimerized Mott Insulators,” *J. Phys. Soc. Jpn.* **76**, 074713 (5 pages) (2007).
- K. YONEMITSU and N. MAESHIMA**, “Photoinduced Melting of Charge Order in a Quarter-Filled Electron System Coupled with Different Types of Phonons,” *Phys. Rev. B* **76**, 075105 (6 pages) (2007).
- Y. OKAMOTO, T. MIKAMI, N. YOSHII and S. OKAZAKI**, “A Molecular Analysis of the Vibrational Energy Relaxation Mechanism of the CN⁻ Ion in Water Based upon Path Integral Influence Functional Theory Combined with a Dipole Expansion of the Solute-Solvent Interaction,” *J. Mol. Liq.* **134**, 34–39 (2007).
- N. YOSHII and S. OKAZAKI**, “Free Energy of Water Permeation into Hydrophobic Core of Sodium Dodecyl Sulfate Micelle by Molecular Dynamics Calculation,” *J. Chem. Phys.* **126**, 096101 (3 pages) (2007).
- S. MIURA**, “Rotational Fluctuation of Molecules in Quantum Clusters. I. Path Integral Hybrid Monte Carlo Algorithm,” *J. Chem. Phys.* **126**, 114308 (10 pages) (2007).
- S. MIURA**, “Rotational Fluctuation of Molecules in Quantum Clusters. II. Molecular Rotation and Superfluidity in OCS-Doped Helium-4 Clusters,” *J. Chem. Phys.* **126**, 114309 (7 pages) (2007).
- S. SAITO and I. OHMINE**, “Fifth-Order Two-Dimensional Raman Spectroscopy of Liquid Water, Crystalline Ice Ih and Amorphous Ices: Sensitivity to Anharmonic Dynamics and Local Hydrogen Bond Network Structure,” *J. Chem. Phys.* **125**, 084506 (12 pages) (2006).
- T. SUMIKAMA, S. SAITO and I. OHMINE**, “Mechanism of Ion Permeation in Model Channel; Free Energy Surface and Dynamics of K⁺ Ion Transport in Anion-Doped Carbon Nanotube,” *J. Phys. Chem. B* **110**, 20671–20677 (2006).
- M. KAMIYA, S. SAITO and I. OHMINE**, “Proton Transfer and Associated Molecular Rearrangements in Photocycle of Photoactive Yellow Protein; Role of Water Molecular Migration on Proton Transfer Reaction,” *J. Phys. Chem. B* **111**, 2948–2956 (2007).
- T. ISHIYAMA and A. MORITA**, “Intermolecular Correlation Effect in Sum Frequency Generation Spectroscopy of Electrolyte Aqueous Solution,” *Chem. Phys. Lett.* **431**, 78–82 (2006).
- T. ISHIYAMA and A. MORITA**, “Molecular Dynamics Study of Gas-Liquid Aqueous Sodium Halide Interfaces I. Flexible and Polarizable Molecular Modeling and Interfacial Properties,” *J. Phys. Chem. C* **111**, 721–737 (2007).
- T. ISHIYAMA and A. MORITA**, “Molecular Dynamics Study of Gas-Liquid Aqueous Sodium Halide Interfaces II. Analysis of Vibrational Sum Frequency Generation Spectra,” *J. Phys. Chem. C* **111**, 738–748 (2007).

Photo-Molecular Science

- K. IMURA, H. OKAMOTO, M. K. HOSSAIN and M. KITAJIMA**, “Visualization of Localized Intense Optical Fields in Single Gold-Nanoparticle Assemblies and Ultrasensitive Raman Active Sites,” *Nano Lett.* **6**, 2173–2176 (2006).
- H. HASEGAWA and Y. OHSHIMA**, “Decoding the State Distribution in a Nonadiabatic Rotational Excitation by a Nonresonant Intense Laser Field,” *Phys. Rev. A* **74**, 061401(R) (4 pages) (2006).
- H. KATSUKI, K. HOSAKA, H. CHIBA and K. OHMORI**, “Read and Write Amplitude and Phase Information by Using High-Precision Molecular Wave-Packet Interferometry,” *Phys. Rev. A* **76**, 013403 (13 pages) (2007).
- I. NAKAI, H. KONDOH, T. SHIMADA, R. YOKOTA, T. KATAYAMA, T. OHTA and N. KOSUGI**, “Geometric and Electronic Structures of NO Dimer Layers on Rh(111) Studied with Near Edge X-Ray Absorption Fine Structure Spectroscopy: Experiment and Theory,” *J. Chem. Phys.* **127**, 024701 (6 pages) (2007).
- V. KIMBERG and N. KOSUGI**, “Calculation of K-Edge Circular Dichroism of Amino Acids: Comparison of Random Phase Approximation with Other Methods,” *J. Chem. Phys.* **126**, 245101 (10 pages) (2007).
- Y. HIKOSAKA, T. KANEYASU, E. SHIGEMASA, Y. TAMENORI and N. KOSUGI**, “Autoionization Dynamics of Core-Valence Doubly Excited States in N₂,” *Phys. Rev. A* **75**, 042708 (5 pages) (2007).
- T. GEJO, M. MACHIDA, K. HONMA, E. SHIGEMASA, E. NAKAMURA, N. KOSUGI and Y. TAMENORI**, “The Vibrational Structure of a Conjugate Shake-Up Satellite Band in the C 1s Core Level Photoemission of CO,” *J. Electron. Spectrosc.* **156**, 274–278 (2007).

- M. FURUKAWA, H. S. KATO, M. TANIGUCHI, T. KAWAI, T. HATSUI, N. KOSUGI, T. YOSHIDA, M. AIDA and M. KAWAI**, "Electronic States of the DNA Polynucleotides Poly(dG)-Poly(dC) in the Presence of Iodine," *Phys. Rev. B* **75**, 045119 (9 pages) (2007).
- B. P. KAFLE, H. KATAYANAGI and K. MITSUKE**, "Photofragment Imaging Apparatus for Measuring Momentum Distributions in Dissociative Photoionization of Fullerenes," *AIP Conf. Proc.* **879**, 1809–1812 (2007).
- K. KANDA, K. MITSUKE, K. SUZUKI and T. IBUKI**, "Photodissociation of Butyl Cyanides and Butyl Isocyanides in the Vacuum UV Region," *AIP Conf. Proc.* **879**, 1817–1820 (2007).
- K. MITSUKE, H. KATAYANAGI, C. HUANG, B. P. KAFLE, MD. S. I. PRODHAN, H. YAGI and Y. KUBOZONO**, "Relative Partial Cross Sections for Single, Double and Triple Photoionization of C₆₀ and C₇₀," *J. Phys. Chem. A* **111**, 8336–8343 (2007).
- T. WANG, S. LI, B. YANG, C. HUANG and Y. LI**, "Thermal Decomposition of Glycidyl Azide Polymer Studied by Synchrotron Photoionization Mass Spectrometry," *J. Phys. Chem. B* **111**, 2449–2455 (2007).
- K. NISHIKAWA, S. WANG, H. KATAYANAGI, S. HAYASHI, H. HAMAGUCHI, Y. KOGA and K. TOZAKI**, "Melting and Freezing Behaviors of Prototype Ionic Liquids, 1-Butyl-3-Methylimidazolium Bromide and Its Chloride, Studied by Using a Nano-Watt Differential Scanning Calorimeter," *J. Phys. Chem. B* **111**, 4894–4900 (2007).
- A. HISHIKAWA, E. J. TAKAHASHI and A. MATSUDA**, "Electronic and Nuclear Responses of Fixed-in-Space H₂S to Ultrashort Intense Laser Fields," *Phys. Rev. Lett.* **96**, 243002 (4 pages) (2006).
- M. LABAT, M. E. COUPRIE, M. HOSAKA, A. MOCHIHASHI, M. KATOH and Y. TAKASHIMA**, "Longitudinal and Transverse Heating of a Relativistic Electron Bunch Induced by a Storage Ring Free Electron Laser," *Phys. Rev. STAB* **9**, 100701 (2006).
- A. MOCHIHASHI, M. KATOH, M. HOSAKA, Y. TAKASHIMA and Y. HORI**, "Touschek Lifetime Measurement with a Spurious Bunch in Single Bunch Operation in the UVSOR-II Electron Storage Ring," *Nucl. Instrum. Methods Phys. Res., Sect. A* **572**, 1033–1041 (2007).
- M. LABAT, M. HOSAKA, A. MOCHIHASHI, M. SHIMADA, M. KATOH, G. LAMBERT, T. HARA, Y. TAKASHIMA and M. E. COUPRIE**, "Coherent Harmonic Generation at UVSOR-II Storage Ring," *Eur. Phys. J. D* **44**, 187–200, e2007-00177-6 (2007).
- Y. SAKURAI, S. KIMURA and K. SEKI**, "Infrared Reflection-Absorption Spectroscopy of Alq₃ Thin Film on Silver Surface Using Synchrotron Radiation," *Appl. Phys. Lett.* **91**, 061922 (3 pages) (2007).
- S. KIMURA, N. KIMURA and H. AOKI**, "Low-Energy Electrodynamics of Heavy Quasiparticles in ZrZn₂," *J. Phys. Soc. Jpn.* **76**, 084710 (5 pages) (2007).
- J. ONOE, T. ITO, S. KIMURA, K. OHNO, Y. NOGUCHI and S. UEDA**, "The Valence Electronic Structure of a Peanut-Shaped C₆₀ Polymer: *In situ* High-Resolution Photoelectron Spectroscopic and Density-Functional Studies," *Phys. Rev. B* **75**, 233410 (4 pages) (2007).
- S. KIMURA, H. J. IM, T. MIZUNO, S. NARAZU, E. MATSUOKA and T. TAKABATAKE**, "Infrared Study on the Electronic Structure of the Alkaline-Earth-Filled Skutterudites AM₄Sb₁₂ (A = Sr, Ba; M = Fe, Ru, Os)," *Phys. Rev. B* **75**, 245106 (6 pages) (2007).
- T. TAKEUCHI, D. FUKAMAKI, H. MIYAZAKI, K. SODA, M. HASEGAWA, H. SATO, U. MIZUTANI, T. ITO and S. KIMURA**, "Electronic Structure and Stability of the Pd-Ni-P Bulk Metallic Glass," *Mater. Trans.* **48**, 1292–1298 (2007).
- J. ONOE, Y. OCHIAI, T. ITO, S. KIMURA, S. UEDA, Y. NOGUCHI and K. OHNO**, "Electronic and Electron-Transport Properties of Peanut-Shaped C₆₀ Polymers," *J. Phys.: Conf. Series* **61**, 899–903 (2007).
- J. ONOE, T. ITO, S. KIMURA and K. OHNO**, "*In situ* High-Resolution Valence Photoelectron Spectra of a Peanut-Shaped C₆₀ Polymer," *Eur. Phys. J. D* **43**, 141–142 (2007).
- K. MATSUBAYASHI, K. IMURA, H. S. SUZUKI, T. MIZUNO, S. KIMURA, T. NISHIOKA, K. KODAMA and N. K. SATO**, "Effect of Single Crystal Composition on Electrical, Optical, Magnetic and Thermodynamic Properties of SmS," *J. Phys. Soc. Jpn.* **76**, 064601 (2007).
- I. OUCHI, I. NAKAI, M. ONO and S. KIMURA**, "Features of Fluorescence Spectra of Polyethylene 2,6-Naphthalate Films," *J. Appl. Polym. Sci.* **105**, 114–121 (2007).
- S. KIMURA and T. MIZUNO**, "Application of Terahertz Synchrotron Radiation at UVSOR-II," *AIP Conf. Proc.* **902**, 67–70 (2007).
- H. J. IM, T. ITO, H. D. KIM, S. KIMURA, J. B. HONG and Y. S. KWON**, "Electronic Structure of CeNiGe_{2-x}Si_x Studied by Resonant Photoemission," *J. Magn. Magn. Mater.* **310**, 411–413 (2007).
- Y. S. KWON, K. E. LEE, M. A. JUNG, E. Y. SONG, H. J. OH, H. J. IM and S. KIMURA**, "Hybridization Gap Collapse at a Quantum Critical Point of CeNi_{1-x}Co_xGe₂," *J. Magn. Magn. Mater.* **310**, 310–312 (2007).
- T. ITO, H. J. IM, S. KIMURA and Y. S. KWON**, "Three-Dimensional Fermi Surface of CeTe₂ Studied by Angle-Resolved Photoemission," *J. Magn. Magn. Mater.* **310**, 431–433 (2007).

LIST OF PUBLICATIONS

- S. KIMURA, T. NISHI, T. TAKAHASHI, T. MIZUNO, K. MIYAGAWA, H. TANIGUCHI, A. KAWAMOTO and K. KANODA**, “Pressure Dependence of Phase Separation in Deuterated κ -(ET)₂Cu[N(CN)₂]Br at the Mott Boundary,” *J. Magn. Magn. Mater.* **310**, 1102–1104 (2007).
- T. NISHI, S. KIMURA, T. TAKAHASHI, H. J. IM, Y. S. KWON, T. ITO, K. MIYAGAWA, H. TANIGUCHI, A. KAWAMOTO and K. KANODA**, “Magnetic-Field-Induced Superconductor–Insulator–Metal Transition in an Organic Conductor: An Infrared Magneto-Optical Imaging Spectroscopic Study,” *Phys. Rev. B* **75**, 014525 (5 pages) (2007).
- T. ITO, S. KIMURA, H. J. IM, E. NAKAMURA, M. SAKAI, T. HORIGOME, K. SODA and T. TAKEUCHI**, “BL5U at UVSOR-II for Three-Dimensional Angle-Resolved Photoemission Spectroscopy,” *AIP Conf. Proc.* **879**, 587–590 (2007).
- S. KIMURA, T. ITO, E. NAKAMURA, M. HOSAKA and M. KATOH**, “Design of a High-Resolution and High-Flux Beamline for VUV Angle-Resolved Photoemission at UVSOR-II,” *AIP Conf. Proc.* **879**, 527–530 (2007).
- S. KIMURA, Y. SAKURAI, E. NAKAMURA and T. MIZUNO**, “Terahertz Microspectroscopy and Infrared Reflection-Absorption Spectroscopy Apparatuses at UVSOR-II,” *AIP Conf. Proc.* **879**, 595–598 (2007).
- S. KIMURA, J. SICHELSCHEMIDT, J. FERSTL, C. KRELLNER, C. GEIBEL and F. STEGLICH**, “Optical Observation of Non-Fermi-Liquid Behavior in the Heavy Fermion State of YbRh₂Si₂,” *Phys. Rev. B* **74**, 132408 (4 pages) (2006).
- S. KIMURA, E. NAKAMURA, T. NISHI, Y. SAKURAI, K. HAYASHI, J. YAMAZAKI and M. KATOH**, “Infrared and Terahertz Spectromicroscopy Beam Line BL6B(IR) at UVSOR-II,” *Infrared Phys. Tech.* **49**, 147–151 (2006).
- Y. HIKOSAKA, T. KANEYASU, E. SHIGEMASA, P. LABLANQUIE, F. PENENT and K. ITO**, “Multielectron Coincidence Spectroscopy for Core-Valence Doubly Ionized States of CO,” *J. Chem. Phys.* **127**, 044305 (4 pages) (2007).
- T. KANEYASU, Y. HIKOSAKA, E. SHIGEMASA, F. PENENT, P. LABLANQUIE, T. AOTO and K. ITO**, “State-Selective Cross Sections of Multiple Photoionization in Ne,” *Phys. Rev. A* **76**, 012717 (7 pages) (2007).
- Y. HIKOSAKA, P. LABLANQUIE, F. PENENT, T. KANEYASU, E. SHIGEMASA, J. H. D. ELAND, T. AOTO and K. ITO**, “Double Photoionization into Double Core-Hole States in Xe,” *Phys. Rev. Lett.* **98**, 183002 (4 pages) (2007).
- Y. HIKOSAKA, T. GEJO, T. TAMURA, K. HONMA, Y. TAMENORI and E. SHIGEMASA**, “Core-Valence Multiply Excited States in N₂ Probed by Detecting Metastable Fragments,” *J. Phys. B* **40**, 2091–2097 (2007).
- Y. HIKOSAKA, T. KANEYASU, E. SHIGEMASA, Y. TAMENORI and N. KOSUGI**, “Autoionization Dynamics of Core-Valence Doubly Excited States in N₂,” *Phys. Rev. A* **75**, 042708 (5 pages) (2007).
- T. KANEYASU, Y. HIKOSAKA and E. SHIGEMASA**, “Electron–Ion Coincidence Spectrometer for Studies on Decay Dynamics of Core-Excited Molecules,” *J. Electron Spectrosc. Relat. Phenom.* **156-158**, 279–283 (2007).
- Y. HIKOSAKA, T. KANEYASU, Y. TAMENORI and E. SHIGEMASA**, “Negative Ion Formation Following Inner-Shell Photoexcitation in CO₂ Studied by Velocity Imaging Spectroscopy,” *J. Electron Spectrosc. Relat. Phenom.* **156-158**, 284–288 (2007).
- T. KANEYASU, Y. HIKOSAKA and E. SHIGEMASA**, “Development of Auger-Electron–Ion Coincidence Spectrometer on Decay Dynamics of Core-Excited Molecules,” *AIP Conf. Proc.* **879**, 1793–1796 (2007).
- E. SHIGEMASA, T. KANEYASU, Y. TAMENORI and Y. HIKOSAKA**, “Photoelectron Recapture through Post-Collision Interaction in N₂,” *J. Electron Spectrosc. Relat. Phenom.* **156-158**, 289–293 (2007).
- T. AOTO, K. ITO, Y. HIKOSAKA, E. SHIGEMASA, F. PENENT and P. LABLANQUIE**, “Properties of Resonant Interatomic Coulombic Decay in Ne Dimers,” *Phys. Rev. Lett.* **97**, 243401 (4 pages) (2006).
- Y. HIKOSAKA, T. KANEYASU and E. SHIGEMASA**, “Ion Pair Formation in the Vacuum Ultraviolet Region of NO Studied by Negative Ion Imaging Spectroscopy,” *J. Electron Spectrosc. Relat. Phenom.* **154**, 43–47 (2006).
- T. KANEYASU, T. AOTO, Y. HIKOSAKA, E. SHIGEMASA and K. ITO**, “Coster-Kronig Decay of the 2s Hole State in HCl Observed by Sub-Natural Linewidth Auger Electron Spectroscopy,” *J. Electron Spectrosc. Relat. Phenom.* **153**, 88–91 (2006).
- Y. SATO and T. TAIRA**, “The Studies of Thermal Conductivity in GdVO₄, YVO₄, and Y₃Al₅O₁₂ Measured by Quasi-One-Dimensional Flash Method,” *Opt. Express* **14**, 10528–10536 (2006).
- J. SAIKAWA, M. FUJII, H. ISHIZUKI and T. TAIRA**, “52 mJ Narrow-Bandwidth Degenerated Optical Parametric System with a Large-Aperture Periodically Poled MgO:LiNbO₃ Device,” *Opt. Lett.* **31**, 3149–3151 (2006).
- M. TSUNEKANE and T. TAIRA**, “High-Power Operation of Diode Edge-Pumped, Composite All-Ceramic Yb:Y₃Al₅O₁₂ Microchip Laser,” *Appl. Phys. Lett.* **90**, 121101 (3 pages) (2007).
- I. SHOJI, T. TAIRA and A. IKESUE**, “Thermally-Induced-Birefringence Effects of Highly Nd³⁺-Doped Y₃Al₅O₁₂ Ceramic Lasers,” *Opt. Mater.* **29**, 1271–1276 (2007).
- Y. SATO, J. SAIKAWA, T. TAIRA and A. IKESUE**, “Characteristics of Nd³⁺-Doped Y₃ScAl₄O₁₂ Ceramic Laser,” *Opt. Mater.* **29**, 1277–1282 (2007).
- J. SAIKAWA, Y. SATO, T. TAIRA and A. IKESUE**, “Femtosecond Yb³⁺-Doped Y₃(Sc_{0.5}Al_{0.5})₂O₁₂ Ceramic Laser,” *Opt. Mater.* **29**, 1283–1288 (2007).
- M. TSUNEKANE and T. TAIRA**, “Design and Performance of Compact Heatsink for High-Power Diode Edge-Pumped, Microchip Lasers,” *IEEE J. Sel. Top. Quantum Electron.* **13**, 619–625 (2007).
- Y. SATO, A. IKESUE and T. TAIRA**, “Tailored Spectral Designing of Layer-by-Layer Type Composite Nd:Y₃ScAl₄O₁₂/Nd:Y₃Al₅O₁₂ Ceramics,” *IEEE J. Sel. Top. Quantum Electron.* **13**, 838–843 (2007).

- M. FUYUKI, K. WATANABE and Y. MATSUMOTO**, "Coherent Surface Phonon Dynamics at K-Covered Pt(111) Surfaces Investigated by Time-Resolved Second Harmonic Generation," *Phys. Rev. B* **74**, 195412 (6 pages) (2006).
- Y. MATSUMOTO**, "Photochemistry and Photo-Induced Ultrafast Dynamics at Metal Surfaces," *Bull. Chem. Soc. Jpn.* **80**, 842–865 (2007).
- H. TSUNOYAMA, P. NICKUT, Y. NEGISHI, K. AL-SHAMERY, Y. MATSUMOTO and T. TSUKUDA**, "Formation of Alkanethiolate-Protected Gold Clusters with Unprecedented Core Sizes in the Thiolation of Polymer-Stabilized Gold Clusters," *J. Phys. Chem. C* **111**, 4153–4158 (2007).
- K. IMURA, H. OKAMOTO, M. K. HOSSAIN and M. KITAJIMA**, "Visualization of Localized Intense Optical Fields in Single Gold-Nanoparticle Assemblies and Ultrasensitive Raman Active Sites," *Nano Lett.* **6**, 2173–2176 (2006).
- M. HASEGAWA, T. TAKEUCHI, K. SODA, H. SATO and U. MIZUTANI**, "Electronic Structure and Phase Stability of Glassy Alloys," *Mater. Sci. Forum* **539-543**, 2048–2053 (2007).
- M. HASEGAWA, K. SODA, H. SATO, T. SUZUKI, T. TAKETOMI, T. TAKEUCHI, H. KATO and U. MIZUTANI**, "Stability and Electronic Structure of Zr-Based Ternary Metallic Glasses and Relevant Compounds," *J. Alloys Compd.* **434-435**, 149–151 (2007).
- H. MIYAZAKI, K. SODA, M. KATO, S. YAGI, T. TAKEUCHI and Y. NISHINO**, "Soft X-Ray Photoemission Study of the Heusler-Type $\text{Fe}_2\text{VAl}_{1-z}\text{Ge}_z$ Alloys," *J. Electron Spectrosc. Relat. Phenom.* **156-158**, 347–350 (2007).
- T. TAKEUCHI, D. FUKAMAKI, H. MIYAZAKI, K. SODA, M. HASEGAWA, H. SATO, U. MIZUTANI, T. ITO and S. KIMURA**, "Electronic Structure and Stability of the Pd-Ni-P Bulk Metallic Glass," *Mater. Trans.* **48**, 1292–1298 (2007).
- K. SODA, S. OTA, T. SUZUKI, H. MIYAZAKI, M. INUKAI, M. KATO, S. YAGI, T. TAKEUCHI, M. HASEGAWA, H. SATO and U. MIZUTANI**, "Electronic Structure of Pd- and Zr-Based Bulk Metallic Glasses Studied by Use of Hard X-Ray Photoelectron Spectroscopy," *AIP Conf. Proc.* **879**, 1821–1824 (2007).

Materials Molecular Science

- J. NISHIJO, C. OKABE, O. OISHI and N. NISHI**, "Synthesis, Structures and Magnetic Properties of Carbon-Encapsulated Nanoparticles via Thermal Decomposition of Metal Acetylide," *Carbon* **44**, 2943–2949 (2006).
- K. JUDAI, J. NISHIJO and N. NISHI**, "Self-Assembly of Copper Acetylide Molecules into Extremely Thin Nanowires and Nanocables," *Adv. Mater.* **18**, 2842–2846 (2006).
- T. IINO, K. OHASHI, Y. MUNE, Y. INOKUCHI, K. JUDAI, N. NISHI and H. SEKIYA**, "Infrared Photodissociation Spectra and Solvation Structures of $\text{Cu}^+(\text{H}_2\text{O})_n$ ($n = 1-4$)," *Chem. Phys. Lett.* **427**, 24–28 (2006).
- Y. MUNE, K. OHASHI, T. IINO, Y. INOKUCHI, K. JUDAI, N. NISHI and H. SEKIYA**, "Infrared Photodissociation Spectroscopy of $[\text{Al}(\text{NH}_3)_n]^+$ ($n = 1-5$): Solvation Structures and Insertion Reactions of Al^+ into NH_3 ," *Chem. Phys. Lett.* **419**, 201–206 (2006).
- T. IINO, K. OHASHI, K. INOUE, K. JUDAI, N. NISHI and H. SEKIYA**, "Coordination and Solvation of Noble Metal Ions: Infrared Spectroscopy of $\text{Ag}^+(\text{H}_2\text{O})_n$," *Eur. Phys. J. D* **43**, 37–40 (2007).
- N. NISHI, J. NISHIJO, K. JUDAI, C. OKABE and O. OISHI**, "Photo-Induced Evolution of Copper Sheets from Cluster Molecules and Its Application to Photolithographic Copper Patterning," *Eur. Phys. J. D* **43**, 287–290 (2007).
- A. FURUYA, M. TSURUTA, F. MISAIZU, K. OHNO, Y. INOKUCHI, K. JUDAI and N. NISHI**, "Infrared Photodissociation Spectroscopy of $\text{Al}^+(\text{CH}_3\text{OH})_n$ ($n = 1-4$)," *J. Phys. Chem. A* **111**, 5995–6002 (2007).
- K. INOUE, K. OHASHI, T. IINO, K. JUDAI, N. NISHI and H. SEKIYA**, "Coordination and Solvation of Copper Ion: Infrared Photodissociation Spectroscopy of $\text{Cu}^+(\text{NH}_3)_n$ ($n = 3-8$)," *Phys. Chem. Chem. Phys.* **9**, 4793–4802 (2007).
- Y. NEGISHI, H. TSUNOYAMA, M. SUZUKI, N. KAWAMURA, M. M. MATSUSHITA, K. MARUYAMA, T. SUGAWARA, T. YOKOYAMA and T. TSUKUDA**, "X-Ray Magnetic Circular Dichroism of Size-Selected, Thiolated Gold Clusters," *J. Am. Chem. Soc.* **128**, 12034–12035 (2006).
- X. -D. MA, T. NAKAGAWA and T. YOKOYAMA**, "Effect of Surface Chemisorption on the Spin Reorientation Transition in Magnetic Ultrathin Fe Film on Ag(001)," *Surf. Sci.* **600**, 4605–4612 (2006).
- T. NAKAGAWA, H. WATANABE and T. YOKOYAMA**, "Adatom-Induced Spin Reorientation Transitions and Spin Canting in Co Films on a Stepped Cu(001) Surface," *Phys. Rev. B* **74**, 134422 (6 pages) (2006).
- J. MIYAWAKI, D. MATSUMURA, A. NOJIMA, T. YOKOYAMA and T. OHTA**, "Structural Study of Co/Pd(111) and Co/Co/Pd(111) by Surface X-Ray Absorption Fine Structure Spectroscopy," *Surf. Sci.* **601**, 95–103 (2007).
- T. NAKAGAWA, T. YOKOYAMA, M. HOSAKA and M. KATOH**, "Measurements of Threshold Photoemission Magnetic Dichroism Using Ultraviolet Lasers and a Photoelastic Modulator," *Rev. Sci. Instrum.* **78**, 023907 (5 pages) (2007).
- H. ABE, K. AMEMIYA, D. MATSUMURA, T. OHTSUKI, E. SAKAI, T. YOKOYAMA and T. OHTA**, "Depth-Resolved XMCD Application to Fe/Ni/Cu(001) Films," *AIP Conf. Proc.* **882**, 384 (2007).

LIST OF PUBLICATIONS

- Y. NEGISHI, H. TSUNOYAMA, M. SUZUKI, N. KAWAMURA, M. M. MATSUSHITA, K. MARUYAMA, T. SUGAWARA, T. YOKOYAMA and T. TSUKUDA**, "X-Ray Magnetic Circular Dichroism of Size-Selected, Thiolated Gold Clusters," *J. Am. Chem. Soc.* **128**, 12034–12035 (2006).
- H. TSUNOYAMA, H. SAKURAI and T. TSUKUDA**, "Size Effect on the Catalysis of Gold Clusters Dispersed in Water for Aerobic Oxidation of Alcohol," *Chem. Phys. Lett.* **429**, 528–532 (2006).
- H. SAKURAI, H. TSUNOYAMA and T. TSUKUDA**, "Oxidative Homo-Coupling of Potassium Aryltrifluoroborates Catalyzed by Gold Nanocluster under Aerobic Conditions," *J. Organomet. Chem.* **692**, 368–374 (2007).
- H. TSUNOYAMA, T. TSUKUDA and H. SAKURAI**, "Synthetic Application of PVP-Stabilized Au Nanocluster Catalyst to Aerobic Oxidation of Alcohols in Aqueous Solution under Ambient Conditions," *Chem. Lett.* **36**, 212–213 (2007).
- H. TSUNOYAMA, P. NICKUT, Y. NEGISHI, K. AL-SHAMERY, Y. MATSUMOTO and T. TSUKUDA**, "Formation of Alkanethiolate-Protected Gold Clusters with Unprecedented Core Sizes in the Thiolation of Polymer-Stabilized Gold Clusters," *J. Phys. Chem. C* **111**, 4153–4158 (2007).
- N. K. CHAKI, H. TSUNOYAMA, Y. NEGISHI, H. SAKURAI and T. TSUKUDA**, "Effect of Ag-Doping on Catalytic Activity of PVP-Stabilized Au Clusters in Aerobic Oxidation of Alcohol," *J. Phys. Chem. C* **111**, 4885–4888 (2007).
- I. KAMIYA, H. TSUNOYAMA, T. TSUKUDA and H. SAKURAI**, "Lewis Acidic Character of Zero-Valent Gold Nanoclusters under Aerobic Conditions: Intramolecular Hydroalkoxylation of Alkenes," *Chem. Lett.* **36**, 646–647 (2007).
- Y. SHICHIBU, Y. NEGISHI, H. TSUNOYAMA, M. KANEHARA, T. TERANISHI and T. TSUKUDA**, "Extremely High Stability of Glutathionate-Protected Au₂₅ Clusters Against Core Etching," *Small* **3**, 835–839 (2007).
- Y. SHICHIBU, Y. NEGISHI, T. WATANABE, N. K. CHAKI, H. KAWAGUCHI and T. TSUKUDA**, "Bicosahedral Gold Clusters [Au₂₅(PPh₃)₁₀(SC_nH_{2n+1})₅Cl₂]²⁺ (n = 2–18): A Stepping Stone to Cluster-Assembled Materials," *J. Phys. Chem. C* **111**, 7485–7487 (2007).
- K. IKEDA, Y. KOBAYASHI, Y. NEGISHI, M. SETO, T. IWASA, K. NOBUSADA, T. TSUKUDA and N. KOJIMA**, "Thiolate-Induced Structural Reconstruction of Gold Clusters Probed by ¹⁹⁷Au Mössbauer Spectroscopy," *J. Am. Chem. Soc.* **129**, 7230–7231 (2007).
- M. IMAMURA, T. MIYASHITA, A. TANAKA, H. YASUDA, Y. NEGISHI and T. TSUKUDA**, "Electronic Structure of Dendrimer-Encapsulated Au Nanocluster," *Eur. Phys. J. D* **43**, 233–236 (2007).
- S. PANDE, S. K. GHOSH, S. PRAHARAJ, S. PANIGRAHI, S. BASU, S. JANA, A. PAL, T. TSUKUDA and T. PAL**, "Synthesis of Normal and Inverted Gold-Silver Core-Shell Architectures in β-Cyclodextrin and Their Application in SERS," *J. Phys. Chem. C* **111**, 10806–10813 (2007).
- S. IWAI, K. YAMAMOTO, A. KASHIWAZAKI, H. NAKAYA, K. YAKUSHI, H. OKAMOTO, H. MORI and Y. NISHIO**, "Photoinduced Melting of Stripe-Type Charge Order and Metallic-Domain Formation in Layered BEDT-TTF Based Salt," *Phys. Rev. Lett.* **98**, 09740 (4 pages) (2007).
- T. YAMAMOTO, J. EDA, A. NAKAO, R. KATO and K. YAKUSHI**, "Charge Ordered State and Frustration of the Site-Charges in (ET)₃Te₂I₆ and (BETS)₂Te₂I₆," *Phys. Rev. B* **75**, 205132 (17 pages) (2007).
- I. SHIROTANI, J. HAYASHI, K. TAKEDA, H. KAWAMURA, M. INOKUCHI, K. YAKUSHI and H. INOKUCHI**, "Effects of Pressure and Shear Stress on the Absorption Spectra of Thin Films of Pentacene," *Mol. Cryst. Liq. Cryst.* **461**, 111–122 (2007).
- I. SHIROTANI, J. HAYASHI, K. TAKEDA, H. KAWAMURA, M. INOKUCHI and K. YAKUSHI**, "Shear Stress Effect on the Absorption Spectra of Organic Thin Films under High Pressure," *Mol. Cryst. Liq. Cryst.* **455**, 75–79 (2006).
- M. URUICHI, K. YAKUSHI and T. MOCHIDA**, "Phase Separation in the Monovalent-to-Divalent Phase Transition of Biferrocenium-(F₁TCNQ)₃," *J. Low Temp. Phys.* **143**, 655–658 (2006).
- K. YAKUSHI, K. SUZUKI, K. YAMAMOTO, T. YAMAMOTO and A. KAWAMOTO**, "Unusual Electronic State of Layered θ-(ET)₂X Studied by Raman Spectroscopy," *J. Low Temp. Phys.* **143**, 659–662 (2006).
- K. YABUUCHI, D. KAWAMURA, M. INOKUCHI, I. SHIROTANI, J. HAYASHI, K. YAKUSHI, H. KAWAMURA and H. INOKUCHI**, "Raman Spectroscopic Study of Bis(diphenylglyoximato)metal Complexes under High Pressure," *Mol. Cryst. Liq. Cryst.* **455**, 81–85 (2006).
- M. INOKUCHI, Y. SAKKA, K. YABUUCHI, I. SHIROTANI, J. HAYASHI, K. YAKUSHI, H. KAWAMURA and H. INOKUCHI**, "Shear Stress Effect on Thin Films of Molecular Crystals," *J. Low Temp. Phys.* **143**, 211–214 (2006).
- A. KAWAMOTO, Y. HONMA, K. KUMAGAI, K. YAMAMOTO and K. YAKUSHI**, "Incoherent-Coherent Crossover Behavior of Electron on κ-(BEDT-TTF)₂X System, Probed by ¹³C-NMR and Optical Studies," *J. Low Temp. Phys.* **143**, 519–522 (2006).
- K. TAKEDA, J. HAYASHI, I. SHIROTANI, H. FUKUDA and K. YAKUSHI**, "Structural, Optical, and Electrical Properties of One-Dimensional Bis(dimethylglyoximato) Nickel(II), Ni(dmg)₂ at High Pressure," *Mol. Cryst. Liq. Cryst.* **460**, 131–144 (2006).
- S. UJI, T. TERASHIMA, M. NISHIMURA, Y. TAKAHIDE, K. ENOMOTO, T. KONOIKE, M. NISHIMURA, H. CUI, H. KOBAYASHI, A. KOBAYASHI, H. TANAKA, M. TOKUMOTO, E. S. CHOI, T. TOKUMOTO, D. GRAF and J. S. BROOKS**, "Vortex Dynamics and Fulde-Ferrell-Larkin-Ovchinnikov State in a Magnetic-Field-Induced Organic Superconductor," *Phys. Rev. Lett.* **97**, 157001 (4 pages) (2006).

- H. CUI, Z. WANG, K. TAKAHASHI, Y. OKANO, H. KOBAYASHI and A. KOBAYASHI**, "Ferroelectric Porous Molecular Crystal, $[\text{Mn}_3(\text{HCOO})_6](\text{C}_2\text{H}_5\text{OH})$, Exhibiting Ferrimagnetic Transition," *J. Am. Chem. Soc.* **128**, 15074–15075 (2006).
- H. CUI, H. KOBAYASHI and A. KOBAYASHI**, "Phase Diagram and Anomalous Constant Resistivity State of Magnetic Organic Superconducting Alloy, λ - $(\text{BETS})_2\text{Fe}_x\text{Ga}_{1-x}\text{Cl}_4$," *J. Mater. Chem.* **17**, 45–48 (2007).
- Z. WANG, B. ZHANG, K. INOUE, H. FUJIWARA, T. OTSUKA, H. KOBAYASHI and M. KURMOO**, "Occurrence of a Rare 4⁹-6⁶ Structural Topology, Chirality, and Weak Ferromagnetism in the $[\text{NH}_4][\text{M}^{\text{II}}(\text{HCOO})_3]$ (M = Mn, Co, Ni) Frameworks," *Inorg. Chem.* **46**, 437–445 (2007).
- B. ZHANG, Z. WANG, M. KURMOO, S. GAO, K. INOUE and H. KOBAYASHI**, "Guest-Induced Chirality in the Ferrimagnetic Nanoporous Diamond Framework $\text{Mn}_3(\text{HCOO})_6$," *Adv. Funct. Mater.* **17**, 577–584 (2007).
- H. TANAKA, S. HARA, M. TOKUMOTO, A. KOBAYASHI and H. KOBAYASHI**, "Resistance Measurements of Microcrystals of Single-Component Molecular Metals Using Finely Patterned Interdigitated Electrodes," *Chem. Lett.* **36**, 1006–1007 (2007).
- E. FUJIWARA, K. YAMAMOTO, M. SHIMSMURA, B. ZHOU, A. KOBAYASHI, K. TAKAHASHI, Y. OKANO, H. CUI and H. KOBAYASHI**, " $(^n\text{Bu}_4\text{N})[\text{Ni}(\text{dmstfdt})_2]$: A Planar Nickel Coordination Complex with an Extended-TTF Ligand Exhibiting Metallic Conduction, Metal–Insulator Transition and Weak Ferromagnetism," *Chem. Mater.* **19**, 553–558 (2007).
- P. MONCEAU, F. NAD, J. M. FABRE and T. NAKAMURA**, "Charge and Anion Ordering in $(\text{TMTTF})_2\text{X}$ Quasi-One-Dimensional Conductors," *J. Low Temp. Phys.* **142**, 367–372 (2006).
- M. HIRAOKA, H. SAKAMOTO, K. MIZOGUCHI, R. KATO, T. KATO, T. NAKAMURA, K. FURUKAWA, K. HIRAKI, T. TAKAHASHI, T. YAMAMOTO and H. TAJIMA**, "Electron Spin Dynamics in $(\text{DMe-DCNQI})_2\text{M}$ (M = $\text{Li}_{1-x}\text{Cu}_x$ ($x < 0.14$), Ag)," *J. Low Temp. Phys.* **142**, 617–620 (2006).
- S. KONNO, S. KAZAMA, M. HIRAOKA, H. SAKAMOTO, K. MIZOGUCHI, H. TANIGUCHI, T. NAKAMURA and K. FURUKAWA**, "EPR Study of the Electronic States of β' - $(\text{BEDT-TTF})(\text{TCNQ})$," *J. Low Temp. Phys.* **142**, 621–624 (2006).
- T. NAKAMURA, T. HARA and K. FURUKAWA**, "Redistribution of Electronic Charge in $(\text{TMTTF})_2\text{ReO}_4$: ¹³C NMR Investigation," *J. Low Temp. Phys.* **142**, 629–632 (2006).
- K. MIZOGUCHI, S. TANAKA, M. OJIMA, S. SANO, M. NAGATORI, H. SAKAMOTO, Y. YONEZAWA, Y. AOKI, H. SATO, K. FURUKAWA and T. NAKAMURA**, "AF-Like Ground State of Mn-DNA and Charge Transfer from Fe to Base- π -Band in Fe-DNA," *J. Phys. Soc. Jpn.* **76**, 043801 (4 pages) (2007).
- M. ITOI, M. KANO, N. KURITA, M. HEDO, Y. UWATOKO and T. NAKAMURA**, "Pressure-Induced Superconductivity in Quasi-One-Dimensional Organic Conductor $(\text{TMTTF})_2\text{AsF}_6$," *J. Phys. Soc. Jpn.* **76**, 053703 (5 pages) (2007).
- T. NAKAMURA, K. FURUKAWA and T. HARA**, "Redistribution of Charge in the Proximity of the Spin-Peierls Transition: ¹³C NMR Investigation of $(\text{TMTTF})_2\text{PF}_6$," *J. Phys. Soc. Jpn.* **76**, 064715 (5 pages) (2007).
- I. KAWAMURA, N. KIHARA, M. OHMINE, K. NISHIMURA, S. TUZI, H. SAITO and A. NAITO**, "Solid State NMR Studies of Two Different Backbone Conformation at Tyr185 as a Function of Retinal Configurations in the Dark, Light, and Pressure Adapted Bacteriorhodopsin," *J. Am. Chem. Soc.* **129**, 1016–1017 (2007).
- I. KAWAMURA, Y. DEGAWA, S. YAMAGUCHI, K. NISHIMURA, S. TUZI, H. SAITO and A. NAITO**, "Pressure Induced Isomerization of Retinal on Bacteriorhodopsin as Disclosed by Fast Magic Angle Spinning NMR," *Photochem. Photobiol.* **83**, 346–350 (2007).
- M. UMEYAMA, A. KIRA, K. NISHIMURA and A. NAITO**, "Interaction of Bovine Lactoferricin with Acidic Phospholipid Bilayers and Its Antimicrobial Activity as Studied by Solid State NMR," *Biochim. Biophys. Acta* **1758**, 1523–1528 (2006).
- R. NEGISHI, T. HASEGAWA, K. TERABE, M. AONO, H. TANAKA, H. OZAWA and T. OGAWA**, "Different I-V Characteristic of Single Electron Tunneling Induced by Using Double-Barrier Tunneling Junctions with Differing Symmetric Structures," *Appl. Phys. Lett.* **90**, 223112 (2007).
- T. OGAWA, H. OZAWA, M. KAWAO and H. TANAKA**, "Photo Responsibility of Au Nano-Particle/Porphyrin Polymer Composite Device Using Nano-Gap Electrodes," *J. Mater. Sci.* **18**, 939–942 (2007).
- H. OZAWA, M. KAWAO, H. TANAKA and T. OGAWA**, "Synthesis of Dendron Protected Porphyrin Wires and Preparation of a One-Dimensional Assembly of Gold Nanoparticles Chemically Linked to the π -Conjugated Wires," *Langmuir* **23**, 6365–6371 (2007).
- W. HUANG, Z. CHU, S. GOU and T. OGAWA**, "Construction of Macrocyclic-Based Molecular Stairs Having Pendant 4-Aminopyridine, 4-Dimethylaminopyridine and Isonicotinonitrile Groups," *Polyhedron* **26**, 1483–1492 (2007).
- T. YAJIMA, H. TANAKA, T. MATSUMOTO, Y. OTSUKA, Y. SUGAWARA and T. OGAWA**, "Refinement of Conditions of Point-Contact Current Imaging Atomic Force Microscopy for Molecular-Scale Conduction Measurements," *Nanotechnology* **18**, 095501 (5 pages) (2007).
- H. TANAKA, M. W. HORN and P. S. WEISS**, "A Method for the Fabrication of Sculptured Thin Films of Periodic Arrays of Standing Nanorods," *J. Nanosci. Nanotechnol.* **6**, 3799 (2006).

LIST OF PUBLICATIONS

- Y. SAKAMOTO, T. SUZUKI, M. KOBAYASHI, Y. GAO, Y. INOUE and S. TOKITO**, “Perfluoropentacene and Perfluorotetracene: Syntheses, Crystal Structures, and FET Characteristics,” *Mol. Cryst. Liq. Cryst.* **444**, 225–232 (2006).
- N. KOCH, A. VOLLMER, S. DUHM, Y. SAKAMOTO and T. SUZUKI**, “The Effect of Fluorination on Pentacene/Gold Interface Energetics and Charge Reorganization Energy,” *Adv. Mater.* **19**, 112–116 (2007).
- Y. KIKUZAWA, T. NAGATA, T. TAHARA and K. ISHII**, “Photo- and Redox-Active Dendritic Molecules with Soft, Layered Nanostructures,” *Chem. Asian J.* **1**, 516–528 (2006).
- T. NAGATA**, “Automated Design of Protecting Molecules for Metal Nanoparticles by Combinatorial Molecular Simulations,” *J. Organomet. Chem.* **692**, 225–233 (2007).
- T. NAGATA and Y. KIKUZAWA**, “An Approach towards Artificial Quinone Pools by Use of Photo- and Redox-Active Dendritic Molecules,” *Biochim. Biophys. Acta* **1767**, 648–652 (2007).
- T. NAGASAWA and T. NAGATA**, “Synthesis and Electrochemistry of Co(III) and Co(I) Complexes Having C₅Me₅ Auxiliary,” *Biochim. Biophys. Acta* **1767**, 666–670 (2007).
- T. NAGATA, T. NAGASAWA, S. K. ZHARMUKHAMEDOV, V. V. KLIMOV and S. I. ALLAKHVERDIEV**, “Reconstitution of the Water-Oxidizing Complex in Manganese-Depleted Photosystem II Preparations Using Synthetic Binuclear Mn(II) and Mn(IV) Complexes: Production of Hydrogen Peroxide,” *Photosynth. Res.* **93**, 133–138 (2007).
- H. SAKURAI, H. TSUNOYAMA and T. TSUKUDA**, “Oxidative Homo-Coupling of Potassium Aryltrifluoroborates Catalyzed by Gold Nanocluster under Aerobic Conditions,” *J. Organomet. Chem.* **692**, 368–374 (2007).
- S. HIGASHIBAYASHI and H. SAKURAI**, “Synthesis of an Enantiopure *syn*-Benzocyclootrimer through Regio-Selective Cyclootrimerization of a Halonorbornene Derivative under the Palladium Nanocluster Conditions,” *Chem. Lett.* **36**, 18–19 (2007).
- H. TSUNOYAMA, T. TSUKUDA and H. SAKURAI**, “Synthetic Application of PVP-Stabilized Au Nanocluster Catalyst to Aerobic Oxidation of Alcohols in Aqueous Solution under Ambient Conditions,” *Chem. Lett.* **36**, 212–213 (2007).
- I. KAMIYA, H. TSUNOYAMA, T. TSUKUDA and H. SAKURAI**, “Lewis Acid Character of Zero-Valent Gold Nanoclusters under Aerobic Conditions: Intramolecular Hydroalkoxylation of Alkenes,” *Chem. Lett.* **36**, 646–647 (2007).
- S. MATSUMIYA, Y. YAMAGUCHI, J. SAITO, M. NAGANO, H. SASAKAWA, S. OTAKI, M. SATOH, K. SHITARA and K. KATO**, “Structural Comparison of Fucosylated and Nonfucosylated Fc Fragments of Human Immunoglobulin G1,” *J. Mol. Biol.* **368**, 767–779 (2007).
- E. SAKATA, Y. YAMAGUCHI, Y. MIYAUCHI, K. IWAI, T. CHIBA, Y. SAEKI, N. MATSUDA, K. TANAKA and K. KATO**, “Direct Interactions between NEDD8 and Ubiquitin E2 Conjugating Enzymes Upregulate Cullin-Based E3 Ligase Activity,” *Nature Struct. Mol. Biol.* **14**, 167–168 (2007).
- M. NAKANO, C. MURAKAMI, Y. YAMAGUCHI, H. SASAKAWA, T. HARADA, E. KURIMOTO, O. ASAMI, T. KAJINO and K. KATO**, “NMR Assignments of the *b'* and *a'* Domains of Thermophilic Fungal Protein Disulfide Isomerase,” *J. Biomol. NMR* **36**, 44 (2006).
- R. KITAHARA, Y. YAMAGUCHI, E. SAKATA, T. KASUYA, K. TANAKA, K. KATO, S. YOKOYAMA and K. AKASAKA**, “Evolutionally Conserved Intermediates between Ubiquitin and NEDD8,” *J. Mol. Biol.* **363**, 395–404 (2006).
- T. YOKOYAMA, S. KURATA and S. TANAKA**, “Direct Identification of Conformational Isomers of Adsorbed Oligothiophene on Cu(100),” *J. Phys. Chem. B* **110**, 18130–18133 (2006).
- K. ONO, M. JOHO, K. SAITO, M. TOMURA, Y. MATSUSHITA, S. NAKA, H. OKADA and H. ONNAGAWA**, “Synthesis and Electroluminescence Properties of *fac*-Tris(2-phenylpyridine)iridium Derivatives Containing Hole-Accepting Moieties,” *Eur. J. Inorg. Chem.* 3676–3683 (2006).
- M. KUJIME, T. KURAHASHI, M. TOMURA and H. FUJII**, “⁶³Cu NMR Spectroscopy of Copper(I) Complexes with Various Tridentate Ligands: CO as a Useful ⁶³Cu NMR Probe for Sharpening ⁶³Cu NMR Signals and Analyzing the Electronic Donor Effect of a Ligand,” *Inorg. Chem.* **46**, 541–551 (2007).
- K. ONO, K. YOSHIKAWA, Y. TSUJI, H. YAMAGUCHI, R. UOZUMI, M. TOMURA, K. TAGA and K. SAITO**, “Synthesis and Photoluminescence Properties of BF₂ Complexes with 1,3-Diketone Ligands,” *Tetrahedron* **63**, 9354–9358 (2007).
- H. MAEDA and Y. ITO**, “BF₂ Complex of Fluorinated Dipyrrolyldiketone: A New Class of Efficient Receptor for Acetate Anions,” *Inorg. Chem.* **45**, 8205–8210 (2006).
- H. MAEDA, Y. ITO, Y. KUSUNOSE and T. NAKANISHI**, “Dipyrrolylpyrazoles: Anion Receptors in Protonated Form and Efficient Building Blocks for Organized Structures,” *Chem. Commun.* 1136–1138 (2007).
- H. MAEDA, Y. KUSUNOSE, M. TERASAKI, Y. ITO, C. FUJIMOTO, R. FUJII and T. NAKANISHI**, “Micro- and Nanometer-Scale Porous, Fibrous, and Sheet Architectures Fabricated by Supramolecular Assemblies of Dipyrrolyldiketones,” *Chem. Asian J.* **2**, 350–370 (2007).

H. MAEDA, Y. KUSUNOSE, Y. MIHASHI and T. MIZOGUCHI, “BF₂ Complexes of β -Tetraethyl-Substituted Dipyrrolyl-diketones as Anion Receptors: Potential Building Subunits for Oligomeric Systems,” *J. Org. Chem.* **72**, 2612–2616 (2007).

H. MAEDA, M. HASEGAWA and A. UEDA, “Hydrogen Bonding Self-Assemblies with 1-D Linear, Dimeric and Hexagonal Nanostructures of *meso*-Pyridyl-Substituted Dipyrromethanes,” *Chem. Commun.* 2276–2278 (2007).

Life and Coordination-Complex Molecular Science

H. YOSHIMURA, S. YOSHIOKA, Y. MIZUTANI and S. AONO, “The Formation of Hydrogen Bond in the Proximal Heme Pocket of HemAT-Bs upon Ligand Binding,” *Biochem. Biophys. Res. Commun.* **357**, 1053–1057 (2007).

H. KOMORI, S. INAGAKI, S. YOSHIOKA, S. AONO and Y. HIGUCHI, “Crystal Structure of CO-Sensing Transcription Activator CooA Bound to Exogenous Ligand Imidazole,” *J. Mol. Biol.* **367**, 864–871 (2007).

E. PINAKOULAKI, H. YOSHIMURA, V. DASKALAKIS, S. YOSHIOKA, S. AONO and C. VAROTSIS, “Two Ligand Binding Sites in the O₂-Sensing Signal Transducer HemAT: Implication for Ligand Recognition/Discrimination and Signaling,” *Proc. Natl. Acad. Sci. U. S. A.* **103**, 14796–14801 (2006).

K. KOBAYASHI, M. KUBO, S. YOSHIOKA, T. KITAGAWA, K. KATO, Y. ASANO and S. AONO, “Systematic Regulation of the Enzymatic Activity of Phenylacetaldoxime Dehydratase by Exogenous Ligand,” *ChemBioChem* **7**, 2004–2009 (2006).

T. OROGUCHI, M. IKEGUCHI, M. OTA, K. KUWAJIMA and A. KIDERA, “Unfolding Pathways of Goat α -Lactalbumin as Revealed in Multiple Alignment of Molecular Dynamics Trajectories,” *J. Mol. Biol.* **371**, 1354–1364 (2007).

H. NAKATANI, K. MAKI, K. SAEKI, T. AIZAWA, M. DEMURA, K. KAWANO, S. TOMODA and K. KUWAJIMA, “Equilibrium and Kinetics of the Folding and Unfolding of Canine Milk Lysozyme,” *Biochemistry* **46**, 5238–5251 (2007).

A. KATO, K. MAKI, T. EBINA, K. KUWAJIMA, K. SODA and Y. KURODA, “Mutational Analysis of Protein Solubility Enhancement Using Short Peptide Tags,” *Biopolymers* **85**, 12–18 (2007).

S. ENOKI, K. MAKI, T. INOBE, K. TAKAHASHI, K. KAMAGATA, T. OROGUCHI, H. NAKATANI, K. TOMOYORI and K. KUWAJIMA, “The Equilibrium Unfolding Intermediate Observed at pH 4 and Its Relationship with the Kinetic Folding Intermediates in Green Fluorescent Protein,” *J. Mol. Biol.* **361**, 969–982 (2006).

T. KURAHASHI, K. ODA, M. SUGIMOTO, T. OGURA and H. FUJII, “A Trigonal-Bipyramidal Geometry Induced by an External Water Ligand in a Sterically Hindered Iron Salen Complex, Related to the Active Site of Protocatechuate 3,4-Dioxygenase,” *Inorg. Chem.* **45**, 7709–7721 (2006).

A. TAKAHASHI, T. KURAHASHI and H. FUJII, “Activation Parameters for Cyclohexene Oxygenation by an Oxoiron(IV) Porphyrin π -Cation Radical Complex: Entropy Control of an Allylic Hydroxylation Reaction,” *Inorg. Chem.* **46**, 6227–6229 (2007).

M. KUJIME, T. KURAHASHI, M. TOMURA and H. FUJII, “⁶³Cu NMR Spectroscopy of Copper(I) Complexes with Various Tridentate Ligands: CO as a Useful ⁶³Cu NMR Probe for Sharpening ⁶³Cu NMR Signals and Analyzing the Electronic Donor Effect of a Ligand,” *Inorg. Chem.* **46**, 541–551 (2007).

H. UNO, Z. L. ZHANG, M. SUZUI, R. TERO, Y. NONOGAKI, S. NAKAO, S. SEKI, S. TAGAWA, S. OIKI and T. URISU, “Noise Analysis of Si-Based Planar-Type Ion-Channel Biosensors,” *Jpn. J. Appl. Phys.* **45**, L1334–L1336 (2006).

C. S. WANG, X. PAN, C. Y. SUN and T. URISU, “Area-Selective Deposition of Self-Assembled Monolayers on SiO₂/Si(100) Patterns,” *Appl. Phys. Lett.* **89**, 233105 (3 pages) (2006).

C. S. WANG, X. Q. ZHANG and T. URISU, “Synchrotron-Radiation-Stimulated Etching of SiO₂ Thin Films with a Tungsten Nano-Pillar Mask,” *J. Synchrotron Radiat.* **13**, 432–434 (2006).

S. B. LEI, R. TERO, N. MISAWA, S. YAMAMURA, L. J. WAN and T. URISU, “AFM Characterization of Gramicidin-A in Tethered Lipid Membrane on Silicon Surface,” *Chem. Phys. Lett.* **429**, 244–249 (2006).

T. OZAWA, Y. NATORI, M. SATO and Y. UMEZAWA, “Imaging Dynamics of Endogenous Mitochondrial RNA in Single Living Cells,” *Nat. Methods* **4**, 413–419 (2007).

T. OZAWA, Y. NATORI, Y. SAKO, H. KUROIWA, T. KUROIWA and Y. UMEZAWA, “A Minimal Peptide Sequence That Targets Fluorescent and Functional Proteins into the Mitochondrial Intermembrane Space,” *ACS Chem. Biol.* **2**, 176–186 (2007).

S. B. KIM, A. KANNO, T. OZAWA, H. TAO and Y. UMEZAWA, “Nongenomic Activity of Ligands in the Association of Androgen Receptor with Src,” *ACS Chem. Biol.* **2**, 484–492 (2007).

S. B. KIM, T. OZAWA, H. TAO and Y. UMEZAWA, “A Proinflammatory Cytokine Sensor Cell for Assaying Inflammatory Activities of Nanoparticles,” *Anal. Biochem.* **362**, 148–150 (2007).

A. KANNO, T. OZAWA and Y. UMEZAWA, “A Genetically Encoded Optical Probe for Detecting Release of Proteins from Mitochondria toward Cytosol in Living Cells and Animals,” *Anal. Chem.* **78**, 8076–8081 (2006).

LIST OF PUBLICATIONS

- S. B. KIM, Y. NATORI, T. OZAWA, H. TAO and Y. UMEZAWA**, “A Method for Determining the Activities of Cytokines Based on the Nuclear Transport of Nuclear Factor- κ B,” *Anal. Biochem.* **359**, 147–149 (2006).
- M. MINAKAWA, K. TAKENAKA and Y. UOZUMI**, “Indexation of the Coordination Ability of Ligands,” *Eur. J. Inorg. Chem.* 1629–1631 (2007).
- Y. M. A. YAMADA, H. GUO and Y. UOZUMI**, “Tightly Convolved Polymeric Phosphotungstate Catalyst: Oxidative Cyclization of Alkenols and Alkenoic Acids,” *Org. Lett.* **9**, 1501–1504 (2007).
- M. KIMURA and Y. UOZUMI**, “Development of New P-Chiral Phosphorodiamidite Ligands Having a Pyrrolo[1,2-c]diazaphosphol-1-one Unit and Their Application to Regio- and Enantioselective Iridium-Catalyzed Allylic Etherification,” *J. Org. Chem.* **72**, 707–714 (2007).
- Y. UOZUMI, R. NAKAO and H. RHEE**, “Development of Amphiphilic Resin-Dispersion of Nano-Palladium Catalysts: Design, Preparation, and Its Use in Aquacatalytic Hydrodechlorination and Aerobic Oxidation,” *J. Organomet. Chem.* **692**, 420–427 (2007).
- Y. M. A. YAMADA, T. ARAKAWA, H. HOCCKE and Y. UOZUMI**, “A Nanoplatinum Catalyst for Aerobic Oxidation of Alcohols in Water,” *Angew. Chem., Int. Ed.* **46**, 704–706 (2007).
- Y. UOZUMI, Y. M. A. YAMADA, T. BEPPU, N. FUKUYAMA, M. UENO and T. KITAMORI**, “Instantaneous Carbon–Carbon Bond Formation Using a Microchannel Reactor with a Catalytic Membrane,” *J. Am. Chem. Soc.* **128**, 15994–15995 (2006).
- Y. UOZUMI and T. SUZUKA**, “Allylic C1-Substitution in Water with Nitromethane Using Amphiphilic Resin-Supported Palladium Complexes,” *J. Org. Chem.* **71**, 8644–8646 (2006).
- Y. NAKAI, T. KIMURA and Y. UOZUMI**, “Alkylative Cyclization of 1,6-Enynes in Water with an Amphiphilic Resin-Supported Palladium Catalyst,” *Synlett* 3065–3068 (2006).
- T. KIMURA and Y. UOZUMI**, “PCP Pincer Palladium Complexes and Their Catalytic Properties: Synthesis via the Electrophilic Ligand Introduction Route,” *Organometallics* **25**, 4883–4887 (2006).
- Y. M. A. YAMADA, Y. MAEDA and Y. UOZUMI**, “A Novel 3D Coordination Palladium-Network Complex: A Recyclable Catalyst for Suzuki-Miyaura Reaction,” *Org. Lett.* **8**, 4259–4262 (2006).
- Y. UOZUMI, T. SUZUKA, R. KAWADE and H. TAKENAKA**, “Allylic Azidation in Water with an Amphiphilic Resin-Supported Palladium-Phosphine Complex,” *Synlett* 2109–2113 (2006).
- Y. MIYAZATO, T. WADA, J. T. MUCKERMAN, E. FUJITA and K. TANAKA**, “Generation of a Ru^{II}-Semiquinone-Anilino-Radical Complex through the Deprotonation of a Ru^{III}-Semiquinone-Anilino Complex,” *Angew. Chem., Int. Ed.* **46**, 5728–5730 (2007).
- H. TANNAI, T. KOIZUMI and K. TANAKA**, “Palladium(II) Complexes Bearing the Terpyridine-Type Tridentate Ligand with Benzo[b]-1,5-Naphthyridin-2-yl Groups,” *Inorg. Chim. Acta* **360**, 3075–3082 (2007).
- K. TSUTSUI, T. KOIZUMI, T. TANAKA, H. HAYASHI and K. TANAKA**, “Anion-Dependent Selective Formation of Intermolecular Non-Covalent Bonds,” *J. Mol. Struct.* **829**, 168–175 (2007).
- R. OKAMURA, T. WADA and K. TANAKA**, “Novel Platinum-Ruthenium Dinuclear Complex Bridged by 2-Aminoethanethiol,” *Bull. Chem. Soc. Jpn.* **79**, 1535–1540 (2006).
- T. WADA, M. YAMANAKA, T. FUJIHARA, Y. MIYAZATO and K. TANAKA**, “Experimental and Theoretical Evaluation of the Charge Distribution over the Ruthenium and Dioxolene Framework of [Ru(OAc)(dioxolene)(terpy)] (terpy = 2,2':6',2''-terpyridine) Depending on the Substituents,” *Inorg. Chem.* **45**, 8887–8894 (2006).
- Y. MIYAZATO, T. WADA and K. TANAKA**, “Redox Behavior and Catalytic Oxidation Reactions of Alcohols by a New Ruthenium(III)-Dioxolene-Amine Complex of Bis(2-pyridylmethyl)-2-Aminoethylamine,” *Bull. Chem. Soc. Jpn.* **79**, 745–747 (2006).
- J. CHO, H. FURUTACHI, S. FUJINAMI, T. TOSHA, H. OHTSU, K. TANAKA, T. KITAGAWA and M. SUZUKI**, “Sequential Reaction Intermediates in Aliphatic C–H Bond Functionalization Initiated by a Bis(μ -oxo)nickel(III) Complex,” *Inorg. Chem.* **45**, 2873–2885 (2006).
- T. MATSUO and H. KAWAGUCHI**, “From Carbon Dioxide to Methane: Homogeneous Reduction of Carbon Dioxide with Hydrosilanes Catalyzed by Zirconium-Borane Complexes,” *J. Am. Chem. Soc.* **128**, 12362–12363 (2006).
- W. -L. MENG, G. -X. LIU, T. OKAMURA, H. KAWAGUCHI, Z. -H. ZHANG, W. -Y. SUN and N. UEYAMA**, “Syntheses, Crystal Structures, and Magnetic Properties of Novel Copper(II) Complexes with the Flexible Bidentate Ligand 1-Bromo-3,5-bis(imidazol-1-ylmethyl)benzen,” *Cryst. Growth Des.* **6**, 2092–2102 (2006).
- W. -L. MENG, J. FAN, T. OKAMURA, H. KAWAGUCHI, Y. LV, W. -Y. SUN and N. UEYAMA**, “Molecular Cage, One-Dimensional Tube and Two-Dimensional Polycatenane Obtained from Reactions of Flexible Tripodal Ligand 1,3,5-Tris(imidazol-1-ylmethyl)-2,4,6-Trimethylbenzene with Copper Salts,” *Z. Anorg. Allg. Chem.* **632**, 1890–1896 (2006).
- W. -L. MENG, Z. -H. ZHANG, Y. LV, H. KAWAGUCHI and W. -Y. SUN**, “Synthesis, Crystal Structure and Magnetic Property of a Two-Dimensional Herringbone-Like Network with Praseodymium(III) Nitrate and 1-Bromo-3,5-bis(imidazol-1-ylmethyl) benzene (bib),” *Appl. Organomet. Chem.* **20**, 399–403 (2006).

- S. SENDA, Y. OHKI, T. HIRAYAMA, D. TODA, J. -L. CHEN, T. MATSUMOTO, H. KAWAGUCHI and K. TATSUMI**, "Mono{hydrotris(mercaptoimidazolyl)borato} Complexes of Manganese(II), Iron(II), Cobalt(II), and Nickel(II) Halides," *Inorg. Chem.* **45**, 9914–9925 (2006).
- D. ZHANG, H. AIHARA, T. WATANABE, T. MATSUO and H. KAWAGUCHI**, "Zirconium Complexes of the Tridentate Bis(aryloxy)-*N*-Heterocyclic-Carbene Ligand: Chloride and Alkyl Functionalized Derivatives," *J. Organomet. Chem.* **692**, 234–242 (2007).
- M. KONDO, Y. IRIE, M. MIYAKAWA, H. KAWAGUCHI, S. YASUE, K. MAEDA and F. UCHIDA**, "Synthesis and Structural Determination of New Multidimensional Coordination Polymers with 4,4'-Oxybis(benzoate) Building Ligands: Construction of Coordination Polymers with Heteroorganic Bridges," *J. Organomet. Chem.* **692**, 136–141 (2007).
- T. KOMURO, H. KAWAGUCHI, J. LANG, T. NAGASAWA and K. TATSUMI**, "[MoFe₃S₄]³⁺ and [MoFe₃S₄]²⁺ Cubane Clusters Containing a Pentamethylcyclopentadienyl Molybdenum Moiety," *J. Organomet. Chem.* **692**, 1–9 (2007).
- G. WU, Y. WANG, X. -F. WANG, H. KAWAGUCHI and W. -Y. SUN**, "Synthesis and Crystal Structure of Mn(II) and Zn(II) Complexes with 1,3,5-Tris(carboxymethoxy)benzene Ligand," *J. Chem. Crystallogr.* **37**, 199–205 (2007).
- L. -Y. KONG, X. -H. LU, Y. -Q. HUANG, H. KAWAGUCHI, Q. CHU, H. -F. ZHU and W. -Y. SUN**, "Unusual One-Dimensional Branched-Chain Structures Assembled by a Novel Imidazole-Containing Tripodal Ligand with Cadmium(II) Salts and Their Fluorescent Property," *J. Solid State Chem.* **180**, 331–338 (2007).
- A. KOBAYASHI and H. KITAGAWA**, "Mixed-Valence Two-Legged MX-Ladder Complex with a Pair of Out-of-Phase Charge-Density Waves," *J. Am. Chem. Soc.* **128**, 12066–12067 (2006).
- M. TADOKORO, S. FUKUI, T. KITAJIMA, Y. NAGAO, S. ISHIMARU, H. KITAGAWA, K. ISOBE and K. NAKASUJI**, "Structures and Phase Transition of Multi-Layered Water Nanotube Confined to Nanochannels," *Chem. Commun.* 1274–1276 (2006).
- C. YAMAMOTO, H. NISHIKAWA, M. NIHEI, T. SHIGA, M. HEDO, Y. UWATOKO, H. SAWA, H. KITAGAWA, Y. TAGUCHI, Y. IWASA and H. OSHIO**, "Electrical Conducting Bis(oxalato)platinate with Direct Connection of Cu(II) Ions," *Inorg. Chem.* **45**, 10270–10276 (2006).
- M. FUJISHIMA, M. YAMAUCHI, R. IKEDA, T. KUBO, K. NAKASUJI and H. KITAGAWA**, "Powder XRD and Solid-State ²H-NMR Studies of RAP-Protected Palladium Nanoparticle (RAP = Rubanic Acid Polymer)," *Solid State Phenomena* **111**, 107–110 (2006).
- S. SHIBAHARA, H. KITAGAWA, Y. OZAWA, K. TORIUMI, T. KUBO and K. NAKASUJI**, "Syntheses and Unusual Segregated-Alternated Hybrid Stacking Structure of Hydrogen-Bonded Charge-Transfer Complexes Composed of Bis[2,3-pyridinedithiolate]Metal Complexes," *Inorg. Chem.* **45**, 1162–1170 (2007).
- M. NAKAYA, M. KANEHARA, M. YAMAUCHI, H. KITAGAWA and T. TERANISHI**, "Hydrogen-Induced Crystal Structural Transformation of FePt Nanoparticles at Low Temperature," *J. Phys. Chem. C* **111**, 7231–7234 (2007).

Theoretical and Computational Molecular Science

T. MAEDA, T. HASEGAWA, T. AKASAK and S. NAGASE, “Chemical Functionalization and Dispersion of Single-Walled Carbon Nanotubes,” in *Handbook of Nano Carbon* (in Japanese), M. Endo and S. Iijima, Eds., NTS; Tokyo, pp. 253–260 (2007).

T. TSUCHYA, T. AKASAK and S. NAGASE, “Chemical Modification of Endohedral Metallofullerenes,” in *Handbook of Nano Carbon* (in Japanese), M. Endo and S. Iijima, Eds., NTS; Tokyo, pp. 608–613 (2007).

N. MAESHIMA and K. YONEMITSU, “Theory of Optical Responses of Photoexcited Halogen-Bridged Metal Complexes in Different Insulating Phases,” in *Multifunctional Conducting Molecular Materials*, G. Saito, F. Wudl, R. C. Haddon, K. Tanigaki, T. Enoki, H. E. Katz and M. Maesato, Eds., RSC Publishing; Cambridge, pp. 185–188 (2007).

K. YONEMITSU, “Mechanism of Ambipolar Field-Effect Transistors on One-Dimensional Organic Mott Insulators,” in *Multifunctional Conducting Molecular Materials*, G. Saito, F. Wudl, R. C. Haddon, K. Tanigaki, T. Enoki, H. E. Katz and M. Maesato, Eds., RSC Publishing; Cambridge, pp. 276–281 (2007).

K. YONEMITSU, “Theory about Mechanism of Transferring Many Electrons at Once and Changing Material Properties by Photoexcitations,” *Optical Alliance* (in Japanese) **18**, 29–33 (2007).

Y. ASAI and T. SHIMAZAKI, “Vibronic Mechanism for Charge Transport and Migration Through DNA and Single Molecules,” in *Charge Migration in DNA, Perspectives from Physics, Chemistry and Biology*, T. Chakraborty, Ed., Springer-Verlag; Heidelberg (2007).

Photo-Molecular Science

H. OKAMOTO, “Near-Field Imaging of Plasmon Wavefunctions in Metal Nanostructures,” in *Recent Advances on Design and Applications of Plasmonic Nanomaterials* (in Japanese), S. Yamada, Ed., CMC Publishing Co., Ltd.; Tokyo, pp. 128–140 (2006).

H. OKAMOTO and K. IMURA, “Near-Field Imaging of Optical Field and Plasmon Wavefunctions in Metal Nanoparticles,” *J. Mater. Chem.* **16**, 3920–3928 (2006).

K. IMURA, “Near-Field Studies of Plasmon Wavefunctions and Optical Fields in Gold Nanoparticles,” *Mol. Sci.* (in Japanese) **1**, A0006 (7 pages) (2007).

A. HISHIKAWA and K. YAMANOUCHI, “Coulomb Explosion Imaging of Molecular Dynamics in Intense Laser Fields,” in *Progress in Ultrafast Intense Laser Science II*, K. Yamanouchi, S. L. Chin, P. Agostini, G. Ferrante, Eds., Springer; Berlin (2007).

A. HISHIKAWA, “Molecules in Sub-10 fs Intense Laser Fields,” *Shototou* (in Japanese) **3**, 7–14 (2007).

M. KATOH, T. HARA and M. HOSAKA, “Generation of Short Wavelength Coherent Radiation with Seeding,” *J. Jpn. Soc. Synchrotron Radiat. Res.* (in Japanese) **20**, 226–232 (2007).

T. TAIRA, “Laser,” *KOGAKU* (in Japanese) **35**, 185–187 (2006).

T. TAIRA and M. TSUNEKANE, “High-Power Edge-Pumped Yb:YAG Single Crystal/YAG Ceramics Hybrid Microchip Laser,” *Proc. SPIE* **6216**, 621607 (8 pages) (2006).

A. IKESUE, Y. L. AUNG, T. TAIRA, T. KAMIMURA, K. YOSHIDA and G. MESSING, “Progress in Ceramic Lasers,” *Annu. Rev. Mater. Res.* **36**, 397–429 (2006).

T. TAIRA, Y. SATO, J. SAIKAWA and A. IKESUE, “Spectroscopic Properties and Laser Operation of RE³⁺-Ion Doped Garnet Materials,” *Proc. SPIE* **6216**, 62160J (12 pages) (2006).

T. TAIRA, “Single Frequency Micro Solid-State Lasers,” in *Systems, Devices and Materials for the Holographic Data Storage* (in Japanese), CMC Publishing Co., Ltd., Chapter 6.2, pp. 228–247 (2006).

T. TAIRA, “Microchip Laser,” *O PLUS E* (in Japanese) **29**, 374–380 (2007).

T. TAIRA, “RE³⁺-Ion-Doped YAG Ceramic Lasers,” *IEEE J. Sel. Top. Quantum Electron.* **13**, 798–809 (2007).

T. TAIRA, “Report on Advanced Solid-State Photonics 2007,” *The Review of Laser Engineering* (in Japanese) **35**, 402–406 (2007).

T. TAIRA, “Conference Report on Advanced Solid-State Photonics 2007,” *OptoNews* (in Japanese) **1**, 37–40 (2007).

T. TAIRA, “Ceramic YAG Lasers,” in *Comptes Rendus Physique*, ELSEVIER, **8**, pp. 138–152 (2007).

Y. MATSUMOTO and K. WATANABE, “Coherent Vibrations of Adsorbates Induced by Femtosecond Laser Excitation,” *Chem. Rev.* **106**, 4234–4260 (2006).

Materials Molecular Science

T. YOKOYAMA, "General Introduction," in *Core-shell Spectroscopy: History, Theory, Experiments and Application of Element-Specific X-ray Inner-Shell Spectroscopy* (in Japanese), T. Ohta and T. Yokoyama, Eds., IPC Pub.; Tokyo, Chapter 1, pp. 1–5 (2007).

T. YOKOYAMA, "Introduction of XAFS," in *Core-shell Spectroscopy: History, Theory, Experiments and Application of Element-Specific X-ray Inner-Shell Spectroscopy* (in Japanese), T. Ohta and T. Yokoyama, Eds., IPC Pub.; Tokyo, Chapter 4.1, pp. 79–79 (2007).

T. YOKOYAMA, "Thermal Vibration in EXAFS," in *Core-shell Spectroscopy: History, Theory, Experiments and Application of Element-Specific X-ray Inner-Shell Spectroscopy* (in Japanese), T. Ohta and T. Yokoyama, Eds., IPC Pub.; Tokyo, Chapter 4.2, pp. 80–86 (2007).

T. NAKAGAWA and T. YOKOYAMA, "Photoelectron Magnetic Circular Dichroism on Magnetic Thin Films Using Visible and Ultraviolet Lasers," *Butsuri* (in Japanese) **62**, 522–526 (2007).

T. TSUKUDA, "Size Specific Properties and Function of Polymer-Protected Gold Nanoclusters," *Electrochemistry* (in Japanese) **74**, 346–350 (2006).

T. TSUKUDA, H. TSUNOYAMA and Y. NEGISHI, "Systematic Synthesis of Monolayer-Protected Gold Clusters with Well-Defined Chemical Compositions," in *Metal Nanoclusters in Catalysis and Materials Science: the Issue of Size-Control*, B. Corain, G. Schmid and N. Toshima, Eds. Elsevier, pp. 373–382 (2007).

T. NAKAMURA, T. HARA and K. FURUKAWA, "Pronounced Enhancement of Charge Ordering Transition Temperatures in TMTTF Salts with Deuteration," in *Multifunctional Conducting Molecular Materials*, G. Saito, F. Wudl, R. C. Haddon, K. Tanigaki, T. Enoki, H. E. Katz and M. Maesato, Eds. RSC Publishing; Cambridge, pp. 83–86 (2007).

T. NAKAMURA, "Magnetic Resonance Measurements for Organic Conductors under Pressure," in *High-Pressure Technical Handbook* (in Japanese), N. Mori, K. Murata, Y. Uwatoko and H. Takahashi, Eds. Maruzen; Tokyo, pp. 274–280 (2007).

K. NISHIMURA and A. NAITO, "REDOR in Multiple Spin System," in *Modern Magnetic Resonance*, G. Webb, Ed., Kluwer Academic, pp. 715–720 (2006).

A. NAITO, S. TORAYA and K. NISHIMURA, "Nuclear Magnetic Resonance of Oriented Bilayer Systems," in *Modern Magnetic Resonance*, G. Webb, Ed., Kluwer Academic, pp. 237–243 (2006).

Y. YAMAGUCHI and K. KATO, "Structural Analyses of Antibody by NMR Spectroscopy," in *Frontier of Development of Antibody Medicine*, M. Ueda, Ed., CMC Publishing; Tokyo, pp. 116–126 (2007).

Y. YAMAGUCHI and K. KATO, "NMR Analyses of Carbohydrate–Protein Interactions," *Jikken Igaku* (in Japanese) **25**, 1137–1144 (2007).

Y. YAMAGUCHI, N. TAKAHASHI and K. KATO, "Antibody Structures," in *Comprehensive Glycoscience*, J. P. Kamerling, Ed., Elsevier Ltd.; Oxford OX5 1GB UK, **vol. 3**, pp. 745–763 (2007).

Y. YAMAGUCHI and K. KATO, "Structural Glycobiology by Stable-Isotope-Assisted NMR Spectroscopy," in *Modern Magnetic Resonance*, G. M. Webb, Ed., Springer; The Netherlands, **vol. 1**, pp. 219–225 (2006).

Y. BABA, "Biomolecular Chemistry Research by Micro- and Nanodevice," *Mirai Zairyuu* (in Japanese) **7**, 2–9 (2007).

Y. BABA, "Perspective for Future Medicine Derived by Nanobiotechnology," *Kagaku* (in Japanese) **62**, 23–27 (2007).

Life and Coordination-Complex Molecular Science

K. KUWAJIMA, "Unfolding and Folding of Proteins," in *Biophysics Handbook* (in Japanese), S. Ishiwata, I. Katsura, Y. Kirino and S. Mitaku, Eds., Asakura Publishing Co. Ltd.; Tokyo (2007).

R. TERO and T. URISU, "Biomaterials I: Proteins and Biochips," in *Introduction to Bio-Science for Nanotechnology* (in Japanese), the Surface Science Society of Japan, Ed., Kyoritsu Shuppan Co., Ltd; Tokyo (2007).

M. TAKEUCHI and T. OZAWA, "Methods for Imaging and Analyses of Intracellular Organelles Using Fluorescent and Luminescent Proteins," *Anal. Sci.* **23**, 25–29 (2007).

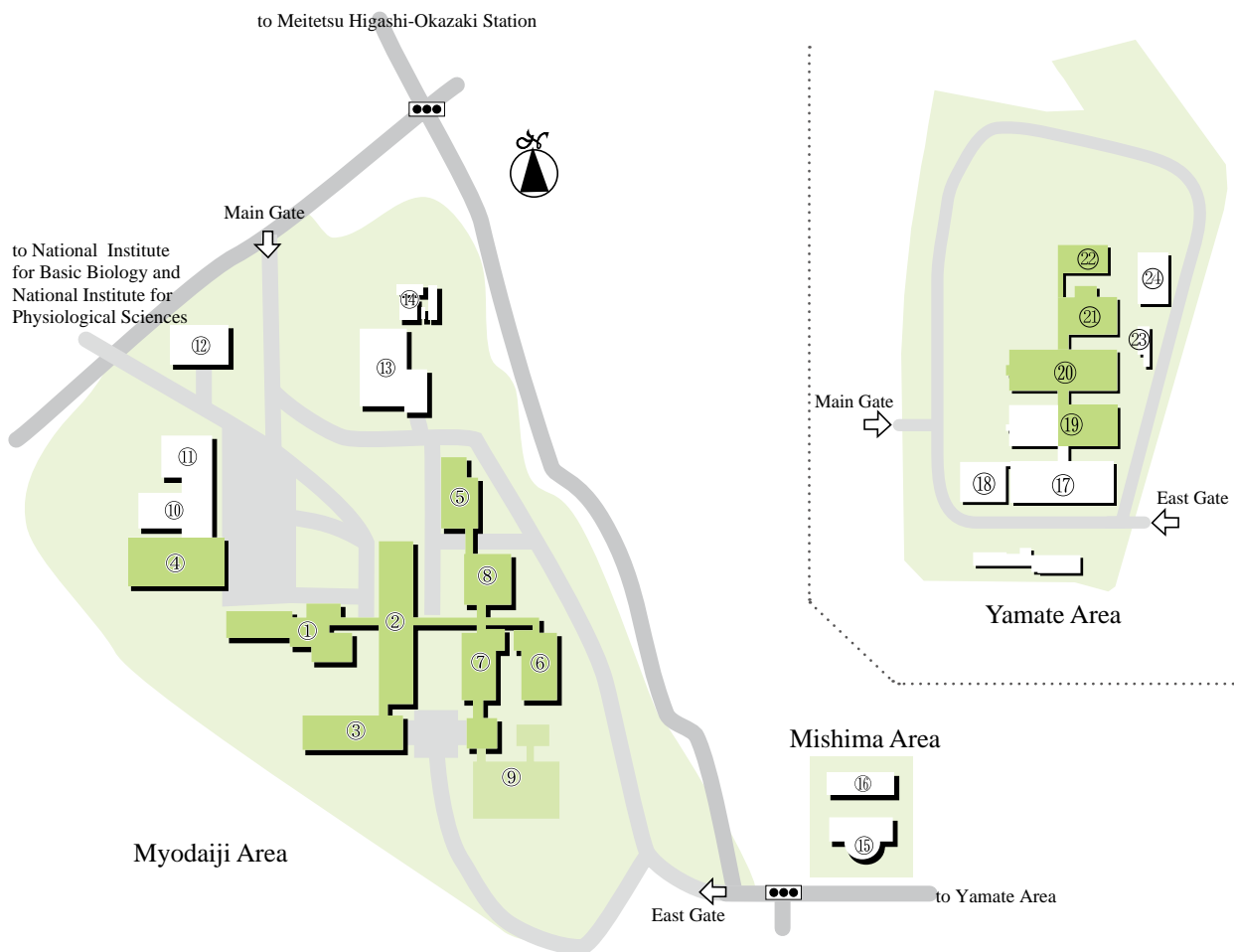
T. OZAWA and Y. UMEZAWA, "Identification of Proteins Targeted into the Endoplasmic Reticulum by cDNA Library Screening," *Methods Mol. Biol.* **390**, 269–280 (2007).

T. OZAWA and Y. UMEZAWA, "A Genetic Method to Identify Mitochondrial Proteins in Living Mammalian Cells," *Methods Mol. Biol.* **390**, 119–130 (2007).

A			KATSUKI, Hiroyuki	28	OKANO, Yoshinori	56	
AKIYAMA, Ryo	22		KAWAGUCHI, Hiroyuki	92	OKAZAKI, Susumu	16	
ALLAKHVERDIEV, Suleyman I.	68		KIM, Bongsoo	12	OZAWA, Takeaki	86	
AONO, Shigetoshi	78		KIM, Kang	18			
ASAI, Yoshihiro	22		KIMURA, Shin-ichi	38	S		
B			KITAGAWA, Hiroshi	94	SAITO, Shinji	18	
BABA, Masaaki	46		KITAJIMA, Masahiro	46	SAKAMOTO, Youichi	66	
BABA, Yoshinobu	76		KOBAYASHI, Hayao	56	SAKURAI, Hidehiro	70	
C			KONDO, Mitsuru	94	SASAKAWA, Hiroaki	72	
CHOI, Cheol Ho	6		KOSUGI, Nobuhiro	30	SHIGEMASA, Eiji	40	
CHONG, Song-ho	12		KURAHASHI, Takuya	82	SODA, Kazuo	46	
F			KUWAJIMA, Kunihiko	80	SUZUKI, Toshiyasu	66	
FUJII, Hiroshi	82		L				
FURUKAWA, Ko	58		LU, Xin	6	T		
FUSHITANI, Mizuho	34		M				
H			MAEDA, Hiromitsu	76	TAIRA, Takunori	42	
HASEGAWA, Hirokazu	26		MAKI, Kosuke	80	TAKAHASHI, Kazuyuki	56	
HATSUI, Takaki	30		MATSUMOTO, Taketoshi	44	TAKEUCHI, Masaki	86	
HAYASHI, Michitoshi	22		MATSUMOTO, Yoshiyasu	44	TANAKA, Hirofumi	64	
HIGASHIBAYASHI, Shuhei	70		MATSUO, Tsukasa	92	TANAKA, Koji	90	
HIGUCHI, Masayoshi	76		MITSUKE, Koichiro	32	TANAKA, Shoji	74	
HIKOSAKA, Yasumasa	40		MIURA, Shinichi	16	TERO, Ryugo	84	
HIRATA, Fumio	12		MOCHIHASHI, Akira	36	TOMURA, Masaaki	75	
HISHIKAWA, Akiyoshi	34		MORITA, Akihiro	20	TSUKUDA, Tatsuya	52	
HOSAKA, Masahito	36		N				
I			NAGASAKA, Masanari	30	U		
IJIMA, Takahiro	62		NAGASAWA, Takayuki	68	UOZUMI, Yasuhiro	88	
IMURA, Kohei	24		NAGASE, Shigeru	6	URISU, Tsuneo	84	
ISHIDA, Tateki	20		NAGATA, Toshi	68	URUICHI, Mikio	54	
ISHIMURA, Kazuya	6		NAKAGAWA, Takeshi	50	W		
ISHIZUKA, Tomoya	60		NAKAMURA, Toshikazu	58	WADA, Tohru	90	
ISHIZUKI, Hideki	42		NARUSHIMA, Tetsuya	24	WANG, Wenping	60	
ITO, Takahiro	38		NEGISHI, Yuichi	52	WATANABE, Kazuya	44	
J			NISHI, Nobuyuki	48	Y		
JIANG, Donglin	60		NISHIJO, Junichi	48	YAKUSHI, Kyuya	54	
JUDAI, Ken	48		NISHIMURA, Katsuyuki	62	YAMADA, Atsushi	16	
K			NOBUSADA, Katsuyuki	8	YAMADA, Yoichi M. A.	88	
KANAMORI-KATAYAMA, Mutsumi	94		O			YAMAMOTO, Kaoru	54
KATAYANAGI, Hideki	32		OGAWA, Takuji	64	YAMASHITA, Yasufumi	14	
KATO, Koichi	72		OHMORI, Kenji	28	YANAI, Takeshi	10	
KATO, Masahiro	36		OHSHIMA, Yasuhiro	26	YASUIKE, Tomokazu	8	
			OHTSUKA, Yuki	6	YOKOYAMA, Toshihiko	50	
			OISHI, Osamu	48	YONEMITSU, Kenji	14	
			OKADA, Kazumasa	46	YOSHIDA, Norio	12	
			OKAMOTO, Hiromi	24	YOSHII, Noriyuki	16	
					YOSHIOKA, Shiro	78	

The IMS campus covering 62,343 m² is situated on a low hill in the midst of Okazaki city. The inequality in the surface of the location, the hill and growing trees are preserved as much as possible, and low-storied buildings are adopted for conservation of the environment. The buildings of IMS are separated according to their functions as shown in the map below. The Research Office Building and all Research Facilities, except for the Computer Center, are linked organically to the Main Laboratory Buildings by corridors. The computer Center, Library and Administration Buildings are situated between IMS and neighboring National Institute for Basic Biology and National Institute for Physiological Sciences, since the latter two facilities are for common use amongst these three institutes.

The lodging facility of IMS called Mishima Lodge, located within four minutes' walk east of IMS can accommodate 74 guests and 20 families. Scientists visiting IMS, as well as the two other institutes, can make use of these facilities. Foreign visiting scientists can also live in this lodging with their families during their stays. The Okazaki Conference Center, with four conference rooms capable of attendance between 50~250, was built in April, 1997 in the Mishima area. The two buildings, Center for Integrative Bioscience, and Research Center for Computational Science, and research facilities of ONRI were built in February, 2002 in the Yamate Area. Four other buildings were also built in March, 2004 in the Yamate Area.



- | | |
|---|--|
| <ul style="list-style-type: none"> 1. Research Office Building 2. Main Laboratory Building 3. South Laboratory Building 4. Computer Center 5. Low-Temperature Facilities Building 6. Research Center for Molecular Scale Nanoscience 7. Laser Research Center for Molecular Science 8. Equipment Development Center 9. UVSOR Facility 10. Central Administration 11. Library 12. Faculty Club | <ul style="list-style-type: none"> 13. Power Station 14. Waste-Water Disposition Facilities 15. Okazaki Conference Center 16. Mishima Lodge 17. Yamate Bldg. 1A 18. Yamate Bldg. 1B 19. Yamate Bldg. 2 20. Yamate Bldg. 3 21. Yamate Bldg. 4 22. Yamate Bldg. 5 23. Waste-Water Disposition Facilities 24. Power Station |
|---|--|

BUILDINGS AND CAMPUS



Okazaki (population 351,000) is 260 km west of Tokyo, and can be reached by train in approximately 3 hours from Tokyo via Shinkansen and the Meitetsu Line.

The nearest large city is Nagoya, about 40 km northwest of Okazaki.





NATIONAL INSTITUTES OF NATURAL SCIENCES

Institute for Molecular Science

Myodaiji Area: 38 Nishigo-Naka, Myodaiji, Okazaki 444-8585, Japan